ELECTRON DIFFRACTION BY GASES

a

thesis

presented for the degree

of Ph.D. in the

University of Glasgow

by

Allan Hugh Clark B.Sc.

July 1968

ProQuest LLC.
789 East Eisenhower Parkway
P.O. Box 1346
Ann Arbor, MI 48106 – 1346

SUMMARY

This thesis contains an account of six gas phase electron diffraction molecular structure determinations carried out at the University of Glasgow for various oxygen-containing compounds of chlorine and sulphur. The apparatus used to record diffraction patterns was a modern, commercial, high accuracy, electron diffraction machine, and scattered electron intensities were measured using an automatic microdensitometer. Normal coordinate calculations, based on published infrared spectroscopic data, are also reported for most of the molecules studied.

Of the first five chapters of the work, Chapter One is devoted to a review of the electron diffraction technique, Chapter Two to a description of the theory on which this technique is based, Chapter Three to a discussion of the experimental methods followed, Chapter Four to an outline of the data processing procedures adopted, and Chapter Five to a summary of the theory of molecular vibrations.

Chapters Six and Seven describe normal coordinate, and root mean square amplitude of vibration, calculations for perchloryl fluoride ($FClO_3$) and perchloric acid ($HClO_4$), whilst Chapter Eight, in addition to providing

an introduction to the diffraction work discussed in subsequent chapters, includes a table of vibrational amplitudes calculated for dichlorine monoxide (Cl_2O), chlorine dioxide (ClO_2), and sulphur dioxide (SO_2), from published force constant data.

In Chapters Nine to Fourteen structural results, obtained by gas phase electron diffraction experiments, are presented for the molecules of dichlorine monoxide, perchloric acid, perchloryl fluoride, chlorine dioxide, sulphur dioxide and sulphur trioxide (SO_3), values being obtained, not only for the internuclear distances present in these systems, but also for the corresponding root mean square amplitudes of vibration. In the cases of dichlorine monoxide, chlorine dioxide, sulphur dioxide and sulphur trioxide, force constant and thermal data are used to correct $r_g(1)$ bond lengths obtained by least squares refinement, to the more fundamentally significant r_e values. For all six molecules studied, qualitative remarks are made concerning the chemical bonding present, the $d\pi$-$p\pi$ bonding theory, described by Cruickshank for tetrahedrally coordinated second row elements, being invoked to help rationalise the structural parameters obtained for perchloric acid and perchloryl fluoride.

In Chapter Fifteen, sources of systematic error

liable to have affected the accuracy of the electron diffraction results of Chapters Nine to Fourteen, are considered, and future improvements to the experimental technique, intended to reduce such errors, are suggested. It is concluded, however, that these uncertainties must be fairly small, since in most cases where checks are possible, the best determined molecular dimensions and root mean square amplitudes of vibration obtained, agree to within a few thousandths of an Angstrom unit with corresponding results determined by other independent physical methods.

In Chapter Sixteen, certain force constant, bond length, and force constant, bond order, relationships, originally published for the Cl-O bond by Robinson, are redetermined, this revision being worthwhile, not only in the light of the present work, but also in view of recently published results for other Cl-O containing compounds. The revised relationships obtained should be of considerable value in predicting Cl-O bond lengths for molecules whose infrared and Raman spectra have been thoroughly investigated, and for which there is therefore a possibility of calculating force constants.

Finally, five appendices are included which describe computer programmes written to carry out

the vibrational calculations of Chapters Six, Seven and Eight.

The work described in this thesis is original, and was carried out in partial fulfillment of the requirements for the degree of Ph.D. in the University of Glasgow.

June 1968 A. H. Clark

ACKNOWLEDGMENTS

The author wishes to express gratitude to his supervisors, Professor D. W. J. Cruickshank, and Dr. B. Beagley, for the valuable advice and stimulating encouragement which they gave him throughout the course of the researches described in this thesis.

He also thanks Dr. J. K. Tyler for much advice and helpful discussion, Dr. M. S. Child for advice on the subject of normal coordinate analysis, Dr. T. G. Hewitt for assistance in the matter of experimentation, Professor D. S. Payne for advice on the preparation of dichlorine monoxide, and the Pennsalt Chemical Corporation, Pennsylvania U. S. A., for their generous gift of a sample of perchloryl fluoride.

The author acknowledges the provision of certain electron diffraction data processing computer programmes by Dr. B. Beagley and Dr. T. G. Hewitt, and also thanks his colleagues in the electron diffraction and microwave laboratories for many hours of helpful discussion.

Finally he acknowledges with gratitude the award of a Carnegie Research Scholarship.

June 1968 A. H. Clark

LIST OF CONTENTS

CHAPTER ONE

AN INTRODUCTION TO GAS PHASE ELECTRON DIFFRACTION

The gas phase electron diffraction technique is a powerful tool for investigating the structure and internal motion of free molecules. Average values for internuclear distances, and values for the root mean square amplitudes of vibration corresponding to these, may be obtained with an accuracy of a few thousandths of an Angstrom unit, and in certain cases, internal rotation may be studied, barrier heights estimated, and conformational problems solved.

The method is subject to a number of limitations, however, and of these, three principal examples may be mentioned. First, and most important, the technique is restricted in its applicability to small or medium-sized molecules, as the methods used by it to derive structural parameters, become steadily less practicable as the number of interatomic distances in a molecule increases, and the symmetry decreases. Second, the molecule studied must be reasonably volatile at ordinary temperatures, as a considerable vapour pressure (around fifty millimetres of mercury) is required to produce a satisfactory diffraction

pattern. In some cases, however, this problem may be overcome by applying high temperature gas-nozzle techniques, though the success of such a procedure depends on the reaction of the compound concerned to heating. Third, the quantity of sample substance necessary for a full structure determination, can amount to several grams, and even if a less rigorous analysis is attempted, and only a single photographic plate record of the diffraction pattern taken, up to half a gram of material may be required. Such quantities of sample as these, are inconveniently large, if a rare compound is to be studied, or one of an extremely explosive nature.

It is of value in assessing gas phase electron diffraction, to compare it with microwave spectroscopy, which, although based on different principles, also produces structural results for small gas molecules. The most complete studies made by this technique, generally determine bond lengths and valence angles more accurately, and using much less sample substance, than is possible by electron diffraction, but the latter method can treat a wider range of molecules, and treat them more rapidly, as it does not involve the time consuming and difficult procedure of isotopic substitution, nor is it restricted to molecules which

possess an electric dipole moment. Whenever possible, it is advantageous to study a compound by both methods, as neither normally enables a direct determination of an equilibrium bond length to be made, and comparison of the $r_g(1)$ and r_s values obtained by the diffraction and spectroscopic experiments, respectively, is of great interest. In addition, each method can produce information which the other is not capable of obtaining, and hence the two techniques must be regarded as supplementing eachother, rather than being in any sense in competition.

Electron diffraction by gases has not always enjoyed its present status as a high accuracy structural tool. In common with most other structural techniques, it has undergone numerous stages of development, stretching over a period of many years. The earliest experimental studies were those of Wierl[1] in the 1930's, and in the following decade, the structural results produced were, by modern standards, rather inaccurate. One of the basic reasons for this, was that the circularly symmetric diffraction patterns recorded during these early experiments, showed a rapid fall-off of electron intensity with scattering angle, and, consequently,

microphotometer traces of such patterns were extremely steep, and showed little sign of diffraction rings. Because of the consequent inaccuracies involved in measuring the intensity function from these patterns, either by visual estimation or from traces, it was impossible to calculate internuclear distances with any great precision, and for a time progress in gas phase electron diffraction was impeded.

The introduction, however, in the 1940's, of a rotating metal sector (see Chapter Three) situated a small distance above the photographic plate, a development suggested by Debye[2] and Finbak[3], enabled patterns to be obtained whose microphotometer traces were much less steep, and showed clear indications of diffraction rings. Thus the oscillating component of the scattered intensity which depends on the molecular geometry and internal motion, could be much more accurately determined than had previously been possible. Consequently, as the sector technique became more refined, it was possible in the early 1950's to apply the theories of Debye[4] and Karle[5-10], on the effects of intramolecular motion on the scattered intensity, to the problem of interpreting diffraction patterns, and more precise molecular dimensions began to be obtained. From this point

onwards, that is during the last fifteen to twenty years, the electron diffraction technique has been steadily improved by extension of the underlying theory, development of instrumentation, and adoption of more sophisticated data processing methods.

For example, in the early 1950's, it was discovered that the use of real atomic amplitudes of scattering (see Chapter Two), based on the first Born approximation, often led to errors in interpreting radial distribution curves, and Schomaker and Glauber discussed[11] the necessity of introducing amplitudes which are complex functions of the scattering angle. This aspect of scattering theory has subsequently been developed, for example, by Ibers and Hoerni[12], Bartell and Brockway[13], Bonham and Ukaji[14], Karle and Bonham[15], and Seip[16], whilst problems concerning inelastic scattering, and the effects of chemical bonding on scattering, have been considered by Karle[17], and Bonham and Iijima[18-20].

Considerable advances have also been made in treating the vibrational problem. The effects of anharmonicity on electron diffraction results were shown to be significant by Bartell[21] in 1955, and this problem has been further developed by Bartell et al.[21-24], Morino[25], and Reitan[26]. In his original

paper [21], Bartell defined the type of internuclear distance obtained by electron diffraction studies, and he indicated a way in which this distance, symbolised $r_g(1)$, could be related to the corresponding equilibrium value r_e. Subsequently, electron diffraction experiments (see for example references 23 and 24) coupled with spectroscopic and thermal measurements, have in favourable cases enabled equilibrium configurations to be accurately determined.

Root mean square amplitudes of vibration, calculated from infrared and Raman spectroscopic data, have been extensively compared with the corresponding values obtained by electron diffraction work, and although the spectroscopic values have normally been calculated on the assumption of harmonic motion, the agreement found is usually very good. A large number of comparisons of this sort are listed in a work by Cyvin [27], and in this reference the possibility of using electron diffraction amplitudes to determine the force constants of molecules, is discussed.

The so-called shrinkage effect found to occur for linear or planar molecules when these are investigated by electron diffraction, was first observed by Bastiansen [28] in 1956, and has been

attributed to non-linear and out-of-plane vibrational motion. This effect, which makes such molecules seem to be non-linear or non-planar, has been treated theoretically by a number of authors, for example, Morino[29], and Cyvin et al.[30]

Among the improvements which have been made to instrumentation and to the data reduction procedure, have been the production of automatic microdensitometers which output intensity data on punched paper tape, and application[31-35] of the method of least squares refinement to the problem of extracting structural parameters from such data. The manufacture of bigger and faster electronic computers has also played an important part in automating and increasing the rate of structure analysis.

The modern state of gas phase electron diffraction has been discussed from several points of view, in reference 32, and in references 36-40. At the present time there are numerous electron diffraction groups working in different parts of the world, and particular mention should be made of those in America, Norway, Japan and Russia, whose contributions to the subject have been large. The structural results produced are of great interest to many types of chemist, and it is probable, as instrumentation improves still

further, and becomes more readily available, that in the future, the technique will be more extensively practised than it is today.

CHAPTER TWO

THE THEORY UNDERLYING THE SCATTERING PROCESS

1. Introduction

In this chapter an outline is given of the quantum mechanical theory of scattering of fast electrons by molecules. No attempt is made to present a rigorous analysis of the problem, and for detailed discussions of the topics covered, and justification of those steps assumed below, without proof, textbooks (41-46) and review articles (16,39,40,47 and 48) should be consulted.

2. A general statement of the problem

In an electron diffraction experiment, a narrow, cylindrical, monochromatic beam of electrons, collides at right angles with a small jet of vapour expanding from a nozzle.

The wavelength of the electrons, λ , is given by de Broglie's relationship,

$$\lambda = h/p \quad \ldots\ldots\ldots\ldots 2.1,$$

where h is Planck's constant, and the momentum p* of an electron is determined by the accelerating voltage gap

* p is the relativistic momentum.

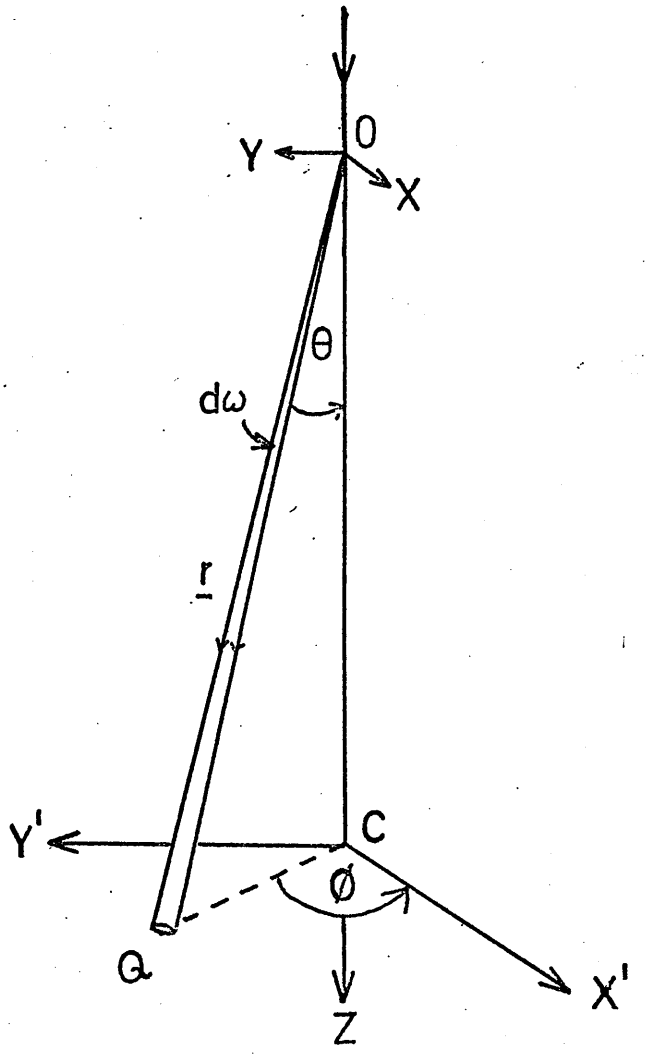

fig. 2.1

used to produce the beam.

When collision occurs, the electrons in the beam interact with gas molecules, and are deflected from their initial paths. The incident beam is thus spread out, and electrons travel away, in all directions, from the scattering centre.

In experiments, a proportion of these scattered particles is received on a rectangular, glass, photographic plate, whose position relative to the gas sample and incident beam may be understood from figure 2.1. In this diagram the incident beam is shown as travelling along the z axis, in a positive direction, and is assumed to strike a small volume of vapour situated at the origin O. The plate lies in the plane Y'CX', with its centre at the point C, and it receives electrons which have been deflected through an angle θ, where θ varies from 0° at C, to some limiting value determined by the size of the plate and its distance from O.

From the nature of the incident beam and the gas volume producing diffraction, it is evident that the distribution of scattered electrons is axially symmetric about the z axis, and hence is independent of the dihedral angle ϕ. It follows from this that the pattern obtained should be circularly

symmetric about C, and in fact, as is well known, electron diffraction photographs, particularly those taken using a rotating sector, show a series of diffuse, concentric, rings of maximum and minimum intensity.

The variation of intensity occurring along any radius may be expressed as a function of the angle θ, and this function, which characterises the entire pattern, is determined experimentally using a microdensitometer (see Chapter Three).

The object of the present chapter is to discuss the relation between this measured intensity variation, and the nature of the molecule producing diffraction.

The problem may be approached mathematically as follows. If the incident beam has intensity I_o, then the number of particles scattered in unit time, through angle θ, into an element of solid angle $d\omega$ (see fig. 2.1), may be written,

$$dN = I_o \cdot \sigma(\theta,\phi) \cdot d\omega \qquad 2.2,$$

where $\sigma(\theta,\phi)$ is called the scattering cross section or differential cross section. The number of electrons incident per unit time, at right angles, upon unit area situated at the point Q, with position vector $\underline{r}$, is the scattered intensity at Q, and

is therefore given by,

$$I(\underline{r}) = I_0 \cdot \sigma(\theta,\emptyset) / r^2 \qquad 2.3.$$

If the r^{-2} factor above, is required to be a constant of proportionality, then equation 2.3 describes the intensity which would be received on a spherical photographic plate of radius r, and a geometric consideration is required to convert the predicted spherical plate intensities to the actual intensity values measured on a flat plate r from O. This correction is discussed in section six of the present chapter.

The basic problem to be solved is that of finding $\sigma(\theta)$ (the $\emptyset$ dependence has been dropped because of the axial symmetry mentioned above), by quantum mechanical methods. Ideally this could be achieved by solving the time independent Schrodinger equation applicable to the case of an electron moving in the presence of a molecule, but this equation is too difficult to solve exactly, even for simple cases. A discussion of an approximate treatment, based on such an equation, is given in review article (47), but in the present chapter, the scattering of electrons by a single atom will be examined first, and then the molecule will be treated as equivalent to a configuration

of independent atoms, and an appropriate expression for $\sigma(\theta)$ derived.

3. The theory of elastic scattering by single atoms

If no exchange of energy is considered, the problem of an electron colliding with an atom, may be treated as that of an electron moving in the vicinity of a spherical potential V(r), centred on the origin of a Cartesian reference frame.

If the electron travels along the positive direction of the z axis, and comes from minus infinity, then during interaction with V(r) it is deflected through angle θ , and after interaction, passes off to infinity once more.

The Schrodinger equation appropriate to the problem is,

$$[-\hbar^2/8\pi^2 m_e \cdot \nabla^2 + V(r)]\psi(\underline{r}) = E.\psi(\underline{r}) \quad \ldots\ldots 2.4,$$

where $\underline{r}$ is the position vector of the electron and V(r) is dependent only on the modulus of $\underline{r}$. The quantity $|\psi(\underline{r})|^2$ may be interpreted as an electron density if scattering of a beam containing many identical electrons is being considered.

An appropriate asymptotic solution to equation 2.4, valid when r is large compared with the extent

of V(r), and if V(r) falls to zero faster than a Coulomb field, is

$$\psi^{\infty}(\underline{r}) \propto e^{ikz} + (r)^{-1} \cdot e^{ikr} \cdot f(\theta) \qquad 2.5,$$

where

$$k^2 = 8\pi^2 m_e \cdot E / h^2 \qquad 2.6.$$

This solution consists of an incident plane wave e^{ikz}, and a spherical scattered wave. Its validity can be verified by substitution in 2.4.* An expression for $\sigma(\theta)$ for atoms, can be obtained from this equation by considering the intensity of electrons it predicts at Q, with position vector $\underline{r}$, where r is very large. This intensity can be shown to be proportional to $|\psi^{\infty}(r)|^2$, and since, in practice, the incident plane wave is not infinite, but has a tiny cross section, only the second term in 2.5 need be considered. Hence the intensity at the point $\underline{r}$ is,

$$I(\underline{r}) \propto (r)^{-2} \cdot |f(\theta)|^2 \qquad 2.7,$$

and comparison of this result with 2.3 shows that,

$$\sigma(\theta) \propto |f(\theta)|^2 \qquad 2.8.^{**}$$

The problem of finding $\sigma(\theta)$ therefore reduces to that of finding $f(\theta)$, a quantity called the atomic

* V(r) must be assumed zero when substitution is made.
** The constant of proportionality turns out to be unity.

scattering amplitude for electrons.

This is done by writing the general solution to 2.4, with axial symmetry, as

$$\psi(\underline{r}) = \sum_{l=0}^{\infty} A_l \cdot P_l(\cos(\theta)) \cdot F_l(r) \qquad 2.9,$$

where each term in this series is itself a solution to 2.4, of the general type,

$$\psi_l(\underline{r}) \propto F_l(r) \cdot Y_l(\theta) \qquad 2.10.$$

In 2.9 the A_l are arbitrary constants, the $P_l(\cos\theta)$ are Legendre polynomials, and, as can be verified by substituting 2.10 in 2.4, each of the $F_l(r)$ must satisfy a differential equation of the type,

$$r^{-2} \cdot \frac{d}{dr}\left(r^2 \cdot \frac{dF}{dr}\right) + \left(k^2 - U(r) - l(l+1)/r^2\right) F = 0 \qquad 2.11,$$

where

$$U(r) = [8\pi^2 m_e/h^2] \cdot V(r) \qquad 2.12.$$

Since only the asymptotic form of 2.9 is required, when r tends to infinity, then only the asymptotic solution to 2.11 is required as r tends to infinity. This latter can be shown to be,

$$F_l(r) \propto (kr)^{-1} \cdot \sin(kr - l\pi/2 + \delta_l) \qquad 2.13,$$

where δ_l is a small phase shift characteristic of

the lth solution. It follows that the appropriate form of 2.9 valid for large r is,

$$\psi(\underline{r}) = \sum_{l=0}^{\infty} A_l \cdot P_l(\cos(\theta)) \cdot (kr)^{-1} \cdot \sin(kr - l\pi/2 + \delta_l) \qquad 2.14.$$

Comparison of this result with 2.5 requires the expansion,

$$[e^{ikz}]^{\infty} = \sum_{l=0}^{\infty} (2l+1) \cdot i^l \cdot P_l(\cos(\theta)) \cdot (kr)^{-1} \cdot \sin(kr - l\pi/2) \qquad 2.15.$$

This latter result may be obtained by writing the solution to 2.4, for the case where $V(r) = 0$, in the form 2.9, and obtaining an asymptotic solution to 2.11, for this the case of a freely moving electron. This solution is already known to have the plane wave form, e^{ikz}, and hence comparison of these two results leads to 2.15. When 2.14 is compared with 2.5, bearing 2.15 in mind, algebraic manipulation based on the necessary equivalence of 2.14 and 2.5, leads to the expression for $f(\theta)$ first derived by Faxen and Holtsmark,[49]

$$f(\theta) = (2ik)^{-1} \cdot \sum_{l=0}^{\infty} (2l+1) \cdot (e^{2i\delta_l} - 1) \cdot P_l(\cos(\theta)) \qquad 2.16.$$

It is evident that $f(\theta)$ is in general a complex number. The principal obstacle encountered in evaluating $f(\theta)$ from 2.16, is the problem of finding the phase shifts δ_l. These can be calculated by applying numerical methods to 2.11, and the series 2.16

summed, but a useful, approximate, real expression for $f(\theta)$ was obtained by Born,[50,51] which is very often used, and will be referred to as $f(\theta)^{Born}$. Born showed that if the phase shifts are small, and the potential $V(r)$ is weak for large r, then

$$f(\theta)^{Born} = -\int_0^\infty U(r).[\sin(rs)/(rs)].r^2.dr \qquad 2.17,$$

where

$$s = 4\pi.\sin(\theta/2)/\lambda \qquad 2.18.$$

The approximation made in deriving this result is known as the first Born approximation, and it is best for fast electrons and light atoms.

If the potential $U(r)$ for an atom is written in the form,

$$U(r) = 8\pi^2 m_e/h^2.\ [-Ze^2/r + V'(r)] \qquad 2.19,$$

where $V'(r)$ is the potential arising from the electron charge cloud, of density $\rho(r)$ in the atom, and this expression is substituted in 2.17 and integration performed, then the result obtained is the familiar one for the electron scattering amplitude, namely,

$$f(\theta)^{Born} \propto (Z - F(s))/s^2 \qquad 2.20,$$

where $F(s)$ is the X-ray scattering factor given by the

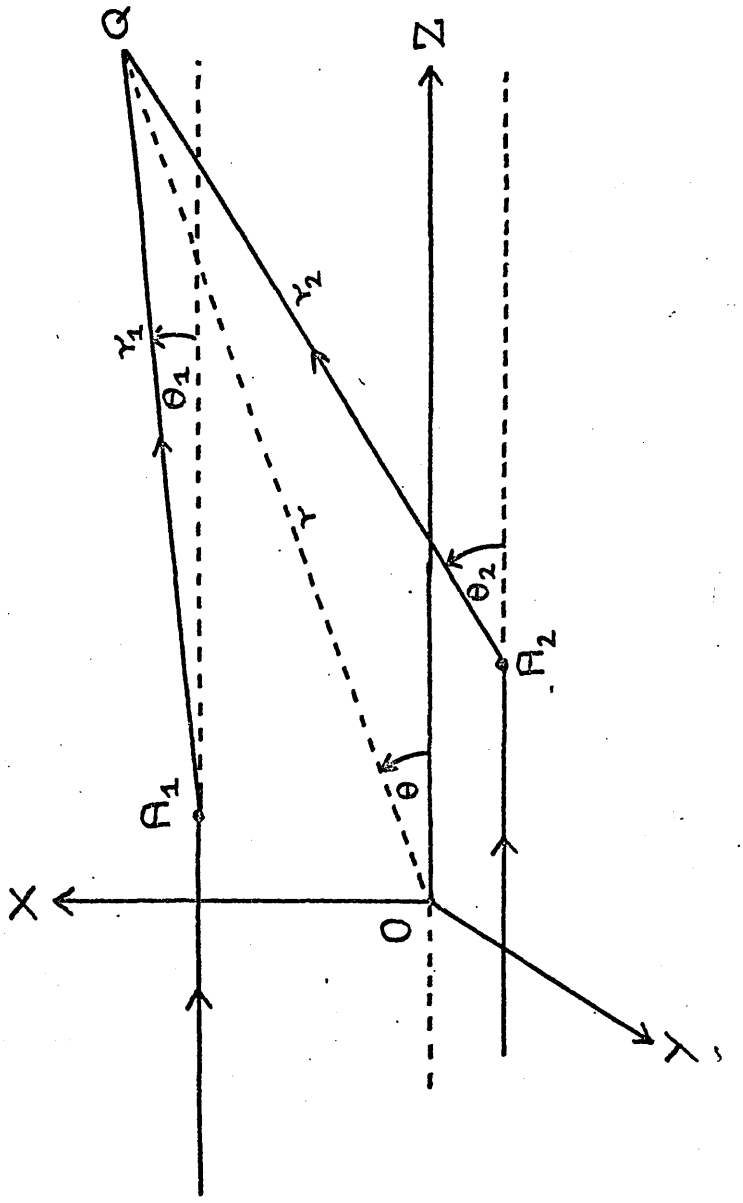

fig. 2.2

expression,

$$F(s) = 4\pi \int_0^\infty [\sin(sr)/(sr)] \cdot \rho(r) \cdot r^2 dr \quad \ldots 2.21,$$

and Z is the atomic number.

The results, 2.20 and 2.16, will now be used to describe scattering by molecules.

4. Treatment of the scattering of electrons by molecules using the independent atom approximation

If chemical bonding is neglected, and a molecule is treated as a configuration of independent atoms, then the molecular scattering problem may be treated by summing the spherical waves scattered by each atom. The independent atom approximation should be valid if the range of interaction of the electron with any atom, and the electron wavelength λ, are much smaller than the distance between atoms. The approximation should therefore be best for light atoms and fast electrons.

Let the molecule be a rigid assembly of atoms, fixed relative to a Cartesian system, with the atoms distributed among various positions in space (fig. 2.2). The elastically scattered wave travelling outwards from any atom j, to the point Q, with position vector $\underline{r}$, where r is very much larger than the interatomic distances, has equation,

$$\psi_j^{\infty}(\underline{r}) = (r_j)^{-1} \cdot f_j(\theta_j) \cdot e^{i\phi_j} \quad \ldots\ldots\ldots\ldots 2.22,$$

where ϕ_j is a phase angle which depends on the position of the jth. atom in space. If $f_j(\theta_j)$ is written as a complex number with the form,

$$f_j(\theta_j) = \left| f_j(\theta_j) \right| \cdot e^{i\eta_j} \quad \ldots\ldots\ldots\ldots 2.23,$$

where η_j is a phase angle dependent on θ_j, and the nature of atom j, then the expression for the outgoing wave may be written in the form,

$$\psi_j^{\infty}(\underline{r}) = (r_j)^{-1} \cdot \left| f_j(\theta_j) \right| \cdot e^{i\eta_j} \cdot e^{i\phi_j} \quad \ldots\ldots\ldots 2.24,$$

If r_j and θ_j are approximated to by r and θ measured relative to O (see fig. 2.2), the resultant wave at Q is therefore,

$$\psi_R^{\infty}(\underline{r}) = \sum_{j=1}^{N} (r)^{-1} \cdot \left| f_j(\theta) \right| \cdot e^{i(\eta_j + \phi_j)} \quad \ldots\ldots\ldots 2.25,$$

where the summation is over all atoms in the molecule. The scattered intensity at Q is proportional to $\psi_R^{\infty}(\underline{r}) \cdot \psi_R^{\infty *}(\underline{r})$, and hence,

$$I(\underline{r}) \propto \sum_{j=1}^{N} (r)^{-1} \cdot \left| f_j(\theta) \right| \cdot e^{i(\eta_j + \phi_j)} \; \chi \; \sum_{k=1}^{N} (r)^{-1} \cdot \left| f_k(\theta) \right| \cdot e^{-i(\eta_k + \phi_k)} \quad \ldots 2.26,$$

or

$$I(\underline{r}) \propto \sum_{j,k=1}^{N} (r)^{-2} \cdot \left| f_j(\theta) \right| \cdot \left| f_k(\theta) \right| \cdot e^{i(\eta_j - \eta_k + \phi_j - \phi_k)} \quad \ldots 2.27,$$

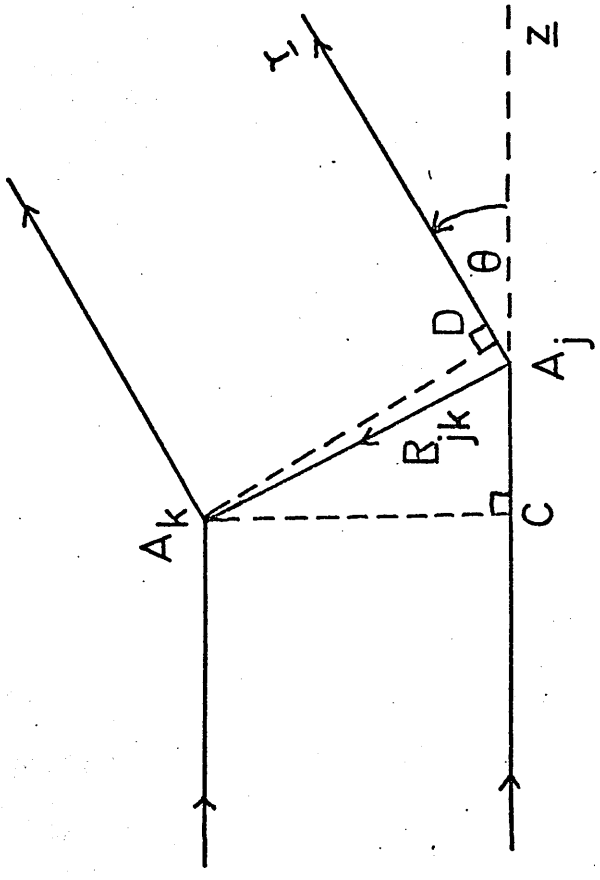

fig. 2.3

and therefore,

$$I(\underline{r}) \propto \sum_{jk=1}^{N} (r)^{-2} \cdot \left|f(\theta)_j\right| \cdot \left|f(\theta)_k\right| \cdot e^{i\Delta\eta_{jk}} \cdot e^{i\Delta\phi_{jk}} \qquad 2.28.$$

In this summation the kjth term is,

$$(r)^{-2} \cdot \left|f_k(\theta)\right| \cdot \left|f_j(\theta)\right| \cdot e^{-i\Delta\eta_{jk}} \cdot e^{-i\Delta\phi_{jk}} \qquad 2.29,$$

and the jjth term is,

$$(r)^{-2} \cdot \left|f_j(\theta)\right|^2 \qquad 2.30.$$

Hence the scattered intensity at Q may be written as,

$$I(\underline{r}) \propto (r)^{-2} \left\{ \sum_{j=1}^{N} \left|f(\theta)_j\right|^2 + \sum_{jk=1(j\neq k)}^{N} \left|f_j(\theta)\right| \cdot \left|f_k(\theta)\right| \cdot \cos(\Delta\eta_{jk} + \Delta\phi_{jk}) \right\} \qquad 2.31,$$

where $\Delta\eta_{jk}$ is independent of the spatial positions of the atoms, but is a function of the scattering angle θ, and $\Delta\phi_{jk}$ is the difference in phase between the waves scattered from atoms j and k. This phase difference may be calculated by finding the path difference D_{jk}, between these two waves. In figure 2.3, $\underline{Z}$ is a unit vector in the direction of the incident beam, and $\underline{r}$ is a unit vector in the direction of the beams scattered to Q, a very long distance away. For the pair of atoms shown, the path difference is $CA_j + A_jD$, and if this pair of atoms is the general pair, then

$$D_{jk} = 2R_{jk} \cdot \sin(\theta/2) \cdot \cos\alpha_{jk} \qquad 2.32,$$

where α_{jk} is the angle between the vector $\underline{R}_{jk}$ and the vector ($\underline{r} - \underline{z}$). It follows that,

$$\Delta\phi_{jk} = (2\pi D_{jk})/\lambda = (4\pi \sin(\theta/2)/\lambda).R_{jk}\cos\alpha_{jk} = s.R_{jk}\cos\alpha_{jk} \quad \ldots 2.33.$$

Hence the intensity at Q may now be written as,

$$I(\underline{r}) \propto (r)^{-2}\left\{\sum_{j=1}^{N}|f_j(\theta)|^2 + \sum_{jk=1(j\neq k)}^{N}|f_j(\theta)|.|f_k(\theta)|.\cos(\Delta\eta_{jk} + s.R_{jk}\cos\alpha_{jk})\right\} \quad 2.34.$$

Now in the diffraction experiment the beam is scattered by a very large number of gas molecules in all possible orientations relative to it, no particular orientation being preferred. Hence equation 2.34 must be averaged over all possible values for the $\cos\alpha_{jk}$. Each of these quantities may vary continuously between the limits 1 and -1, and so integration produces the required average intensity at Q,

$$\bar{I}(\underline{r}) \propto (r)^{-2}\left\{\sum_{j}|f_j(\theta)|^2 + \sum_{jk(j\neq k)}|f_j(\theta)|.|f_k(\theta)|.\cos\Delta\eta_{jk}.[\sin(sR_{jk})/(sR_{jk})]\right\}^{*} \quad \ldots 2.35.$$

In the work described in this thesis, because the molecules examined contained light atoms, of fairly similar atomic number, the $\cos\Delta\eta_{jk}$ term was assumed to be always very near to unity, and the amplitudes $|f_j(\theta)|$ and $|f_k(\theta)|$, were assumed to be given by Born's expression 2.17, and hence by 2.20. Thus for a rigid configuration of atoms, allowed to take up all possible orientations relative to the incident beam, the

* Note that the quantity in brackets is just $\sigma(\theta)$, of equation 2.3.

average intensity of electrons elastically scattered to Q, is given by,

$$\bar{I}(\underline{r}) \propto (r^{-2}.s^{-4}).\left\{\sum_{i=1}^{N}(Z_i-F_i)^2+\sum_{ij=1(i\neq j)}^{N}(Z_i-F_i).(Z_j-F_j).\sin(sR_{ij})/(sR_{ij})\right\}$$

52 2.36.

If a term S_i is added to take atomic inelastic scattering into account, $\bar{I}(\underline{r})$ is replaced by $I(s)$, and the r^{-2} factor treated as a constant of proportionality, and omitted, then

$$I(s) \propto (s^{-4}).\left\{\sum_{i=1}^{N}[(Z_i-F_i)^2+S_i]+\sum_{ij=1(i\neq j)}^{N}(Z_i-F_i).(Z_j-F_j).\sin(sR_{ij})/(sR_{ij})\right\}$$

is the final expression obtained. 2.37

5. Modification of the intensity expression to take into account molecular vibration

Molecules are in reality non-rigid, and undergo internal vibration and other forms of internal motion. At any instant, the electron beam not only interacts with molecules in all possible orientations relative to it, but also with molecules in a very large number of distorted configurations, distorted that is, relative to the equilibrium configuration of minimum potential energy. As the population of vibrational energy levels is temperature dependent, the exact distribution of the molecules among possible states of distortion, is also temperature dependent.

The modification which must be made to 2.37 to

take these effects into account can be derived as follows (see ref. 4). Let R_{ij} be any interatomic distance present in the molecule. As a result of internal motion, a large collection of molecules will, at any instant, show a practically continuous range of R_{ij} values surrounding the equilibrium value R_{ij}^{e}. This distribution may be described by a probability function $P_{ij}(R)$, where $P_{ij}(R)dR$ is the fraction of the total number of molecules which have a value of R_{ij} in the range R to R+dR. Each $\sin(sR_{ij})/(sR_{ij})$ term appearing in 2.37 can now be averaged using this probability function. The average is just,

$$\int_0^\infty P_{ij}(R)\cdot(\sin(sR)/(sR))\,dR \quad \ldots\ldots 2.38,$$

and hence the correct form for I(s), which takes into account internal motion, may be written,

$$I(s) \propto s^{-4}\left\{\sum_i[(Z_i-F_i)^2+S_i]+\sum_{ij(i\neq j)}(Z_i-F_i)\cdot(Z_j-F_j)\int_0^\infty P_{ij}(R)\cdot(\sin(sR)/(sR))\,dR\right\} \quad \ldots 2.39.$$

If the molecule is assumed to undergo only harmonic vibrational motion, a Gaussian function may be assumed for each $P_{ij}(R)$ function, not only for any particular vibrational energy level, but also for the function required above, which is temperature dependent, and takes into account the distribution of molecules among all the possible vibrational levels.

The Gaussian distribution assumed is symmetric about the equilibrium distance R_{ij}^{e} and integration of 2.39, using it, gives the result,*

$$I(s) \propto s^{-4}\left\{\sum_{i}[(Z_i-F_i)^2+S_i]+\sum_{ij(i\neq j)}(Z_i-F_i).(Z_j-F_j).[\sin(sR_{ij})/(sR_{ij})].e^{-u_{ij}^2s^2/2}\right\} \quad \text{2.40.}$$

In this equation the R_{ij} appearing in the sine term, is related to the centre of gravity value for the Gaussian distribution, by the equation (see ref. 21),

$$R_{ij}^{g}(1)\ [\text{i.e. } R_{ij} \text{ above}] = R_{ij}^{g}(0) - u_{ij}^2/R_{ij}^{e} \quad \ldots\ldots \text{2.41,}$$

and is in fact the centre of gravity value of the function $P_{ij}(R)/R$. The u_{ij} quantities appearing above, are the root mean square deviations of the R_{ij}'s from the R_{ij}^{e}'s, and are temperature dependent. The nomenclature used in equation 2.41 is that used by Bartell[21], and will be discussed further in section eight. The u_{ij}'s , or root mean square amplitudes of vibration, will be discussed at length in Chapter Five. For completely harmonic vibration R_{ij}^{e} is equal to $R_{ij}^{g}(0)$. Equation 2.41 has been mentioned at this stage to emphasise the fact that it is an $R_{ij}^{g}(1)$ distance that is obtained , when 2.40 is used to describe the experimental intensity data.

In reality the assumed Gaussian $P_{ij}(R)$ function is invalid because of anharmonicity of vibration, and

* This step involves certain approximations but is sufficiently accurate for most purposes.

a less symmetric type of distribution should be used. In 1955 Bartell[21] extended the theory to include the effects of anharmonicity. By assuming a Morse type of potential, and by extending the results obtained for diatomic systems to actual polyatomic molecules, he suggested a better expression for the scattered intensity I(s). This is,

$$I(s) \propto s^{-4}\left\{\sum_i [(Z_i - F_i)^2 + S_i] + \sum_{ij(i\neq j)} (Z_i - F_i)(Z_j - F_j)\left[\frac{\sin s(R_{ij} - x_{ij}s^2)}{sR_{ij}}\right] e^{-u_{ij}^2 s^2/2}\right\} \quad 2.42,$$

where x_{ij} is a small constant* related to the 'a' of the Morse function. (see equn. 2.54)

In the work described in this thesis the function used to describe the intensity was of the type 2.40, and the x_{ij} were not considered.

In the cases of molecules capable of internal rotation, the treatment given above is invalid, as the $P_{ij}(R)$ functions for certain distances are no longer even nearly Gaussian. Discussions of internal motion of this sort have been given by Debye[4] and Karle[5-10], and the problem is reviewed in reference (48).

* This asymmetry constant x_{ij} is related to 'a' by $x_{ij} = au_{ij}^4/6$.

6. The relation between the I(s) of 2.40 and the measured intensity

Expression 2.40 is proportional to the intensity of electrons received at any point Q, on a spherical surface, of radius r and centre 0, when an electron beam travelling along the positive direction of the z axis, is scattered by a small gas sample situated at 0. In experiments a flat photographic plate is used to record this intensity, and is situated r from 0, at right angles to the z axis, and parallel to the xy plane. In addition , a metal sector (see Chapter Three) is allowed to rotate above the plate, and multiplies the intensity of scattered electrons by a known function $\alpha(s)$.

The intensity observed at any point on the plate has to be divided by $\alpha(s)$, and then by $\cos^3(\theta)$, to convert it into a quantity proportional to the I(s) of 2.40. The $\cos^3(\theta)$ factor arises because an area element on the spherical surface is nearer the origin 0, by a factor of $\cos(\theta)$, than its projection on the plate, and also, on projection, the area is increased by a factor of $\cos(\theta)$.

In practice the experimental data are further multiplied by s^4, to give a function, called an uphill curve because of its appearance, and this has the

theoretical form,

$$I_{up}(s) \propto \sum_i [(Z_i - F_i)^2 + S_i] + \sum_{ij\,(i\neq j)} (Z_i - F_i).(Z_j - F_j).[\sin(sR_{ij})/(sR_{ij})].e^{-u_{ij}^2 s^2/2} \qquad 2.43,$$

if the approximations made in previous sections are accepted.

In practice it is found necessary to add an extra unknown function of s, E(s) , to this equation. This term is required to take into account extraneous scattering of electrons by the internal parts of the diffraction apparatus itself. A final expression for the uphill curve is therefore,

$$I_{up}(s) \propto \sum_i [(Z_i - F_i)^2 + S_i] + E(s) + \sum_{ij\,(i\neq j)} (Z_i - F_i).(Z_j - F_j).[\sin(sR_{ij})/(sR_{ij})].e^{-u_{ij}^2 s^2/2} \qquad 2.44.$$

It is clear that the first two terms are independent of the geometry of the scattering molecule, and it is normally assumed that this sum, called the background scattering curve, is a smooth steadily* increasing function of s, which has no wavelike characteristics. In electron diffraction work , although the atomic scattering factors, both elastic and inelastic, are known, the background curve is usually drawn empirically through the uphill curve and subtracted from this. The unknown nature of E(s) makes this necessary.

The function obtained on subtraction depends on

*Not in a mathematical sense, the gradient changes, see fig. 4.3.

the molecular structure and motion, and may be called the molecular intensity curve $I_{mol}(s)$. If the assumed background curve is correct, then the molecular intensity function obtained, should have the theoretical form,

$$I_{mol}(s) \propto \sum_{ij=1(i\neq j)}^{N} (Z_i - F_i).(Z_j - F_j).[\sin(sR_{ij})/(sR_{ij})]\, e^{-u_{ij}^2 s^2/2} \qquad 2.45.$$

In the work described in this thesis, the $I_{mol}(s)$ function was modified by multiplying it by,

$$s \Big/ \left\{ [1 - F_m/Z_m][1 - F_n/Z_n] \right\},$$

where the labels m and n refer to two commonly occurring atom types in the molecule. The resulting function may be written as,

$$I_m(s) \propto \sum A_{ij} [\sin(sR_{ij})/R_{ij}]\, e^{-u_{ij}^2 s^2/2} \qquad 2.46,$$

where

$$A_{ij} = N_{ij}.Z_i.Z_j.(1 - F_i/Z_i).(1 - F_j/Z_j) \Big/ (1 - F_m/Z_m)(1 - F_n/Z_n) \qquad 2.47.$$

N_{ij} is the number of equivalent distances of type ij and the summation is over all nonequivalent distance types.

The reason for carrying out this modification is, that the A_{ij} coefficient is independent of s, if i and j refer to the same atom types as m and n. In the

case where this is not so, A_{ij} is still very nearly independent of s, and in some least squares refinement procedures A_{ij} has been treated as constant.

In the present work the intensity curve finally obtained after correction, subtraction of the background, and modification (for details see Chapter Four), was assumed to have the theoretical form 2.46, and the method of least squares refinement was applied to calculate the best values of the R_{ij} and u_{ij} parameters consistent with this assumption. The A_{ij} factors were, where necessary, calculated as functions of s, and were not assumed constant.

7. The radial distribution function [53]

Equation 2.46 for the $I_m(s)$ function may be written in the more general form,

$$I_m(s) \propto \sum_{\substack{\text{all types} \\ ij}} A_{ij} \cdot \int_0^\infty [\sin(sR)/R] \cdot P_{ij}(R) \cdot dR \qquad \ldots 2.48,$$

where the assumption of harmonic motion has not been made. This is equivalent to,

$$I_m(s) \propto \int_0^\infty \left(\sum A_{ij} P_{ij}(R)/R \right) \cdot \sin(sR) \cdot dR \qquad \ldots 2.48',$$

and, by applying Fourier transformation theory to this equation, it follows that,

* For the purposes of this step A_{ij} should be taken as $\sim N_{ij} Z_i Z_j$.

$$\frac{\sigma(R)}{R} = \sum A_{ij}.[P_{ij}(R)/R] \propto \int_0^{\infty} I_m(s).\sin sR.ds \quad \ldots 2.49.$$

The function of R defined by 2.49 is known as the radial distribution function, $\sigma(R)/R$ and it is evident that it consists of a sum of probability distributions (note, however, the division by R), one for each of the non-equivalent distances ij.

Visual examination of such a curve immediately provides information about the structure and internal motion of a molecule, information which is not apparent from a similar examination of the corresponding $I_m(s)$ curve.

In practice the $I_m(s)$ data obtained stretch from some non-zero lower s limit, to some finite upper s limit, and the integral appearing in 2.49 cannot be evaluated as it stands. If it is approximated to by,

$$\int_{smin}^{smax} I_m(s).\sin sR.ds \quad \ldots 2.50,$$

then the $\sigma(R)/R$ curve obtained is distorted from its true form (2.49) in two ways. The omission of data from s = 0 to s = smin causes the R axis base line to be curved instead of straight (the envelope effect), whilst the omission of data beyond smax introduces a noise ripple, which spreads out in either direction from the base of each peak in the radial distribution

curve. The envelope and noise ripple effects make interpretation of the σ (R)/R curve difficult.

The two effects are normally dealt with in the following ways. The envelope effect may be removed by adding theoretical intensity data, based on some knowledge of the structure to be determined, up to smin, and then transforming, or it may be allowed for empirically by drawing in an envelope for the σ(R)/R function obtained, and then subtracting this to produce a curve properly based on the R axis.

The lack of high s data is compensated for by multiplying $I_M(s)$ by e^{-ks^2}*, where k is a suitable small constant, and then transforming it according to 2.50. The damping function has the effect of making the missing high s data contribute little to the integral, and hence the result approximates very closely to what would have been obtained by integrating to infinity as in 2.49. Clearly the great disadvantage of this procedure is that the peaks in the resulting radial distribution function are all artificially broadened, and resolution is greatly reduced. Normally k is chosen in such a way as to produce a balance between the effects of 'noise' and broadening.

If the vibrational motion of a molecule were strictly harmonic, then the peaks appearing in the

* the damping function.

$\sigma(R)/R$ plot would be very nearly Gaussian, and the R value corresponding to the peak maximum would be very close to the equilibrium value for the distance concerned. These remarks are in fact more appropriate to the function $\sigma(R)$ itself, but the effects produced by dividing by R , are comparatively small. The half band width of these peaks would also be related to the mean amplitude of vibration u_{ij} for the distance concerned, though naturally this width also depends on the choice of damping constant, (k).

Since $I_m(s)$ can be written in the form 2.46 for the case of completely harmonic vibration, this expression may be substituted into

$$\frac{\sigma(R)}{R} \propto \int_0^{\infty} I_m(s).e^{-ks^2} \cdot \sin sR \, .ds \quad \ldots 2.51,$$

and if the A_{ij} are assumed to be constants, integration may be performed to give,

$$\frac{\sigma(R)}{R} \propto \sum_{(\text{all types } ij)} \left\{ A_{ij} / [R_{ij}\sqrt{k + u_{ij}^2/2}] \right\} \cdot e^{\frac{-(R_{ij}-R)^2}{4(k+u_{ij}^2/2)}} \quad \ldots 2.52.$$

This theoretical equation for the $\sigma(R)/R$ curve , based on the assumptions of harmonicity, constant A_{ij}'s, and the first Born approximation, may be compared with experimental curves, obtained by numerical integration of 2.51 between the limits smin and smax. The envelope effect should be removed before comparison.

* $\sim N_{ij}Z_iZ_j$.

Deviations found to occur between the experimental and theoretical $\sigma(R)/R$ curves may be assigned to failure of the approximations made in deriving expression 2.52, or to an inadequate damping function e^{-ks^2}. There is the additional possibility that the theoretical $I_m(s)$ function assumed is based on an incorrect model or set of parameters u_{ij} and R_{ij}.

8. A discussion of the types of bond length obtained

The electron diffraction experiment leads, on data processing, to an $I_m(s)$ curve, and this on Fourier transformation, using a suitable damping function, produces a radial distribution curve. The problem to be discussed in this section concerns the nature of the R_{ij} parameters which may be extracted from the experimental data.

Normally these are obtained by fitting a theoretical intensity expression to the experimental $I_m(s)$ curve. In the work described in this thesis an expression of type 2.46 was used for this purpose, and the least squares refinement procedure was adopted to achieve the best fit. The experimental radial distribution curve was used in a qualitative way only.

It is useful, however, to define various types of internuclear distance in terms of the radial

distribution function (see ref. 21). The general expression $\sigma(R)/R^N$ will be considered where N may take on the values 0, 1, etc., and the molecular vibrations will be assumed slightly anharmonic.

Following Bartell[21], the peak maximum of the $\sigma(R)/R^N$ function, corresponding to a particular interatomic distance, may be written $r_m(N)$, and is related to the equilibrium r_e value by,

$$r_m(N) \simeq r_e - Nu^2/r_e + au^2 \qquad 2.53,$$

where u is the root mean square amplitude of vibration for the distance concerned, and 'a' is the constant appearing in the Morse potential,

$$V(r) = D^*[\, e^{-2a(r-r_e)} - 2e^{-a(r-r_e)}\,] \qquad 2.54,$$

and is usually in the order of 2.0 Å^{-1} for single bonds. Thus 'a' describes the amount of anharmonicity involved.

The centre of gravity value for a peak in the $\sigma(R)/R^N$ function has already been mentioned in section five , where the values for N = 0 and N = 1 were considered. A general relationship relating the N th value $r_g(N)$ to the equilibrium distance r_e, is

* D = a dissociation energy.

$$r_g(N) \simeq r_e - Nu^2/r_e + 3au^2/2 \qquad 2.55.$$

If an expression of type 2.46 is used to fit the experimental $I_m(s)$ curve, an $r_g(1)$ distance is obtained. This follows from the nature of equation 2.40 discussed in section five, from which 2.46 was derived. If N is given the value 1 in 2.55 above, the relationship between the $r_g(1)$ distance and r_e is just,

$$r_g(1) = r_e - u^2/r_e + 3au^2/2 \qquad 2.56.$$

The r_e appearing in the second term may be approximated to by $r_g(1)$ itself. The constant u is normally available from the electron diffraction study or from spectroscopic data, and often 'a' may be estimated from spectroscopic and/or thermal data (see Chapter Eight).

It is clear from 2.55 that the relationship between $r_g(1)$ and $r_g(0)$ is that given by equation 2.41 of section five, and again the r_e appearing in the denominator may be approximated to by $r_g(1)$.

9. Failure of the first Born approximation

In section four the independent atom approximation was used to calculate the electron intensity scattered by a molecule, and equation 2.35, containing a $\cos \Delta\eta_{jk}$

term was derived. This factor was shown to arise because of the complex number amplitudes of scattering predicted by 2.16.

Assumption of the first Born approximation, the assumption made in the second half of section four, is equivalent to saying that the cosine term is always close to unity, and that the moduli of the scattering amplitudes are given by 2.20. As has been stated previously, these assumptions are most justified if the molecule contains light atoms, all having closely similar atomic numbers, and if fast (e.g. 50 -60 kV) electrons are employed in scattering experiments.

In the early 1950's use of this approximate treatment for molecules containing both heavy and light atoms (e.g. UF_6), led to errors in interpreting the radial distribution curves obtained by transforming the experimental intensity functions. For example, the peak corresponding to the U-F distance in UF_6 was found[54] to be split into two components, and hence UF_6 was thought to be slightly distorted from a regular octahedral structure. Two types of U-F bond were presumed to be present.

This splitting may easily be explained, however, if the cosine factor in 2.35 is a non-zero function of s , for in such a case the $\cos\Delta\eta_{jk} \cdot \sin sR_{jk}$ factor

behaves as the sum of two sine functions sin sR_1 and sine sR_2, where the difference between R_1 and R_2 is small.

At the present time complex scattering factors are used where necessary, and an important list of values has been given by Ibers and Hoerni.[12] An analytical expression for $\Delta\eta_{jk}$ has been given by Bonham and Ukaji.[14] Theoretical radial distribution functions, taking into account failure of the Born approximation, may be calculated by transforming theoretical molecular intensity curves by numerical integration.

For molecules having no atomic number difference greater than ten, the u values alone should be affected by assuming real scattering factors. In the present work only the Cl..H distance in perchloric acid failed to satisfy this condition, but as is shown in Chapter Ten this distance is exceedingly badly determined anyway. Accordingly expression 2.46 was adopted for the theoretical $I_m(s)$ function, and the cosine term was neglected.

The vibrational amplitudes obtained for the Cl-O, Cl-F and S-O distances were corrected using the formula suggested by Bonham and Ukaji[14]. This correction is discussed in Chapter Eight.

10. Conclusion

The equations discussed in previous sections give a quantitative explanation of the electron diffraction pattern. The oscillating component of the scattered intensity is shown to depend on the structure and internal motion of the gas molecule, and to be superimposed upon a smooth background function which depends, among other things, on the nature of the atoms present, and not on their spatial distribution or vibrational motion.

Although these equations are sufficiently exact to enable a great deal of information to be extracted from measured intensity data, the theory presented here is necessarily approximate.

For example, the independent atom treatment ignores the effects of chemical bonding on the distribution of electrons in the scattering molecule, and hence on the scattered intensity. These effects have, it is true, been shown to be small for the cases of H_2 and H_2^+, by Bonham and Iijima [18-20], but they are observable, particularly at low scattering angles, and should be compensated for by proper adjustment of the background function in this region. The independent atom approximation also makes no allowance for molecular inelastic scattering, multiple interatomic scattering,

or electron exchange, and again it is necessary to assume that these effects are small and may be allowed for by suitable choice of the background curve.

The vibrational effects considered in section five were restricted to those produced by harmonic (and slightly anharmonic) motion, and hence the equations presented in that section are limited in their applicability.

The gas sample has been assumed throughout to be infinitesimally small, but the effects of sample size are not insignificant, and have been shown by Kuchitsu[55], and Rundgren[56], to affect the accuracy of the u values obtained.

The electron beam has also been assumed ideal, that is, completely monochromatic and of extremely low density, and these conditions are probably fairly well satisfied in modern experimental work.

Despite the sources of error mentioned, the theory in its present simple form, has been very successful, and structural results obtained by applying it usually compare favourably with equivalent information produced by other physical methods (e.g. microwave spectroscopy).

CHAPTER THREE

A DESCRIPTION OF THE ELECTRON DIFFRACTION INSTRUMENT AND EXPERIMENTAL PROCEDURE

1. Introduction

In the structural investigations discussed in Chapters Nine to Fourteen, the scattered electron intensities were recorded using a modern commercial electron diffraction machine, built in Swizerland by Balzers of Zurich. This machine, known as the Balzers Eldigraph KD-G2[57], is described in some detail in the present chapter. A photograph of it is shown in plate 3.1, and a schematic diagram in figure 3.1.

Two microdensitometers, manufactured by Joyce-Loebl, and used to measure intensities recorded on photographic plates by the Eldigraph, are also described. A photograph of one of these, the more often used, and more convenient, automatic instrument, is shown in plate 3.2.

At various stages of the description, details of the experimental procedure followed in using the diffraction equipment, are also given.

THE BALZERS ELDIGRAPH KD G2

PLATE 3.1

THE BALZERS ELDIGRAPH

KD G2

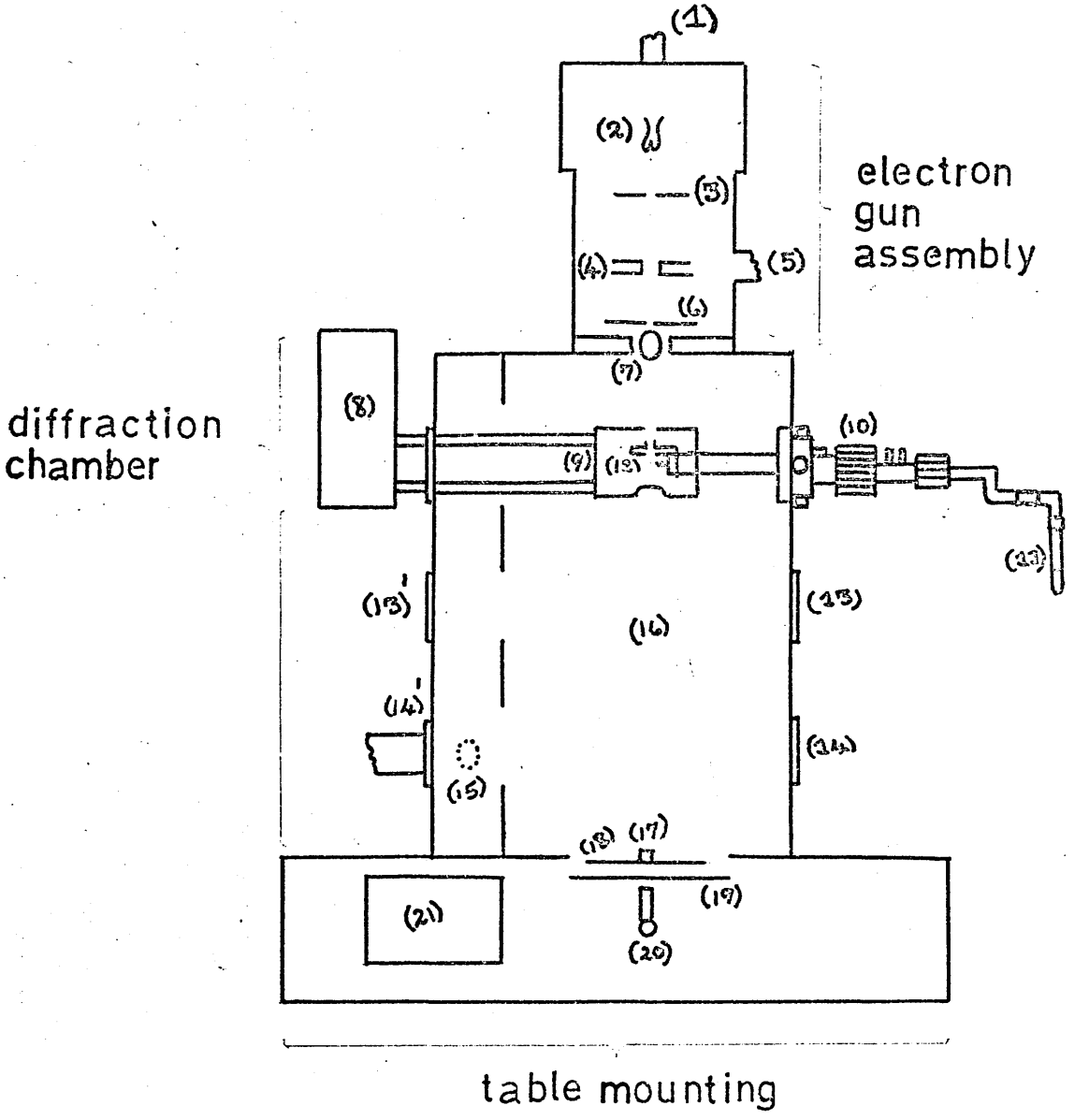

fig. 3.1

KEY

TO FIGURE 3.1

1. The high tension supply line.
2. The cathode.
3. The anode aperture.
4. The condenser lens.
5. The outlet to the electron gun vacuum pumping assembly.
6. The condenser aperture.
7. A ball valve separating the gun from the diffraction chamber.
8. A liquid nitrogen container connected to the cold trap.
9. The cold trap.
10. The nozzle assembly.
11. The sample tube.
12. The nozzle tip and attached collimeter.
13. The nozzle position for the twentyfive centimetre distance.
13.' The cold trap position for the twentyfive centimetre distance.
14. The nozzle position for the eleven centimetre distance.
14.' The cold trap position for the eleven centimetre distance.
15. The outlet to the diffraction chamber pumping assembly.
16. Scattered electrons.
17. The beam stop.
18. The rotating sector.
19. The photographic plate.
20. The microscope.
21. The photographic plate box.

THE JOYCE-LOEBL AUTOMATIC MICRODENSITOMETER

PLATE 3.2

2. A preliminary description of the Balzers Eldigraph

As may be seen from figure 3.1, the Balzers Eldigraph can be considered as consisting of two sections separated by a ball valve (7). The smaller one of these is the electron gun assembly, whilst the larger one comprises the diffraction chamber, the gas nozzle (10), the cold trap (9), the sector assembly (18), and the table which supports the machine, and contains the photographic plate box (21).

The diffraction chamber has a number of observation windows set into it, and these are fitted with shutters (visible in plate 3.1) so that light can be excluded when necessary.

A control consul, visible to the right of the apparatus in the photograph, is used to operate the vacuum pumping system and to produce and regulate the electron beam.

Other pieces of equipment, not shown in either the figure, or plate 3.1, are the transformer and stabiliser units required to provide the high tension voltage supply, and the digital voltmeter used to monitor it.

An hydraulic lifting device is also available, and is required to raise or lower the gun and diffraction chamber relative to the table.

3. The vacuum pumping system

Provision is made in the Balzers Eldigraph for separate pumping of the electron gun and the diffraction chamber, when the ball valve is closed. The gun is evacuated by means of a small rotary backing pump, and small oil diffusion pump, whilst a similar, but more powerful arrangement, is required for the larger volume of the diffraction chamber and the table. These pumps are situated behind the apparatus, as it is viewed in plate 3.1.

Gauges, located in the control consul, indicate the gas pressure at various points in the machine, and the best vacuum normally obtained in the diffraction chamber is approximately 5.10^{-5} mm of mercury.

4. Production of the electron beam

The high tension supply, required to accelerate the electrons, is normally adjusted to a value of approximately fifty thousand volts, and is highly stabilised (one part in ten thousand) to ensure that the wavelength of the beam (around 0.051 Å) does not fluctuate during experiments.

The electrons are generated by a heated filament, the cathode (2), charged to a high negative potential, and accelerate towards an anode (3), at zero potential.

A small metal cylinder, called the wehnelt, which is more negative than the cathode, is situated round the latter, and allows a rough, preliminary, focussing of the beam onto the anode. The potential difference between cathode and wehnelt may be varied, and in experiments it is usually set at an optimum value.

The accelerated electrons pass through an adjustable aperture in the anode, and are focussed into a narrow cylindrical beam by an electromagnetic condenser lens (4). The beam then passes through a variable aperture, the condenser aperture (6), and finally enters the diffraction chamber, if the ball valve is open. A further aperture of constant size called the gross aperture, is swung into position inside the diffraction chamber if either of the two shortest camera distances (see section five) are in operation.

The beam diameter normally used in diffraction work is in the order of 0.2mm, and is determined by the choice made of the aperture sizes.

Various centering devices are available on the outside of the gun, and these are used to ensure that the beam passes centrally through the apertures and lens described above. A fluorescent screen can

be swung into position above the sector, to enable the behaviour of the beam to be viewed, and the centering adjustments carried out.

An adjustment is also present on the gun, which enables the beam to be centred through the beam stop (17), situated at the axis of the sector. A microscope (20), and small fluorescent screen, situated below the beam stop, are necessary to achieve this latter centering process.

In the diffraction experiments described in this thesis, a beam current of between 80 and 120 μA was normally used. The beam voltage was always adjusted until a standard reading was obtained on a five window digital voltmeter, connected across a particular resistance in the high tension voltage supply unit. By monitoring the high tension voltage in this way, it was possible to work at a constant wavelength for a period of several days.

5. The nozzle assembly and cold trap

The gas nozzle is effectively a metal tube, with a specially designed platinum jet at one end, and an external connection to a glass sample tube (11) at the other. The flow of vapour through the jet, into the diffraction chamber, is regulated by a needle valve,

and the inlet tube is surrounded by a water jacket, through which hot water (up to about 90^{o} C) may be passed, if it is necessary to warm the incoming gas.

The Balzers Eldigraph allows four possible locations of the nozzle relative to the plate. Three of these, the one actually shown, and positions 13 and 14, are indicated in figure 3.1, and correspond to jet-to-plate distances of fifty, twentyfive and eleven centimetres, respectively. The fourth location, the hundred centimetre position, can be attained if an extra section is bolted between the gun and diffraction chamber. In plate 3.1 the nozzle position shown is the hundred centimetre one, and the extra section of diffraction chamber required may also be seen.

The jet-to-plate distances are calibrated before an experiment, by setting up standard measuring rods mounted in a tripod, inside the diffraction chamber. A vertical travel adjustment on the nozzle enables this calibration to be made, and the adjustment device is locked when the operation has been completed. The horizontal, radial, and in-out adjustment controls also available, are still variable, and are required at a later stage of the experiment to centre the nozzle and attached collimeter tube (12), relative to the

beam.

Two other items situated near the nozzle tip, and not shown in figure 3.1, are (a) a small thermocouple used to estimate the temperature of the gas jet, and (b) a holder containing a polycrystalline solid specimen. This holder may be swung into the line of the beam, instead of the collimeter, and an electron diffraction powder photograph obtained, showing a series of sharp, concentric rings. This pattern is always recorded during diffraction experiments, and is used to measure the wavelength of the beam. In the present work thallium chloride was the substance used for this purpose.

When diffraction is in progress, and a vapour sample continuously enters the diffraction chamber, it is necessary to remove the gas immediately after scattering has taken place. This is achieved by condensing the sample on a liquid nitrogen cooled surface. The device used is called the cold trap (9) and it surrounds the nozzle in the manner indicated in figure 3.1. The liquid nitrogen required to cool it, is placed in the insulated can (8). The trap is supported by a ledge (not shown in fig. 3.1), attached to the nozzle, and it has holes of a suitable size cut out of its top and bottom, to permit the

THE SECTOR

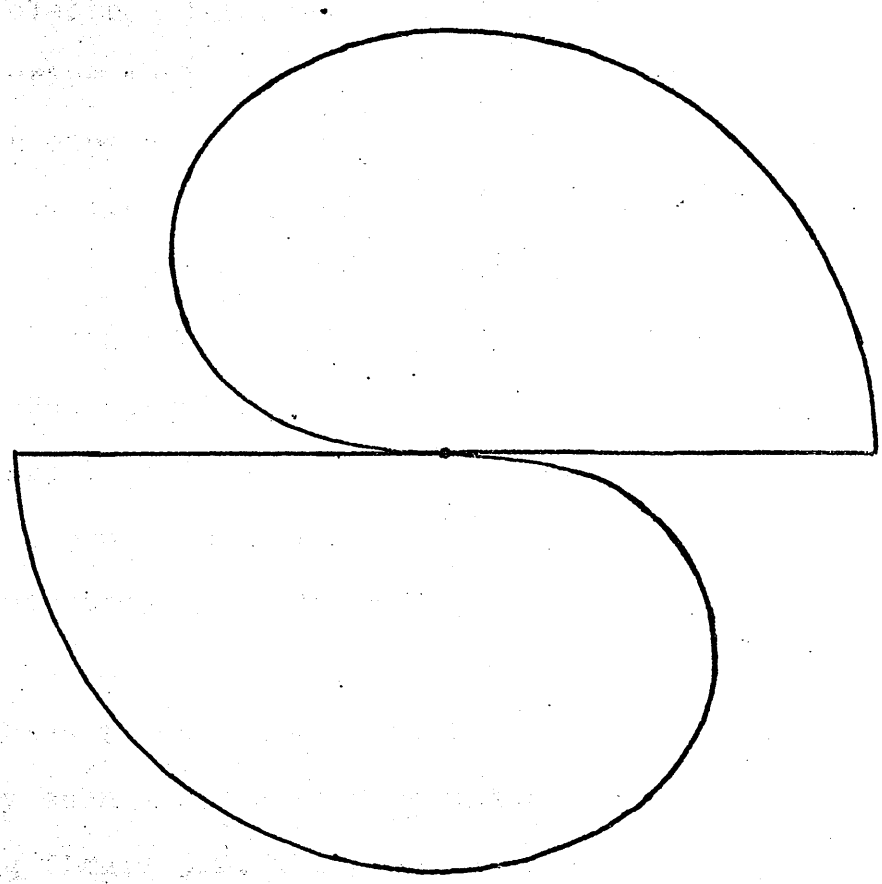

fig. 3.2

incident beam and scattered electrons to pass through unimpeded.

6. The sector assembly

The expression for I(s) given by equation 2.40 of Chapter Two, contains an s^{-4} factor, and hence the scattered electron intensity should fall off rapidly with scattering angle. The earliest electron diffraction experiments confirmed this, and the photographic plates obtained showed large gradients in blackness along the radius of the diffraction pattern. Furthermore, microdensitometer traces of these patterns showed little sign of the diffraction rings so important in determining molecular structure.

To overcome these difficulties Debye[2], and Finbak[3], suggested in the late 1930's, that a flat, specially cut, metal sector should be rotated a small distance above the photographic plate. The effect produced by such a device may be understood by considering figure 3.2, which shows the general shape of the sector used in the present work. Because of the continuously increasing angle of opening, from the centre to the edge, the sector multiplies the intensity predicted by 2.40, by a function of s, which is such that the recorded pattern shows a much smaller

radial variation in optical density. The diffraction rings are clearly visible, both on the plate and on the microdensitometer traces. These latter are less steep than the old ones, and enable the oscillating component of the scattered intensity, to be much more accurately measured than was previously possible.

The sector geometry must of course be accurately known if the measured intensities are to be compared with theory, and this is normally determined by examining the sector with a travelling microscope.

At the time when the present work was carried out, the Balzers Eldigraph was equipped with two distinct sectors, one suitable for the hundred and fifty centimetre distances, and the other for the remaining two . Two speeds of sector rotation are also available, these being eight hundred and four hundred revolutions per minute respectively.

7. Introduction of the sample

When the beam has been produced, and satisfactorily centred through the apertures, lens, cold trap, collimeter and beam stop, and the cold trap is at a suitably low temperature, it is possible to introduce the vapour sample into the apparatus.

Before this is done, however, the ball valve is closed to isolate the electron gun from the main chamber. A sample tube is attached to the end of the nozzle assembly as shown in figure 3.1 and plate 3.1, and is surrounded by a cooling bath to reduce the sample vapour pressure to a negligibly small value. When this has been achieved the needle valve is opened. A pressure gauge on the panel of the control consul immediately registers a pressure increase in the diffraction chamber, as air from the sample tube, and dissolved gases in the sample, are pumped off. When these have been removed, the sample is heated to a suitable temperature (the vapour pressure should be roughly fifty millimetres of mercury in diffraction experiments), and the vapour is allowed to flow through the nozzle and to condense out continuously on the cold trap surface.

When the pressure in the main chamber has fallen to about 5.10^{-5} mm Hg , the ball valve is opened to allow entry of the electron beam, and a diffraction pattern should be observed on the larger fluorescent screen, if this is in position above the sector.

Visual examination of this pattern enables adjustments to be made to the beam current, sample temperature, centering etc., until a satisfactory

diffraction pattern is obtained on the screen.

8. The photographic procedure

Before the apparatus is pumped down, that is right at the start of an experiment, a lightproof plate box, containing six to twelve rectangular photographic plates, of size 13cm by 18cm, mounted in metal frames, is loaded into the lower part of the table. This box is divided into two sections, one for unexposed, and the other for exposed plates. When it is in position, the apparatus is pumped down, and beam production and centering carried out as has already been described.

When the stage described at the end of the previous section is reached, and a good pattern is observed on the screen, this latter is swung out of the line of the scattered electrons, and all observation windows shuttered. A plate is withdrawn from the plate box by rotating the plate carrier control on the outside of the table. At this stage it is still possible to check that the beam passes centrally through the beam stop, and this is done by looking through the microscope (20). If the beam is central, the microscope is fitted with a cap to prevent light admission, and an electrostatic exposure shutter in the electron gun

is switched on, to prevent the beam from passing into the diffraction chamber. The plate is then wound into position beneath the sector, and the sector allowed to rotate. An exposure timer on the control consul is set to a suitable value, and the exposure shutter opened. At various instants during the exposure the beam voltage is checked by examining the reading on the digital voltmeter, and small corrections made if necessary. After exposure the sector is stopped, and the plate wound back and deposited in the plate box. The whole procedure may then be repeated for a second plate and so on. After a complete run the vapour supply is cut off, and the ball valve closed. The apparatus is allowed to fill up with dry nitrogen, and the plate box removed to the darkroom.

The exposure times required for plates taken during the present work were found to vary from compound to compound, but as a general rule, the order of decreasing time was that of increasing jet-to-plate distance. Typical values were thirty seconds for the hundred centimetre distance, one minute for the fifty, three to four minutes for the twentyfive, and perhaps ten minutes or longer for the eleven centimetre distance. These values, however, depend

THE ELECTRON DIFFRACTION PATTERN

FOR $FClO_3$ AT FIFTY CM

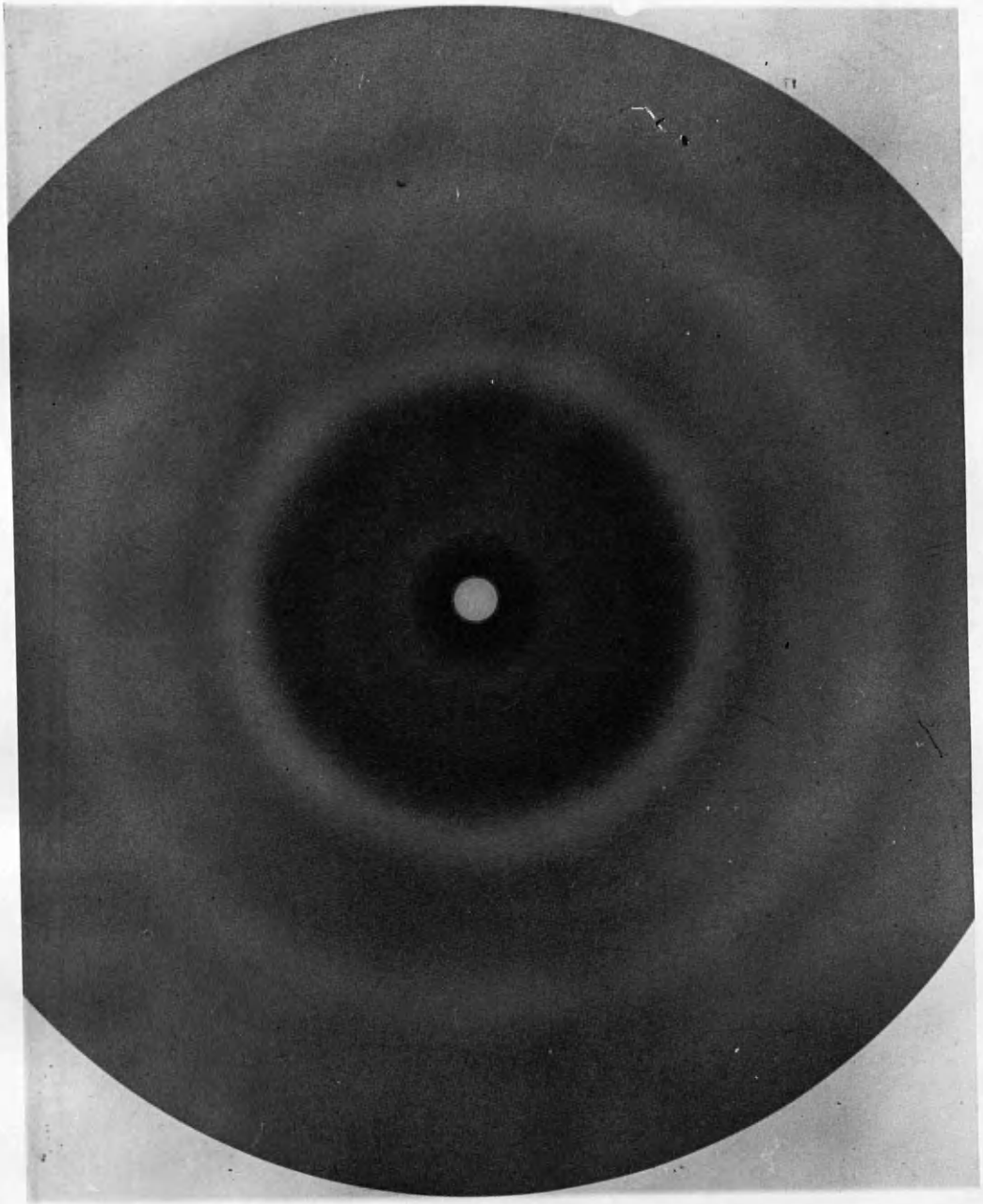

PLATE 3.3

THE ELECTRON DIFFRACTION PATTERN

FOR $FClO_3$ AT TWENTYFIVE CM

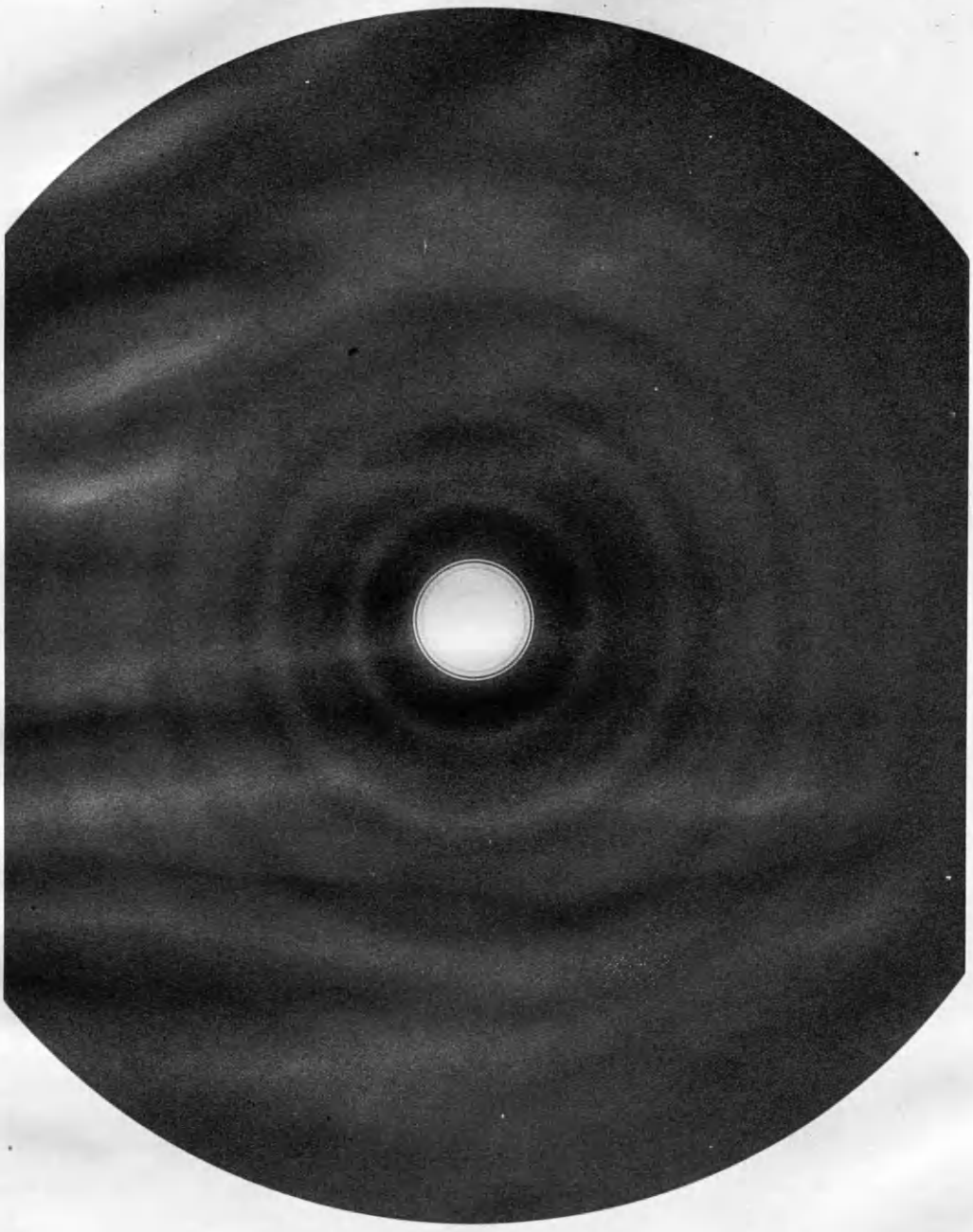

PLATE 3.4

Note: The uneven blackness visible in certain regions of the above print, and not forming part of the diffraction pattern itself, was not a property of the actual photographic plate.

not only on the compound studied, but also on the type of plate used and the beam current. The figures quoted above are for chlorine containing molecules, Ilford N60 plates, and a beam current of roughly 100μ A.

The photographic plates were developed using the standard techniques of developing, stopping, and fixing, a suitable safety lamp being employed. After fixing the plates were washed for half an hour in running water, then allowed to dry.

The backs of the dry plates were then cleaned using distilled water and sometimes acetone, to remove any remaining backing material, and polished using tissues. The emulsion surface was never touched by hand or tissue.

Photographs of plates taken at fifty and twentyfive centimetres for perchloryl fluoride ($FClO_3$), are shown in plates 3.3 and 3.4.

9. Microdensitometry

During the course of the experimental work discussed in this thesis, two types of microdensitometer were available. Most of the results quoted in Chapters Nine to Fourteen were obtained using the second of these instruments, the automatic microdensitometer

shown in plate 3.2. The principles underlying the operation of these pieces of equipment may be summarised as follows.

A source of light is split by prisms into two identical beams. One of these is passed through a small area on the photographic plate studied, whilst the other beam passes through an optical wedge. This latter is a rectangular glass plate, blackened in such a way that it presents a continuous gradient of optical density along its length. The two transmitted beams are compared, and if an inequality of intensity is observed, the optical wedge moves lengthwise until a balance is achieved.

In the case of the pen trace microdensitometer (the manual instrument), the first beam scans slowly across a diameter of the electron diffraction pattern, and the resulting wedge movement causes a pen to trace out a curve (usually a little ' noisy ') on graph paper. This plot can be converted to an optical density trace if suitable wedge calibration data are used to correct the original graph. A zero base line is also output in experiments of this kind, and is traced out when the beam passes continuously through a clear glass region of the plate.

The automatic microdensitometer operates a little

differently. In this case the beam no longer scans across the plate continuously, but moves in a stepwise fashion from point to point along a diameter of the pattern. This movement is controlled by a carefully manufactured leadscrew, and in the present work the scan interval chosen was as near to 0.2 mm as the accuracy of the instrument would allow.

At each point on the plate, the compensating position taken up by the optical wedge, is recorded by a potentiometer, and a three figure number punched out on paper tape, in a code suitable for the computer. This punch is shown nearest the camera in plate 3.2. A zero base line value, defined as before, is also punched out.

Both microdensitometers allow accurate centering of the pattern relative to the light beam, and this operation must be carefully carried out to ensure that the beam scans along the pattern diameter, to a sufficient degree of precision. In the present work 750 readings were recorded during each scan of the automatic microdensitometer.

The graphs produced by the manual instrument were treated as follows. The curve and base line recorded were traced onto transparent paper, some hand-smoothing being applied simultaneously. The ordinates of the resulting plot were then read off visually, by placing

the tracing paper on top of graph paper, and taking readings at millimetre intervals along the base line. About 750 readings were again obtained, as the ratio arm on the manual instrument, relating the movement of the graph paper to that of the photographic plate, produces almost exactly, a fivefold magnification of the trace when recorded on graph paper. Hence one millimetre on the baseline corresponds to very nearly 0.2 mm on the plate.

Comparison of the traces obtained by the two microdensitometers, showed that the automatic one produces a far more ragged curve than the manual one. This is only to be expected, however, as hand-smoothing was applied in the manual microdensitometer procedure. The automatic instrument must be assumed, from the nature of its operation, to produce data points which are much less correlated than those finally obtained by the tracing and reading-off methods.

Since the automatic data curves are fed into the computer directly, without any smoothing being applied, a larger number of traces must be averaged if smooth uphill and molecular intensity curves are finally to be obtained. This remark is particularly true if the data concerned, have been recorded at the shortest two camera distances, as such data are always poorer

in quality, owing to a low signal to noise ratio.

In conclusion, it may be said that the manual method is time-consuming and tedious to apply, and almost certainly is subject to greater errors than the procedure followed when using the automatic instrument. This latter microdensitometer produces results extremely quickly, on paper tape, and it is very easy to record a large number of traces at each camera distance. One improvement which might be made to this instrument would be to allow the plates to rotate slowly about the centre of the pattern during scanning, as this should improve the quality of each trace.

10. Wavelength determination

Diffraction by a polycrystalline sample has already been discussed in section five. In the present work a powder photograph taken using TlCl as diffracting material, was used to determine the wavelength of the electron beam.

Ring diameters on the pattern were measured using a travelling microscope, or the automatic microdensitometer operating at a very small scan interval. About twelve different rings were usually measured, and often each final accepted value was an

average of several readings taken from more than one plate recording.

Each diameter was used to give a separate estimate of the wavelength, and finally an average of these results was taken, and a standard deviation calculated. The value assumed for the cell dimension of the cubic thallium chloride crystal was obtained from the literature[58], and the calculations described were carried out on the computer using the theory applicable to X-ray powder patterns.

A typical result for the wavelength was,

$$\lambda = 0.05116 \pm 0.00002 \text{ Å}.$$

Wherever possible the solid sample pattern was recorded at the hundred centimetre camera distance, as in this case the rings usually measured are well spaced out on the plate and hence their diameters can be estimated with the minimum error.

CHAPTER FOUR

THE ELECTRON DIFFRACTION DATA PROCESSING ROUTINE

1. Introduction

This chapter outlines the computational methods which were employed to extract R_{ij} and u_{ij} parameters for the molecules studied, from microdensitometer trace readings. The computer programmes required to carry out the necessary calculations have already been described by Beagley et al.,[59] and the sections below merely enlarge upon this description.

2. Conversion of the trace readings to optical density values

The 'three in one' computer programme required calibration data for the optical wedges used, to carry out its function of converting microdensitometer readings to optical densities. A typical example of the kind of corrected trace output by this programme, is shown in figure 4.1 for dichlorine monoxide photographed at a jet-to-plate distance of fifty centimetres. The automatic microdensitometer was used to produce this set of readings, and some hand-smoothing has been applied for presentation purposes.

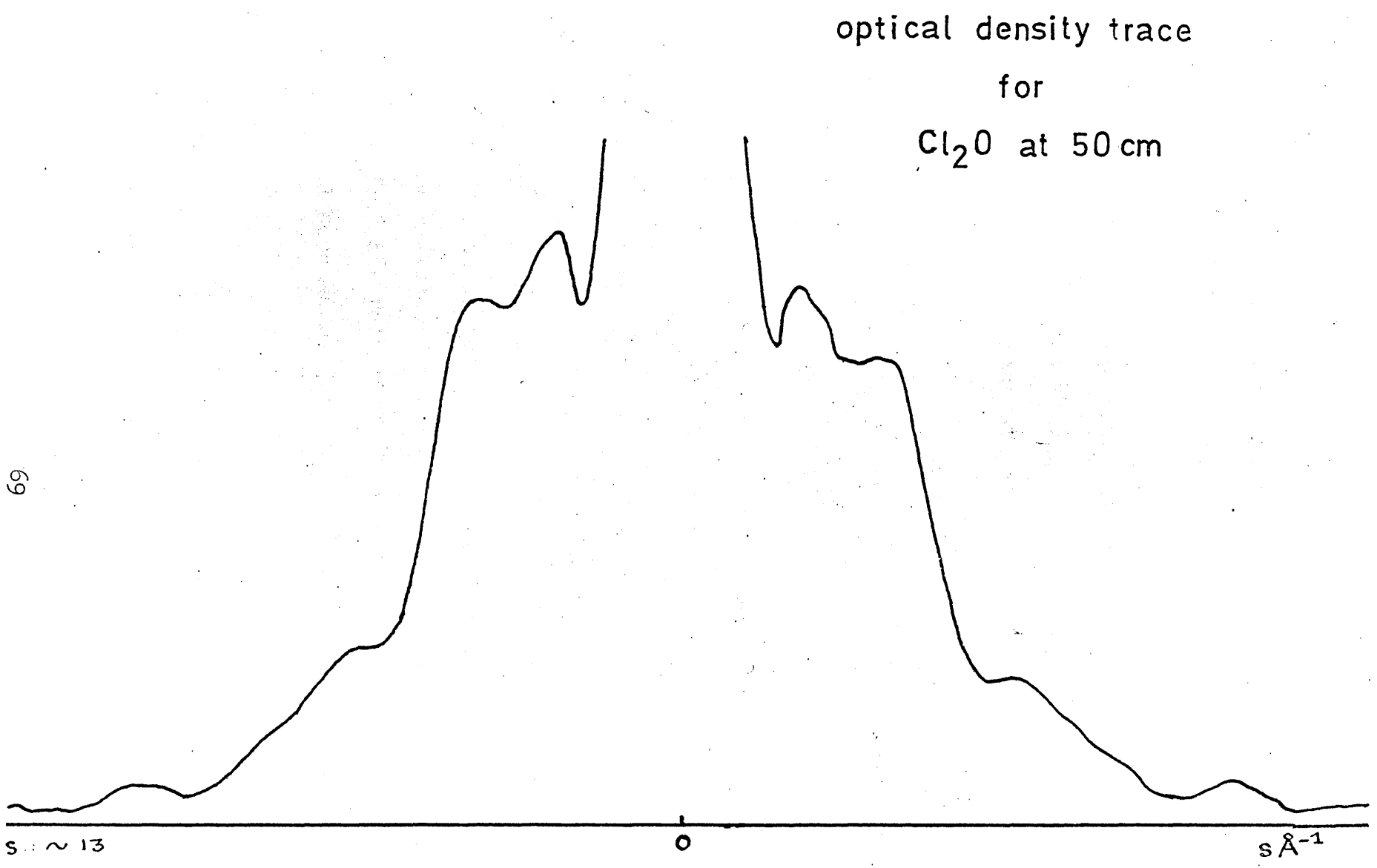

fig. 4.1

3. Calculation of the position of the trace centre

Ideally, the trace shown in figure 4.1 should be symmetrical about the point marked 0. The position of this centre may be defined as the number of data point intervals from the beginning of the trace to 0. In the present work this quantity was determined by finding the positions of pairs of symmetrically equivalent features, such as ring maxima and minima, and the edges of the central hole in the pattern caused by the beam stop. Both a manual and a computer procedure were adopted to do this, and the calculated error on the value produced (~ 375), varied between 0.5 and 0.9 of a unit.

4. Calculation of the s scale

The function of the s scale programme was to assign s values, at equal intervals, to points on the optical density curve. The information required to do this included the beam wavelength, the jet-to-plate distance, the radius of the central part of the pattern, omitted because of the beam stop, the position of the trace centre, and finally the microdensitometer scan interval (0.2 mm).

Using this information, the programme first calculated Δs, the interval in s corresponding to a

0.2 mm step on the plate. The radius of the omitted section was then used to find smin, the lower s limit, whilst smax, the upper limit, was determined by counting the number of data point intervals from the trace centre to the nearer of the two outermost intensity readings.

The range in s between smin and smax was divided into a number of Δs segments, and the intensity values corresponding to s = smin + n. Δs, where s was less than or equal to smax, and n took on the integer values, 0,1,2, etc., were calculated by interpolating the original optical density data. Two values were obtained for each s, as there are two symmetrically equivalent points on either side of the trace centre. These intensities were output in corresponding pairs.

5. The blackness, planar plate, and sector corrections

The corrections programme first averaged the two equivalent sets of readings output by the s scale procedure, and then modified these results to take into account nonlinear response of the photographic plate to incident electron intensity. The blackness correction factors necessary to do this, were determined experimentally for the N60 Ilford plates employed, and were fed into the computer. Each

trace optical density value was then multiplied by a correction factor interpolated from this input set of numbers.

The next step was to convert the intensity data to corresponding spherical plate values by dividing each reading by $\cos^3\theta$, as described in Chapter Two, section six.

The following correction allowed for the effects produced by the rotating sector. The function $\alpha(s)$, determined by the sector geometry, was calculated for each s, and the data points divided by it to convert them to unsectored values.

Finally, the uphill curve discussed in section six of Chapter Two, was formed by multiplying the intensities by s^4. It was then output as a series of numbers, running from smin to smax, in Δs intervals.

6. Combination of a set of uphill curves obtained for a particular jet-to-plate distance

In most experiments a number of microdensitometer traces were processed for each jet-to-plate distance. The resulting uphill curves were averaged to form a single set of readings, by the computer programme 'combination one', and this combined uphill curve output.

The uphill curve and final background

for $FClO_3$ at 100 cm

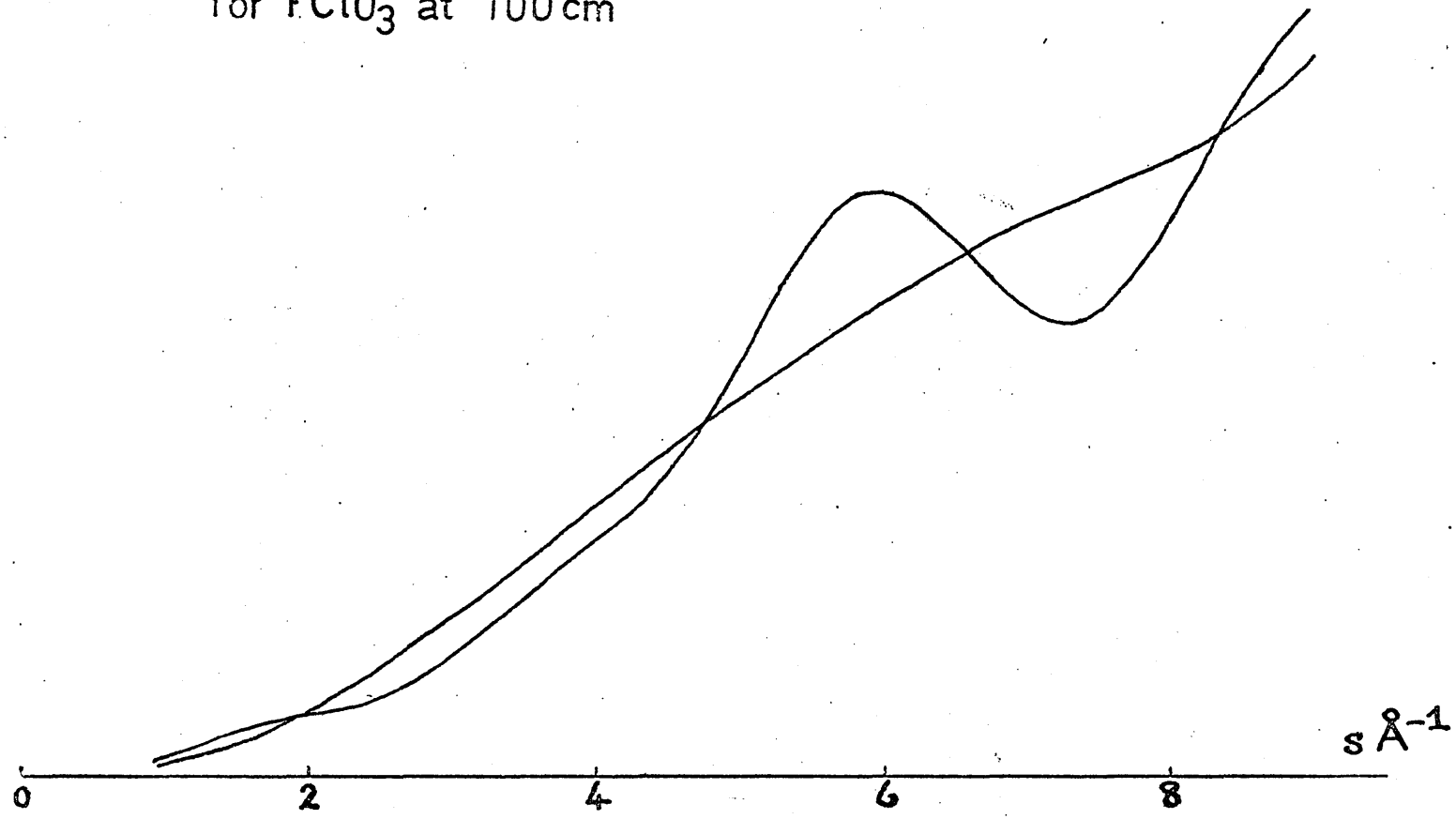

fig. 4.2

fig. 4.3

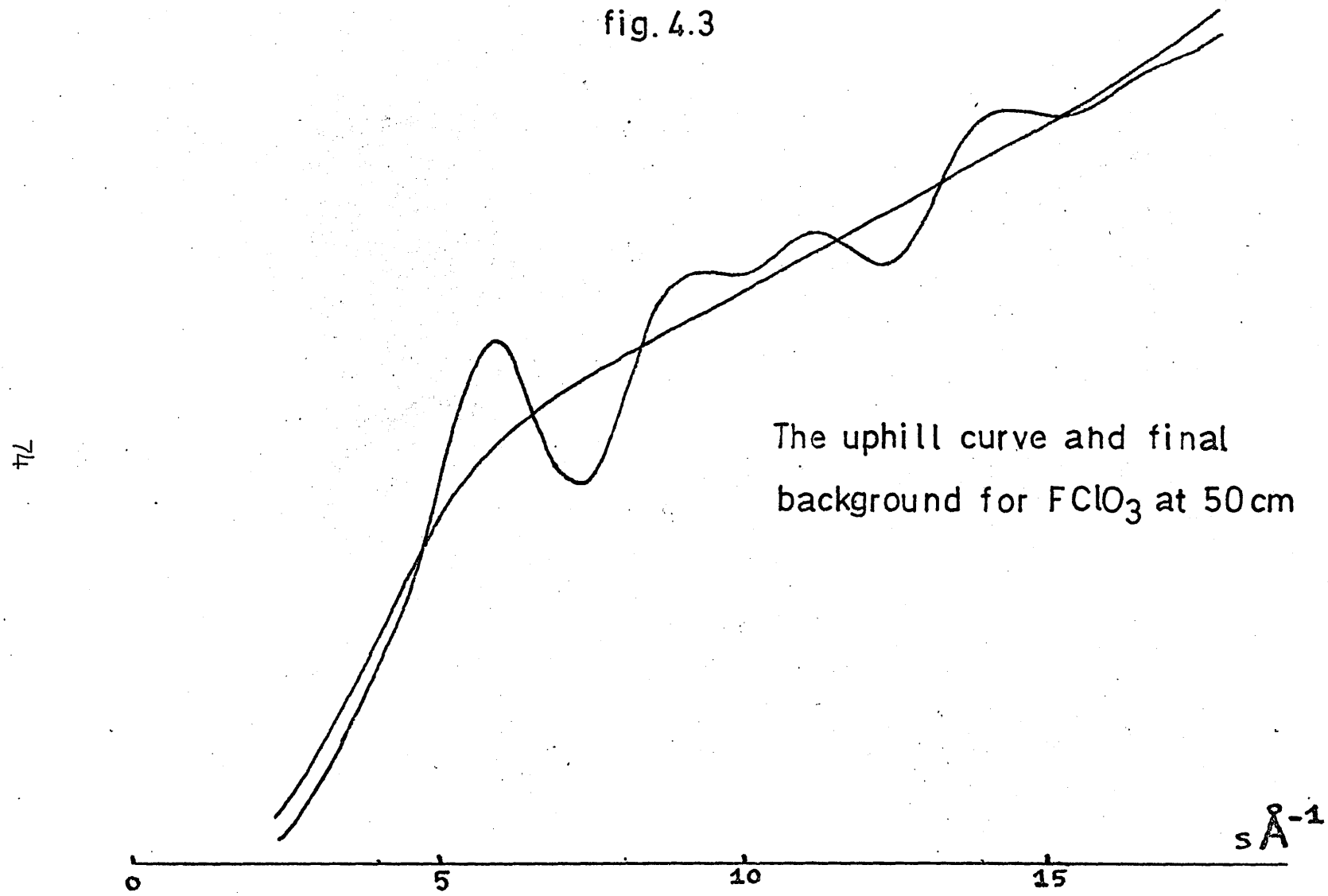
The uphill curve and final background for $FClO_3$ at 50 cm
sÅ^{-1}
0
5
10
15

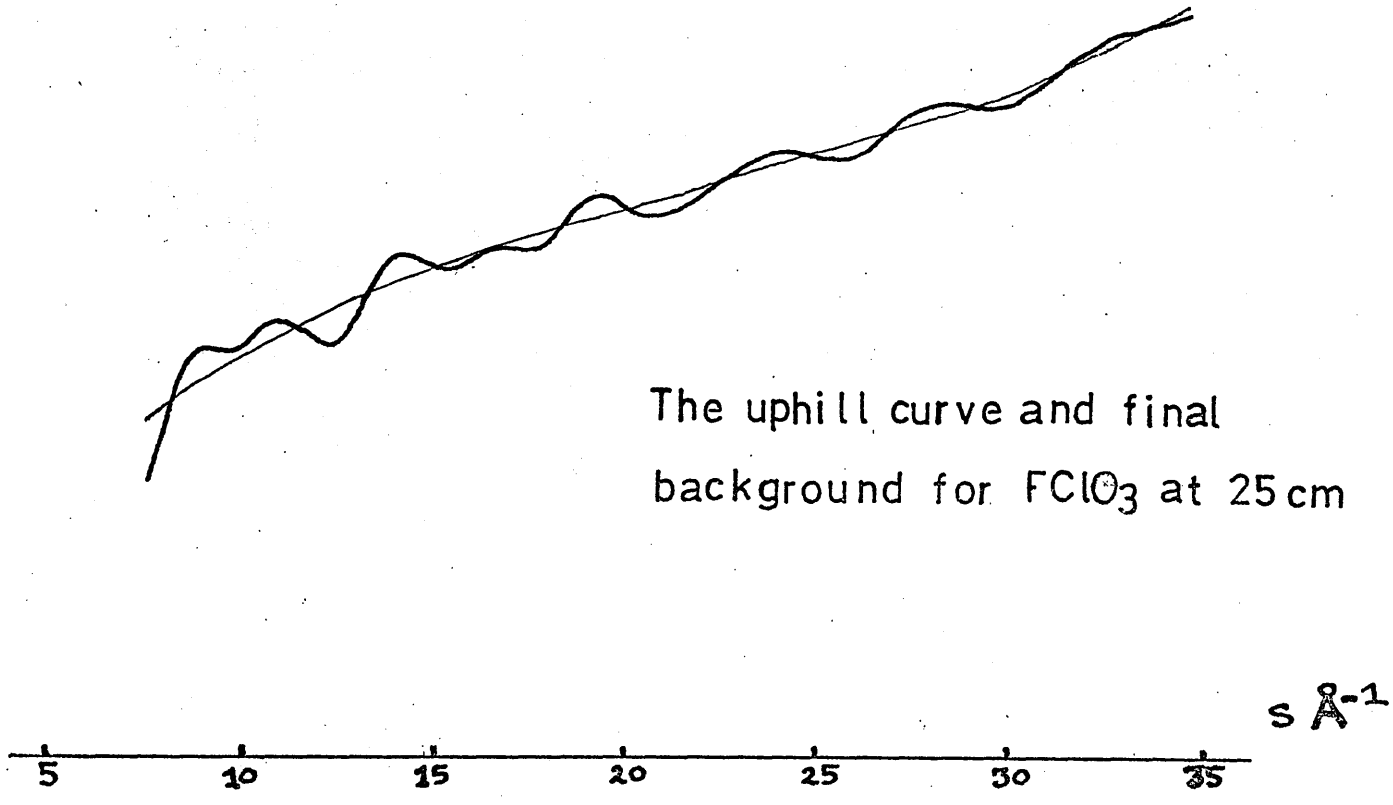

The uphill curve and final background for $FClO_3$ at 25 cm

fig. 4.4

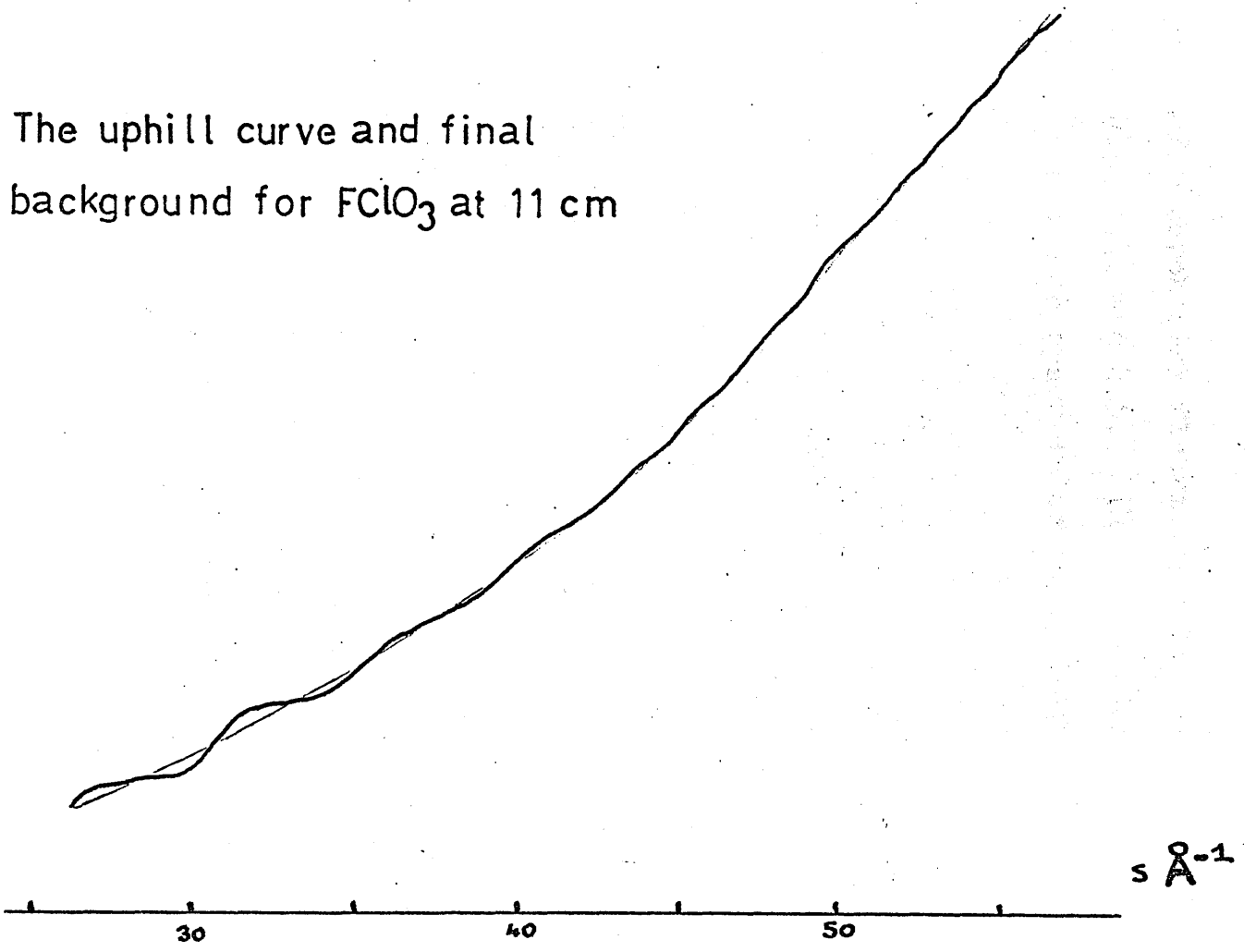
The uphill curve and final
background for $FClO_3$ at 11 cm
s Å^{-1}
30
40
50

fig. 4.5

In thorough investigations, combined uphill curves were obtained for at least the first three of the four available jet-to-plate distances. A complete set of four combined uphill curves is given for perchloryl fluoride ($FClO_3$) in figures 4.2, 4.3, 4.4, and 4.5. The final background curves adopted are also drawn in on these diagrams.

7. The first background

The nature of the background function, and its relationship to the uphill curve, have been discussed in section six of Chapter Two. In the present work the first background curve adopted, was drawn by computer, in a purely empirical way, through the combined uphill curve. It was constrained to be a smooth steadily increasing function of s, and was constructed by drastically smoothing the set of data output by 'combination one'. In the case of hundred centimetre data, the computer background had to be further hand-smoothed, in the low s region, as it failed to curve round sufficiently sharply to pass through the s equals zero point.

The background curve so produced, was subtracted from the uphill curve and an $I_{mol}(s)$ curve output.

8. Modification of the $I_{mol}(s)$ curve

The $I_m(s)$ function, convenient for Fourier transformation and least squares refinement, was produced from the previously output $I_{mol}(s)$ curve, by the procedure described in section six of Chapter Two. The sets of X-ray scattering factors required for this, were taken from reference (60), and were interpolated for each s value. The modified $I_m(s)$ function (theoretical form 2.46) was then output.

9. Combination of $I_m(s)$ functions calculated for more than one jet-to-plate distance

Each combined uphill curve obtained, was treated as described in sections seven and eight, and a corresponding $I_m(s)$ function produced. The $I_m(s)$ curves obtained in this way, for the four jet-to-plate distances, normally had the following s limits and Δs intervals,

distance(cm)	smin($\AA^{-1}$)	smax($\AA^{-1}$)	Δs($\AA^{-1}$)
100	0.8	9.0	0.02
50	2.4	18.0	0.05
25	7.6	36.0	0.10
11	22.0	~ 40.0	0.22

Before Fourier transformation or complete least squares refinement were carried out, however, these

curves had to be put on the same scale, and combined into a single set of data, running from the lowest s limit measured, to an upper limit, determined by the quality of the data obtained, in intervals of s which varied discontinuously in the manner indicated by the following typical set of s limits and Δ s intervals.

data set	smin($\mathring{A}^{-1}$)	smax($\mathring{A}^{-1}$)	Δ s($\mathring{A}^{-1}$)
1	0.8	9.0	0.02
2	9.05	18.0	0.05
3	18.10	36.0	0.10
4	36.22	~ 40.0	0.22

This combined molecular intensity curve was computed from the single distance $I_m(s)$ data, by a programme called 'combination two'. The method used was as follows. The first two single distance curves were compared in the s region where they overlapped, and the set which had the larger Δ s interval was interpolated to give data points showing a one to one correspondence with those of the first curve. A standard technique was then used to scale the second curve to the first. The resulting corresponding pairs of data points in the overlap region were fused into a single set by finding a weighted average for each pair. The resulting values were then output along with the remaining readings

belonging to the first trace. This process was repeated for the second overlap region, using the scaled second trace produced as described above, and the third single distance $I_m(s)$ curve, and then for the third region if eleven centimetre data were available.

In this way four curves, all on the same scale, and having the s limits and s intervals shown in the second table above, were produced. The three connecting scale factors were also output by the programme as these were required at the background adjustment stage described in section twelve.

10. Fourier transformation

The combined $I_m(s)$ function was Fourier transformed by calculating the integral,

$$\int_{smin}^{smax} I_m(s) . e^{-ks^2} \sin(sR)\, ds$$

for a series of equally spaced R values running from 0 to some suitable upper limit. The approximate method of adding strips was used to do this, and the damping constant k was normally assigned a value between 0.001 and 0.005 Å^2, the exact value depending on the upper s limit of the data transformed. The resulting $\sigma'(R)/R$ function was plotted on graph paper and interpreted in terms of the molecule studied.

11. Least squares refinement

Very often the Fourier transformation described in section ten, produces a plot which gives a good indication of the structure of the molecule studied. It is sometimes possible to use this $\sigma'(R)/R$ function to estimate the principal bond lengths and valence angles present, and to propose a reasonable starting model on which to base a least squares refinement.

In the present work, the method of iterative least squares refinement[61] was applied to the problem of fitting an expression of type 2.46 of Chapter Two to the experimental combined $I_m(s)$ curve.

The A_{ij} factors appearing in equation 2.46 were defined for the model chosen, by classifying the interatomic distances present into equivalent and nonequivalent types, molecular symmetry being used to do this. The least squares programme calculated these A_{ij}'s as functions of s, by interpolating input sets of X-ray scattering factors.

Both R_{ij} and u_{ij} parameters, and an overall scale factor were refineable, and provision was made in the programme to keep any number of these variables constant, whilst the remainder were refined alone.

For most molecules the nonequivalent distance types present, that is the R_{ij}'s of 2.46, do not form

an independent set of variables, and certain of them have to be expressed as functions of a chosen subset of independent values. In the present work, when this occurred, only the independent R_{ij}'s were refined by the least squares method, and the remaining distances were calculated after each cycle, by a specially written subroutine. This latter had to be varied for each new molecule studied, and in addition to finding dependent distances, it calculated partial derivatives of the type, $\partial R_{dependent} / \partial R_{independent}$, these being required for correct application of the least squares method. In the present work the u_{ij} values were always treated as independent quantities, and hence there were no similar problems relating to them.

The least squares programme minimised the function,

$$\sum_{all\,data} w_i \cdot \Delta_i^2 = \sum w_i \cdot (I_i^{obs.} - I_i^{calc.})^2,$$

where w_i is a weight factor and was allowed to vary with s in an almost trapezoidal manner. The analytical form adopted for this function is presented in Chapter Eight.

When convergence was reached, the final cycle of refinement ended by outputting zero shifts for the

parameters varied, and corresponding estimated standard deviations. In addition, the quantity,

$$R = \sum_i |\Delta_i| \Big/ \sum_i |I_i^{obs}|,$$

called the residual, was also output, and was used to estimate the quality of the fit obtained for the particular model adopted.

In the case of refinements involving $I_m(s)$ data corresponding to a first empirical background curve, the u_{ij} quantities were normally held constant at estimated values, and the well determined independent distances and the overall scale factor refined alone. The resulting parameters output after completion of this first refinement, were then used to improve the background as described in the next section. After this it was possible to undertake more complete rèfinements.

At the empirical background stage, it was common to obtain an R value of around forty percent, but after background adjustment, this value usually fell, and in final refinements it was found to lie between twelve and fifteen percent.

The R_{ij} parameters output were quoted as $r_g(1)$ distances, and a correction was applied to certain of the mean amplitudes to take into account failure of

the Born approximation. This correction[14] has already been mentioned in Chapter Two section ten, and will be discussed again in more detail in Chapter Eight.

12. The background adjustment procedure

The background curve was often reassessed after least squares refinement, by using the R_{ij} and u_{ij} parameters and the scale factors available.

The programme 'adjust background' used these pieces of information to calculate a theoretical $I_{mol}(s)$ curve, on the same scale as each uphill curve, and for the same s values. Subtraction of this from the uphill data* produced an unsmooth curve which was then subjected to a smoothing procedure and an improved background produced. In the present work the last background adjustment performed involved handsmoothing at this stage to obtain the best possible result.

$I_m(s)$ functions were calculated as before using the new background functions obtained, and the process of recombination repeated. This was followed by Fourier transformation and least squares refinement of the combined $I_m(s)$ function as before.

If the background was indeed an improved one

* i.e. from the uphill curve corresponding to it.

this was reflected in the lower residual and lower estimated standard deviations output by the least squares refinement, and in the reduction of the ' noise level ' of the Fourier transform.

The whole cycle of operations was repeated until no further improvement was achieved, and the R_{ij}'s, u_{ij}'s, and scales, all reached steady values. At this stage if the residual and standard deviations were reasonable, the structure determination was assumed to be complete, and errors were estimated on the independent R_{ij}'s using the formula,

$$\text{reproducibility} = \sqrt{(3\sigma)^2 + (R_{ij}/2000)^2}$$

The second term in the root sign is intended to take into account sources of systematic error. The first term is three times the standard deviation (σ).

The reproducibilities of the dependent R_{ij}'s, and of angles, were calculated using the conventional methods for combining errors.

The systematic error appropriate to the u_{ij} values, is difficult to assess because of the large number of factors (see Chapter Fifteen) which affect amplitudes, and in the present work the reproducibility for these was always calculated as three standard deviations.

CHAPTER FIVE

CALCULATION OF ROOT MEAN SQUARE AMPLITUDES OF VIBRATION FROM SPECTROSCOPIC DATA

1. Introduction

The purpose of the present chapter is to provide a theoretical background to the force constant and root mean square amplitude calculations presented in Chapters Six to Eight.

The theory given below is applicable to harmonic vibration only, and has been merely outlined, as detailed discussions of the vibrational problem are already available in the textbook[62] by Wilson, Decius and Cross, the monograph[27] by Cyvin, the papers[63-65] by Morino et al., and in a review article[48] by Rambidi, Spiridonov and Alekseev.

2. An outline of the quantum mechanical and classical mechanical approaches to molecular vibration

In a quantum mechanical approach to the molecular vibration problem, it is necessary to make the Born Oppenheimer assumption, and to regard the overall molecular wave function as separable into two factors,

one describing the electronic motion, and the other the nuclear motion. It is also necessary to make the further assumption that the nuclear wave function may be similarly factored, and written as a product of three terms $\psi_{TRANS.}$, $\psi_{ROT.}$, and $\psi_{VIB.}$, corresponding respectively to translational, rotational, and vibrational motions. In this approximation, the vibrational problem reduces to calculating the wave functions ψ_{VIB} alone, and the corresponding energy levels E_{vib}. If these are known, then the observed infrared and Raman vibrational spectra may be predicted, and the root mean square amplitudes of vibration calculated.

In the case of molecules for which the assumptions outlined above are reasonably valid, the procedure of calculating the vibrational wave functions is as follows. A classical approach to the problem is first made, and the results of this treatment are used to write down a Schrodinger equation for the corresponding quantum mechanical problem. This equation is then solved for the ψ_{VIB} and E_{vib} quantities.

From the classical point of view the molecule may be assumed to be equivalent to a collection of point masses, held in an equilibrium configuration by certain restoring forces. A total of 3N-6 coordinates

are needed to describe the vibrational motion if the number of atoms in the molecule equals N. This is true as six constraints must be assumed to ensure that the centre of mass of the system remains at rest, and that there is no possibility of rotation. In an initial approach, a set of Cartesian mass-weighted displacement coordinates (see ref. 62 page 14) may be adopted, and if the assumption is made that all atomic displacements from equilibrium are minute, the kinetic and potential energies of the system may then be written as quadratic forms (see next section), in terms of this coordinate set. Application of Lagrange's equations of motion [66] to the problem, leads to the conclusion that the most general solution to the vibrational equations, may be written as a linear combination of certain particular solutions, called normal modes of vibration. These modes have the physical significance, that they are motions in which the atoms oscillate about their equilibrium positions with simple harmonic motion, all moving in phase, with the same frequency, but with amplitudes which vary from atom to atom in the molecule. Each mode is thus characterised by a certain frequency (ν), and the Lagrangian treatment leads to a secular equation, which defines the values which these so-called fundamental

frequencies of vibration may take on, for any particular set of masses, and restoring forces. The theory predicts that these frequencies are just the eigenvalues[67] of a certain matrix of order 3N-6. The corresponding eigenvectors[67] of this matrix determine the amplitudes of oscillation, and hence the actual physical forms of the normal modes.

The Cartesian treatment outlined above is unsatisfactory in one respect. The force constants involved in the quadratic potential energy expression have no chemical significance, and are not those discussed in chemical literature. To overcome this difficulty, it is necessary to make a linear transformation of coordinates to a set of 3N-6 independent internal displacement values, which are changes in interatomic distances (usually bonded distances) and valence angles. The force constants appearing in the new potential energy expression in terms of these coordinates, are once again the elements of a matrix $\underline{f}$, but the diagonal elements of this matrix are the familiar force constants used to characterise the strength of chemical bonds.

One major disadvantage of the new treatment, however, is that the kinetic energy expression appropriate to the internal displacement coordinates

loses its previous simplicity, and involves a matrix g whose elements g_{ij} are complicated functions of the molecular geometry and atomic masses. A new secular equation is obtained as before, by applying the Lagrangian equations of motion, and this equation states that the fundamental frequencies of vibration are the eigenvalues of the gf matrix, and that the amplitudes are given by the corresponding eigenvectors.

Because the order of the gf matrix (3N-6) is large for most molecules, it is necessary to factor this array into a block-diagonal form, by linearly transforming the internal displacement coordinates to a set of so-called symmetry coordinates. These form a completely reduced representation of the molecular point group, and in terms of them, the G, F and GF matrices, corresponding to g, f and gf in the above treatment, have a suitable block-diagonal form. Not only is factorisation of the secular equation achieved, but also, the frequencies emerging from each block correspond to normal modes of vibration, which belong to the same symmetry species as the symmetry coordinates of the block concerned. Thus a classification of the fundamental frequencies is automatically determined.

The treatment given so far is inadequate for the purposes of the quantum mechanical approach, and yet

another linear transformation of coordinates must be defined. This is from the set of symmetry coordinates, to a specially significant coordinate set, the so-called normal coordinates (the Q's). The transformation is defined in such a way, that not only do the Q's form a completely reduced representation of the molecular point group, but also, they have the property that the kinetic and potential energies may be written in extremely simple, diagonal, quadratic forms in terms of them.

A Hamiltonian operator can be written as a function of the normal coordinates, and a corresponding Schrodinger equation is immediately defined. Because of the diagonal nature of the energy expressions, and the one to one correspondence which the normal coordinates have with each normal mode and frequency, this Schrodinger equation can be factored into 3N-6 distinct differential equations, one for each of the Q's. Each of these separate equations is of the linear harmonic oscillator type, and hence is readily soluble to give wavefunctions $\psi_{v_k}(Q_k)$ which are the so-called Hermite orthogonal functions (see ref. 62 page 37). The corresponding energy expressions are $E_{v_k} = (v_k+\frac{1}{2})h\nu_k$. In the above expressions k is a label, v_k is a quantum number which can take on the values 0,1,2 etc., and ν_k

is the classical frequency of the kth normal mode. It follows from the nature of the Schrodinger equation concerned, that the overall solution to it, may be written as a product of the 3N-6 $\psi_{V_k}(Q_k)$'s, and the energy levels as sums of the 3N-6 Ev_k's. Each energy level is thus defined by 3N-6 quantum numbers, and is expressed in terms of the 3N-6 classical vibrational frequencies. If, as is often the case, some of these fundamental frequencies are identical, then degenerate vibrational levels occur, and the frequencies concerned are also called degenerate (twofold, threefold etc.).

Using wavefunctions derived in this way, it is possible to decide upon the selection rules which govern transitions between energy levels, and for this, the case of harmonic vibration, it can be shown (see ref. 62 Chapter Three) that the frequencies expected in the infrared and Raman vibrational spectra, are noneother than the classical fundamental values.

Further consideration of the possible transitions, reveals, that only those fundamentals corresponding to certain symmetry species of the molecular point group, will be infrared active or Raman active. The familiar rule emerges that a mode of vibration must involve a change in electric dipole moment, if it is to be infrared active, and a change in molecular

polarisability, if it is to be Raman active.

The calculation of root mean square amplitudes of vibration requires use of the vibrational wave functions discussed above, to obtain expectation values for squares of the normal coordinates. This problem will be dealt with in section five. A mathematical treatment of the classical theory described qualitatively above, follows in the next section.

3. The equations of normal coordinate analysis

Let $\underline{s}$ be a column vector containing 3N-6 independent internal displacement coordinates. In terms of these the kinetic energy of the molecule (T), and the potential energy (V), may be written,

$$2T = (\dot{\underline{s}})' \cdot (\underline{g}^{-1}) \cdot (\dot{\underline{s}}) \qquad 5.1,$$

$$2V = (\underline{s})' \cdot \underline{f} \cdot (\underline{s}) \qquad 5.2,$$

where the matrix $\underline{g}^{-1}$ is that discussed in Appendix One, and must be calculated from a knowledge of the molecular geometry, and atomic masses. The matrix $\underline{f}$. is the force constant array which defines the nature of the force field holding the atoms together, and constitutes the basic unknown of the vibrational

problem.

Application of the equations of Lagrange, using the energy expressions given above, leads to a secular equation which has as its solutions a set of quantities λ_k, which are related to the fundamental frequencies by the expression $\nu_k = \lambda_k^{1/2}/2\pi$. This secular equation may be written in determinantal form,

$$\left| \underline{g}.\underline{f} - \underline{E}\lambda \right| = 0 \qquad 5.3,$$

where $\underline{E}$ is the unit matrix. The eigenvector $\underline{a}_k$ of the $\underline{gf}$ matrix, corresponding to the eigenvalue λ_k, is defined by the following set of simultaneous, homogeneous linear equations,

$$\left[\underline{g}.\underline{f} - \underline{E}\lambda_k\right]\left[\underline{a}\right]_k = \underline{0} \qquad 5.4.$$

The vector $\underline{a}_k$ appearing in this expression is undetermined to the extent of an arbitrary multiplying scalar. This vector contains a set of amplitudes of the internal displacement coordinates, and so provides a physical description of the kth normal mode.

The factorisation of the above secular equation is achieved by making the transformation of coordinates,

$$\underline{s} = \underline{U}.\underline{S} \qquad 5.5$$

and since this transformation is usually an orthogonal one, the inverse relation may be written,

$$\underline{S} = \underline{U}' \cdot \underline{s} \qquad 5.6$$

where $\underline{U}'$ is the transpose of the matrix $\underline{U}$. Here the vector $\underline{S}$ is a column vector containing a set of 3N-6 symmetry coordinates. The matrix $\underline{U}'$ may be constructed by following the principles given in Chapter Six of reference 62.

In terms of this new set of coordinates, the energy expressions become,

$$2T = (\dot{\underline{S}})'(\underline{G}^{-1})(\dot{\underline{S}}) \qquad 5.7,$$

$$2V = (\underline{S})'\underline{F}(\underline{S}) \qquad 5.8,$$

where the matrices $\underline{G}$ and $\underline{F}$ are related to the $\underline{g}$ and $\underline{f}$ matrices of the previous treatment by,

$$\underline{G} = \underline{U}'\underline{g}\underline{U} \qquad 5.9,$$

$$\underline{F} = \underline{U}'\underline{f}\underline{U} \qquad 5.10,$$

and the new secular equation may be written in the form,

$$\left| \underline{G}\underline{F} - \underline{E}\lambda \right| = 0 \qquad 5.11.$$

The transformation of the symmetry coordinates to the normal coordinates, can be defined by a matrix $\underline{L}$ as follows,

$$\underline{S} = \underline{L}\underline{Q} \qquad 5.12,$$

and $\underline{L}$ is such that the two energy expressions in terms of the normal coordinates are,

$$2T = (\dot{\underline{Q}})'\underline{E}(\dot{\underline{Q}}) \qquad 5.13,$$

$$2V = (\underline{Q})'\underline{\Lambda}(\underline{Q}) \qquad 5.14,$$

where the matrix $\underline{\Lambda}$ is a diagonal matrix whose elements are the λ_k values.

From these expressions for the energy it can be shown that the columns of the $\underline{L}$ matrix are the eigenvectors defined by the equation,

$$[\underline{G}\underline{F} - \underline{E}\lambda_k][\underline{A}]_k = \underline{0} \qquad 5.15,$$

if these are normalised by multiplying them by a factor N_k given by,

$$N_k^2 = \lambda_k \Big/ \sum_{t,t'} F_{tt'} A_{tk} A_{t'k} \qquad 5.16.$$

It is clear from equations 5.6 and 5.12 above, that the transformation between the internal displacement coordinates and the normal coordinates is given by,

$$\underline{s} = (\underline{U}\underline{L})\underline{Q} \qquad 5.17.$$

It should be noted that the transformations to normal coordinates are not usually orthogonal, and hence matrix inversion is required to produce the inverse relationship.

4. The inclusion of redundant coordinates[68]

Often, for reasons of symmetry, it is necessary to treat the vibrational problem in terms of a number of internal displacement coordinates greater than 3N-6. This inclusion of dependent internal coordinates leads to certain consequences when the Lagrangian treatment is applied. If each added dependent coordinate can be written linearly in terms of the independent coordinates, then it is possible to treat the problem exactly as before, and define g and f matrices, whose orders are greater than 3N-6. The resulting gf matrix now has a number of zero eigenvalues and null eigenvectors, corresponding to the redundant coordinates included. Another significant consequence of the inclusion of redundant coordinates, is that in such a case, the f matrix contains redundant force constants, and cannot be determined uniquely. In this case an infinite number of f matrices are theoretically possible, all producing the same set of fundamental frequencies of vibration.

This lack of uniqueness does not apply to all of the f_{ij} elements, but is confined to the rows and columns of the array, whose corresponding $\underline{s}$ elements are linearly related.

For example, in the spectroscopic calculations described in Chapter Six for $FClO_3$, one redundant coordinate has been included. In this case, the six angles surrounding the chlorine atom are not independent of oneanother, and, to an approximation, the corresponding small changes in them, the internal displacement coordinates, are connected by a single linear relation. Hence one of these displacement coordinates is redundant, and its inclusion leads to a zero eigenvalue, null eigenvector, and zero normal coordinate. The zero eigenvalue obtained, is, however, a good check on the correctness of the g and $\underline{G}$ matrices calculated.

In the $FClO_3$ analysis, there will consequently be a lack of uniqueness attached to the angle bending force constants and corresponding interaction constants. The extra redundant coordinate is necessary, however, if the problem is to be factored, by transforming to symmetry coordinates, as for this purpose, all symmetrically equivalent sets of coordinates must be maintained intact.

There are in fact methods available for eliminating redundant symmetry coordinates from the problem (see ref. 62 page 140), and so obtaining unique $\underline{F}$ matrices, but in the present work no such elimination was attempted, as the angle bending force constants were not required for any purpose.

The force field was calculated to give good agreement between the observed and theoretical vibrational frequencies, and only the stretching force constants were considered to have a unique significance.

5. The root mean square amplitudes of vibration [27]

Let $\underline{r}$ be a column vector containing a set of changes in the interatomic distances, whose root mean square amplitudes of vibration are required. This set may be written in terms of the independent internal displacement coordinates, as follows,

$$\underline{r} = \underline{X}.\underline{s} \qquad 5.18,$$

and hence in terms of the normal coordinates by,

$$\underline{r} = (\underline{X}\underline{U}\underline{L})\underline{Q} \qquad 5.19,$$

or

$$\underline{r} = \underline{K}\underline{Q} \qquad 5.20.$$

From this latter result it is evident that,

$$\underline{r}.\underline{r}' = \underline{K}(\underline{Q}.\underline{Q}')\underline{K}' \qquad 5.21,$$

where $\underline{rr}'$ is a matrix containing elements of the type $r_i r_j$, and the matrix $\underline{QQ}'$ likewise contains elements of the form $Q_i Q_j$.

If these matrices are replaced by arrays whose elements are the corresponding average values $\overline{r_i r_j}$ and $\overline{Q_i Q_j}$, then the previous equation may be written in the corresponding form,

$$\overline{\underline{r}.\underline{r}'} = \underline{K}(\overline{\underline{Q}.\underline{Q}})\underline{K}' \qquad 5.22.$$

The u_{ij}^2 quantities appearing in the equations of Chapter Two, are defined by the relationship,

$$u_{ij}^2 = \overline{[R_{ij} - R_{ij}^e]^2} \qquad 5.23,$$

and it follows from this, that the diagonal elements of the matrix $\overline{\underline{rr}'}$ are u_{ij}^2 values for the distances present in $\underline{r}$.

The matrix $\overline{\underline{QQ}}'$ may be evaluated by finding the average values of $Q_i Q_j$ and Q_i^2, averaged that is, not only for a particular vibrational state, but also over all states, populated at any temperature according to the Boltzmann distribution function.

For any vibrational state, the average, or

expectation value for a function of the Q's, is given by the integral,

$$\langle f(Q) \rangle = \int \psi_{vib} f(Q) \psi^*_{vib} \, dQ \qquad 5.24,$$

where integration is over all of the 3N-6 Q's. If the function is simply the products $Q_i Q_j$ or Q_i^2, then the integral may be evaluated, and a further averaging over all levels carried out, each value for a particular vibrational state, being weighted according to the Boltzmann distribution.

The results obtained are discussed in reference 27, and for a polyatomic molecule turn out to be,

$$\overline{Q_i^2} = \{h / 8\pi^2 \nu_i\} . \coth[h\beta\nu_i/2] \qquad 5.25,$$

$$\overline{Q_i Q_j} = 0 \qquad 5.26.$$

The ν_i term is the classical fundamental frequency of vibration, and $\beta = 1/kT$ where T is the absolute temperature.

Substitution of these results into the $\overline{QQ}$' matrix, and consideration of the nature of equation 5.22, shows that each of the $\overline{r_i^2}$ quantities is given by,

$$\overline{r_i^2} = \sum_{k=1}^{3N-6} K_{ik}^2 . [h/8\pi^2\nu_k] . \coth[h\beta\nu_k/2] \qquad 5.27.$$

This expression is the basic formula necessary for

calculating mean square amplitudes of vibration from spectroscopic data. The u_{ij} values are of course the square roots of the $\overline{r_i^2}$ terms above. The $\underline{K}$ matrix and the ν_k must be calculated according to the methods of normal coordinate analysis outlined in previous sections.

6. The computational procedure adopted

In the spectroscopic calculations described for $FClO_3$ and $HClO_4$ in Chapters Six and Seven, the theory discussed in sections two to five above, was applied in the following way.

As a first step, a molecular model was defined by assuming a symmetry and geometry, and the atoms constituting this model were assigned integer number labels for the purpose of identifying coordinates.

The methods of group theory were next employed to decide the symmetry species of the normal modes of vibration, and to determine which of these modes ought to be infrared active and which Raman active.

References to published spectral data for the molecule concerned were then looked up, and if the observed vibrational frequencies were found to be unassigned, or only partially assigned, an attempt was made to identify them with the frequencies expected for the molecular model assumed. Once an assignment

of the observed frequencies had been decided upon, it was possible to begin calculation of theoretical frequency values and force constant matrices.

To do this a choice was first made of a suitable set of internal displacement coordinates to describe the vibrational problem, and the structure of the completely reduced representation of the molecular point group, based on these coordinates, indicated the symmetry species of any redundant symmetry coordinates likely to be present.

The kinetic energy matrix g was then calculated by computer, using the programme described in Appendix One, and a trial f matrix constructed, partly by guesswork, and partly by transferring force constants from other similar molecules.

Because of the fact that the number of observed vibrational frequencies was much less than the number of distinct elements of the f matrix to be determined, it was necessary to make the well-known approximation of valence forces (see ref. 62, Chapter Eight), and to assume that most of the off-diagonal terms of the potential energy matrix, could be set equal to zero. In choosing these zero elements, the policy was adopted of allowing the number of non-zero force constants in the matrix, to equal the

number of observed frequencies, and the variable constants were made up of the diagonal matrix elements plus a small number of cross terms.

In practice there was always a problem in deciding which cross terms were most significant, and should be included, and this problem was usually dealt with by experimenting with a number of types of force field. The one giving best agreement between observed and calculated frquencies was finally chosen for the purposes of amplitude calculations, and force constant comparisons. This somewhat empirical approach had the advantage, that some measure of the accuracy of the diagonal terms could be obtained by studying their variation, as the nature of the chosen cross-terms was varied.

Once a type of field had been decided upon and trial values had been assigned to the non-zero variable force constants, the g and f matrices were transformed to block-diagonal form by constructing symmetry coordinates, and the resulting GF matrix was solved block by block for eigenvalues, and the results compared with the experimental frequency values.

This process of f and F matrix construction, and GF solution, was repeated in cycles, with systematic variation of the elements of f, until the differences

between observed and calculated fundamentals had been reduced to a minimum. This force field variation procedure is described in more detail in Appendix Three, whilst the eigenvalues programme used to solve the secular equations, is described in Appendix Two.

Once a final type of force field and choice of force constants had been decided upon, the $\underline{L}$ transformation matrix was calculated from a set of eigenvectors corresponding to the final calculated frequencies, and the matrix $\underline{K}$, defined by,

$$\underline{K} = \underline{X}\underline{U}\underline{L} \qquad 5.28,$$

was determined for a set of interatomic distances $\underline{r}$, whose u values were required. These latter were calculated according to equation 5.27 of the previous section, the temperature assumed being that of the electron diffraction study.

These methods were employed for the larger systems such as $FClO_3$, but for the XOX molecules discussed in Chapter Eight, a full force field was always available in the literature, and hence a direct calculation of the amplitudes of vibration was possible. The computer programme used to carry out this complete type of analysis, is described in Appendix Four.

7. A discussion of the accuracy of force constants and root mean square amplitudes of vibration calculated by the above methods

The problem of estimating the accuracy of force constants and mean amplitudes of vibration, obtained by calculations of the type discussed above, is not an easy one to solve in quantitative terms. Numerous factors are involved in making this assessment, and these vary considerably from one situation to another. For example, the quality, nature, and extent of the available experimental data, vary from molecule to molecule, and the size and rigidity of the molecule concerned are critical in determining the success of a normal coordinate analysis. In addition to these factors, the error itself varies from parameter to parameter, depending on how well a particular force constant or amplitude is determined by the experimental data, and to what extent it is affected by any approximations which have been made. Despite all this, it is possible to make a few general remarks, of a qualitative nature, which are useful as guides when dealing with specific cases.

Firstly, the theory outlined above is only applicable to the case of a rigid molecule, undergoing harmonic, or very nearly harmonic, vibrational motion.

It follows that poor results will be obtained, if this theory is applied to a loosely bound system, which undergoes anharmonic motion, and for which the separation of rotational and vibrational energies is a bad approximation.

Secondly, even if the molecule is sufficiently rigid, the tendency for the number of distinct $\underline{f}$ matrix elements to be greater than the number of observed data, a tendency which increases as the molecular size increases, leads inevitably to the assumption of an approximate, semi-diagonal force field, and this assumption limits the possibility of ever achieving exact agreement between observed and calculated fundamental frequencies. Neglect of significant off-diagonal interaction terms in the $\underline{f}$ matrix can result from making such an approximation, and this neglect may cause some of the diagonal force constants obtained to be subject to considerable errors. This is not at all satisfactory, when it is recalled that these are the force constants quoted in chemical literature, as characteristic of chemical bonds.

Thirdly, if redundant coordinates are included in the treatment, certain of the diagonal force constants obtained, usually angle bending constants, lack a unique significance, and although this is not really

a source of error, it is a source of uncertainty which should be borne in mind.

Finally, even in the case of a fairly rigid molecule, the observed vibrational frequencies, should be corrected for anharmonicity, to the so-called ' mechanical frequencies ' before being used in calculations. Such correction requires detailed spectral information, and this is not always available.

The ideal case is therefore that of a rigid molecule, for which a great deal of infrared and Raman spectroscopic data have been obtained, for in such a case, the $\underline{f}$ matrix can be calculated with the minimum amount of approximation. This is particularly true if the spectral data includes frequencies for several isotopic species, but the molecular size is always a limitation, as the number of distinct f_{ij} elements increases rapidly with the number of atoms present in the system. In the present work, these ideal conditions were most nearly achieved in the cases of the XOX angular symmetric molecules discussed in Chapter Eight, as for these, full matrix potential functions are available in the literature, and their vibrational motion may be assumed to be reasonably harmonic.

In less favourable situations, where spectral data

are limited, individual circumstances must be taken into account, in estimating errors. In the cases of $FClO_3$ and $HClO_4$, discussed in Chapters Six and Seven, errors were assessed by considering the following three points.

First, the agreement between the observed and calculated frequencies finally achieved, was used as a measure of the validity of the approximate force field adopted.

Second, changes in the diagonal force constants were noted, as the choice of non-zero off-diagonal matrix elements was varied. In this way a rough estimate was obtained of the errors liable to be present in the stretching force constants, as a result of neglect of cross-terms in the force field.

Third, a comparison was made, where possible, of the force constants and amplitudes obtained, with those quoted in the literature, either for the same molecules, or for closely similar systems.

The conclusions reached for $FClO_3$ and $HClO_4$ are discussed in the following two chapters, but a general summary of the reliability and usefulness of spectroscopic amplitudes, may be stated as follows. For calculations carried out on small to medium-sized molecules of the type discussed for $FClO_3$ and $HClO_4$

it seems that most of the amplitudes obtained are as accurate, if not more so, than corresponding electron diffraction values. This tends to be particularly true of the amplitudes calculated for chemical bonds, as the error sources previously discussed, affect these less than they do the amplitudes of many types of non-bonded distance.

The amplitudes of vibration calculated from spectroscopic data are useful to the electron diffractionist, as they may be compared with corresponding electron diffraction results, or included as constants in least squares refinements of intensity data. In this latter capacity they often help to resolve closely similar internuclear distances which are often strongly correlated with amplitudes of vibration.

It may be said in conclusion, that if electron diffraction amplitude results are ever to be used to make precise determinations of molecular force fields, then they will have to be obtained in the future with a much higher accuracy than they are now, as experience of normal coordinate calculations indicates that the amplitudes of bonded distances are fairly insensitive to small changes in the $\underline{f}$ matrix, insensitive, that is, by the present error standards of a few thousandths of an Angstrom unit.

CHAPTER SIX

A CALCULATION OF THE ROOT MEAN SQUARE AMPLITUDES OF VIBRATION OF PERCHLORYL FLUORIDE

1. Introduction

As a result of their infrared study[69] of gaseous perchloryl fluoride ($FClO_3$), Lide and Mann concluded that the molecule has the C_{3v} structure indicated in figure 6.1, and in addition, they obtained values for the six fundamental frequencies of vibration expected for such a model. Their conclusion has subsequently been confirmed by a microwave investigation[70], and by the electron diffraction study described in Chapter Eleven of this thesis.

The calculations of the present chapter were undertaken to obtain spectroscopic values for the root mean square amplitudes of vibration of perchloryl fluoride, the temperature assumed (243° K) being that estimated for the gas in the diffraction experiment.

2. The methods of calculation adopted

A normal coordinate analysis was performed using as data, the vibrational frequencies of reference 69, and structural results produced at an intermediate stage of the electron diffraction study. The GF matrix

PERCHLORYL FLUORIDE

(C_{3v} model)

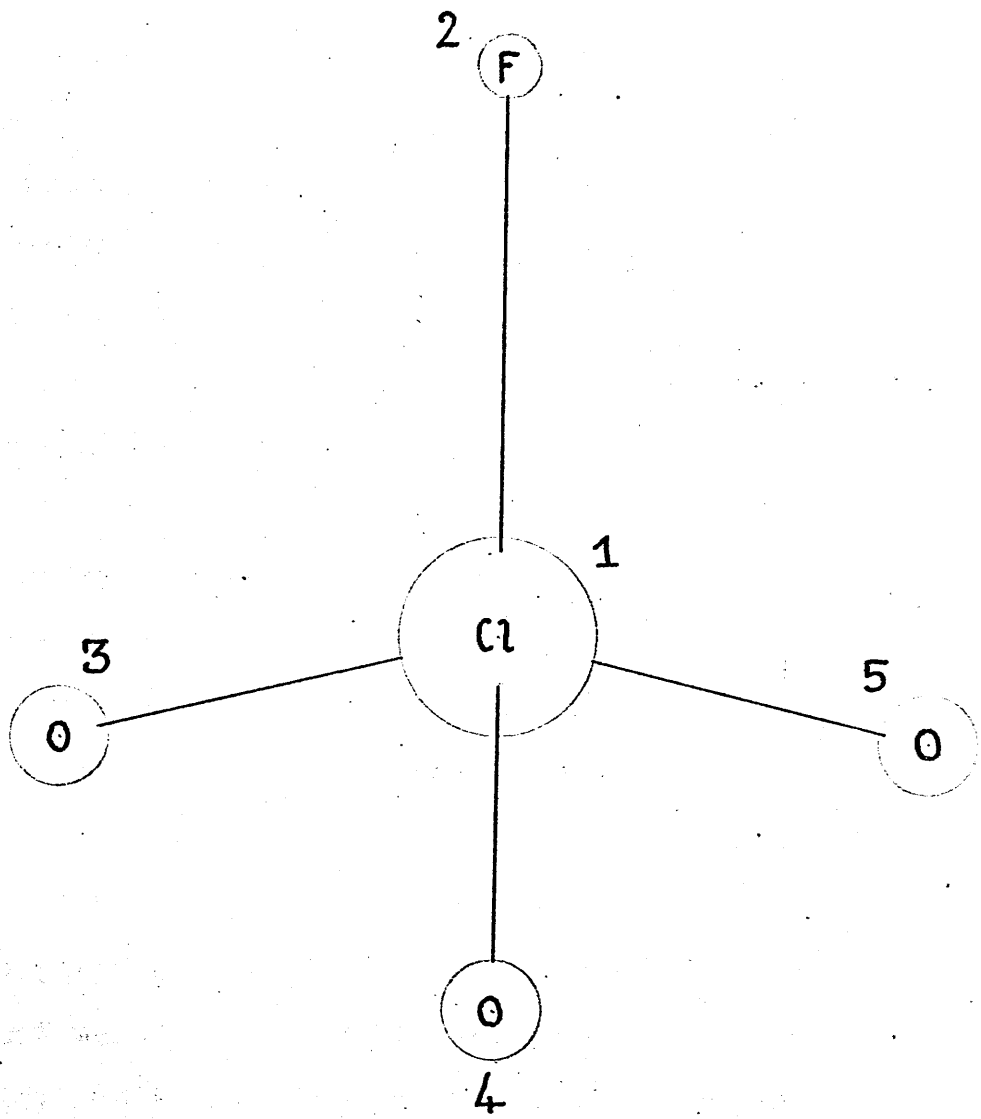

fig. 6.1

method, outlined in Chapter Five, and discussed in detail in reference 62, was employed, and the kinetic energy matrix g was calculated by computer for the Cl^{35} species, using the programme presented in Appendix One. The force constant f matrix was constrained to be semi-diagonal, and to contain only six non-zero force constants, such constraints being necessary in view of the limited nature of the spectroscopic data available (six frequencies). Three distinct selections were made for the non-zero matrix elements, and for each of the force fields so defined, optimum values for the six constants were obtained using the force constant variation procedure of Appendix Three. That field producing frequencies in best agreement with experiment, was finally adopted, and its elements used to calculate the root mean square amplitudes of vibration.

Eigenvalues of the GF matrix blocks were calculated by the method described in Appendix Two, and eigenvectors were computed using a desk calculating machine.

Root mean square amplitudes of vibration for the four distinct types of internuclear distance present in the C_{3v} model, were calculated by finding the transformation matrix K, relating the four internal displacement coordinates s_{12}, r_{13}, p_{45}, and q_{23} (see figure 6.1) to the normal coordinates. This was

achieved by obtaining the linear relationships (defined by the transformation matrix $\underline{X}$ of Chapter Five) expressing these coordinates in terms of the set of internal displacement coordinates $\underline{s}$, used to describe the vibrational motion, and then applying the equation, $\underline{K} = \underline{XUL}$. In this relationship, the matrix $\underline{L}$ (see Chapter Five) was calculated by normalising the eigenvectors of the $\underline{GF}$ matrix, and $\underline{U}$ defines the transformation to symmetry coordinates $\underline{s} = \underline{US}$. The matrix $\underline{X}$ was obtained by writing the distances P_{45} and Q_{23} in terms of the internal coordinates S_{12} etc., listed in table 6.3, using the cosine rule of trigonometry. These two equations were then differentiated to obtain linear relations expressing p_{45} (= dP_{45}) and q_{23} (= dQ_{23}) in terms of the elements of $\underline{s}$. This procedure is described in more detail in reference 27.

The amplitudes of vibration were finally calculated from the $\underline{K}$ matrix elements, by applying equation 5.27 of Chapter Five, and assuming $T = 243^{\circ}$ K.

3. Results

The numbering system used to label the atoms of the C_{3v} model of perchloryl fluoride, is indicated in figure 6.1. A description of the six expected

fundamental modes of vibration is given in table 6.1, together with their point group symmetry species, and symbols ν_1 to ν_6 for the corresponding normal frequencies. Numerical values for these latter were obtained from reference 69, and are listed in table 6.2. They have not been corrected for anharmonicity, nor do they refer to a particular isotopic species, as the spectra of the Cl^{35} and Cl^{37} species were not resolved.

The choice of ten internal, and internal displacement, coordinates, used to describe the vibrational motion, is shown in table 6.3. The bond lengths and valence angles assumed in this table were obtained by the electron diffraction study described in Chapter Eleven, and as there are ten coordinates included in this list, and only nine can be independent for perchloryl fluoride, one is redundant (see Chapter Five). Structures of completely reduced representations of the C_{3v} point group, based on various coordinate sets, including those in the previous table, are given in table 6.4. It is evident from this table that the redundant internal displacement coordinate included will give rise to a redundant symmetry coordinate (A1), when the gf matrix is factored. It is also clear that such factorisation will lead to a GF matrix containing an A1 block of order four, and

two E blocks of order three. The eigenvalues belonging to these latter two blocks will of course be identical, and one of the A1 eigenvalues will be zero on account of the inclusion of the A1 redundant symmetry coordinate. The symmetry coordinate transformation matrix $\underline{U}'$ appearing in $\underline{S} = \underline{U}'\underline{s}$ is shown in table 6.5.

The nature of the unfactored g matrix, consistent with the choice of internal displacement coordinates made in table 6.3, is indicated in table 6.6, and numerical values for the non-identical elements of this matrix, calculated by computer, are listed in table 6.7.

The $\underline{f}$ matrix is of course identical to the g matrix in form, and the final values obtained for the elements of this matrix, and the final choice of non-zero elements, are shown in table 6.8.

The forms of the block-diagonal $\underline{G}$ and $\underline{F}$ matrices, and formulae for the elements of these matrices in terms of the elements of the g and $\underline{f}$ arrays, are given in tables 6.9 and 6.10.

Values for the A1 and E frequencies calculated by solving the blocks of the secular equation $|\underline{GF} - \underline{E}\lambda| = 0$, using for $\underline{F}$ the force constants of table 6.8, are compared with the values of Lide and Mann[69], in table 6.11. The $\underline{K}$ matrix, described in the previous section

is presented in a general form in table 6.12, and the values calculated for the elements of this matrix, in table 6.13. Root mean square amplitudes of vibration, calculated from these matrix elements, assuming T = 243°K, are listed in table 6.14, for the four distances selected.

Consideration of the variations produced both in the diagonal force constants, and in the amplitude values, by altering the choice of non-zero $\underline{f}$ matrix elements (for a discussion see Chapter Five), led to the conclusion that the error limits appropriate to the Cl-F and Cl-O stretching force constants are roughly 0.4 and 0.5 md/Å, respectively, whilst the amplitudes u_{Cl-F}, u_{Cl-O}, $u_{O..O}$, and $u_{O..F}$ may be assigned the error limits 0.003, 0.002, 0.003, and 0.004 Å, respectively. It must be emphasised, however, that these error limits are not based on a particularly rigorous type of analysis, but are essentially empirical and approximate.

4. Discussion

A discussion of the vibrational amplitudes calculated will be given in subsequent Chapters, when both spectroscopic and electron diffraction results have been obtained for other similar molecules, and

for $FClO_3$ itself. It is of interest, however, to compare the calculated Cl-F and Cl-O bond-stretching force constants, with published values obtained for $FClO_3$, and for the molecules ClF and ClF_3.

The bond length of chlorine monofluoride has been accurately determined by microwave spectroscopy[71], and an r_e value of 1.6281 Å obtained. The single fundamental frequency of vibration expected for ClF, has been established by Jones et al., as a result of a spectroscopic study[72], and calculation of the Cl-F stretching force constant using their value of 772 cm^{-1}, led to a result of 4.32 md/Å. This is in good agreement with the stretching force constant of 4.35 md/Å presented in table 6.8 for the ClF bond in $FClO_3$. As, however, this latter bond length is about 0.015 Å shorter than that found in ClF itself, the value of 4.35 md/Å found for perchloryl fluoride must be presumed to be slightly low.

Chlorine trifluoride has been the subject of a fairly accurate microwave study[73] by Smith, and of the three ClF bonds present one is 1.598 Å long, and the other two have a length of 1.698 Å. The structural results obtained by this investigation have been used by Long and Jones, who have carried out force constant calculations[74] for ClF_3, and have obtained ClF

stretching force constants of 4.29 and 2.92 md/Å, respectively, for the two distances quoted above. The first of these results is, as might be hoped from a consideration of the bond length involved, in good agreement with the force constant obtained for perchloryl fluoride. The second value refers of course to a much longer Cl-F distance, and is accordingly a good deal smaller than the 4.35 md/Å of the present study.

A value has been obtained[75] by Robinson, for the Cl-O stretching force constant of $FClO_3$, using a simpler type of calculation than that adopted in the present work. Robinson's value is 9.82 md/Å which is in reasonable agreement with the result given in table 6.8 of 9.3 md/Å, when the errors appropriate to the two results are taken into account. From the nature of the calculations carried out, it may be assumed that the 9.3 value is the more reliable.

No comment or comparison will be made for the other non-zero constants included in the quadratic potential function, as not only are they fairly inaccurate, but they probably lack the transferability of stretching force constants.

TABLE 6.1

A description

of the fundamental frequencies of vibration

of perchloryl fluoride (C_{3v} model)

Mode	Symbol	Symmetry species
Cl-O stretch	v1	A1
Cl-F stretch	v2	A1
ClO_3 bend	v3	A1
Cl-O stretch	v4	E
ClO_3 bend	v5	E
rock	v6	E

Note; all frequencies are infrared and Raman active.

TABLE 6.2

The observed frequencies of vibration for perchloryl fluoride (ref. 69)

frequency	observed value (cm^{-1})
v1	1061
v2	715
v3	549
v4	1315
v5	589
v6	405

TABLE 6.3

The choice of internal coordinates and internal displacement coordinates for $FClO_3$

(one redundancy)

internal coordinate	value assumed	corresponding displacement coordinate
S_{12}	1.610 Å	s_{12}
R_{13}	1.402 Å	r_{13}
R_{14}	"	r_{14}
R_{15}	"	r_{15}
G_{34}	115.1°	g_{34}
G_{35}	"	g_{35}
G_{45}	"	g_{45}
B_{23}	103.0°	b_{23}
B_{24}	"	b_{24}
B_{25}	"	b_{25}

TABLE 6.4

Structures of representations

of the C_{3v} point group

based on various coordinate sets

coordinate set	structure
The Cartesian displacement coordinates	3A1 + 3E *
The ten chosen internal coordinates	4A1 + 3E
The redundant symmetry coordinate	A1
s_{12}	A1
r_{13} r_{14} r_{15}	A1 + E
g_{34} g_{35} g_{45}	A1 + E
b_{23} b_{24} b_{25}	A1 + E

* The species of the six translation and rotation modes have been subtracted.

TABLE 6.5

The symmetry coordinate transformation

		s_{12}	r_{13}	r_{14}	r_{15}	g_{34}	g_{35}	g_{45}	b_{23}	b_{24}	b_{25}
	S1	1									
A1	S2		$1/3^{\frac{1}{2}}$	$1/3^{\frac{1}{2}}$	$1/3^{\frac{1}{2}}$						
	S3					$1/3^{\frac{1}{2}}$	$1/3^{\frac{1}{2}}$	$1/3^{\frac{1}{2}}$			
	S4								$1/3^{\frac{1}{2}}$	$1/3^{\frac{1}{2}}$	$1/3^{\frac{1}{2}}$
	S5		$2/6^{\frac{1}{2}}$	$-1/6^{\frac{1}{2}}$	$-1/6^{\frac{1}{2}}$						
E	S6					$-1/6^{\frac{1}{2}}$	$-1/6^{\frac{1}{2}}$	$2/6^{\frac{1}{2}}$			
	S7								$2/6^{\frac{1}{2}}$	$-1/6^{\frac{1}{2}}$	$-1/6^{\frac{1}{2}}$
	S8			$1/2^{\frac{1}{2}}$	$-1/2^{\frac{1}{2}}$						
E	S9					$-1/2^{\frac{1}{2}}$	$1/2^{\frac{1}{2}}$				
	S10									$-1/2^{\frac{1}{2}}$	$1/2^{\frac{1}{2}}$

Note: The matrix shown above is the U' matrix of Chapter Five. All missing elements are zero.

TABLE 6.6

The nature of the g matrix

	s_{12}	r_{13}	r_{14}	r_{15}	g_{34}	g_{35}	g_{45}	b_{23}	b_{24}	b_{25}
s_{12}	g1	g2	g2	g2	g3	g3	g3	g4	g4	g4
r_{13}		g5	g6	g6	g7	g7	g8	g9	g10	g10
r_{14}			g5	g6	g7	g8	g7	g10	g9	g10
r_{15}				g5	g8	g7	g7	g10	g10	g9
g_{34}					g11	g12	g12	g13	g13	g14
g_{35}						g11	g12	g13	g14	g13
g_{45}							g11	g14	g13	g13
b_{23}								g15	g16	g16
b_{24}									g15	g16
b_{25}										g15

Note: for the elements of the f matrix change g to f above except in the case of the displacement coordinates.

TABLE 6.7

Calculated values for the elements of the g matrix

element	value
g1	0.081203
g2	-0.006423
g3	0.014410
g4	-0.019858
g5	0.091071
g6	-0.012120
g7	-0.018455
g8	0.027192
g9	-0.017293
g10	0.015342
g11	0.104997
g12	-0.033226
g13	-0.009349
g14	-0.034421
g15	0.083357
g16	-0.005075

TABLE 6.8

The final values adopted

for the elements

of the f matrix

element	description	value
f1	Cl-F stretching constant (md/Å)	4.35
f2	Cl-F,Cl-O stretch-stretch interaction constant (md/Å)	-0.25
f3		0.00
f4	Cl-F,O-Cl-F stretch-bend interaction constant (X 10^{-3} dyne/rad)	0.55
f5	Cl-O stretching constant (md/Å)	9.30
f6		0.00
f7		0.00
f8		0.00
f9		0.00
f10		0.00
f11	O-Cl-O bending constant (X 10^{-11} erg/rad^2)	1.95
f12		0.00
f13		0.00
f14		0.00
f15	O-Cl-F bending constant (X 10^{-11} erg/rad^2)	1.60
f16		0.00

TABLE 6.9

The form of the block-diagonal G matrix

	S1	S2	S3	S4	S5	S6	S7	S8	S9	S10
S1	G11	G12	G13	G14	0	0	0	0	0	0
S2		G22	G23	G24	0	0	0	0	0	0
S3			G33	G34	0	0	0	0	0	0
S4				G44	0	0	0	0	0	0
S5					G55	G56	G57	0	0	0
S6						G66	G67	0	0	0
S7							G77	0	0	0
S8								G88	G89	G8,10
S9									G99	G9,10
S10										G10,10

Note: For the matrix F change G to F above.

TABLE 6.10

The elements of the block-diagonal

$\underline{G}$ matrix

in terms of $\underline{g}$ matrix elements

element	expression	element	expression
G11	g1	G56	g8 - g7
G12	$\sqrt{3}$g2	G57	g9 - g10
G13	$\sqrt{3}$g3	G66	g11- g12
G14	$\sqrt{3}$g4	G67	g14- g13
G22	g5 + 2g6	G77	g15- g16
G23	g8 + 2g7	G88	g5 - g6
G24	2g10+ g9	G89	g8 - g7
G33	g11+ 2g12	G8,10	g10- g9
G34	2g13+ g14	G99	g11- g12
G44	g15+ 2g16	G9,10	g13- g14
G55	g5 - g6	G10,10	g15- g16

Note: For the corresponding $\underline{F}$ elements change G and g above to F and f respectively.

TABLE 6.11

A comparison of calculated and observed vibrational frequencies for perchloryl fluoride

frequency	observed value (cm^{-1})	calculated value (cm^{-1})
v1	1061	1060
v2	715	713
v3	549	504
v4	1315	1323
v5	589	611
v6	405	452

TABLE 6.12

The $\underline{K}$ matrix for four kinds

of internuclear distance present in $FClO_3$

$\underline{r}$	Q1	Q2	Q3	Q4	Q5	Q6	Q7	Q8	Q9	Q10
s_{12}	K11	K12	K13	0	0	0	0	0	0	0
r_{13}	K21	K22	K23	0	K25	K26	K27	0	0	0
p_{45}	K31	K32	K33	0	K35	K36	K37	0	0	0
q_{23}	K41	K42	K43	0	K45	K46	K47	0	0	0

Note: Q4 is the redundant (zero) normal coordinate.

TABLE 6.13

Calculated values for the K matrix elements

element	calculated value
K11	0.10683
K12	0.26402
K13	0.00899
K21	-0.14507
K22	0.03457
K23	-0.00631
K25	0.25987
K26	0.03385
K27	0.01063
K31	-0.21720
K32	0.09069
K33	-0.08451
K35	-0.10644
K36	-0.22587
K37	0.01284
K41	-0.06814
K42	0.18608
K43	0.12868
K45	0.10388
K46	0.05562
K47	0.21321

TABLE 6.14

The calculated

root mean square amplitudes of vibration

for $FClO_3$ at 243° K

interatomic distance	calculated u value (Å)
S_{12}	0.043
$R_{13,14,15}$	0.036
$P_{45,34,35}$	0.053
$Q_{23,24,25}$	0.061

CHAPTER SEVEN

A CALCULATION OF THE ROOT MEAN SQUARE AMPLITUDES OF VIBRATION OF PERCHLORIC ACID

1. Introduction

Fairly detailed force constant calculations have already been published for perchloric acid ($HClO_4$) by Siebert in 1954[76], but the accuracy of his analysis was limited by the approximate nature of the structural and spectroscopic data available for the molecule at that time, and no attempt was made to calculate root mean square amplitudes of vibration.

In 1959 an electron diffraction study of gaseous perchloric acid made by Akishin et al.,[77] established the C_{3v} symmetry of the ClO_4 skeleton, and obtained rough dimensions for this part of the molecule. These results have subsequently been refined by the more accurate electron diffraction investigation of the acid, described in Chapter Ten of the present work. Neither study, however, determined the conformation, or internal motion, of the hydrogen atom.

In 1961, Giguère and Savoie supplemented the existing Raman data[78] available for perchloric acid, by publishing a detailed infrared study[79] of $HClO_4$ and

PERCHLORIC ACID

(Cs model)

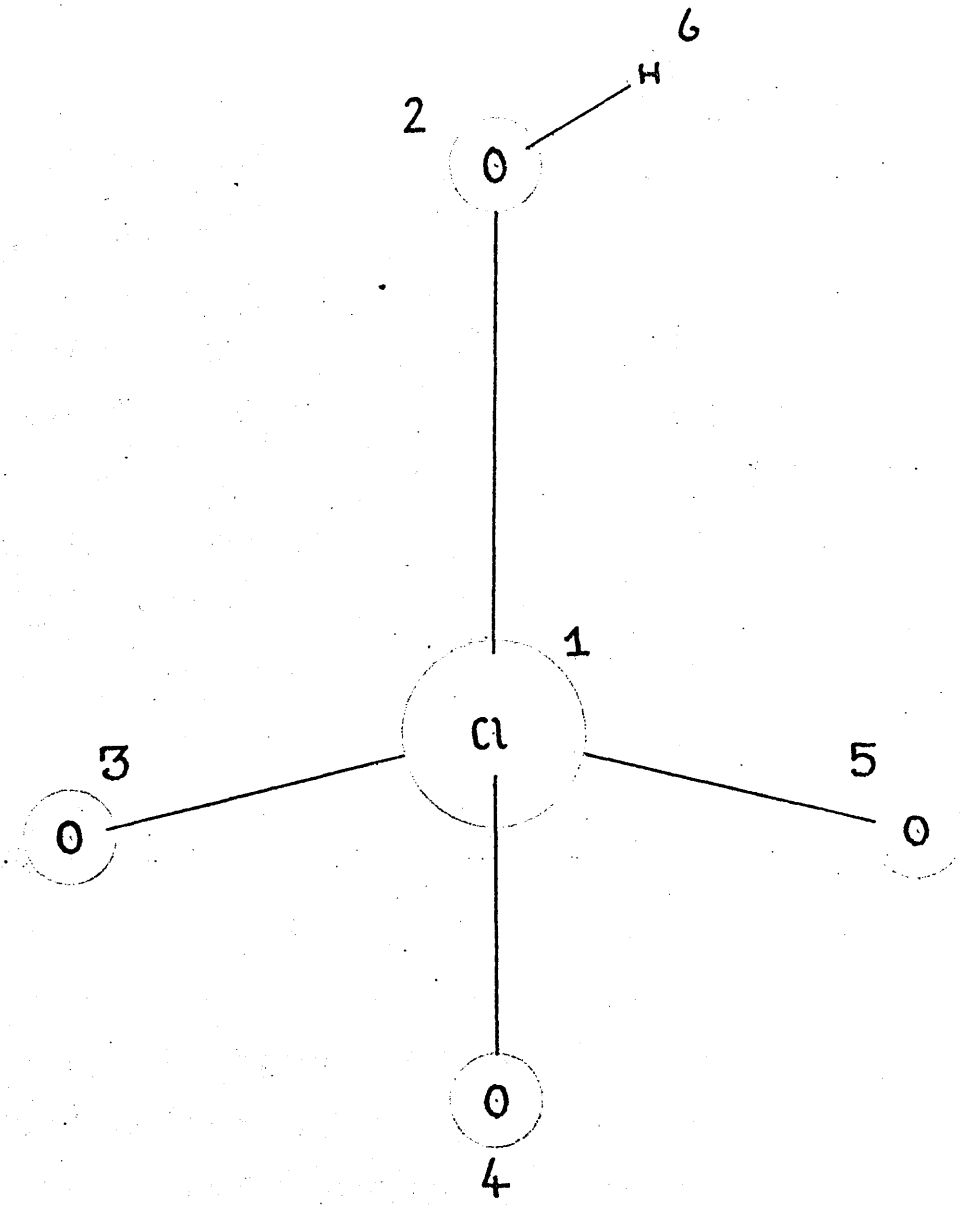

fig. 7.1

$DClO_4$. They recorded spectra for the acid in all three physical states, and assigned the measured frequencies in terms of a molecular model having C_s symmetry, and consisting of a C_{3v} tetrahedral skeleton, with an attached hydrogen atom. This latter was assumed to be either staggered or eclipsed with respect to the oxygen atoms of the symmetrical ClO_3 group, but the infrared study did not distinguish between these two possibilities. One of them, the staggered conformation, is shown schematically in figure 7.1.

The force constant calculations discussed below were undertaken to obtain spectroscopic values for the root mean square amplitudes of vibration of the molecule, the temperature assumed (308°K), being that estimated for the diffracting vapour in the electron diffraction investigation of Chapter Ten.

2. The methods of calculation adopted

Instead of applying the methods of normal coordinate analysis to the complete C_s model of figure 7.1, it was decided to simplify the secular equation by considering the vibrations of the ClO_4 skeleton alone. This was achieved by treating the OH group as a single point mass X, an approximation which was also made by Siebert in his calculations, and which

assumes a separation of the high frequencies of vibration of the light hydrogen atom from the lower frequencies of the ClO_4 skeleton. It is justified in a discussion given in Chapter Four of reference 62.

The $HClO_4$ molecule was therefore treated as an $XClO_3$, C_{3v}, system similar to perchloryl fluoride, and a special correlation procedure carried out when choosing values for the six fundamental frequencies of vibration (3A1+3E), appropriate to such a model. This necessity arises as follows. Since $HClO_4$ is not an $XClO_3$ structure, but has in fact C_s symmetry, the three degenerate E frequencies expected for the C_{3v} skeletal model (see Chapter Six), are in reality split into three pairs of closely similar values. It follows that the observed infrared spectrum of perchloric acid contains twelve distinct fundamental frequencies of vibration (8A'+4A''), and that of these, nine (6A'+3A''), and not six, correspond to motions of the ClO_4 skeleton. Before an approximate C_{3v} treatment of the molecule could be attempted, it was therefore necessary to consider the nine A' and A'' skeletal frequencies published by Giguere and Savoie[79] for the C_s structure, and to calculate from these, three E and three A1 values for the $XClO_3$ model. The E frequencies were obtained by averaging the two members of each

A',A'' pair, split apart by the presence of the vibrating hydrogen atom, whilst the A1 frequencies corresponded to the remaining three A' fundamentals.

Once this process had been carried out, and six ' observed ' frequencies estimated for the $XClO_3$ model, it was possible to proceed exactly as described for $FClO_3$ in Chapter Six. Structural parameters were taken from the results produced at an intermediate stage of the electron diffraction investigation of Chapter Ten, and only the $HCl^{35}O_4^{16}$ species of perchloric acid was considered.

3. Results

The integer numbering system adopted to label the atoms of the C_s model (and hence the C_{3v} model) is shown in figure 7.1. A description of the twelve fundamental modes of vibration expected for this structure, is given in table 7.1, and numerical values for these frequencies selected from the published $HClO_4$ data of Giguère and Savoie, are listed in table 7.2. These values have not been corrected for anharmonicity, and apply equally well to the Cl^{35} and Cl^{37} species. The correlation process adopted to calculate (' observed ') fundamental frequencies for the C_{3v} approximate model is summarised in table 7.3. Tables 7.4 to 7.9 describe

the normal coordinate analysis carried out, and are identical in form to certain of the tables presented in Chapter Six. The final force field obtained is shown in table 7.6, and values for the four types of root mean square amplitude of vibration expected for the ClO_4 skeleton are listed in table 7.9, the assumed temperature being 308°K.

The Cl-OH and Cl-O_p (p = peripheral) stretching force constants calculated were assigned error limits of 0.5 md/Å each, and as in the case of $FClO_3$, these limits are essentially approximate. The errors assigned to the vibrational amplitudes u_{Cl-OH}, u_{Cl-O_p}, $u_{O_p..O_p}$, and $u_{O_p..OH}$ were 0.004, 0.002, 0.003 and 0.004 Å respectively.

A second approximate calculation was carried out for $HClO_4$ treating it as an XOH angular molecule where this time X = ClO_3, and the OH bond length assumed was 0.96 Å, a value fairly typical of OH containing compounds. The valence angle XOH was given the value of 113° in accordance with the results obtained for hypochlorous acid by Badger and Hedberg[80]. Values for the three fundamental frequencies expected for this model were selected in an obvious way from table 7.2, and these were fitted by the force constant variation procedure using as trial starting constants the results

given by Badger and Hedberg for HOCl. The amplitudes u_{OH} and $u_{Cl..H}$ were calculated at 308°K, and found to have the values 0.07 and 0.11 Å respectively. These results are approximate but were used as constants in the least squares refinements of Chapter Ten.

4. Discussion

It is of interest to compare the amplitudes of vibration and stretching force constants obtained for the ClO_4 skeleton, with those determined for $FClO_3$ in Chapter Six. As would be expected from a consideration of bond length and polarity, the force constant obtained for the Cl-F bond in perchloryl fluoride is somewhat larger than that calculated for the Cl-OH bond in perchloric acid. The Cl-F amplitude of vibration should therefore be smaller than that of the Cl-OH bond, and this is in fact found to be the case. Also consistent with these results is the fact that the amplitude of vibration of the nonbonded Op..F distance is smaller than that calculated for the Op..OH distance in $HClO_4$. The force constants calculated for the Cl-Op bonds in both molecules are, however, very similar, and this is entirely consistent with the identical amplitudes of vibration computed for these distances, and also with the closely similar lengths obtained for these bonds by the electron diffraction

investigations of Chapters Ten and Eleven. The amplitudes calculated for the Op..Op nonbonded distances in both molecules are also very similar.

It is also of interest to compare the amplitudes of vibration calculated in this chapter for the Cl-Op and Op..Op distances in perchloric acid, with the values obtained by an electron diffraction study[81] of gaseous chlorine heptoxide (Cl_2O_7). This molecule consists of two perchloric acid units condensed together, and the two ClO_3 groups present in chlorine heptoxide are structurally very similar to those found in $HClO_4$ and $FClO_3$ (see Chapters Ten and Eleven). The electron diffraction results for Cl_2O7 include values for u_{Cl-Op} and $u_{Op..Op}$ of 0.035 and 0.057 Å respectively, the corresponding error limits being given as 0.003 and 0.007 Å. The second of these results is in good agreement with the 0.054 Å obtained by the present work, but when the first amplitude is corrected for failure of the Born approximation (see Chapter Eight), it becomes 0.028 Å, a value considerably lower than the 0.036 Å obtained by the calculations of this chapter and of Chapter Six. This discrepancy is surprising as the $Cl-O_p$ bond length in chlorine heptoxide is very similar to that of $HClO_4$. It is likely, however, that the spectroscopic results

are the more accurate, and this conclusion will be substantiated in Chapters Ten and Eleven when further electron diffraction results will be obtained for the Cl-Op amplitudes of vibration.

As for perchloryl fluoride, it is worthwhile to assess the reliability of the force constants obtained for the Cl-O bonds in perchloric acid , by comparing the results of the present calculations with corresponding values determined for the same or similar systems by other workers.

Thus Siebert[76] calculated values for the Cl-Op and Cl-OH stretching force constants of 8.02 and 4.04 md/Å respectively. The methods he used were similar to those described above, but as was mentioned in section one, the data available to him were considerably inferior to those available at the present time. This must be assumed to explain the discrepancy between the value of 8.02 md/Å he calculated for the Cl-Op bond, and the value of 9.2 md/Å given in table 7.6. His Cl-OH force constant of 4.04 md/Å is, however, in good agreement with the value of 3.85 md/Å calculated in the present analysis.

More recently Robinson[75] published values of 9.55 and 3.79 md/Å for these constants, values which are in good agreement with those of the present work, despite the extremely approximate methods Robinson

adopted to calculate these results.

Finally, it is of interest to consider the Cl-OH bond found in the molecule of hypochlorous acid HOCl. The infrared spectra of both HOCl and DOCl have been examined by two sets of workers, Badger and Hedberg[80] and Schwager and Arkell.[81A] The average Cl-O stretching force constant obtained by considering the results published by these authors is 3.9 md/Å, and this value seems to suggest that the Cl-O bond length in hypochlorous acid is closely similar to that found for the Cl-OH bond in perchloric acid (1.635 Å), and shorter than the 1.70 Å assumed by the above workers in their calculations.

As in the case of $FClO_3$ no comments or comparisons will be made for the other force constants appearing in the quadratic potential energy expression of $HClO_4$.

TABLE 7.1

A description

of the fundamental frequencies of vibration

of perchloric acid (C_s model)

mode		symbol	symmetry species
O-H	stretch	v1	A'
Cl-O	stretch	v2	A'
Cl-O-H	bend	v3	A'
Cl-O	stretch	v4	A'
Cl-OH	stretch	v5	A'
O-Cl-O	bend	v6	A'
O-Cl-O	bend	v7	A'
O-Cl-OH	bend	v8	A'
Cl-O	stretch	v9	A''
O-Cl-O	bend	v10	A''
O-Cl-OH	bend	v11	A''
H	torsion	v12	A''

TABLE 7.2

The observed

frequencies of vibration

for perchloric acid

(H species)

frequency	observed value (cm^{-1})[79]
v1	3560
v2	1263
v3	1200
v4	1050
v5	725
v6	565
v7	519
v8	390
v9	1326
v10	580
v11	430
v12	307

TABLE 7.3

The assumed frequencies for the C_{3v} approximate model

observed frequencies (cm^{-1}) for the C_s model		assumed frequencies (cm^{-1}) for the C_{3v} approximate model
(A') 1050 = v4	→	(A1) 1050 = 'v1'
(A') 725 = v5	→	(A1) 725 = 'v2'
(A') 519 = v7	→	(A1) 519 = 'v3'
(A') 1263 = v2 (A") 1326 = v9	→	(E) 1295 = 'v4'
(A') 565 = v6 (A") 580 = v10	→	(E) 573 = 'v5'
(A') 390 = v8 (A") 430 = v11	→	(E) 410 = 'v6'

Note: The A' and A" pairs were combined by a process of straight averaging.

TABLE 7.4

The choice of internal coordinates and internal displacement coordinates for $HClO_4$ (one redundancy)

internal coordinate	value assumed	corresponding displacement coordinate
S_{12}	1.630 Å	s_{12}
R_{13}	1.408 Å	r_{13}
R_{14}	"	r_{14}
R_{15}	"	r_{15}
G_{34}	112.5°	g_{34}
G_{35}	"	g_{35}
G_{45}	"	g_{45}
B_{23}	106.23°	b_{23}
B_{24}	"	b_{24}
B_{25}	"	b_{25}

TABLE 7.5

Calculated values for the elements of the g matrix

element	value
g1	0.087395
g2	-0.007990
g3	0.016987
g4	-0.019481
g5	0.091071
g6	-0.010934
g7	-0.018748
g8	0.023243
g9	-0.016828
g10	0.016587
g11	0.102908
g12	-0.024322
g13	-0.013486
g14	-0.035261
g15	0.085786
g16	-0.007206

TABLE 7.6

The final values adopted

for the elements

of the f matrix

element	description	value
f1	Cl-OH stretching constant (md/Å)	3.85
f2	Cl-OH,Cl-O stretch-stretch interaction constant (md/Å)	0.30
f3		0.00
f4	Cl-OH,O-Cl-OH stretch-bend interaction constant (X 10^{-3} dyne/rad)	0.462
f5	Cl-O stretching constant (md/Å)	9.20
f6		0.00
f7		0.00
f8		0.00
f9		0.00
f10		0.00
f11	O-Cl-O bending constant (X 10^{-11} erg/rad^2)	1.90
f12		0.00
f13		0.00
f14		0.00
f15	O-Cl-OH bending constant (X 10^{-11} erg/rad^2)	1.35
f16		0.00

TABLE 7.7

A comparison of

calculated and 'observed' *

vibrational frequencies

for perchloric acid

frequency	'observed' value (cm^{-1})	calculated value (cm^{-1})
v1	1050	1044
v2	725	723
v3	519	513
v4	1295	1301
v5	573	583
v6	410	428

* The observed values quoted are those estimated for the approximate C_{3v} model as indicated in table 7.3.

TABLE 7.8

Calculated values for the K matrix elements

elements	calculated value
K11	0.06926
K12	0.28603
K13	0.02807
K21	-0.15129
K22	0.00961
K23	-0.00927
K25	0.25895
K26	0.02912
K27	0.01048
K31	-0.21859
K32	0.06309
K33	-0.10350
K35	-0.10876
K36	-0.22504
K37	0.00679
K41	-0.10203
K42	0.18272
K43	0.13322
K45	0.10980
K46	0.04237
K47	0.21444

TABLE 7.9

The calculated
root mean square amplitudes of vibration
for the approximate C_{3v} model of $HClO_4$
at 308° K

interatomic distance	calculated u value (Å)
S_{12}	0.046
$R_{13,14,15}$	0.036
$P_{45,34,35}$	0.054
$Q_{23,24,25}$	0.064

CHAPTER EIGHT

AN INTRODUCTION TO THE STRUCTURE DETERMINATIONS OF CHAPTERS NINE TO FOURTEEN

Before presenting detailed discussions of the Cl_2O, $HClO_4$, $FClO_3$, ClO_2, SO_2 and SO_3 electron diffraction investigations, it is convenient to collect together in a single chapter, a number of explanatory notes relevant to all of these accounts. Such notes are given in sections one to eight below, and provide an introduction to the subject matter of Chapters Nine to Fourteen.

1. Experimentation

In each of Chapters Nine to Fourteen, a table is given which summarises experimental procedure. This table consists of several columns, one for each of the jet-to-plate distances at which diffraction patterns were recorded, and each column lists the following items of information:

(a) the wavelength of the electron beam

This was determined from powder patterns as described in section ten of Chapter Three, and was measured only once during each investigation, as it could be relied upon to remain constant throughout the

period of several days required for data collection.

(b) the sample temperature

This was normally adjusted until the sample vapour pressure was sufficient to enable a strong diffraction pattern to be recorded, and temperatures below 0° C were attained by immersing the sample tube in a carefully controlled acetone solid carbon dioxide bath.

(c) the nozzle temperature

Owing to the tendency shown by certain of the compounds studied (e.g. Cl_2O and SO_3) to condense on the nozzle tip, it was necessary to warm the incoming sample vapour by passing thermostatically regulated hot water through an appropriate part of the nozzle assembly. Nozzle temperatures up to 85° C were attained in this way.

(d) the temperature assumed for the diffracting vapour

In the case of Cl_2O this was determined roughly by carrying out a separate experiment, in which a thermocouple was suspended in the gas stream. In subsequent investigations, however, it was considered satisfactory to accept the arithmetic mean of the nozzle and sample temperatures as a reasonable estimate of this quantity.

(e) the number of plates used to provide intensity data

A minimum of four photographic plates was normally

required for each jet-to-plate distance.

(f) a description of the diffraction patterns obtained

Ideally electron diffraction patterns should be of medium blackness, and should show clear indications of diffraction rings right out to their outer limits. In tables 9.1 to 14.1, comments, based on these criteria, are given for the plates actually obtained.

(g) the number of microdensitometer traces measured

This number was increased from one investigation to the next, in an attempt to improve the accuracy of the uphill curves obtained, and in any one study it was found necessary to average more traces for twentyfive and eleven centimetre plates, than for those taken at the other two jet-to-plate distances.

This ends the list of items included in the columns of tables 9.1 to 14.1.

Since the substances studied in the present work were reactive, oxygen-containing, compounds of chlorine and sulphur, considerable care was taken when handling them, and all joints and stopcocks forming part of the glassware connected to the nozzle, and parts of the nozzle itself, were lubricated with KEL-F fluorocarbon grease. All samples, whether they were obtained commercially, or specially prepared, were purified using the electron diffraction apparatus to pump off

volatile contaminants, and diffraction patterns were normally recorded when a middle fraction of sample flowed into the diffraction chamber.

2. The diagrams presented

In each of Chapters Nine to Fourteen, uphill curves are quoted numerically, in tables, but the corresponding background curves are not discussed at all, and these should be assumed to be smooth increasing functions of s, similar in form to the curves shown in figures 4.2 to 4.5 for perchloryl fluoride. The experimental combined molecular intensity function $I_m(s)$ is presented graphically in each chapter, as is the corresponding radial distribution curve $O'(R)/R$.

Experimental radial distribution functions were calculated by numerical integration as described in section ten of Chapter Four, and to avoid the envelope effect, theoretical intensities were in each case added to the experimental $I_m(s)$ data, from s = 0 to s = smin, before applying Fourier transformation. The damping constant k was normally given the value 0.004 Å^2 in these calculations, unless particularly high resolution of similar internuclear distances was required. This value is larger than the 0.002-0.003 Å^2 strictly appropriate to $I_m(s)$ data terminating at S = 35 Å^{-1}, but

the extra damping was adopted to weight out high s intensity data of poor quality, and so reduce the ' noise level ' of the resulting $\sigma'(R)/R$ function.

In figures 9.1 to 14.1 and 9.2 to 14.2, the $I_m(s)$ and $\sigma'(R)/R$ curves presented are compared with corresponding theoretical functions calculated using equations 2.46 and 2.52 of Chapter Two. In these calculations the R_{ij} distances, and the overall scale factor assumed, were final values derived from least squares results, but the root mean square amplitudes of vibration also required, were chosen to be the spectroscopic results calculated in Chapters Six, Seven, and section eight of the present chapter. This choice was made in the hope of demonstrating systematic deviations between the observed and theoretical intensity functions. Such deviations should arise on account of the approximate nature of equation 2.46 which assumes the first Born approximation, and neglects anharmonicity of vibration. Examination of figures 9.1 to 14.1 reveals no definite indications of the extra damping, and slight phase shift, expected for the experimental curve relative to the theoretical one, but such effects should be most obvious at the higher s values, and the data presented have, with the possible exception of the $FClO_3$ case, rather low upper s limits.

A number of non-systematic deviations* are, however, illustrated in figures 9.1 to 14.1, and in certain cases it is evident that these could have been reduced by altering the final background curves chosen. Such discrepancies, particularly those occurring below s equals 25 A^{o-1}, are presumably responsible for the fairly large ' noise ripples ' appearing in certain of the experimental $O'(R)/R$ plots of figures 9.2 to 14.2 (see for example figure 12.2 for ClO_2). The final background curves adopted in the present work, may be justified, however, by the fact that they were constrained to be extremely smooth, and are therefore in no way biased towards a particular set of R_{ij} and u_{ij} results. This inflexibility did, however, lead to somewhat higher estimated standard deviations in these parameters, than might otherwise have been obtained.

3. The types of refinement carried out

In Chapters Nine to Fourteen, results obtained by three types of least squares refinement of $I_m(s)$ molecular intensity data, are presented in tabular form. These refinements, which differ in the nature of the $I_m(s)$ data fitted, may be described as follows:

(a) the single distance refinement

The $I_m(s)$ curve fitted in this case consisted of

* More correctly, a localised divergence is apparent in some of these figs., randomly situated.

a set of intensity values derived from microdensitometer data measured from plates taken at one jet-to-plate distance only. In this type of refinement, amplitudes of vibration were held constant at spectroscopic values to facilitate convergence.

(b) the ' combtwo ' refinement

The $I_m(s)$ curve fitted in this case was calculated from several sets of $I_m(s)$ data obtained at different jet-to-plate distances, by the processes of scaling and fusion described in Chapter Four, section nine. In this type of refinement, amplitudes were either varied, or held constant at spectroscopic values.

(c) the ' combscaled ' refinement

In this case the $I_m(s)$ data fitted consisted of a set of separate intensity curves obtained at different jet-to-plate distances, but put on the same scale, by the procedure described in section nine of Chapter Four, the fusion step being completely omitted. In this type of refinement, amplitudes were either varied, or held constant at spectroscopic values.

In those tables of Chapters Nine to Fourteen which present results of the least squares refinements carried out, only the final values obtained for the independent, refineable, R_{ij} parameters are quoted, together with those u_{ij} values also varied. The errors quoted in

these tables are in every case least squares estimated standard deviations. The residual R (see Chapter Four, section eleven) and the minimum value obtained for the function $\sum_i w\Delta_i^2$, are also included. In these tables, the amplitudes of vibration presented have not been corrected for failure of the first Born approximation.

4. The weighting schemes adopted

The function w(s) used to assign a weight factor to each intensity value fitted by least squares, has already been discussed in section eleven of Chapter Four. In the present work this function was assumed to consist of a horizontal, linear, w = 1 region, flanked by two exponential damping curves (w<1), and the exact analytical forms given to it for the various $I_m(s)$ data sets refined, are listed in table 8.1. The low s exponential section was intended to weight out intensity data subject to errors arising from background uncertainty, whilst the object of the high s section was to damp out the poorer quality intensity data measured at the edges of twentyfive, and over most of eleven centimetre, plates. The s limits of the horizontal region were decided by considering experimental uphill and $I_m(s)$ curves.

It is evident from table 8.1 that the damping function applied to the all-data-combined $I_m(s)$ curves is somewhat unrealistic insofar as it hardly weights out the poor quality high s data at all. In the present work such a function was adopted in an attempt to obtain the best possible values for the root mean square amplitudes of vibration, as these were of particular interest. In reality, refinements carried out using much steeper high s exponential curves resulted in no significant alterations in the R_{ij} and u_{ij} parameters, though their e.s.d.'s were reduced. It was therefore concluded that for data sets of the type collected in the present work, the outer damping function was not of critical importance.

For similar reasons, no special elaborate weighting scheme was adopted for the combscaled data, but instead the somewhat less realistic procedure of using the same scheme in both combtwo and combscaled refinements was followed.

5. The final R_{ij} and u_{ij} parameters accepted

The two principles adhered to when calculating final values for the structural parameters were (a) to average sets of R_{ij} and u_{ij} parameters obtained by all-data-combined least squares refinements, and

(b) to weight all sets of results equally when making this average, irrespective of whether the refinement producing a particular set was a combtwo or combscaled type, or whether amplitudes were varied or held constant at spectroscopic values. In this latter case, the spectroscopic amplitudes were not of course included in the averaging process. It should also be mentioned that in certain respects the dichlorine monoxide investigation was exceptional, and the above principles were modified somewhat in treating this particular case.

The procedure described above may be criticised on the grounds that combtwo and combscaled refinements should in principle be weighted differently, and that in many cases an amplitudes constant refinement is capable of producing more accurate R_{ij} parameters than a corresponding amplitudes variable one. The refinements carried out in the present work provided no strong evidence, however, to suggest that the combscaled method was a great deal more reliable than the combtwo procedure, and since equation 2.46 does not contain a $\cos\Delta\eta_{ij}$ factor, the amplitudes constant refinements were in the present work subject to uncertainties arising from this omission. In fact the amplitudes included as constants in these refinements, should have been first corrected to

' apparent values ' to compensate for failure of the first Born approximation, as described in section six below, but unfortunately the magnitude of this correction was not appreciated at the time of refinement.

In view of these remarks it was finally decided to adopt principles (a) and (b) above. The least squares e.s.d. values were also averaged in this way and reproducibilities calculated from the final results by applying the methods outlined in section twelve of Chapter Four.

The final average independent R_{ij} and u_{ij} parameters are listed together with their reproducibilities in certain of the tables of Chapters Nine to Fourteen. Dependent R_{ij} values, and valence angles, calculated from the independent distances, are also included in these tables, and the reproducibilities of these dependent parameters were derived using the standard methods available for combining errors. The amplitude values quoted in these tables have been corrected for failure of the first Born approximation according to the methods described in the section which follows.

6. Amplitude correction

Equation 2.46 assumes that the $\cos \Delta\eta_{ij}$ factor,

which should be included in any rigorous expression for the scattered electron intensity, is always close to unity for the molecules considered in Chapters Nine to Fourteen. When atom i is not the same type of atom as atom j, this assumption is not strictly correct, and its validity decreases as the difference in atomic number between atoms i and j increases. In the case of a Cl-O bond, for example, the effect of the cosine term is to damp the sine wave expected for this internuclear distance, and the damping produced is similar in nature to that caused by the vibrational $\exp(-\frac{1}{2}u^2s^2)$ factor, though considerably smaller in magnitude. It follows that if equation 2.46 is used to fit the experimental intensity data, certain of the u_{ij} parameters produced (those for which i and j refer to different types of atom) will have abnormally high values, owing to the assumption that all observed damping stems from the exponential factor.

Bonham and Ukaji[14] have derived equations which predict the correction necessary to convert the 'apparent amplitudes' obtained, to real values. Their method is based on the assumption, that for each atom, $\eta_i(s)$ can be written in the polynomial form $a+bs+cs^2$ where the coefficients a, b and c depend on the atomic number of the atom i. Hence $\Delta\eta_{ij}$ can be similarly expressed

and the effect of the cos $\Delta\eta_{ij}$ term assessed.

A list of apparent and corrected amplitude values calculated according to the more approximate equation given by Bonham and Ukaji, is presented in table 8.2, and these results may be used to construct correction curves, so that any observed Cl-O, S-O or Cl-F amplitudes may automatically be corrected for failure of the first Born approximation. The corrections given are probably accurate to 0.001 Å. In Chapters Nine to Fourteen, whenever corrected amplitudes are quoted, it may be assumed that table 8.2 has been consulted.

7. Correction of $r_g(1)$ bond lengths to r_e values

It is clearly of interest when comparing bond lengths obtained by electron diffraction, with those derived by other methods, to have $r_g(0)$ and r_e values available, as well as the $r_g(1)$ quantities obtained by least squares refinement. The relationships connecting these three types of distance have already been discussed in section eight of Chapter Two. To apply these equations it is necessary to know the root mean square amplitude of vibration u_{ij} corresponding to the bond concerned, and also the 'a' constant of the Morse potential. The first of these may be obtained either from the electron diffraction study itself, or

from spectroscopic calculations, but the second requires a knowledge of the force constant k, and the dissociation energy D, appropriate to the bond concerned. Of these latter two quantities, the first can be obtained by spectroscopic calculations, and the second can often be derived for simple molecules, by combining the heats of reaction of a series of chemical processes. Thus for Cl_2O, ClO_2, SO_2 and SO_3, stretching force constants were obtained from references 82, 83, 84 and 85, and average Cl-O and S-O dissociation energies from tables of thermodynamic data for these molecules. The ' a ' values calculated were obtained from the equation $a = (k/2D)^{\frac{1}{2}}$ given in reference 36, which is applicable when a Morse potential is assumed for the bond concerned. The results obtained are listed in table 8.3.

It should be added that a second set of ' a ' values was obtained for the Cl-O bonds in Cl_2O and ClO_2, and the S-O bond in SO_2, from the spectroscopic anharmonicity constants X_{33} , measured for the antisymmetrical stretching frequencies of vibration of these systems, and given in references 82, 86, and 87. The equation applied was $a = (8\pi^2\mu X_{33}/h)^{\frac{1}{2}}$, where μ is the reduced mass of the molecule if it is treated as an X-Y diatomic system. This method did

not seem as reliable as the first, and gave values for 'a' which were a good deal smaller than those listed in table 8.3. This second approach was therefore neglected.

No corrections to r_e values were made for the bonds of $HClO_4$ and $FClO_3$, although the 'a' values appropriate to the Cl_2O and ClO_2 molecules could presumably be used to give rough estimates of the equilibrium distances in these systems.

8. Calculation of spectroscopic amplitudes

Calculations of the amplitudes of vibration for perchloryl fluoride and perchloric acid have already been described in Chapters Six and Seven, and the values obtained were included as constants in certain of the least squares refinements discussed in Chapters Ten and Eleven. No such refinements were made for the remaining molecules Cl_2O, ClO_2, SO_2 and SO_3, however, as these systems do not contain similar internuclear distances. Nonetheless, amplitudes of vibration were calculated for the first three of these molecules for comparison purposes, amplitudes having already been calculated for SO_3 by Stølevik et al.[88]

For an XOX angular symmetrical molecule, four force constants are necessary to define the harmonic

potential function, if changes in the two X-O bond lengths, and the XOX angle, are chosen as internal displacement coordinates. These constants are defined in table 8.4, where the units appropriate to them are also indicated. Table 8.5 presents results calculated using the computer programme discussed in Appendix Four. Electron diffraction, or in some cases microwave structural parameters, were used as data in these calculations, and the temperature assumed was that estimated for the diffracting vapour in the electron diffraction experiment. The force constant information used was obtained from the infrared and microwave studies given in references 82, 83 and 84, and should be very reliable, though a correction[89] made to the results of reference 82, should, however, be noted. The amplitudes calculated for the bonded distances are almost certainly accurate to better than 0.001 Å, and those for the nonbonded distances to better than 0.003 Å.

TABLE 8.1

The weight functions adopted in least squares refinements

data set	s range	w
100 cm distance	$s<4$	$\exp(-0.07(4-s))$
	$4\leq s\leq 7$	1
	$s>7$	$\exp(-0.01(s-7))$
50 cm distance	$s<5$	$\exp(-0.07(5-s))$
	$5\leq s\leq 15$	1
	$s>15$	$\exp(-0.01(s-15))$
25 cm distance	$s<10$	$\exp(-0.07(10-s))$
	$10\leq s\leq 25$	1
	$s>25$	$\exp(-0.01(s-25))$
11 cm distance	$s<30$	$\exp(-0.07(30-s))$
	$30\leq s\leq 40$	1
	$s>40$	$\exp(-0.01(s-40))$
all distances combined	$s<5$	$\exp(-0.07(5-s))$
	$5\leq s\leq 30$	1
	$s>30$	$\exp(-0.01(s-30))$

TABLE 8.2

Correction of the u values

for failure of the Born approximation

distance type	real amplitude (Å)	apparent amplitude (Å)	correction (Å)
Cl-O	0.054	0.060	-0.006
	0.043	0.050	-0.007
	0.032	0.040	-0.008
S-O and Cl-F	0.055	0.060	-0.005
	0.044	0.050	-0.006
	0.033	0.040	-0.007

Note: These results were calculated according to equation 21 of reference 14.

TABLE 8.3

Morse potential 'a' values

calculated for certain Cl-O and S-O

bonds

from thermodynamic and force constant data

bond	estimated* dissocn. energy (kcals/mol)	force constant (md/A^{o})	a value (A^{o-1})
Cl-O (Cl_2O)	50	2.75	2.0
Cl-O (ClO_2)	63	7.00	2.8
S-O (SO_2)	120	10.02	2.5
S-O (SO_3)	110	10.60	2.6

Note: The dissociation energies of the ClO and SO radicals are 64 and 120 kcals/mole respectively.

* These energies were calculated by combining heats of reaction obtained from tables of thermodynamic data.

TABLE 8.4

A description of the XOX valence force field adopted

constant	symbol	units
X-O stretching constant	f_r	md/Å
X-O,X-O stretch-stretch interaction constant	f_{rr}	md/Å
X-O-X,X-O stretch-bend interaction constant	$f_{r\theta}$	10^{-3} dyn/rad
X-O-X bending constant	f_θ	10^{-11} erg/rad^2

TABLE 8.5

Calculated u values for the

XOX molecules studied by electron diffraction

molecule*	Cl_2O	ClO_2	SO_2
source of the force field used	ref. 82	ref. 83	ref. 84
f_r	2.75	7.01	10.02
f_{rr}	0.40	-0.16	0.03
$f_{r\theta}$	0.26	0.00	0.29
f_θ	1.32	1.41	1.63
temp. (^oK)	295	283	253
u_{O-X} ($\AA$)	0.051	0.039	0.035
$u_{X..X}$ ($\AA$)	0.068	0.063	0.055

* These calculations were performed for the Cl^{35}, S^{32} and O^{16} species of the molecules.

CHAPTER NINE

AN ELECTRON DIFFRACTION INVESTIGATION OF GASEOUS DICHLORINE MONOXIDE

1. Introduction

A number of previous electron diffraction investigations[90-92] have been carried out for dichlorine monoxide (Cl_2O), and of these, the most recent by Dunitz and Hedberg[92] in 1950, established moderately accurate dimensions for the molecule, but did not determine root mean square amplitudes of vibration.

In 1965 Rochkind and Pimentel published a detailed infrared investigation[82] of several isotopic species of the compound, and determined values for the four force constants necessary to define the molecule's harmonic potential function. One of their results, however, the stretch-bend interaction force constant $f_{r\theta}$, has subsequently been shown to be in error, and has been corrected by Beagley, Clark and Cruickshank[89].

In a recent microwave investigation[93] of the oxide, Millen et al. recorded spectra for the three chlorine substituted isotopic species, and determined r_s and r_o structural parameters with a high degree of precision. These authors also calculated the four force constants of the potential function, and the results they obtained agree well with those of Rochkind and Pimentel, if the

correction to $f_{r\theta}$, mentioned above, is taken into account.

The present electron diffraction investigation was undertaken to obtain accurate $r_g(1)$ internuclear distances for the molecule, and also values for the root mean square amplitudes of vibration. It was intended to compare these latter with corresponding spectroscopic results calculated from the force constant data of references 82 and 89.

2. Experimental

The sample of dichlorine monoxide studied was prepared according to a method described by Cady[94], and details of the experimental electron diffraction procedure adopted are given in table 9.1.

Two sets of microdensitometer traces were recorded from the photographic plates obtained, these sets of intensities being measured by means of the manual and automatic microdensitometers respectively. The automatic data were originally collected merely to check the results of the manual study, and accordingly eleven centimetre data were not included in this second investigation.

Uphill curves for the first and second studies are listed in tables 9.2 and 9.3 respectively, and a combined $I_m(s)$ function, calculated by averaging the two separate

experimental combined molecular intensity curves of the first and second investigations, is presented in figure 9.1. A corresponding radial distribution function is shown in figure 9.2, and confirms the angular symmetric nature of the molecule.

3. Results

The two internuclear distances R_{Cl-O} and $R_{Cl..Cl}$ were used to define the molecular geometry, and in least squares refinements these were varied independently together with their corresponding root mean square amplitudes of vibration.

Results of single distance refinements carried out as part of the manual and automatic microdensitometer studies are presented in tables 9.4 and 9.5 respectively, and it is evident, that of the two sets of data collected, the automatic set has the higher quality. This is indicated by the low residuals listed in table 9.5 for the hundred and fifty centimetre distance refinements, and also by the consistency of the R_{ij} parameters presented in this table. The automatic twentyfive centimetre data residual is anomalously high, however, owing to a lack of averaging of intensities, and to a poor choice of optical wedge made when using the automatic microdensitometer.

Table 9.6 presents results obtained by combtwo refinements carried out for both complete sets of intensity data collected. It is clear from this table that the automatic results are higher than those produced by the manual study, and a lower residual is achieved by the automatic data refinement.

The final structural parameters accepted for dichlorine monoxide are presented in table 9.7, and were obtained by making a 1:2 average of the two columns of table 9.6, the results derived from automatic data being favoured for the reasons mentioned above. The average standard deviations so calculated were reduced somewhat, as the two sets of results given in table 9.6 constitute to some extent independent measurements of the structural parameters. Reproducibilities were calculated from these reduced values.

4. Discussion

The molecular dimensions obtained by the present study are in agreement with those of previous electron diffraction investigations[90-92], if all error limits involved are taken into account, and the amplitudes of vibration also determined, agree well with the corresponding spectroscopic results presented in table 8.5.

It is of interest to compare the Cl-O bond length

and ClOCl valence angle obtained, with corresponding values determined by the microwave study of reference 93. In making such a comparison a difficulty arises, however, in knowing which of the three electron diffraction Cl-O distance types $r_g(1)$, $r_g(0)$ or r_e listed in table 9.8, to compare with the corresponding microwave r_s value. Clearly the $r_g(0)$ result is in best agreement with this latter, but since the r_s and r_o internuclear distances quoted in reference 93 are almost identical, it seems probable[96] that the microwave r_s bond length should in fact be compared with the electron diffraction r_e value, and as may be seen from table 9.8, such a comparison reveals a rather poor agreement between these quantities. This lack of consistency may, however, be a consequence of the fact that the microwave Cl-O internuclear distance is not in the full sense of the term an r_s parameter, since no attempt was made in the work described in reference 93 to isotopically substitute the central oxygen atom in the molecule. It follows that a more critical comparison of the two investigations may be made by comparing the $R_{Cl..Cl}$ distances obtained. In the microwave publication this parameter is not in fact quoted, but it is certainly the best determined one of the study and may be described absolutely correctly as

an r_s distance. A value of 2.800 Å can be calculated for this quantity from the published data, and this result agrees well with both the $r_g(1)$ and $r_g(0)$ electron diffraction values listed in table 9.8. Unfortunately, a corresponding electron diffraction r_e distance is difficult to estimate, but should not be much more than 0.005 Å shorter than the $r_g(1)$ value, and hence is still within error limit of the microwave r_s result. Such agreement suggests that the Cl-O distance obtained by the microwave investigation may be less accurate than originally claimed, and that a microwave study of the O^{18} species of Cl_2O would be worthwhile.

It is also of interest to compare the bond length and valence angle obtained for Cl_2O with corresponding $r_g(1)$ values determined for the ClOCl bridge in the molecule of chlorine heptoxide (Cl_2O_7). This latter compound has been studied by electron diffraction by Beagley[81], and the bridge dimensions he determined are 1.709 Å and 118.6° respectively, the corresponding reproducibilities being 0.004 Å and 0.7°. Thus the bond length in Cl_2O lengthens, and the valence angle increases on transition to $O_3ClOClO_3$. The second of these observations may be rationalised in terms of repulsion between the two ClO_3 groups in the heptoxide,

but the first is less obviously explained. A possible rationalisation may, however, be outlined as follows. In the case of chlorine heptoxide Beagley[81] has concluded that the Cl-O bridge bonds are bent, and has given a value of 109.2^{o} as the true angle between the two hybrid orbitals of the oxygen atom forming these bonds. Thus the bridging oxygen atom of the heptoxide may be described as sp^3 hybridised, and for this reason cannot become involved in the $d\pi$-$p\pi$ bonding suggested by Cruickshank[95] for molecules containing second row elements tetrahedrally coordinated by oxygen atoms. The bridge bonds in this compound may therefore be assumed to have no double bond character. In Cl_2O a similar state of affairs must exist, but in this case the Cl-O bonds are straight, and the valence angle of 111^{o} suggests that the hybrid orbitals used for bonding by the oxygen atom contain higher s character than those involved in the bridge bonding of chlorine heptoxide. Any slight amount of $d\pi$-$p\pi$ overlap made possible by the increased size of this angle when compared with the tetrahedral value, is presumably opposed by the presence of lone pairs of electrons on chlorine as discussed in reference 95. It may therefore be concluded that the bonds in dichlorine monoxide have little or no π character*, and are shorter than

* Wagner (ref. 104) also concluded this as a result of m.o. calculations.

the Cl-O bridge bonds found in Cl_2O_7 on account of the greater s character involved in the hybrid orbitals used for bonding by the central oxygen atom of Cl_2O, and the less efficient orbital overlap possible in forming the bent bonds of the heptoxide.

Most of the work presented in this chapter has been described in a recent publication[96] and it should be mentioned to avoid confusion, that the parameters given in this publication were obtained by making a 1:1 and not 1:2 average of the manual and automatic microdensitometer results, and that less rigorously smoothed background curves were assumed.

TABLE 9.1

A summary of experimental details

for the dichlorine monoxide investigation

jet to plate distance	100 cm	50 cm	25 cm	11 cm
wavelength (Å)	0.051162	0.051162	0.051162	0.051162
e.s.d.	0.000015	0.000015	0.000015	0.000015
sample temperature (°K)	246	246	246	246
nozzle temperature (°K)	363	363	363	363
gas temperature assumed (°K)	295	295	295	295
number of plates used	4	4	4	4
quality	good	good	good	good
number of traces measured (MMDM)	4	4	4	4
(AMDM)	4	4	4	0

MMDM = manual microdensitometer
AMDM = automatic microdensitometer

TABLE 9.2

Cl_2O intensity data(1) as combined uphill curves

range (1): s = 1.06 by 0.02 to 8.92 $Å^{-1}$

8.600_{10}	+2;	8.926_{10}	+2;	9.291_{10}	+2;	9.670_{10}	+2;	1.006_{10}	+3;
1.047_{10}	+3;	1.088_{10}	+3;	1.127_{10}	+3;	1.167_{10}	+3;	1.206_{10}	+3;
1.244_{10}	+3;	1.282_{10}	+3;	1.319_{10}	+3;	1.355_{10}	+3;	1.390_{10}	+3;
1.427_{10}	+3;	1.463_{10}	+3;	1.501_{10}	+3;	1.541_{10}	+3;	1.583_{10}	+3;
1.625_{10}	+3;	1.668_{10}	+3;	1.710_{10}	+3;	1.754_{10}	+3;	1.798_{10}	+3;
1.841_{10}	+3;	1.885_{10}	+3;	1.929_{10}	+3;	1.974_{10}	+3;	2.021_{10}	+3;
2.067_{10}	+3;	2.116_{10}	+3;	2.166_{10}	+3;	2.218_{10}	+3;	2.270_{10}	+3;
2.325_{10}	+3;	2.382_{10}	+3;	2.439_{10}	+3;	2.500_{10}	+3;	2.562_{10}	+3;
2.624_{10}	+3;	2.690_{10}	+3;	2.757_{10}	+3;	2.828_{10}	+3;	2.899_{10}	+3;
2.973_{10}	+3;	3.049_{10}	+3;	3.129_{10}	+3;	3.207_{10}	+3;	3.287_{10}	+3;
3.368_{10}	+3;	3.451_{10}	+3;	3.535_{10}	+3;	3.618_{10}	+3;	3.704_{10}	+3;
3.791_{10}	+3;	3.880_{10}	+3;	3.973_{10}	+3;	4.065_{10}	+3;	4.160_{10}	+3;
4.256_{10}	+3;	4.351_{10}	+3;	4.450_{10}	+3;	4.548_{10}	+3;	4.650_{10}	+3;
4.753_{10}	+3;	4.855_{10}	+3;	4.959_{10}	+3;	5.064_{10}	+3;	5.171_{10}	+3;
5.276_{10}	+3;	5.386_{10}	+3;	5.496_{10}	+3;	5.604_{10}	+3;	5.716_{10}	+3;
5.825_{10}	+3;	5.934_{10}	+3;	6.043_{10}	+3;	6.155_{10}	+3;	6.264_{10}	+3;
6.374_{10}	+3;	6.484_{10}	+3;	6.590_{10}	+3;	6.696_{10}	+3;	6.799_{10}	+3;
6.905_{10}	+3;	7.011_{10}	+3;	7.119_{10}	+3;	7.224_{10}	+3;	7.331_{10}	+3;
7.435_{10}	+3;	7.533_{10}	+3;	7.636_{10}	+3;	7.735_{10}	+3;	7.834_{10}	+3;
7.933_{10}	+3;	8.034_{10}	+3;	8.131_{10}	+3;	8.232_{10}	+3;	8.335_{10}	+3;
8.432_{10}	+3;	8.530_{10}	+3;	8.625_{10}	+3;	8.724_{10}	+3;	8.821_{10}	+3;
8.917_{10}	+3;	9.011_{10}	+3;	9.105_{10}	+3;	9.198_{10}	+3;	9.292_{10}	+3;
9.382_{10}	+3;	9.475_{10}	+3;	9.567_{10}	+3;	9.661_{10}	+3;	9.756_{10}	+3;
9.851_{10}	+3;	9.950_{10}	+3;	1.004_{10}	+4;	1.014_{10}	+4;	1.024_{10}	+4;
1.034_{10}	+4;	1.044_{10}	+4;	1.055_{10}	+4;	1.065_{10}	+4;	1.076_{10}	+4;
1.086_{10}	+4;	1.097_{10}	+4;	1.108_{10}	+4;	1.119_{10}	+4;	1.131_{10}	+4;
1.142_{10}	+4;	1.154_{10}	+4;	1.166_{10}	+4;	1.178_{10}	+4;	1.191_{10}	+4;
1.204_{10}	+4;	1.217_{10}	+4;	1.230_{10}	+4;	1.244_{10}	+4;	1.257_{10}	+4;
1.271_{10}	+4;	1.285_{10}	+4;	1.299_{10}	+4;	1.313_{10}	+4;	1.327_{10}	+4;
1.342_{10}	+4;	1.358_{10}	+4;	1.374_{10}	+4;	1.389_{10}	+4;	1.405_{10}	+4;
1.422_{10}	+4;	1.439_{10}	+4;	1.455_{10}	+4;	1.472_{10}	+4;	1.488_{10}	+4;
1.506_{10}	+4;	1.522_{10}	+4;	1.539_{10}	+4;	1.556_{10}	+4;	1.573_{10}	+4;
1.590_{10}	+4;	1.607_{10}	+4;	1.624_{10}	+4;	1.640_{10}	+4;	1.656_{10}	+4;
1.672_{10}	+4;	1.688_{10}	+4;	1.705_{10}	+4;	1.721_{10}	+4;	1.736_{10}	+4;
1.751_{10}	+4;	1.767_{10}	+4;	1.784_{10}	+4;	1.798_{10}	+4;	1.813_{10}	+4;
1.829_{10}	+4;	1.844_{10}	+4;	1.857_{10}	+4;	1.872_{10}	+4;	1.885_{10}	+4;
1.897_{10}	+4;	1.910_{10}	+4;	1.922_{10}	+4;	1.935_{10}	+4;	1.947_{10}	+4;
1.959_{10}	+4;	1.969_{10}	+4;	1.980_{10}	+4;	1.990_{10}	+4;	1.998_{10}	+4;
2.008_{10}	+4;	2.017_{10}	+4;	2.025_{10}	+4;	2.032_{10}	+4;	2.039_{10}	+4;
2.046_{10}	+4;	2.052_{10}	+4;	2.058_{10}	+4;	2.064_{10}	+4;	2.068_{10}	+4;
2.073_{10}	+4;	2.077_{10}	+4;	2.080_{10}	+4;	2.083_{10}	+4;	2.085_{10}	+4;
2.087_{10}	+4;	2.089_{10}	+4;	2.089_{10}	+4;	2.090_{10}	+4;	2.089_{10}	+4;
2.089_{10}	+4;	2.088_{10}	+4;	2.086_{10}	+4;	2.085_{10}	+4;	2.083_{10}	+4;
2.081_{10}	+4;	2.079_{10}	+4;	2.077_{10}	+4;	2.074_{10}	+4;	2.072_{10}	+4;
2.068_{10}	+4;	2.064_{10}	+4;	2.059_{10}	+4;	2.056_{10}	+4;	2.052_{10}	+4;

TABLE 9.2 (cont'd)

2.048_{10}	+4;	2.044_{10}	+4;	2.041_{10}	+4;	2.039_{10}	+4;	2.034_{10}	+4;
2.032_{10}	+4;	2.027_{10}	+4;	2.023_{10}	+4;	2.021_{10}	+4;	2.018_{10}	+4;
2.013_{10}	+4;	2.010_{10}	+4;	2.008_{10}	+4;	2.005_{10}	+4;	2.002_{10}	+4;
2.001_{10}	+4;	1.997_{10}	+4;	1.995_{10}	+4;	1.993_{10}	+4;	1.991_{10}	+4;
1.990_{10}	+4;	1.991_{10}	+4;	1.990_{10}	+4;	1.992_{10}	+4;	1.992_{10}	+4;
1.993_{10}	+4;	1.994_{10}	+4;	1.996_{10}	+4;	1.997_{10}	+4;	2.000_{10}	+4;
2.004_{10}	+4;	2.008_{10}	+4;	2.012_{10}	+4;	2.016_{10}	+4;	2.021_{10}	+4;
2.026_{10}	+4;	2.031_{10}	+4;	2.038_{10}	+4;	2.044_{10}	+4;	2.052_{10}	+4;
2.059_{10}	+4;	2.068_{10}	+4;	2.076_{10}	+4;	2.087_{10}	+4;	2.095_{10}	+4;
2.104_{10}	+4;	2.113_{10}	+4;	2.124_{10}	+4;	2.135_{10}	+4;	2.145_{10}	+4;
2.156_{10}	+4;	2.165_{10}	+4;	2.177_{10}	+4;	2.188_{10}	+4;	2.200_{10}	+4;
2.214_{10}	+4;	2.228_{10}	+4;	2.240_{10}	+4;	2.254_{10}	+4;	2.267_{10}	+4;
2.281_{10}	+4;	2.294_{10}	+4;	2.308_{10}	+4;	2.322_{10}	+4;	2.336_{10}	+4;
2.350_{10}	+4;	2.364_{10}	+4;	2.378_{10}	+4;	2.393_{10}	+4;	2.407_{10}	+4;
2.420_{10}	+4;	2.434_{10}	+4;	2.447_{10}	+4;	2.461_{10}	+4;	2.476_{10}	+4;
2.490_{10}	+4;	2.504_{10}	+4;	2.518_{10}	+4;	2.531_{10}	+4;	2.546_{10}	+4;
2.560_{10}	+4;	2.572_{10}	+4;	2.585_{10}	+4;	2.599_{10}	+4;	2.611_{10}	+4;
2.623_{10}	+4;	2.635_{10}	+4;	2.646_{10}	+4;	2.659_{10}	+4;	2.670_{10}	+4;
2.681_{10}	+4;	2.692_{10}	+4;	2.705_{10}	+4;	2.716_{10}	+4;	2.725_{10}	+4;
2.736_{10}	+4;	2.746_{10}	+4;	2.757_{10}	+4;	2.764_{10}	+4;	2.774_{10}	+4;
2.785_{10}	+4;	2.792_{10}	+4;	2.802_{10}	+4;	2.812_{10}	+4;	2.821_{10}	+4;
2.831_{10}	+4;	2.840_{10}	+4;	2.847_{10}	+4;	2.855_{10}	+4;	2.861_{10}	+4;
2.870_{10}	+4;	2.876_{10}	+4;	2.885_{10}	+4;	2.894_{10}	+4;	2.900_{10}	+4;
2.905_{10}	+4;	2.914_{10}	+4;	2.920_{10}	+4;	2.926_{10}	+4;	2.932_{10}	+4;
2.938_{10}	+4;	2.945_{10}	+4;	2.951_{10}	+4;	2.957_{10}	+4;	2.963_{10}	+4;
2.970_{10}	+4;	2.977_{10}	+4;	2.983_{10}	+4;	2.988_{10}	+4;	2.994_{10}	+4;
3.003_{10}	+4;	3.010_{10}	+4;	3.018_{10}	+4;	3.026_{10}	+4;	3.033_{10}	+4;
3.039_{10}	+4;	3.046_{10}	+4;	3.051_{10}	+4;	3.058_{10}	+4;	3.064_{10}	+4;
3.072_{10}	+4;	3.080_{10}	+4;	3.090_{10}	+4;	3.098_{10}	+4;	3.106_{10}	+4;
3.114_{10}	+4;	3.121_{10}	+4;	3.130_{10}	+4;	3.138_{10}	+4;	3.146_{10}	+4;
3.155_{10}	+4;	3.165_{10}	+4;	3.174_{10}	+4;	3.184_{10}	+4;	3.193_{10}	+4;
3.201_{10}	+4;	3.210_{10}	+4;	3.219_{10}	+4;	3.227_{10}	+4;	3.236_{10}	+4;
3.244_{10}	+4;	3.254_{10}	+4;	3.262_{10}	+4;	3.271_{10}	+4;	3.278_{10}	+4;
3.287_{10}	+4;	3.294_{10}	+4;	3.303_{10}	+4;	3.310_{10}	+4;		

range (2): s = 2.85 by 0.05 to 18.00 Å^{-1}

5.241_{10}	+4;	5.410_{10}	+4;	5.571_{10}	+4;	5.730_{10}	+4;	5.881_{10}	+4;
6.026_{10}	+4;	6.165_{10}	+4;	6.304_{10}	+4;	6.437_{10}	+4;	6.570_{10}	+4;
6.712_{10}	+4;	6.871_{10}	+4;	7.033_{10}	+4;	7.198_{10}	+4;	7.372_{10}	+4;
7.555_{10}	+4;	7.741_{10}	+4;	7.942_{10}	+4;	8.149_{10}	+4;	8.365_{10}	+4;
8.596_{10}	+4;	8.831_{10}	+4;	9.074_{10}	+4;	9.325_{10}	+4;	9.585_{10}	+4;

TABLE 9.2 (cont'd)

9.848_{10} +4;	1.011_{10} +5;	1.039_{10} +5;	1.065_{10} +5;	1.091_{10} +5;
1.116_{10} +5;	1.140_{10} +5;	1.164_{10} +5;	1.187_{10} +5;	1.208_{10} +5;
1.228_{10} +5;	1.246_{10} +5;	1.264_{10} +5;	1.280_{10} +5;	1.296_{10} +5;
1.309_{10} +5;	1.319_{10} +5;	1.327_{10} +5;	1.333_{10} +5;	1.338_{10} +5;
1.341_{10} +5;	1.342_{10} +5;	1.341_{10} +5;	1.339_{10} +5;	1.333_{10} +5;
1.327_{10} +5;	1.320_{10} +5;	1.312_{10} +5;	1.303_{10} +5;	1.293_{10} +5;
1.286_{10} +5;	1.275_{10} +5;	1.267_{10} +5;	1.260_{10} +5;	1.254_{10} +5;
1.249_{10} +5;	1.246_{10} +5;	1.242_{10} +5;	1.239_{10} +5;	1.238_{10} +5;
1.239_{10} +5;	1.241_{10} +5;	1.246_{10} +5;	1.252_{10} +5;	1.261_{10} +5;
1.271_{10} +5;	1.283_{10} +5;	1.295_{10} +5;	1.309_{10} +5;	1.322_{10} +5;
1.337_{10} +5;	1.354_{10} +5;	1.372_{10} +5;	1.390_{10} +5;	1.409_{10} +5;
1.428_{10} +5;	1.446_{10} +5;	1.466_{10} +5;	1.484_{10} +5;	1.502_{10} +5;
1.522_{10} +5;	1.539_{10} +5;	1.557_{10} +5;	1.574_{10} +5;	1.589_{10} +5;
1.603_{10} +5;	1.615_{10} +5;	1.625_{10} +5;	1.636_{10} +5;	1.649_{10} +5;
1.658_{10} +5;	1.666_{10} +5;	1.674_{10} +5;	1.683_{10} +5;	1.692_{10} +5;
1.698_{10} +5;	1.704_{10} +5;	1.711_{10} +5;	1.717_{10} +5;	1.723_{10} +5;
1.729_{10} +5;	1.736_{10} +5;	1.742_{10} +5;	1.748_{10} +5;	1.755_{10} +5;
1.761_{10} +5;	1.768_{10} +5;	1.774_{10} +5;	1.781_{10} +5;	1.788_{10} +5;
1.797_{10} +5;	1.802_{10} +5;	1.814_{10} +5;	1.824_{10} +5;	1.833_{10} +5;
1.841_{10} +5;	1.847_{10} +5;	1.856_{10} +5;	1.862_{10} +5;	1.871_{10} +5;
1.879_{10} +5;	1.889_{10} +5;	1.896_{10} +5;	1.903_{10} +5;	1.910_{10} +5;
1.918_{10} +5;	1.924_{10} +5;	1.927_{10} +5;	1.931_{10} +5;	1.932_{10} +5;
1.930_{10} +5;	1.932_{10} +5;	1.934_{10} +5;	1.933_{10} +5;	1.933_{10} +5;
1.937_{10} +5;	1.941_{10} +5;	1.942_{10} +5;	1.942_{10} +5;	1.500_{10} +5;
1.948_{10} +5;	1.950_{10} +5;	1.955_{10} +5;	1.959_{10} +5;	1.967_{10} +5;
1.976_{10} +5;	1.984_{10} +5;	1.992_{10} +5;	2.002_{10} +5;	2.012_{10} +5;
2.026_{10} +5;	2.039_{10} +5;	2.052_{10} +5;	2.065_{10} +5;	2.083_{10} +5;
2.100_{10} +5;	2.124_{10} +5;	2.146_{10} +5;	2.168_{10} +5;	2.190_{10} +5;
2.209_{10} +5;	2.227_{10} +5;	2.244_{10} +5;	2.265_{10} +5;	2.283_{10} +5;
2.301_{10} +5;	2.318_{10} +5;	2.340_{10} +5;	2.359_{10} +5;	2.376_{10} +5;
2.391_{10} +5;	2.404_{10} +5;	2.414_{10} +5;	2.426_{10} +5;	2.435_{10} +5;
2.441_{10} +5;	2.449_{10} +5;	2.458_{10} +5;	2.466_{10} +5;	2.473_{10} +5;
2.477_{10} +5;	2.485_{10} +5;	2.485_{10} +5;	2.489_{10} +5;	2.494_{10} +5;
2.494_{10} +5;	2.492_{10} +5;	2.494_{10} +5;	2.502_{10} +5;	2.503_{10} +5;
2.500_{10} +5;	2.501_{10} +5;	2.502_{10} +5;	2.500_{10} +5;	2.504_{10} +5;
2.506_{10} +5;	2.509_{10} +5;	2.512_{10} +5;	2.518_{10} +5;	2.525_{10} +5;
2.533_{10} +5;	2.540_{10} +5;	2.546_{10} +5;	2.551_{10} +5;	2.559_{10} +5;
2.568_{10} +5;	2.578_{10} +5;	2.587_{10} +5;	2.594_{10} +5;	2.605_{10} +5;
2.614_{10} +5;	2.627_{10} +5;	2.637_{10} +5;	2.647_{10} +5;	2.659_{10} +5;
2.669_{10} +5;	2.684_{10} +5;	2.695_{10} +5;	2.705_{10} +5;	2.716_{10} +5;
2.726_{10} +5;	2.735_{10} +5;	2.741_{10} +5;	2.751_{10} +5;	2.762_{10} +5;
2.772_{10} +5;	2.781_{10} +5;	2.786_{10} +5;	2.795_{10} +5;	2.806_{10} +5;
2.816_{10} +5;	2.824_{10} +5;	2.833_{10} +5;	2.846_{10} +5;	2.857_{10} +5;
2.870_{10} +5;	2.881_{10} +5;	2.891_{10} +5;	2.901_{10} +5;	2.910_{10} +5;
2.923_{10} +5;	2.934_{10} +5;	2.946_{10} +5;	2.960_{10} +5;	2.976_{10} +5;
2.992_{10} +5;	3.003_{10} +5;	3.018_{10} +5;	3.031_{10} +5;	3.047_{10} +5;
3.066_{10} +5;	3.079_{10} +5;	3.092_{10} +5;	3.105_{10} +5;	3.116_{10} +5;
3.133_{10} +5;	3.148_{10} +5;	3.155_{10} +5;	3.164_{10} +5;	3.172_{10} +5;
3.180_{10} +5;	3.186_{10} +5;	3.197_{10} +5;	3.209_{10} +5;	3.218_{10} +5;

3.229_{10} +5; 3.234_{10} +5; 3.244_{10} +5; 3.249_{10} +5; 3.257_{10} +5;
3.261_{10} +5; 3.267_{10} +5; 3.273_{10} +5; 3.276_{10} +5; 3.283_{10} +5;
3.288_{10} +5; 3.292_{10} +5; 3.293_{10} +5; 3.299_{10} +5; 3.304_{10} +5;
3.305_{10} +5; 3.309_{10} +5; 3.312_{10} +5; 3.316_{10} +5; 3.318_{10} +5;
3.324_{10} +5; 3.330_{10} +5; 3.340_{10} +5; 3.342_{10} +5; 3.348_{10} +5;
3.353_{10} +5; 3.353_{10} +5; 3.358_{10} +5; 3.361_{10} +5; 3.363_{10} +5;
3.365_{10} +5; 3.363_{10} +5; 3.362_{10} +5; 3.356_{10} +5;

range (3): s= 10.3 by 0.10 to 32.30 Å^{-1}

7.876_{10} +6; 7.901_{10} +6; 7.944_{10} +6; 8.005_{10} +6; 8.081_{10} +6;
8.158_{10} +6; 8.266_{10} +6; 8.402_{10} +6; 8.533_{10} +6; 8.653_{10} +6;
8.783_{10} +6; 8.881_{10} +6; 8.991_{10} +6; 9.078_{10} +6; 9.153_{10} +6;
9.218_{10} +6; 9.257_{10} +6; 9.292_{10} +6; 9.296_{10} +6; 9.308_{10} +6;
9.308_{10} +6; 9.281_{10} +6; 9.250_{10} +6; 9.235_{10} +6; 9.196_{10} +6;
9.169_{10} +6; 9.167_{10} +6; 9.179_{10} +6; 9.198_{10} +6; 9.247_{10} +6;
9.301_{10} +6; 9.357_{10} +6; 9.425_{10} +6; 9.491_{10} +6; 9.568_{10} +6;
9.627_{10} +6; 9.683_{10} +6; 9.742_{10} +6; 9.787_{10} +6; 9.836_{10} +6;
9.872_{10} +6; 9.904_{10} +6; 9.927_{10} +6; 9.971_{10} +6; 9.996_{10} +6;
1.004_{10} +7; 1.008_{10} +7; 1.013_{10} +7; 1.019_{10} +7; 1.027_{10} +7;
1.035_{10} +7; 1.041_{10} +7; 1.049_{10} +7; 1.057_{10} +7; 1.064_{10} +7;
1.069_{10} +7; 1.076_{10} +7; 1.082_{10} +7; 1.085_{10} +7; 1.089_{10} +7;
1.092_{10} +7; 1.093_{10} +7; 1.092_{10} +7; 1.092_{10} +7; 1.091_{10} +7;
1.088_{10} +7; 1.085_{10} +7; 1.083_{10} +7; 1.081_{10} +7; 1.081_{10} +7;
1.079_{10} +7; 1.081_{10} +7; 1.084_{10} +7; 1.089_{10} +7; 1.094_{10} +7;
1.101_{10} +7; 1.107_{10} +7; 1.115_{10} +7; 1.123_{10} +7; 1.132_{10} +7;
1.139_{10} +7; 1.146_{10} +7; 1.153_{10} +7; 1.159_{10} +7; 1.165_{10} +7;
1.172_{10} +7; 1.178_{10} +7; 1.184_{10} +7; 1.190_{10} +7; 1.192_{10} +7;
1.195_{10} +7; 1.197_{10} +7; 1.200_{10} +7; 1.202_{10} +7; 1.204_{10} +7;
1.208_{10} +7; 1.209_{10} +7; 1.211_{10} +7; 1.215_{10} +7; 1.216_{10} +7;
1.218_{10} +7; 1.220_{10} +7; 1.222_{10} +7; 1.225_{10} +7; 1.228_{10} +7;
1.231_{10} +7; 1.234_{10} +7; 1.236_{10} +7; 1.236_{10} +7; 1.238_{10} +7;
1.241_{10} +7; 1.243_{10} +7; 1.246_{10} +7; 1.250_{10} +7; 1.256_{10} +7;
1.259_{10} +7; 1.264_{10} +7; 1.270_{10} +7; 1.275_{10} +7; 1.279_{10} +7;
1.287_{10} +7; 1.297_{10} +7; 1.303_{10} +7; 1.311_{10} +7; 1.317_{10} +7;
1.323_{10} +7; 1.330_{10} +7; 1.335_{10} +7; 1.340_{10} +7; 1.345_{10} +7;
1.349_{10} +7; 1.351_{10} +7; 1.353_{10} +7; 1.355_{10} +7; 1.357_{10} +7;
1.359_{10} +7; 1.360_{10} +7; 1.362_{10} +7; 1.364_{10} +7; 1.365_{10} +7;
1.368_{10} +7; 1.371_{10} +7; 1.373_{10} +7; 1.378_{10} +7; 1.381_{10} +7;
1.386_{10} +7; 1.393_{10} +7; 1.398_{10} +7; 1.403_{10} +7; 1.408_{10} +7;
1.413_{10} +7; 1.417_{10} +7; 1.420_{10} +7; 1.424_{10} +7; 1.428_{10} +7;
1.432_{10} +7; 1.435_{10} +7; 1.440_{10} +7; 1.446_{10} +7; 1.450_{10} +7;

TABLE 9.2 (cont'd)

1.454_{10} +7; 1.459_{10} +7; 1.464_{10} +7; 1.471_{10} +7; 1.477_{10} +7;
1.484_{10} +7; 1.492_{10} +7; 1.497_{10} +7; 1.505_{10} +7; 1.508_{10} +7;
1.515_{10} +7; 1.518_{10} +7; 1.523_{10} +7; 1.528_{10} +7; 1.532_{10} +7;
1.536_{10} +7; 1.540_{10} +7; 1.543_{10} +7; 1.546_{10} +7; 1.550_{10} +7;
1.554_{10} +7; 1.560_{10} +7; 1.565_{10} +7; 1.570_{10} +7; 1.576_{10} +7;
1.582_{10} +7; 1.588_{10} +7; 1.596_{10} +7; 1.603_{10} +7; 1.611_{10} +7;
1.619_{10} +7; 1.629_{10} +7; 1.636_{10} +7; 1.642_{10} +7; 1.648_{10} +7;
1.656_{10} +7; 1.663_{10} +7; 1.669_{10} +7; 1.676_{10} +7; 1.682_{10} +7;
1.688_{10} +7; 1.693_{10} +7; 1.697_{10} +7; 1.703_{10} +7; 1.708_{10} +7;
1.712_{10} +7; 1.721_{10} +7; 1.727_{10} +7; 1.735_{10} +7; 1.743_{10} +7;
1.752_{10} +7; 1.758_{10} +7; 1.767_{10} +7; 1.774_{10} +7; 1.781_{10} +7;
1.789_{10} +7; 1.796_{10} +7; 1.802_{10} +7; 1.809_{10} +7; 1.818_{10} +7;
1.825_{10} +7;

range (4): s = 20.46 by 0.22 to 39.60 Å^{-1}

1.408_{10} +8; 1.403_{10} +8; 1.395_{10} +8; 1.381_{10} +8; 1.371_{10} +8;
1.364_{10} +8; 1.362_{10} +8; 1.362_{10} +8; 1.365_{10} +8; 1.369_{10} +8;
1.374_{10} +8; 1.378_{10} +8; 1.384_{10} +8; 1.386_{10} +8; 1.388_{10} +8;
1.387_{10} +8; 1.384_{10} +8; 1.383_{10} +8; 1.379_{10} +8; 1.380_{10} +8;
1.381_{10} +8; 1.385_{10} +8; 1.391_{10} +8; 1.394_{10} +8; 1.394_{10} +8;
1.398_{10} +8; 1.399_{10} +8; 1.400_{10} +8; 1.398_{10} +8; 1.400_{10} +8;
1.399_{10} +8; 1.398_{10} +8; 1.398_{10} +8; 1.395_{10} +8; 1.395_{10} +8;
1.392_{10} +8; 1.389_{10} +8; 1.390_{10} +8; 1.391_{10} +8; 1.393_{10} +8;
1.399_{10} +8; 1.405_{10} +8; 1.410_{10} +8; 1.415_{10} +8; 1.421_{10} +8;
1.424_{10} +8; 1.430_{10} +8; 1.435_{10} +8; 1.438_{10} +8; 1.444_{10} +8;
1.450_{10} +8; 1.453_{10} +8; 1.458_{10} +8; 1.459_{10} +8; 1.461_{10} +8;
1.463_{10} +8; 1.465_{10} +8; 1.468_{10} +8; 1.474_{10} +8; 1.479_{10} +8;
1.484_{10} +8; 1.491_{10} +8; 1.496_{10} +8; 1.500_{10} +8; 1.506_{10} +8;
1.510_{10} +8; 1.510_{10} +8; 1.514_{10} +8; 1.518_{10} +8; 1.521_{10} +8;
1.525_{10} +8; 1.531_{10} +8; 1.538_{10} +8; 1.543_{10} +8; 1.550_{10} +8;
1.555_{10} +8; 1.560_{10} +8; 1.567_{10} +8; 1.574_{10} +8; 1.581_{10} +8;
1.587_{10} +8; 1.595_{10} +8; 1.601_{10} +8; 1.608_{10} +8; 1.615_{10} +8;
1.623_{10} +8; 1.631_{10} +8; 1.639_{10} +8;

TABLE 9.2 (cont'd)

1.454_{10} +7; 1.459_{10} +7; 1.464_{10} +7; 1.471_{10} +7; 1.477_{10} +7;
1.484_{10} +7; 1.492_{10} +7; 1.497_{10} +7; 1.505_{10} +7; 1.508_{10} +7;
1.515_{10} +7; 1.518_{10} +7; 1.523_{10} +7; 1.528_{10} +7; 1.532_{10} +7;
1.536_{10} +7; 1.540_{10} +7; 1.543_{10} +7; 1.546_{10} +7; 1.550_{10} +7;
1.554_{10} +7; 1.560_{10} +7; 1.565_{10} +7; 1.570_{10} +7; 1.576_{10} +7;
1.582_{10} +7; 1.588_{10} +7; 1.596_{10} +7; 1.603_{10} +7; 1.611_{10} +7;
1.619_{10} +7; 1.629_{10} +7; 1.636_{10} +7; 1.642_{10} +7; 1.648_{10} +7;
1.656_{10} +7; 1.663_{10} +7; 1.669_{10} +7; 1.676_{10} +7; 1.682_{10} +7;
1.688_{10} +7; 1.693_{10} +7; 1.697_{10} +7; 1.703_{10} +7; 1.708_{10} +7;
1.712_{10} +7; 1.721_{10} +7; 1.727_{10} +7; 1.735_{10} +7; 1.743_{10} +7;
1.752_{10} +7; 1.758_{10} +7; 1.767_{10} +7; 1.774_{10} +7; 1.781_{10} +7;
1.789_{10} +7; 1.796_{10} +7; 1.802_{10} +7; 1.809_{10} +7; 1.818_{10} +7;
1.825_{10} +7;

range (4): s = 20.46 by 0.22 to 39.60 $\mathring{A}^{-1}$

1.408_{10} +8; 1.403_{10} +8; 1.395_{10} +8; 1.381_{10} +8; 1.371_{10} +8;
1.364_{10} +8; 1.362_{10} +8; 1.362_{10} +8; 1.365_{10} +8; 1.369_{10} +8;
1.374_{10} +8; 1.378_{10} +8; 1.384_{10} +8; 1.386_{10} +8; 1.388_{10} +8;
1.387_{10} +8; 1.384_{10} +8; 1.383_{10} +8; 1.379_{10} +8; 1.380_{10} +8;
1.381_{10} +8; 1.385_{10} +8; 1.391_{10} +8; 1.394_{10} +8; 1.394_{10} +8;
1.398_{10} +8; 1.399_{10} +8; 1.400_{10} +8; 1.398_{10} +8; 1.400_{10} +8;
1.399_{10} +8; 1.398_{10} +8; 1.398_{10} +8; 1.395_{10} +8; 1.395_{10} +8;
1.392_{10} +8; 1.389_{10} +8; 1.390_{10} +8; 1.391_{10} +8; 1.393_{10} +8;
1.399_{10} +8; 1.405_{10} +8; 1.410_{10} +8; 1.415_{10} +8; 1.421_{10} +8;
1.424_{10} +8; 1.430_{10} +8; 1.435_{10} +8; 1.438_{10} +8; 1.444_{10} +8;
1.450_{10} +8; 1.453_{10} +8; 1.458_{10} +8; 1.459_{10} +8; 1.461_{10} +8;
1.463_{10} +8; 1.465_{10} +8; 1.468_{10} +8; 1.474_{10} +8; 1.479_{10} +8;
1.484_{10} +8; 1.491_{10} +8; 1.496_{10} +8; 1.500_{10} +8; 1.506_{10} +8;
1.510_{10} +8; 1.510_{10} +8; 1.514_{10} +8; 1.518_{10} +8; 1.521_{10} +8;
1.525_{10} +8; 1.531_{10} +8; 1.538_{10} +8; 1.543_{10} +8; 1.550_{10} +8;
1.555_{10} +8; 1.560_{10} +8; 1.567_{10} +8; 1.574_{10} +8; 1.581_{10} +8;
1.587_{10} +8; 1.595_{10} +8; 1.601_{10} +8; 1.608_{10} +8; 1.615_{10} +8;
1.623_{10} +8; 1.631_{10} +8; 1.639_{10} +8;

TABLE 9.3

Cl_2O intensity data(2) as combined uphill curves

range (1): s = 0.86 by 0.02 to 8.98 $Å^{-1}$

5.703_{10} +2;	5.899_{10} +2;	6.127_{10} +2;	6.365_{10} +2;	6.601_{10} +2;
6.821_{10} +2;	7.043_{10} +2;	7.262_{10} +2;	7.491_{10} +2;	7.742_{10} +2;
8.039_{10} +2;	8.353_{10} +2;	8.706_{10} +2;	9.076_{10} +2;	9.449_{10} +2;
9.814_{10} +2;	1.018_{10} +3;	1.054_{10} +3;	1.090_{10} +3;	1.126_{10} +3;
1.163_{10} +3;	1.198_{10} +3;	1.233_{10} +3;	1.266_{10} +3;	1.299_{10} +3;
1.332_{10} +3;	1.365_{10} +3;	1.401_{10} +3;	1.438_{10} +3;	1.478_{10} +3;
1.519_{10} +3;	1.559_{10} +3;	1.599_{10} +3;	1.639_{10} +3;	1.680_{10} +3;
1.720_{10} +3;	1.761_{10} +3;	1.802_{10} +3;	1.843_{10} +3;	1.884_{10} +3;
1.925_{10} +3;	1.968_{10} +3;	2.015_{10} +3;	2.066_{10} +3;	2.118_{10} +3;
2.173_{10} +3;	2.229_{10} +3;	2.286_{10} +3;	2.343_{10} +3;	2.401_{10} +3;
2.460_{10} +3;	2.521_{10} +3;	2.583_{10} +3;	2.647_{10} +3;	2.714_{10} +3;
2.782_{10} +3;	2.852_{10} +3;	2.923_{10} +3;	2.996_{10} +3;	3.070_{10} +3;
3.146_{10} +3;	3.223_{10} +3;	3.301_{10} +3;	3.380_{10} +3;	3.460_{10} +3;
3.542_{10} +3;	3.624_{10} +3;	3.707_{10} +3;	3.793_{10} +3;	3.882_{10} +3;
3.974_{10} +3;	4.068_{10} +3;	4.168_{10} +3;	4.267_{10} +3;	4.361_{10} +3;
4.442_{10} +3;	4.525_{10} +3;	4.599_{10} +3;	4.679_{10} +3;	4.776_{10} +3;
4.892_{10} +3;	5.008_{10} +3;	5.142_{10} +3;	5.269_{10} +3;	5.381_{10} +3;
5.485_{10} +3;	5.583_{10} +3;	5.684_{10} +3;	5.783_{10} +3;	5.886_{10} +3;
5.989_{10} +3;	6.092_{10} +3;	6.195_{10} +3;	6.294_{10} +3;	6.392_{10} +3;
6.491_{10} +3;	6.592_{10} +3;	6.695_{10} +3;	6.798_{10} +3;	6.900_{10} +3;
7.003_{10} +3;	7.112_{10} +3;	7.222_{10} +3;	7.323_{10} +3;	7.424_{10} +3;
7.517_{10} +3;	7.603_{10} +3;	7.688_{10} +3;	7.779_{10} +3;	7.867_{10} +3;
7.961_{10} +3;	8.058_{10} +3;	8.152_{10} +3;	8.249_{10} +3;	8.346_{10} +3;
8.443_{10} +3;	8.537_{10} +3;	8.629_{10} +3;	8.717_{10} +3;	8.806_{10} +3;
8.897_{10} +3;	8.992_{10} +3;	9.085_{10} +3;	9.174_{10} +3;	9.260_{10} +3;
9.349_{10} +3;	9.437_{10} +3;	9.528_{10} +3;	9.624_{10} +3;	9.720_{10} +3;
9.815_{10} +3;	9.910_{10} +3;	1.000_{10} +4;	1.010_{10} +4;	1.019_{10} +4;
1.029_{10} +4;	1.039_{10} +4;	1.050_{10} +4;	1.061_{10} +4;	1.073_{10} +4;
1.084_{10} +4;	1.095_{10} +4;	1.106_{10} +4;	1.118_{10} +4;	1.129_{10} +4;
1.141_{10} +4;	1.153_{10} +4;	1.166_{10} +4;	1.179_{10} +4;	1.192_{10} +4;
1.206_{10} +4;	1.219_{10} +4;	1.233_{10} +4;	1.247_{10} +4;	1.262_{10} +4;
1.276_{10} +4;	1.291_{10} +4;	1.305_{10} +4;	1.320_{10} +4;	1.336_{10} +4;
1.352_{10} +4;	1.369_{10} +4;	1.385_{10} +4;	1.401_{10} +4;	1.416_{10} +4;
1.430_{10} +4;	1.445_{10} +4;	1.462_{10} +4;	1.478_{10} +4;	1.497_{10} +4;
1.515_{10} +4;	1.532_{10} +4;	1.547_{10} +4;	1.562_{10} +4;	1.575_{10} +4;
1.589_{10} +4;	1.604_{10} +4;	1.621_{10} +4;	1.637_{10} +4;	1.653_{10} +4;
1.669_{10} +4;	1.684_{10} +4;	1.699_{10} +4;	1.714_{10} +4;	1.729_{10} +4;
1.743_{10} +4;	1.756_{10} +4;	1.769_{10} +4;	1.781_{10} +4;	1.794_{10} +4;
1.806_{10} +4;	1.818_{10} +4;	1.831_{10} +4;	1.844_{10} +4;	1.857_{10} +4;
1.868_{10} +4;	1.878_{10} +4;	1.887_{10} +4;	1.895_{10} +4;	1.902_{10} +4;
1.910_{10} +4;	1.918_{10} +4;	1.926_{10} +4;	1.933_{10} +4;	1.940_{10} +4;

TABLE 9.3 (cont'd)

1.947_{10} +4;	1.952_{10} +4;	1.957_{10} +4;	1.961_{10} +4;	1.964_{10} +4;
1.967_{10} +4;	1.970_{10} +4;	1.973_{10} +4;	1.975_{10} +4;	1.978_{10} +4;
1.979_{10} +4;	1.981_{10} +4;	1.982_{10} +4;	1.983_{10} +4;	1.982_{10} +4;
1.981_{10} +4;	1.980_{10} +4;	1.978_{10} +4;	1.976_{10} +4;	1.974_{10} +4;
1.973_{10} +4;	1.971_{10} +4;	1.969_{10} +4;	1.966_{10} +4;	1.963_{10} +4;
1.960_{10} +4;	1.956_{10} +4;	1.954_{10} +4;	1.950_{10} +4;	1.948_{10} +4;
1.944_{10} +4;	1.940_{10} +4;	1.936_{10} +4;	1.932_{10} +4;	1.928_{10} +4;
1.923_{10} +4;	1.919_{10} +4;	1.914_{10} +4;	1.909_{10} +4;	1.905_{10} +4;
1.901_{10} +4;	1.899_{10} +4;	1.898_{10} +4;	1.897_{10} +4;	1.896_{10} +4;
1.895_{10} +4;	1.893_{10} +4;	1.890_{10} +4;	1.887_{10} +4;	1.884_{10} +4;
1.881_{10} +4;	1.879_{10} +4;	1.880_{10} +4;	1.881_{10} +4;	1.883_{10} +4;
1.885_{10} +4;	1.887_{10} +4;	1.889_{10} +4;	1.891_{10} +4;	1.893_{10} +4;
1.896_{10} +4;	1.899_{10} +4;	1.902_{10} +4;	1.905_{10} +4;	1.908_{10} +4;
1.911_{10} +4;	1.915_{10} +4;	1.921_{10} +4;	1.928_{10} +4;	1.936_{10} +4;
1.946_{10} +4;	1.956_{10} +4;	1.965_{10} +4;	1.975_{10} +4;	1.983_{10} +4;
1.992_{10} +4;	2.000_{10} +4;	2.010_{10} +4;	2.019_{10} +4;	2.030_{10} +4;
2.041_{10} +4;	2.053_{10} +4;	2.064_{10} +4;	2.076_{10} +4;	2.087_{10} +4;
2.099_{10} +4;	2.110_{10} +4;	2.122_{10} +4;	2.134_{10} +4;	2.146_{10} +4;
2.159_{10} +4;	2.173_{10} +4;	2.187_{10} +4;	2.201_{10} +4;	2.215_{10} +4;
2.229_{10} +4;	2.242_{10} +4;	2.255_{10} +4;	2.268_{10} +4;	2.281_{10} +4;
2.294_{10} +4;	2.308_{10} +4;	2.321_{10} +4;	2.334_{10} +4;	2.348_{10} +4;
2.361_{10} +4;	2.375_{10} +4;	2.390_{10} +4;	2.404_{10} +4;	2.419_{10} +4;
2.434_{10} +4;	2.450_{10} +4;	2.464_{10} +4;	2.476_{10} +4;	2.487_{10} +4;
2.498_{10} +4;	2.508_{10} +4;	2.519_{10} +4;	2.533_{10} +4;	2.547_{10} +4;
2.556_{10} +4;	2.566_{10} +4;	2.572_{10} +4;	2.577_{10} +4;	2.587_{10} +4;
2.600_{10} +4;	2.611_{10} +4;	2.626_{10} +4;	2.638_{10} +4;	2.647_{10} +4;
2.654_{10} +4;	2.663_{10} +4;	2.672_{10} +4;	2.681_{10} +4;	2.690_{10} +4;
2.700_{10} +4;	2.709_{10} +4;	2.718_{10} +4;	2.727_{10} +4;	2.736_{10} +4;
2.743_{10} +4;	2.749_{10} +4;	2.754_{10} +4;	2.758_{10} +4;	2.762_{10} +4;
2.766_{10} +4;	2.771_{10} +4;	2.777_{10} +4;	2.783_{10} +4;	2.790_{10} +4;
2.797_{10} +4;	2.803_{10} +4;	2.812_{10} +4;	2.820_{10} +4;	2.826_{10} +4;
2.832_{10} +4;	2.837_{10} +4;	2.839_{10} +4;	2.839_{10} +4;	2.842_{10} +4;
2.845_{10} +4;	2.850_{10} +4;	2.857_{10} +4;	2.866_{10} +4;	2.875_{10} +4;
2.884_{10} +4;	2.892_{10} +4;	2.900_{10} +4;	2.907_{10} +4;	2.916_{10} +4;
2.924_{10} +4;	2.932_{10} +4;	2.939_{10} +4;	2.945_{10} +4;	2.950_{10} +4;
2.956_{10} +4;	2.964_{10} +4;	2.972_{10} +4;	2.982_{10} +4;	2.992_{10} +4;
3.000_{10} +4;	3.008_{10} +4;	3.016_{10} +4;	3.023_{10} +4;	3.030_{10} +4;
3.038_{10} +4;	3.047_{10} +4;	3.057_{10} +4;	3.067_{10} +4;	3.078_{10} +4;
3.090_{10} +4;	3.099_{10} +4;	3.106_{10} +4;	3.111_{10} +4;	3.115_{10} +4;
3.119_{10} +4;	3.123_{10} +4;	3.128_{10} +4;	3.134_{10} +4;	3.140_{10} +4;
3.146_{10} +4;	3.153_{10} +4;			

TABLE 9.3 (cont'd)

range (2): s = 2.40 by 0.05 to 17.90 $\mathring{A}^{-1}$

3.998_{10} +4;	4.206_{10} +4;	4.418_{10} +4;	4.622_{10} +4;	4.814_{10} +4;
5.004_{10} +4;	5.188_{10} +4;	5.365_{10} +4;	5.536_{10} +4;	5.728_{10} +4;
5.923_{10} +4;	6.118_{10} +4;	6.296_{10} +4;	6.471_{10} +4;	6.635_{10} +4;
6.801_{10} +4;	6.958_{10} +4;	7.100_{10} +4;	7.235_{10} +4;	7.382_{10} +4;
7.549_{10} +4;	7.732_{10} +4;	7.922_{10} +4;	8.129_{10} +4;	8.341_{10} +4;
8.545_{10} +4;	8.757_{10} +4;	8.984_{10} +4;	9.223_{10} +4;	9.465_{10} +4;
9.719_{10} +4;	9.982_{10} +4;	1.025_{10} +5;	1.053_{10} +5;	1.082_{10} +5;
1.111_{10} +5;	1.140_{10} +5;	1.169_{10} +5;	1.198_{10} +5;	1.226_{10} +5;
1.253_{10} +5;	1.280_{10} +5;	1.304_{10} +5;	1.325_{10} +5;	1.345_{10} +5;
1.364_{10} +5;	1.383_{10} +5;	1.403_{10} +5;	1.423_{10} +5;	1.438_{10} +5;
1.449_{10} +5;	1.459_{10} +5;	1.467_{10} +5;	1.471_{10} +5;	1.473_{10} +5;
1.472_{10} +5;	1.468_{10} +5;	1.462_{10} +5;	1.453_{10} +5;	1.443_{10} +5;
1.433_{10} +5;	1.422_{10} +5;	1.410_{10} +5;	1.399_{10} +5;	1.388_{10} +5;
1.379_{10} +5;	1.370_{10} +5;	1.359_{10} +5;	1.350_{10} +5;	1.342_{10} +5;
1.337_{10} +5;	1.333_{10} +5;	1.331_{10} +5;	1.330_{10} +5;	1.331_{10} +5;
1.336_{10} +5;	1.342_{10} +5;	1.347_{10} +5;	1.355_{10} +5;	1.366_{10} +5;
1.378_{10} +5;	1.391_{10} +5;	1.406_{10} +5;	1.421_{10} +5;	1.437_{10} +5;
1.455_{10} +5;	1.474_{10} +5;	1.494_{10} +5;	1.514_{10} +5;	1.534_{10} +5;
1.554_{10} +5;	1.574_{10} +5;	1.596_{10} +5;	1.616_{10} +5;	1.632_{10} +5;
1.650_{10} +5;	1.669_{10} +5;	1.686_{10} +5;	1.698_{10} +5;	1.713_{10} +5;
1.728_{10} +5;	1.741_{10} +5;	1.751_{10} +5;	1.761_{10} +5;	1.772_{10} +5;
1.782_{10} +5;	1.791_{10} +5;	1.797_{10} +5;	1.802_{10} +5;	1.808_{10} +5;
1.815_{10} +5;	1.821_{10} +5;	1.827_{10} +5;	1.833_{10} +5;	1.835_{10} +5;
1.840_{10} +5;	1.847_{10} +5;	1.856_{10} +5;	1.862_{10} +5;	1.865_{10} +5;
1.875_{10} +5;	1.885_{10} +5;	1.891_{10} +5;	1.893_{10} +5;	1.898_{10} +5;
1.909_{10} +5;	1.920_{10} +5;	1.926_{10} +5;	1.925_{10} +5;	1.927_{10} +5;
1.934_{10} +5;	1.943_{10} +5;	1.951_{10} +5;	1.959_{10} +5;	1.965_{10} +5;
1.971_{10} +5;	1.977_{10} +5;	1.985_{10} +5;	1.993_{10} +5;	1.999_{10} +5;
1.999_{10} +5;	1.998_{10} +5;	2.001_{10} +5;	2.003_{10} +5;	2.005_{10} +5;
2.006_{10} +5;	2.009_{10} +5;	2.010_{10} +5;	2.009_{10} +5;	2.009_{10} +5;
2.007_{10} +5;	2.004_{10} +5;	2.006_{10} +5;	2.008_{10} +5;	2.006_{10} +5;
2.007_{10} +5;	2.013_{10} +5;	2.019_{10} +5;	2.026_{10} +5;	2.033_{10} +5;
2.043_{10} +5;	2.050_{10} +5;	2.057_{10} +5;	2.067_{10} +5;	2.081_{10} +5;
2.097_{10} +5;	2.114_{10} +5;	2.131_{10} +5;	2.149_{10} +5;	2.166_{10} +5;
2.185_{10} +5;	2.203_{10} +5;	2.219_{10} +5;	2.239_{10} +5;	2.260_{10} +5;
2.279_{10} +5;	2.300_{10} +5;	2.322_{10} +5;	2.344_{10} +5;	2.367_{10} +5;
2.390_{10} +5;	2.408_{10} +5;	2.424_{10} +5;	2.437_{10} +5;	2.449_{10} +5;
2.461_{10} +5;	2.478_{10} +5;	2.494_{10} +5;	2.507_{10} +5;	2.513_{10} +5;
2.520_{10} +5;	2.528_{10} +5;	2.537_{10} +5;	2.543_{10} +5;	2.547_{10} +5;
2.547_{10} +5;	2.544_{10} +5;	2.544_{10} +5;	2.552_{10} +5;	2.558_{10} +5;
2.559_{10} +5;	2.555_{10} +5;	2.552_{10} +5;	2.551_{10} +5;	2.557_{10} +5;
2.569_{10} +5;	2.575_{10} +5;	2.575_{10} +5;	2.572_{10} +5;	2.573_{10} +5;

TABLE 9.3 (cont'd)

2.592_{10} +5;	2.624_{10} +5;	2.633_{10} +5;	2.609_{10} +5;	2.588_{10} +5;
2.594_{10} +5;	2.611_{10} +5;	2.621_{10} +5;	2.630_{10} +5;	2.645_{10} +5;
2.662_{10} +5;	2.672_{10} +5;	2.680_{10} +5;	2.689_{10} +5;	2.699_{10} +5;
2.705_{10} +5;	2.715_{10} +5;	2.730_{10} +5;	2.747_{10} +5;	2.760_{10} +5;
2.771_{10} +5;	2.782_{10} +5;	2.795_{10} +5;	2.807_{10} +5;	2.818_{10} +5;
2.828_{10} +5;	2.836_{10} +5;	2.843_{10} +5;	2.855_{10} +5;	2.870_{10} +5;
2.883_{10} +5;	2.888_{10} +5;	2.891_{10} +5;	2.896_{10} +5;	2.907_{10} +5;
2.919_{10} +5;	2.931_{10} +5;	2.942_{10} +5;	2.958_{10} +5;	2.979_{10} +5;
2.999_{10} +5;	3.011_{10} +5;	3.013_{10} +5;	3.018_{10} +5;	3.030_{10} +5;
3.049_{10} +5;	3.073_{10} +5;	3.101_{10} +5;	3.126_{10} +5;	3.142_{10} +5;
3.154_{10} +5;	3.169_{10} +5;	3.184_{10} +5;	3.199_{10} +5;	3.214_{10} +5;
3.229_{10} +5;	3.245_{10} +5;	3.261_{10} +5;	3.278_{10} +5;	3.293_{10} +5;
3.306_{10} +5;	3.321_{10} +5;	3.342_{10} +5;	3.362_{10} +5;	3.375_{10} +5;
3.378_{10} +5;	3.378_{10} +5;	3.382_{10} +5;	3.396_{10} +5;	3.411_{10} +5;
3.419_{10} +5;	3.419_{10} +5;	3.417_{10} +5;	3.420_{10} +5;	3.424_{10} +5;
3.426_{10} +5;	3.433_{10} +5;	3.434_{10} +5;	3.427_{10} +5;	3.420_{10} +5;
3.432_{10} +5;	3.452_{10} +5;	3.464_{10} +5;	3.457_{10} +5;	3.446_{10} +5;
3.449_{10} +5;	3.457_{10} +5;	3.465_{10} +5;	3.467_{10} +5;	3.476_{10} +5;
3.485_{10} +5;	3.494_{10} +5;	3.507_{10} +5;	3.515_{10} +5;	3.520_{10} +5;
3.531_{10} +5;	3.547_{10} +5;	3.551_{10} +5;	3.553_{10} +5;	3.556_{10} +5;
3.557_{10} +5;				

range (3): s = 7.6 by 0.10 to 34.90 Å^{-1}

3.708_{10} +6;	3.715_{10} +6;	3.733_{10} +6;	3.741_{10} +6;	3.740_{10} +6;
3.732_{10} +6;	3.729_{10} +6;	3.721_{10} +6;	3.727_{10} +6;	3.739_{10} +6;
3.741_{10} +6;	3.763_{10} +6;	3.783_{10} +6;	3.770_{10} +6;	3.778_{10} +6;
3.790_{10} +6;	3.784_{10} +6;	3.769_{10} +6;	3.762_{10} +6;	3.759_{10} +6;
3.737_{10} +6;	3.711_{10} +6;	3.704_{10} +6;	3.683_{10} +6;	3.663_{10} +6;
3.631_{10} +6;	3.627_{10} +6;	3.641_{10} +6;	3.658_{10} +6;	3.682_{10} +6;
3.701_{10} +6;	3.746_{10} +6;	3.794_{10} +6;	3.849_{10} +6;	3.902_{10} +6;
3.963_{10} +6;	4.036_{10} +6;	4.104_{10} +6;	4.146_{10} +6;	4.198_{10} +6;
4.244_{10} +6;	4.283_{10} +6;	4.323_{10} +6;	4.327_{10} +6;	4.352_{10} +6;
4.350_{10} +6;	4.347_{10} +6;	4.336_{10} +6;	4.318_{10} +6;	4.294_{10} +6;
4.270_{10} +6;	4.257_{10} +6;	4.239_{10} +6;	4.250_{10} +6;	4.248_{10} +6;
4.238_{10} +6;	4.243_{10} +6;	4.273_{10} +6;	4.318_{10} +6;	4.349_{10} +6;
4.377_{10} +6;	4.423_{10} +6;	4.451_{10} +6;	4.489_{10} +6;	4.514_{10} +6;
4.537_{10} +6;	4.558_{10} +6;	4.562_{10} +6;	4.592_{10} +6;	4.604_{10} +6;

TABLE 9.3 (concluded)

4.621_{10} +6;	4.634_{10} +6;	4.661_{10} +6;	4.680_{10} +6;	4.701_{10} +6;
4.738_{10} +6;	4.773_{10} +6;	4.782_{10} +6;	4.816_{10} +6;	4.867_{10} +6;
4.918_{10} +6;	4.956_{10} +6;	4.993_{10} +6;	5.011_{10} +6;	5.058_{10} +6;
5.075_{10} +6;	5.094_{10} +6;	5.092_{10} +6;	5.086_{10} +6;	5.117_{10} +6;
5.110_{10} +6;	5.066_{10} +6;	5.060_{10} +6;	5.045_{10} +6;	5.034_{10} +6;
5.026_{10} +6;	5.027_{10} +6;	5.025_{10} +6;	5.052_{10} +6;	5.068_{10} +6;
5.098_{10} +6;	5.120_{10} +6;	5.148_{10} +6;	5.185_{10} +6;	5.211_{10} +6;
5.244_{10} +6;	5.294_{10} +6;	5.334_{10} +6;	5.374_{10} +6;	5.415_{10} +6;
5.441_{10} +6;	5.444_{10} +6;	5.455_{10} +6;	5.502_{10} +6;	5.513_{10} +6;
5.524_{10} +6;	5.529_{10} +6;	5.537_{10} +6;	5.563_{10} +6;	5.569_{10} +6;
5.573_{10} +6;	5.598_{10} +6;	5.602_{10} +6;	5.638_{10} +6;	5.641_{10} +6;
5.642_{10} +6;	5.679_{10} +6;	5.676_{10} +6;	5.686_{10} +6;	5.696_{10} +6;
5.716_{10} +6;	5.724_{10} +6;	5.727_{10} +6;	5.716_{10} +6;	5.760_{10} +6;
5.756_{10} +6;	5.764_{10} +6;	5.762_{10} +6;	5.790_{10} +6;	5.782_{10} +6;
5.798_{10} +6;	5.835_{10} +6;	5.836_{10} +6;	5.864_{10} +6;	5.888_{10} +6;
5.912_{10} +6;	5.957_{10} +6;	5.970_{10} +6;	6.019_{10} +6;	6.044_{10} +6;
6.097_{10} +6;	6.135_{10} +6;	6.130_{10} +6;	6.157_{10} +6;	6.195_{10} +6;
6.215_{10} +6;	6.233_{10} +6;	6.237_{10} +6;	6.255_{10} +6;	6.275_{10} +6;
6.303_{10} +6;	6.314_{10} +6;	6.310_{10} +6;	6.285_{10} +6;	6.281_{10} +6;
6.296_{10} +6;	6.312_{10} +6;	6.318_{10} +6;	6.327_{10} +6;	6.339_{10} +6;
6.347_{10} +6;	6.402_{10} +6;	6.424_{10} +6;	6.411_{10} +6;	6.429_{10} +6;
6.461_{10} +6;	6.487_{10} +6;	6.539_{10} +6;	6.589_{10} +6;	6.599_{10} +6;
6.591_{10} +6;	6.628_{10} +6;	6.647_{10} +6;	6.661_{10} +6;	6.665_{10} +6;
6.668_{10} +6;	6.703_{10} +6;	6.746_{10} +6;	6.753_{10} +6;	6.780_{10} +6;
6.793_{10} +6;	6.853_{10} +6;	6.839_{10} +6;	6.879_{10} +6;	6.949_{10} +6;
6.924_{10} +6;	6.967_{10} +6;	6.995_{10} +6;	6.996_{10} +6;	7.028_{10} +6;
7.071_{10} +6;	7.110_{10} +6;	7.113_{10} +6;	7.111_{10} +6;	7.128_{10} +6;
7.169_{10} +6;	7.137_{10} +6;	7.148_{10} +6;	7.190_{10} +6;	7.207_{10} +6;
7.247_{10} +6;	7.084_{10} +6;	7.252_{10} +6;	7.302_{10} +6;	7.286_{10} +6;
7.336_{10} +6;	7.337_{10} +6;	7.398_{10} +6;	7.458_{10} +6;	7.489_{10} +6;
7.522_{10} +6;	7.573_{10} +6;	7.599_{10} +6;	7.634_{10} +6;	7.683_{10} +6;
7.673_{10} +6;	7.715_{10} +6;	7.744_{10} +6;	7.780_{10} +6;	7.830_{10} +6;
7.869_{10} +6;	7.859_{10} +6;	7.923_{10} +6;	7.940_{10} +6;	7.944_{10} +6;
7.984_{10} +6;	8.023_{10} +6;	8.041_{10} +6;	8.075_{10} +6;	8.146_{10} +6;
8.146_{10} +6;	8.183_{10} +6;	8.242_{10} +6;	8.263_{10} +6;	8.267_{10} +6;
8.326_{10} +6;	8.357_{10} +6;	8.424_{10} +6;	8.431_{10} +6;	8.468_{10} +6;
8.523_{10} +6;	8.602_{10} +6;	8.638_{10} +6;	8.697_{10} +6;	8.756_{10} +6;
8.808_{10} +6;	8.815_{10} +6;	8.843_{10} +6;	8.898_{10} +6;	8.936_{10} +6;
8.936_{10} +6;	8.968_{10} +6;	9.025_{10} +6;	9.092_{10} +6;	9.114_{10} +6;
9.199_{10} +6;	9.239_{10} +6;	9.271_{10} +6;	9.298_{10} +6;	9.313_{10} +6;
9.382_{10} +6;	9.340_{10} +6;	9.367_{10} +6;	9.295_{10} +6;	

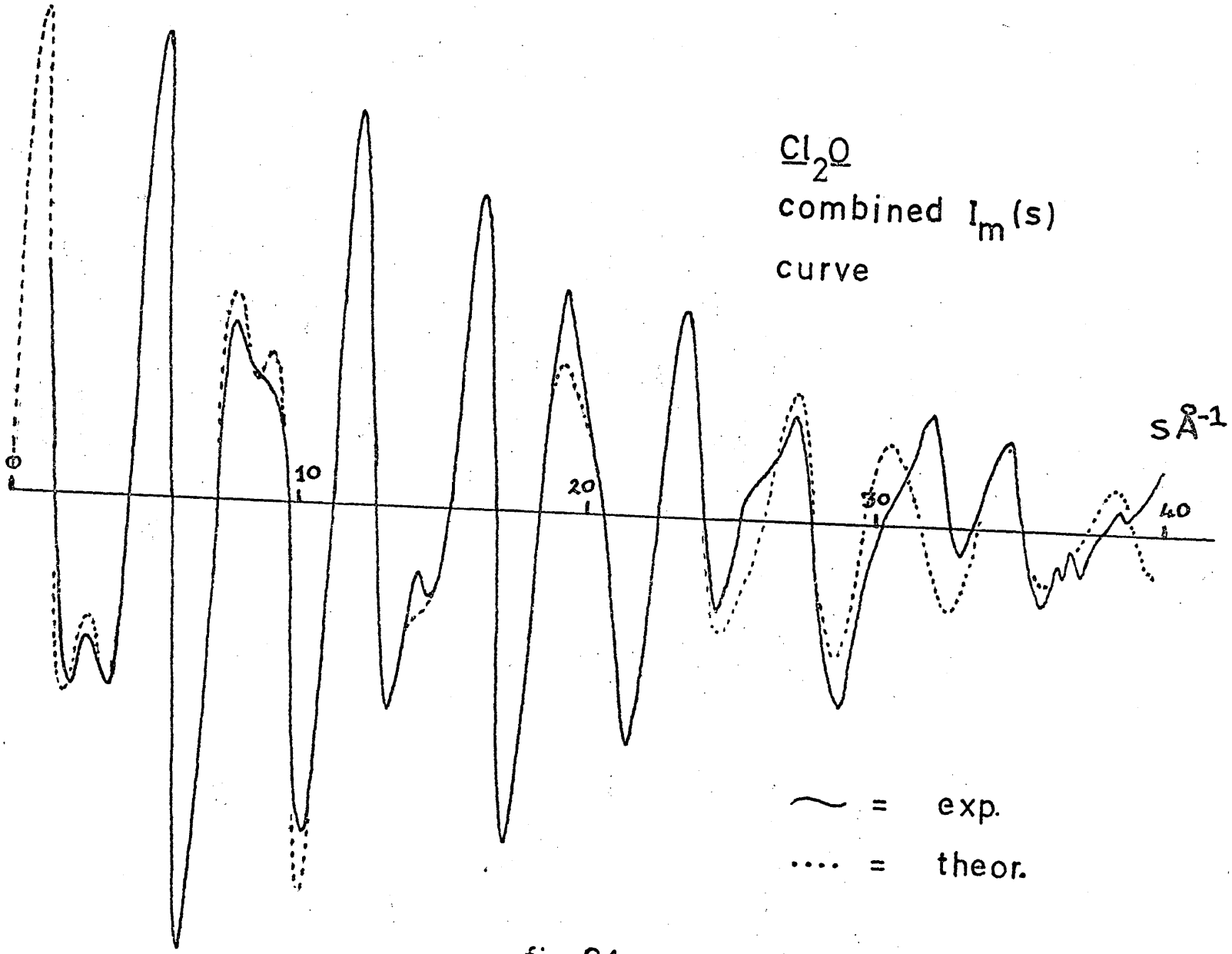

fig. 9.1

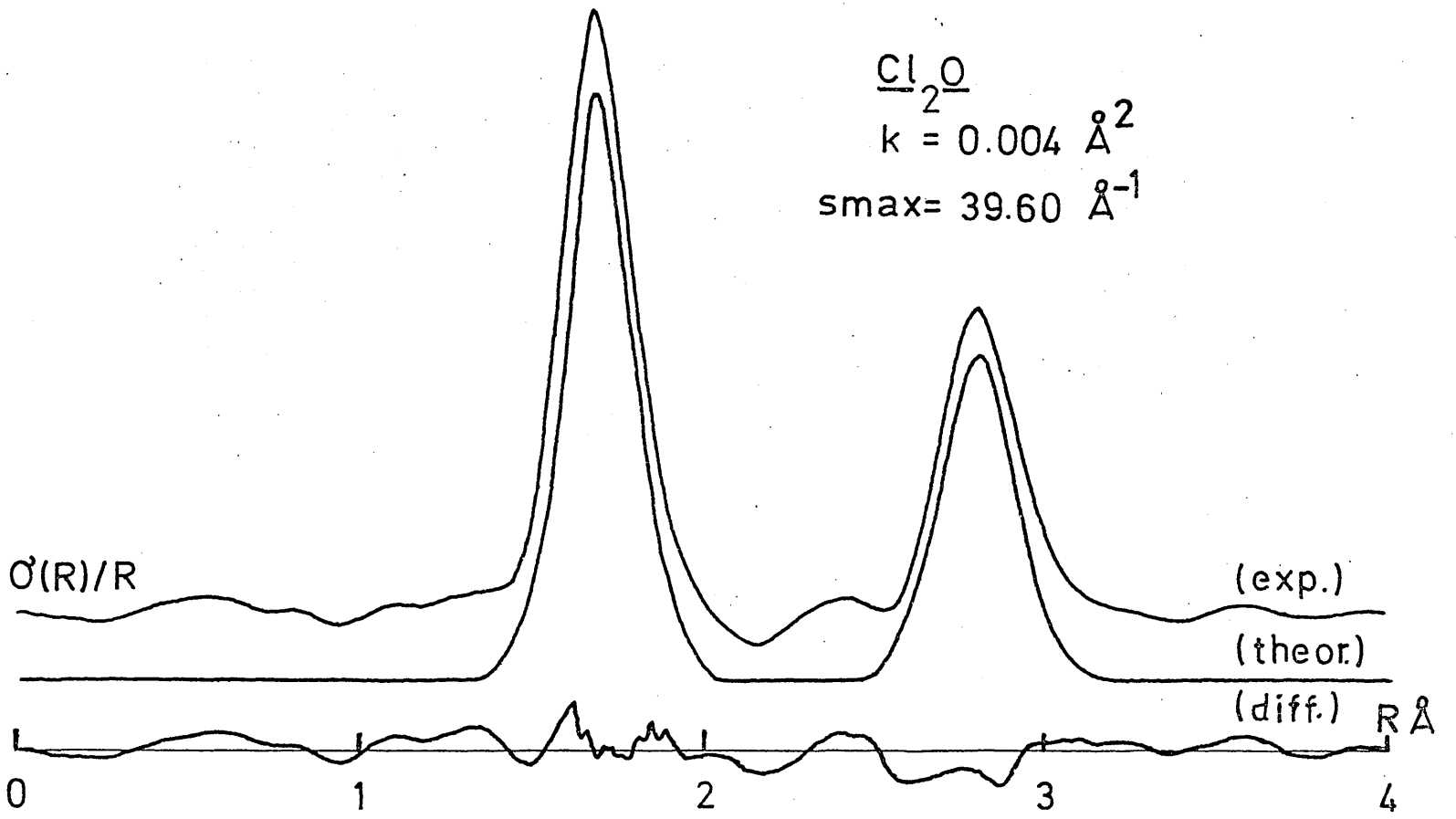

fig. 9.2

TABLE 9.4

Results of individual distance refinements

for Cl_2O

(manual microdensitometer data)

jet to plate distance	100 cm	50 cm	25 cm	11 cm
r_{Cl-O} (Å)	1.6829	1.6883	1.6920	1.6757
σ	0.0020	0.0031	0.0012	0.0061
$r_{Cl..Cl}$ (Å)	2.8198	2.7903	2.7913	2.7849
σ	0.0037	0.0061	0.0029	0.0213
R (%)	14.77	24.16	28.02	84.90
$\sum w\Delta^2$	6.430×10^{9}	1.053×10^{12}	1.385×10^{14}	2.769×10^{16}

Notes: (1) u values were held constant at spectroscopic values.

(2) σ's are least squares e.s.d.'s.

(3) r values are $r_g(1)$ distances.

TABLE 9.5

Results of individual distance refinements

for Cl_2O

(automatic microdensitometer data)

jet to plate distance	100 cm	50 cm	25 cm
r_{Cl-O} (Å)	1.6966	1.6952	1.6953
σ	0.0005	0.0010	0.0021
$r_{Cl..Cl}$ (Å)	2.7994	2.8034	2.7920
σ	0.0010	0.0020	0.0050
R (%)	4.63	12.91	41.72
$\sum w\Delta^2$	4.046×10^{8}	1.256×10^{11}	1.725×10^{14}

Notes: (1) u values were held constant at spectroscopic values.

(2) σ 's are least squares e.s.d.'s.

(3) r values are $r_g(1)$ distances.

TABLE 9.6

Results of all data combined (combtwo)

refinements

refinement	manual MDM data	automatic MDM data
r_{Cl-O} (Å)	1.6907	1.6961
σ'	0.0014	0.0015
u_{Cl-O} (Å)	0.0503	0.0618
σ'	0.0018	0.0017
$r_{Cl..Cl}$ (Å)	2.7991	2.7982
σ'	0.0028	0.0026
$u_{Cl..Cl}$ (Å)	0.0596	0.0653
σ'	0.0029	0.0026
R (%)	20.64	15.06
$\sum w\Delta^2$	3.506×10^{10}	2.017×10^{10}

Notes: (1) σ''s are least squares e.s.d.'s.

(2) The u values have not been corrected for failure of the Born approximation.

TABLE 9.7

The final structural parameters

for Cl_2O

parameter	final result	reproducibility
r_{Cl-O} (Å)	1.694	0.004
$r_{Cl..Cl}$ (Å)	2.799	0.006
$\angle ClOCl$ (°)	111.4	0.6
u_{Cl-O} (Å)	0.052	0.004
$u_{Cl..Cl}$ (Å)	0.063	0.006

Notes: (1) These results were obtained by averaging the manual and automatic microdensitometer results of the previous table, the average being weighted 2:1 in favour of the automatic data. The σ's were combined using the standard methods for combining errors, and the reproducibilities were calculated according to the methods outlined in Chapter Four, section 12.

(2) The distances quoted are $r_g(1)$ values.

(3) The amplitude u_{Cl-O} has been corrected for failure of the Born approximation by subtracting 0.006 from the final least squares result, as described in Chapter Eight.

(4) The spectroscopic amplitude values for Cl_2O at 295°K are u_{Cl-O} = 0.051 and $u_{Cl..Cl}$ = 0.068 Ångstrom units resp, as is stated in Chapter Eight.

TABLE 9.8

A comparison of the structural results obtained for Cl_2O by the present study with those of a recent microwave study

parameter	e.d. present work	microwave study ref. 93
r_{Cl-O} (Å)		
$r_g(1)$	1.694	-
$r_g(0)$	1.696	-
r_e	1.688	~1.700
r_s	-	1.700
estimated error in the r_{Cl-O}'s	0.004	< 0.001
$r_{Cl..Cl}$ (Å)		
$r_g(1)$	2.799	-
$r_g(0)$	2.801	-
r_s	-	2.800*
estimated error in the $r_{Cl..Cl}$'s	0.006	< 0.001*
$\widehat{ClOCl}$ (°)	111.4 $r_g(1)$	110.86
error in angle	0.6	0.1

* Calculated by the author from published results.

CHAPTER TEN

AN ELECTRON DIFFRACTION INVESTIGATION OF PERCHLORIC ACID VAPOUR*

1. Introduction

In 1959 Akishin et al. published an electron diffraction investigation[77] of perchloric acid vapour ($HClO_4$). As a result of this study they proposed a C_{3v} tetrahedral structure for the ClO_4 part of the molecule, and obtained moderately accurate dimensions for this skeleton without locating the position of the attached hydrogen atom, or determining root mean square amplitudes of vibration.

In 1963 Giguère and Savoie supplemented existing Raman spectroscopic data[78] for the acid by publishing an infrared study[79] of $HClO_4$ and $DClO_4$ in the vapour and condensed phases. They assigned observed frequencies in terms of a C_s molecular model also having a C_{3v} skeleton, with the hydrogen atom either eclipsed or staggered with respect to the symmetrical ClO_3 group.

The present electron diffraction investigation was undertaken to obtain more precise molecular dimensions than were determined in reference 77, and to locate if possible the position of the hydrogen atom. It was also hoped to obtain values for the root mean

* A preliminary summary of this study is given in ref. 98.

square amplitudes of vibration for comparison with corresponding spectroscopic results calculated from the data of Giguère and Savoie.

2. Experimental

A sample of the anhydrous compound was prepared by dehydrating aqueous perchloric acid according to a method described by Smith[97], and the experimental conditions adopted during the electron diffraction investigation are summarised in table 10.1.

Owing to a strong tendency for the acid to attack oil present in the sector bearing, long exposure times were difficult to achieve at the shortest jet-to-plate distances, and consequently, only a single underexposed twentyfive centimetre diffraction pattern was obtained. For this reason also, no eleven centimetre data were collected.

Uphill curves are listed in table 10.2, and the experimental combined $I_m(s)$ function is shown graphically in figure 10.1. Two Fourier transforms of this function are presented in figures 10.2 and 10.3, these having been calculated for damping constants of 0.001 and 0.004 A^{o2} respectively. The first of these radial distribution curves shows a considerable amount of ' noise ripple ' because of the low damping employed,

but resolves the two types of Cl-O bonded distance present in the molecule, and indicates the C_{3v} nature of the ClO_4 skeleton. Any distortion from this symmetry must, if it exists, be presumed fairly small. Neither Fourier transform gives definite information about the position or motion of the attached hydrogen atom.

3. Results

The C_s molecular model assumed for the purposes of least squares refinement, consisted of a ClO_4 skeleton of C_{3v} symmetry similar to that assumed in references 77 and 79, with the attached hydrogen atom staggered with respect to the oxygen atoms of the ClO_3 group as indicated in figure 7.1. The molecular geometry was therefore defined by five parameters, and these were chosen to be the five independent internuclear distances R_{Cl-Op}, R_{Cl-OH}, $R_{Op..Op}$, R_{O-H} and $R_{Cl..H}$. Attempts to refine R_{O-H} and $R_{Cl..H}$ soon indicated that the position of the hydrogen atom was poorly determined by the intensity data collected, and hence it was decided to fix the position of this atom by setting the O-H distance equal to 0.96 Å and the ClOH valence angle to 113°, values already discussed in Chapter Seven. The

amplitudes of vibration corresponding to R_{O-H}, $R_{Cl..H}$ and to the two non-bonded $R_{Op..H}$ distance types, were all held constant as well. The first two of these were given the values 0.07 and 0.11 Å respectively, whilst the second two were each assigned a guessed value of 0.2 Å, consistent with a torsional motion of the hydrogen atom. The remaining vibrational amplitudes u_{Cl-Op}, u_{Cl-OH}, $u_{Op..Op}$ and $u_{Op..OH}$ were all refinable, and the three types of dependent internuclear distance implied by the C_s model, were calculated during least squares refinement by the subroutine described in Appendix Five.

Results of single distance refinements are presented in table 10.3, and show a good consistency from one jet-to-plate distance to another, whilst results of all-data-combined least squares refinements of both the combtwo and combscaled types, are listed in the columns of table 10.4. The figures presented in this latter table immediately indicate that the $R_{Op..Op}$ parameter is very poorly determined by the data available, particularly if the amplitudes of vibration $u_{Op..Op}$ and $u_{Op..OH}$ are included in the refinement. Two explanations of this effect seem possible. It may be that the somewhat inferior twentyfive centimetre data collected, are not of sufficiently high quality

to resolve the similar Op..Op and Op..OH tetrahedral edges which have of course identical A factors, or alternatively, it may be that these edges are in reality extremely similar, being more nearly identical than those found in $FClO_3$ (see Chapter Eleven), or suggested by the results of table 10.4. The second of these explanations seems to be confirmed by the facts (a) that if the Op..Op distance is assumed to have a value around 2.38 Å, the result obtained for it in such molecules as $FClO_3$ and Cl_2O_7 (see Chapter Eleven and reference 81) and if the Cl-Op and Cl-OH distances are given the values shown in table 10.4, then the dependent Op..OH distance calculated is also close to 2.38 Å in magnitude, and (b) in the case of the all-data-combined least squares refinements, attempts made to locate false minima, by altering the initial trial value given to $R_{Op..Op}$ indicated a tendency for this parameter to first converge towards a fairly well defined value of 2.38 Å, but then to diverge from this, and finally to converge to a much less well determined result of smaller magnitude.

Final parameters and reproducibilities calculated for the molecule by averaging the columns of table 10.4 are listed in table 10.5. The final OpClOp angle obtained has a large error limit associated with it

as a result of the indeterminacy mentioned above, and this angle could easily be as large as the corresponding value of 115.2° obtained by Beagley[81] for the two ClO_3 groups in chlorine heptoxide.

4. Discussion

The structural results obtained by the present study are in reasonable agreement with values given by Akishin et al.[77] of 1.42 (0.01) Å for R_{Cl-Op}, 1.64 (0.02) Å for R_{Cl-OH} and 100(2)° for the OpClO(H) valence angle, though the latter result is somewhat different from the corresponding angle quoted in table 10.5. In neither electron diffraction study was any information obtained about the hydrogen atom, and in the present investigation no evidence was established to suggest that the threefold axis of the symmetrical ClO_3 group in perchloric acid, does not lie along the Cl-OH bond. Various theoretical radial distribution curves were calculated for such a tilted model and compared with the experimental $\sigma(R)/R$ function in an effort to investigate such a possibility, but best agreement was obtained when the angle of tilt was close to 0°. It may therefore be concluded that any such distortion from C_{3v} symmetry of the ClO_4 skeleton is very small.

With the exception of u_{Cl-Op}, the vibrational amplitudes obtained by the present work are very poorly determined. All of the amplitude results listed in table 10.5 do in fact agree with the corresponding spectroscopic values of Chapter Seven, if error limits are considered, but only in the case of u_{Cl-Op} can the agreement obtained be described as both significant and good.

The dimensions presented in table 10.5 for the ClO_4 skeleton may be compared with corresponding results determined by Beagley[81] for the two ClO_4 tetrahedra in the molecule of chlorine heptoxide. The dimensions he obtained for Cl_2O_7 are $R_{Cl-Op} = 1.405$ Å, $R_{Cl-OCl} = 1.709$ Å, and the angle $OpClOp = 115.2^\circ$. The reproducibilities assigned to these quantities in reference 81 are 0.002 Å, 0.004 Å and 0.2° respectively. The most striking difference between these $r_g(1)$ results and corresponding values given in table 10.5, is the lengthening of the Cl-OH bond in the acid as it becomes the bridge bond in the heptoxide. It is also noticeable that the Cl-Op bonds in perchloric acid are slightly longer than those of Cl_2O_7, but this difference cannot be regarded as particularly significant when error limits are taken into account.

The bonding in Cl_2O_7 has been described by Beagley[81]

in terms of two single Cl-O bridge bonds, and six Cl-Op bonds each having a π bond order of two thirds. The occurrence of π bonding may be explained in terms of overlap of two p orbitals on each peripheral oxygen atom with the d_{z^2} and $d_{x^2-y^2}$ orbitals on chlorine, a type of bonding which has been discussed in some detail in a paper by Cruickshank[95], and which may be postulated for a good many compounds containing a second row element tetrahedrally coordinated by oxygen atoms. As has been mentioned in Chapter Nine, the true valence angle of 109.2° suggested for the Cl_2O_7 bridge excludes the possibility of a suitable p orbital being available on the bridging oxygen atom of this compound for a similar type of overlap.

In the molecule of perchloric acid, however, the ClOH angle is presumably greater than 109.2°, being probably about 113° (see reference 80 for HOCl and reference 120 for CH_3OCl), and hence it is possible that the Cl-OH bond in this molecule involves a certain amount of $d\pi$-$p\pi$ bonding. Cruickshank[95] has suggested π bond orders of 1/4+1/3 for the X-Op bonds in an O_3XOY system, and 1/4 for the X-OY bond, but these bond orders are based on the assumptions that the angle XOY is close to 120° and that the energy of the p orbital on the bridging oxygen atom is similar to the energies

of the p orbitals available on each peripheral oxygen atom. In perchloric acid, where Y = H, the XOY angle appears to be only 113°, and hence this factor alone should reduce the amount of Cl-OH π bonding possible in the $HClO_4$ molecule. The similarity found to exist between the Cl-Op distances in Cl_2O_7 and $HClO_4$ also suggests that the Cl-OH π bond order in the acid is a good deal less than 0.25, for if this were not so, the Cl-Op distance in $HClO_4$ would be longer than in Cl_2O_7 on account of its having a π bond order less than two thirds. It will be shown later (Chapter 16) that the Cl-OH bond order is approximately 0.1 in $HClO_4$.

The results obtained by the present work do not contradict the general statement made in reference 95, that for O_3XOH systems, where X is a second row element, the difference between the X-Op and X-OH bonds is usually greater for the free molecule, than for the corresponding molecule in a crystal, this effect being explained in terms of hydrogen bonding in the condensed phase.

It is of interest that the average Cl-O bond length of 1.46 Å obtained by the present work for $HClO_4$, is equal to the empirical estimate suggested by Cruickshank[95] for ClO_4 tetrahedra in general.

In the present work no evidence was obtained for dimerisation of $HClO_4$ in the vapour phase. Intramolecular hydrogen bonding cannot be excluded however.

TABLE 10.1

A summary of experimental details

for the perchloric acid investigation

jet to plate distance	100 cm	50 cm	25 cm	-
wavelength (A)	0.051190	0.051190	0.051190	
e.s.d.	0.000022	0.000022	0.000022	
sample temperature (^{o}K)	288	288	288	
nozzle temperature (^{o}K)	328	328	328	
gas temperature assumed (^{o}K)	308	308	308	
number of plates used	4	4	1	
quality	good	good	very light	
number of traces measured (AMDM)	4	4	8	

TABLE 10.2

$HClO_4$ intensity data as combined uphill curves

range (1): s = 0.74 by 0.02 to 9.00 $Å^{-1}$

3.443_{10} +2;	3.584_{10} +2;	3.720_{10} +2;	3.854_{10} +2;	4.005_{10} +2;
4.186_{10} +2;	4.396_{10} +2;	4.633_{10} +2;	4.892_{10} +2;	5.163_{10} +2;
5.427_{10} +2;	5.696_{10} +2;	5.972_{10} +2;	6.245_{10} +2;	6.533_{10} +2;
6.839_{10} +2;	7.169_{10} +2;	7.526_{10} +2;	7.913_{10} +2;	8.326_{10} +2;
8.746_{10} +2;	9.163_{10} +2;	9.576_{10} +2;	9.971_{10} +2;	1.035_{10} +3;
1.073_{10} +3;	1.109_{10} +3;	1.144_{10} +3;	1.177_{10} +3;	1.210_{10} +3;
1.241_{10} +3;	1.272_{10} +3;	1.305_{10} +3;	1.338_{10} +3;	1.372_{10} +3;
1.407_{10} +3;	1.443_{10} +3;	1.476_{10} +3;	1.509_{10} +3;	1.539_{10} +3;
1.567_{10} +3;	1.593_{10} +3;	1.619_{10} +3;	1.644_{10} +3;	1.668_{10} +3;
1.692_{10} +3;	1.715_{10} +3;	1.737_{10} +3;	1.760_{10} +3;	1.784_{10} +3;
1.808_{10} +3;	1.834_{10} +3;	1.860_{10} +3;	1.885_{10} +3;	1.910_{10} +3;
1.934_{10} +3;	1.959_{10} +3;	1.982_{10} +3;	2.005_{10} +3;	2.028_{10} +3;
2.049_{10} +3;	2.072_{10} +3;	2.095_{10} +3;	2.118_{10} +3;	2.142_{10} +3;
2.166_{10} +3;	2.188_{10} +3;	2.211_{10} +3;	2.233_{10} +3;	2.254_{10} +3;
2.277_{10} +3;	2.302_{10} +3;	2.327_{10} +3;	2.353_{10} +3;	2.381_{10} +3;
2.409_{10} +3;	2.437_{10} +3;	2.467_{10} +3;	2.498_{10} +3;	2.529_{10} +3;
2.562_{10} +3;	2.596_{10} +3;	2.631_{10} +3;	2.669_{10} +3;	2.709_{10} +3;
2.749_{10} +3;	2.790_{10} +3;	2.832_{10} +3;	2.876_{10} +3;	2.920_{10} +3;
2.966_{10} +3;	3.016_{10} +3;	3.069_{10} +3;	3.122_{10} +3;	3.179_{10} +3;
3.238_{10} +3;	3.296_{10} +3;	3.354_{10} +3;	3.410_{10} +3;	3.464_{10} +3;
3.518_{10} +3;	3.574_{10} +3;	3.634_{10} +3;	3.694_{10} +3;	3.759_{10} +3;
3.826_{10} +3;	3.892_{10} +3;	3.962_{10} +3;	4.034_{10} +3;	4.107_{10} +3;
4.179_{10} +3;	4.253_{10} +3;	4.328_{10} +3;	4.402_{10} +3;	4.476_{10} +3;
4.552_{10} +3;	4.627_{10} +3;	4.702_{10} +3;	4.777_{10} +3;	4.852_{10} +3;
4.928_{10} +3;	5.006_{10} +3;	5.084_{10} +3;	5.161_{10} +3;	5.237_{10} +3;
5.312_{10} +3;	5.386_{10} +3;	5.460_{10} +3;	5.533_{10} +3;	5.606_{10} +3;
5.680_{10} +3;	5.755_{10} +3;	5.828_{10} +3;	5.901_{10} +3;	5.971_{10} +3;
6.044_{10} +3;	6.113_{10} +3;	6.183_{10} +3;	6.252_{10} +3;	6.323_{10} +3;
6.391_{10} +3;	6.459_{10} +3;	6.526_{10} +3;	6.592_{10} +3;	6.661_{10} +3;
6.729_{10} +3;	6.798_{10} +3;	6.866_{10} +3;	6.932_{10} +3;	6.997_{10} +3;
7.065_{10} +3;	7.134_{10} +3;	7.204_{10} +3;	7.277_{10} +3;	7.347_{10} +3;
7.415_{10} +3;	7.481_{10} +3;	7.546_{10} +3;	7.614_{10} +3;	7.684_{10} +3;
7.755_{10} +3;	7.828_{10} +3;	7.901_{10} +3;	7.978_{10} +3;	8.056_{10} +3;
8.137_{10} +3;	8.221_{10} +3;	8.306_{10} +3;	8.388_{10} +3;	8.469_{10} +3;
8.547_{10} +3;	8.630_{10} +3;	8.716_{10} +3;	8.805_{10} +3;	8.895_{10} +3;
8.984_{10} +3;	9.073_{10} +3;	9.164_{10} +3;	9.261_{10} +3;	9.361_{10} +3;
9.466_{10} +3;	9.576_{10} +3;	9.688_{10} +3;	9.797_{10} +3;	9.906_{10} +3;
1.002_{10} +4;	1.014_{10} +4;	1.026_{10} +4;	1.038_{10} +4;	1.050_{10} +4;

1.063_{10} +4;	1.076_{10} +4;	1.090_{10} +4;	1.104_{10} +4;	1.119_{10} +4;
1.135_{10} +4;	1.150_{10} +4;	1.165_{10} +4;	1.179_{10} +4;	1.192_{10} +4;
1.205_{10} +4;	1.218_{10} +4;	1.232_{10} +4;	1.247_{10} +4;	1.261_{10} +4;
1.276_{10} +4;	1.290_{10} +4;	1.305_{10} +4;	1.318_{10} +4;	1.333_{10} +4;
1.348_{10} +4;	1.363_{10} +4;	1.378_{10} +4;	1.394_{10} +4;	1.410_{10} +4;
1.426_{10} +4;	1.442_{10} +4;	1.458_{10} +4;	1.475_{10} +4;	1.491_{10} +4;
1.507_{10} +4;	1.523_{10} +4;	1.539_{10} +4;	1.554_{10} +4;	1.568_{10} +4;
1.583_{10} +4;	1.597_{10} +4;	1.611_{10} +4;	1.626_{10} +4;	1.641_{10} +4;
1.655_{10} +4;	1.669_{10} +4;	1.681_{10} +4;	1.693_{10} +4;	1.705_{10} +4;
1.716_{10} +4;	1.727_{10} +4;	1.738_{10} +4;	1.750_{10} +4;	1.762_{10} +4;
1.772_{10} +4;	1.783_{10} +4;	1.792_{10} +4;	1.801_{10} +4;	1.809_{10} +4;
1.817_{10} +4;	1.824_{10} +4;	1.831_{10} +4;	1.838_{10} +4;	1.843_{10} +4;
1.848_{10} +4;	1.853_{10} +4;	1.858_{10} +4;	1.863_{10} +4;	1.867_{10} +4;
1.871_{10} +4;	1.874_{10} +4;	1.875_{10} +4;	1.877_{10} +4;	1.877_{10} +4;
1.877_{10} +4;	1.876_{10} +4;	1.876_{10} +4;	1.876_{10} +4;	1.876_{10} +4;
1.876_{10} +4;	1.874_{10} +4;	1.871_{10} +4;	1.867_{10} +4;	1.862_{10} +4;
1.856_{10} +4;	1.850_{10} +4;	1.845_{10} +4;	1.839_{10} +4;	1.834_{10} +4;
1.829_{10} +4;	1.824_{10} +4;	1.818_{10} +4;	1.812_{10} +4;	1.805_{10} +4;
1.798_{10} +4;	1.792_{10} +4;	1.786_{10} +4;	1.779_{10} +4;	1.772_{10} +4;
1.764_{10} +4;	1.754_{10} +4;	1.744_{10} +4;	1.734_{10} +4;	1.724_{10} +4;
1.713_{10} +4;	1.703_{10} +4;	1.692_{10} +4;	1.681_{10} +4;	1.671_{10} +4;
1.662_{10} +4;	1.653_{10} +4;	1.645_{10} +4;	1.636_{10} +4;	1.627_{10} +4;
1.618_{10} +4;	1.608_{10} +4;	1.599_{10} +4;	1.591_{10} +4;	1.583_{10} +4;
1.576_{10} +4;	1.569_{10} +4;	1.563_{10} +4;	1.558_{10} +4;	1.553_{10} +4;
1.548_{10} +4;	1.542_{10} +4;	1.537_{10} +4;	1.531_{10} +4;	1.527_{10} +4;
1.523_{10} +4;	1.520_{10} +4;	1.517_{10} +4;	1.513_{10} +4;	1.511_{10} +4;
1.509_{10} +4;	1.508_{10} +4;	1.509_{10} +4;	1.509_{10} +4;	1.510_{10} +4;
1.510_{10} +4;	1.510_{10} +4;	1.511_{10} +4;	1.513_{10} +4;	1.516_{10} +4;
1.520_{10} +4;	1.525_{10} +4;	1.530_{10} +4;	1.536_{10} +4;	1.543_{10} +4;
1.554_{10} +4;	1.567_{10} +4;	1.581_{10} +4;	1.590_{10} +4;	1.600_{10} +4;
1.606_{10} +4;	1.608_{10} +4;	1.610_{10} +4;	1.615_{10} +4;	1.620_{10} +4;
1.629_{10} +4;	1.639_{10} +4;	1.650_{10} +4;	1.660_{10} +4;	1.671_{10} +4;
1.682_{10} +4;	1.693_{10} +4;	1.705_{10} +4;	1.718_{10} +4;	1.731_{10} +4;
1.745_{10} +4;	1.758_{10} +4;	1.772_{10} +4;	1.786_{10} +4;	1.801_{10} +4;
1.816_{10} +4;	1.830_{10} +4;	1.844_{10} +4;	1.858_{10} +4;	1.870_{10} +4;
1.883_{10} +4;	1.896_{10} +4;	1.909_{10} +4;	1.923_{10} +4;	1.935_{10} +4;
1.948_{10} +4;	1.962_{10} +4;	1.975_{10} +4;	1.990_{10} +4;	2.005_{10} +4;
2.020_{10} +4;	2.036_{10} +4;	2.052_{10} +4;	2.067_{10} +4;	2.081_{10} +4;
2.094_{10} +4;	2.106_{10} +4;	2.118_{10} +4;	2.129_{10} +4;	2.140_{10} +4;
2.153_{10} +4;	2.165_{10} +4;	2.179_{10} +4;	2.192_{10} +4;	2.205_{10} +4;
2.215_{10} +4;	2.224_{10} +4;	2.231_{10} +4;	2.236_{10} +4;	2.242_{10} +4;
2.249_{10} +4;	2.255_{10} +4;	2.262_{10} +4;	2.268_{10} +4;	2.272_{10} +4;
2.276_{10} +4;	2.279_{10} +4;	2.283_{10} +4;	2.288_{10} +4;	2.293_{10} +4;
2.297_{10} +4;	2.301_{10} +4;	2.303_{10} +4;	2.304_{10} +4;	2.306_{10} +4;
2.309_{10} +4;	2.311_{10} +4;	2.316_{10} +4;	2.320_{10} +4;	

TABLE 10.2 (cont'd)

range (2): $s = 2.40$ by 0.05 to 18.00 Å^{-1}

$1.886_{10}+4$;	$1.964_{10}+4$;	$2.044_{10}+4$;	$2.127_{10}+4$;	$2.212_{10}+4$;
$2.302_{10}+4$;	$2.399_{10}+4$;	$2.501_{10}+4$;	$2.608_{10}+4$;	$2.723_{10}+4$;
$2.843_{10}+4$;	$2.973_{10}+4$;	$3.107_{10}+4$;	$3.233_{10}+4$;	$3.354_{10}+4$;
$3.476_{10}+4$;	$3.595_{10}+4$;	$3.707_{10}+4$;	$3.825_{10}+4$;	$3.948_{10}+4$;
$4.065_{10}+4$;	$4.180_{10}+4$;	$4.304_{10}+4$;	$4.430_{10}+4$;	$4.553_{10}+4$;
$4.674_{10}+4$;	$4.790_{10}+4$;	$4.906_{10}+4$;	$5.022_{10}+4$;	$5.140_{10}+4$;
$5.257_{10}+4$;	$5.384_{10}+4$;	$5.520_{10}+4$;	$5.659_{10}+4$;	$5.798_{10}+4$;
$5.942_{10}+4$;	$6.092_{10}+4$;	$6.248_{10}+4$;	$6.409_{10}+4$;	$6.583_{10}+4$;
$6.767_{10}+4$;	$6.957_{10}+4$;	$7.156_{10}+4$;	$7.366_{10}+4$;	$7.580_{10}+4$;
$7.798_{10}+4$;	$8.026_{10}+4$;	$8.269_{10}+4$;	$8.536_{10}+4$;	$8.809_{10}+4$;
$9.068_{10}+4$;	$9.318_{10}+4$;	$9.572_{10}+4$;	$9.836_{10}+4$;	$1.009_{10}+5$;
$1.033_{10}+5$;	$1.057_{10}+5$;	$1.082_{10}+5$;	$1.105_{10}+5$;	$1.126_{10}+5$;
$1.147_{10}+5$;	$1.167_{10}+5$;	$1.184_{10}+5$;	$1.200_{10}+5$;	$1.214_{10}+5$;
$1.226_{10}+5$;	$1.237_{10}+5$;	$1.246_{10}+5$;	$1.251_{10}+5$;	$1.255_{10}+5$;
$1.256_{10}+5$;	$1.255_{10}+5$;	$1.253_{10}+5$;	$1.249_{10}+5$;	$1.243_{10}+5$;
$1.235_{10}+5$;	$1.226_{10}+5$;	$1.214_{10}+5$;	$1.201_{10}+5$;	$1.186_{10}+5$;
$1.168_{10}+5$;	$1.150_{10}+5$;	$1.134_{10}+5$;	$1.118_{10}+5$;	$1.103_{10}+5$;
$1.085_{10}+5$;	$1.066_{10}+5$;	$1.048_{10}+5$;	$1.033_{10}+5$;	$1.020_{10}+5$;
$1.011_{10}+5$;	$1.001_{10}+5$;	$9.902_{10}+4$;	$9.797_{10}+4$;	$9.718_{10}+4$;
$9.667_{10}+4$;	$9.645_{10}+4$;	$9.652_{10}+4$;	$9.670_{10}+4$;	$9.697_{10}+4$;
$9.746_{10}+4$;	$9.816_{10}+4$;	$9.911_{10}+4$;	$1.002_{10}+5$;	$1.015_{10}+5$;
$1.029_{10}+5$;	$1.045_{10}+5$;	$1.063_{10}+5$;	$1.080_{10}+5$;	$1.097_{10}+5$;
$1.115_{10}+5$;	$1.134_{10}+5$;	$1.152_{10}+5$;	$1.171_{10}+5$;	$1.191_{10}+5$;
$1.211_{10}+5$;	$1.229_{10}+5$;	$1.247_{10}+5$;	$1.266_{10}+5$;	$1.285_{10}+5$;
$1.301_{10}+5$;	$1.316_{10}+5$;	$1.331_{10}+5$;	$1.343_{10}+5$;	$1.353_{10}+5$;
$1.362_{10}+5$;	$1.371_{10}+5$;	$1.379_{10}+5$;	$1.384_{10}+5$;	$1.389_{10}+5$;
$1.393_{10}+5$;	$1.398_{10}+5$;	$1.401_{10}+5$;	$1.401_{10}+5$;	$1.403_{10}+5$;
$1.404_{10}+5$;	$1.406_{10}+5$;	$1.406_{10}+5$;	$1.405_{10}+5$;	$1.407_{10}+5$;
$1.409_{10}+5$;	$1.409_{10}+5$;	$1.406_{10}+5$;	$1.405_{10}+5$;	$1.405_{10}+5$;
$1.407_{10}+5$;	$1.407_{10}+5$;	$1.407_{10}+5$;	$1.409_{10}+5$;	$1.414_{10}+5$;
$1.421_{10}+5$;	$1.426_{10}+5$;	$1.428_{10}+5$;	$1.432_{10}+5$;	$1.438_{10}+5$;
$1.444_{10}+5$;	$1.447_{10}+5$;	$1.451_{10}+5$;	$1.459_{10}+5$;	$1.467_{10}+5$;
$1.474_{10}+5$;	$1.478_{10}+5$;	$1.482_{10}+5$;	$1.489_{10}+5$;	$1.497_{10}+5$;
$1.503_{10}+5$;	$1.505_{10}+5$;	$1.507_{10}+5$;	$1.510_{10}+5$;	$1.511_{10}+5$;
$1.515_{10}+5$;	$1.518_{10}+5$;	$1.518_{10}+5$;	$1.516_{10}+5$;	$1.519_{10}+5$;
$1.521_{10}+5$;	$1.517_{10}+5$;	$1.511_{10}+5$;	$1.508_{10}+5$;	$1.507_{10}+5$;
$1.503_{10}+5$;	$1.497_{10}+5$;	$1.490_{10}+5$;	$1.484_{10}+5$;	$1.481_{10}+5$;
$1.479_{10}+5$;	$1.474_{10}+5$;	$1.465_{10}+5$;	$1.459_{10}+5$;	$1.455_{10}+5$;
$1.449_{10}+5$;	$1.444_{10}+5$;	$1.441_{10}+5$;	$1.440_{10}+5$;	$1.438_{10}+5$;
$1.436_{10}+5$;	$1.435_{10}+5$;	$1.440_{10}+5$;	$1.447_{10}+5$;	$1.451_{10}+5$;

1.454_{10} +5;	1.459_{10} +5;	1.466_{10} +5;	1.471_{10} +5;	1.475_{10} +5;
1.483_{10} +5;	1.495_{10} +5;	1.506_{10} +5;	1.518_{10} +5;	1.535_{10} +5;
1.551_{10} +5;	1.565_{10} +5;	1.577_{10} +5;	1.589_{10} +5;	1.601_{10} +5;
1.615_{10} +5;	1.629_{10} +5;	1.647_{10} +5;	1.667_{10} +5;	1.681_{10} +5;
1.689_{10} +5;	1.697_{10} +5;	1.717_{10} +5;	1.736_{10} +5;	1.744_{10} +5;
1.746_{10} +5;	1.753_{10} +5;	1.764_{10} +5;	1.772_{10} +5;	1.777_{10} +5;
1.780_{10} +5;	1.782_{10} +5;	1.785_{10} +5;	1.791_{10} +5;	1.796_{10} +5;
1.800_{10} +5;	1.803_{10} +5;	1.803_{10} +5;	1.799_{10} +5;	1.800_{10} +5;
1.811_{10} +5;	1.820_{10} +5;	1.823_{10} +5;	1.822_{10} +5;	1.822_{10} +5;
1.824_{10} +5;	1.827_{10} +5;	1.824_{10} +5;	1.817_{10} +5;	1.811_{10} +5;
1.808_{10} +5;	1.809_{10} +5;	1.817_{10} +5;	1.818_{10} +5;	1.808_{10} +5;
1.800_{10} +5;	1.800_{10} +5;	1.801_{10} +5;	1.801_{10} +5;	1.805_{10} +5;
1.811_{10} +5;	1.813_{10} +5;	1.812_{10} +5;	1.813_{10} +5;	1.815_{10} +5;
1.827_{10} +5;	1.846_{10} +5;	1.850_{10} +5;	1.843_{10} +5;	1.840_{10} +5;
1.849_{10} +5;	1.851_{10} +5;	1.853_{10} +5;	1.855_{10} +5;	1.857_{10} +5;
1.861_{10} +5;	1.867_{10} +5;	1.872_{10} +5;	1.870_{10} +5;	1.876_{10} +5;
1.887_{10} +5;	1.892_{10} +5;	1.887_{10} +5;	1.883_{10} +5;	1.886_{10} +5;
1.886_{10} +5;	1.886_{10} +5;	1.887_{10} +5;	1.890_{10} +5;	1.893_{10} +5;
1.894_{10} +5;	1.892_{10} +5;	1.894_{10} +5;	1.897_{10} +5;	1.902_{10} +5;
1.907_{10} +5;	1.911_{10} +5;	1.915_{10} +5;	1.915_{10} +5;	1.918_{10} +5;
1.926_{10} +5;	1.944_{10} +5;	1.959_{10} +5;	1.959_{10} +5;	1.951_{10} +5;
1.950_{10} +5;	1.953_{10} +5;	1.956_{10} +5;	1.961_{10} +5;	1.967_{10} +5;
1.974_{10} +5;	1.981_{10} +5;	1.991_{10} +5;		

range (3): s = 7.40 by 0.10 to 34.70 Å^{-1}

6.728_{10} +5;	6.891_{10} +5;	6.987_{10} +5;	7.234_{10} +5;	7.483_{10} +5;
7.762_{10} +5;	8.058_{10} +5;	8.346_{10} +5;	8.631_{10} +5;	8.916_{10} +5;
9.141_{10} +5;	9.373_{10} +5;	9.577_{10} +5;	9.726_{10} +5;	9.865_{10} +5;
9.968_{10} +5;	9.992_{10} +5;	1.001_{10} +6;	1.002_{10} +6;	1.003_{10} +6;
1.003_{10} +6;	1.004_{10} +6;	1.008_{10} +6;	1.010_{10} +6;	1.014_{10} +6;
1.017_{10} +6;	1.023_{10} +6;	1.030_{10} +6;	1.039_{10} +6;	1.049_{10} +6;
1.067_{10} +6;	1.080_{10} +6;	1.086_{10} +6;	1.095_{10} +6;	1.103_{10} +6;
1.111_{10} +6;	1.115_{10} +6;	1.111_{10} +6;	1.111_{10} +6;	1.107_{10} +6;
1.100_{10} +6;	1.095_{10} +6;	1.088_{10} +6;	1.082_{10} +6;	1.070_{10} +6;
1.063_{10} +6;	1.057_{10} +6;	1.056_{10} +6;	1.057_{10} +6;	1.055_{10} +6;
1.059_{10} +6;	1.066_{10} +6;	1.075_{10} +6;	1.087_{10} +6;	1.099_{10} +6;
1.117_{10} +6;	1.144_{10} +6;	1.162_{10} +6;	1.180_{10} +6;	1.205_{10} +6;
1.222_{10} +6;	1.239_{10} +6;	1.256_{10} +6;	1.283_{10} +6;	1.326_{10} +6;

TABLE 10.2 (concluded)

1.338_{10} +6;	1.314_{10} +6;	1.320_{10} +6;	1.317_{10} +6;	1.318_{10} +6;
1.320_{10} +6;	1.318_{10} +6;	1.318_{10} +6;	1.319_{10} +6;	1.315_{10} +6;
1.314_{10} +6;	1.316_{10} +6;	1.318_{10} +6;	1.316_{10} +6;	1.314_{10} +6;
1.315_{10} +6;	1.318_{10} +6;	1.326_{10} +6;	1.332_{10} +6;	1.331_{10} +6;
1.333_{10} +6;	1.345_{10} +6;	1.351_{10} +6;	1.370_{10} +6;	1.388_{10} +6;
1.375_{10} +6;	1.354_{10} +6;	1.358_{10} +6;	1.362_{10} +6;	1.365_{10} +6;
1.364_{10} +6;	1.362_{10} +6;	1.368_{10} +6;	1.376_{10} +6;	1.376_{10} +6;
1.382_{10} +6;	1.391_{10} +6;	1.424_{10} +6;	1.479_{10} +6;	1.464_{10} +6;
1.478_{10} +6;	1.459_{10} +6;	1.469_{10} +6;	1.479_{10} +6;	1.504_{10} +6;
1.516_{10} +6;	1.529_{10} +6;	1.543_{10} +6;	1.560_{10} +6;	1.570_{10} +6;
1.579_{10} +6;	1.587_{10} +6;	1.590_{10} +6;	1.594_{10} +6;	1.597_{10} +6;
1.602_{10} +6;	1.599_{10} +6;	1.599_{10} +6;	1.599_{10} +6;	1.598_{10} +6;
1.598_{10} +6;	1.596_{10} +6;	1.585_{10} +6;	1.588_{10} +6;	1.588_{10} +6;
1.591_{10} +6;	1.591_{10} +6;	1.579_{10} +6;	1.683_{10} +6;	1.609_{10} +6;
1.597_{10} +6;	1.604_{10} +6;	1.612_{10} +6;	1.614_{10} +6;	1.623_{10} +6;
1.636_{10} +6;	1.641_{10} +6;	1.651_{10} +6;	1.669_{10} +6;	1.678_{10} +6;
1.688_{10} +6;	1.698_{10} +6;	1.705_{10} +6;	1.714_{10} +6;	1.727_{10} +6;
1.736_{10} +6;	1.751_{10} +6;	1.757_{10} +6;	1.766_{10} +6;	1.781_{10} +6;
1.790_{10} +6;	1.794_{10} +6;	1.806_{10} +6;	1.823_{10} +6;	1.826_{10} +6;
1.832_{10} +6;	1.839_{10} +6;	1.852_{10} +6;	1.865_{10} +6;	1.871_{10} +6;
1.879_{10} +6;	1.881_{10} +6;	1.881_{10} +6;	1.887_{10} +6;	1.892_{10} +6;
1.891_{10} +6;	1.892_{10} +6;	1.900_{10} +6;	1.898_{10} +6;	1.904_{10} +6;
1.902_{10} +6;	1.903_{10} +6;	1.905_{10} +6;	1.910_{10} +6;	1.912_{10} +6;
1.912_{10} +6;	1.915_{10} +6;	1.918_{10} +6;	1.926_{10} +6;	1.934_{10} +6;
1.945_{10} +6;	1.955_{10} +6;	1.965_{10} +6;	1.983_{10} +6;	1.993_{10} +6;
2.003_{10} +6;	2.016_{10} +6;	2.030_{10} +6;	2.041_{10} +6;	2.057_{10} +6;
2.063_{10} +6;	2.076_{10} +6;	2.103_{10} +6;	2.104_{10} +6;	2.106_{10} +6;
2.117_{10} +6;	2.126_{10} +6;	2.137_{10} +6;	2.153_{10} +6;	2.149_{10} +6;
2.159_{10} +6;	2.163_{10} +6;	2.163_{10} +6;	2.165_{10} +6;	2.175_{10} +6;
2.179_{10} +6;	2.180_{10} +6;	2.189_{10} +6;	2.195_{10} +6;	2.196_{10} +6;
2.195_{10} +6;	2.198_{10} +6;	2.204_{10} +6;	2.218_{10} +6;	2.217_{10} +6;
2.219_{10} +6;	2.218_{10} +6;	2.223_{10} +6;	2.228_{10} +6;	2.230_{10} +6;
2.236_{10} +6;	2.244_{10} +6;	2.246_{10} +6;	2.249_{10} +6;	2.257_{10} +6;
2.267_{10} +6;	2.271_{10} +6;	2.284_{10} +6;	2.282_{10} +6;	2.284_{10} +6;
2.305_{10} +6;	2.317_{10} +6;	2.322_{10} +6;	2.333_{10} +6;	2.347_{10} +6;
2.363_{10} +6;	2.370_{10} +6;	2.385_{10} +6;	2.408_{10} +6;	2.418_{10} +6;
2.427_{10} +6;	2.432_{10} +6;	2.439_{10} +6;	2.454_{10} +6;	2.460_{10} +6;
2.472_{10} +6;	2.483_{10} +6;	2.489_{10} +6;	2.497_{10} +6;	2.510_{10} +6;
2.521_{10} +6;	2.521_{10} +6;	2.529_{10} +6;	2.535_{10} +6;	2.540_{10} +6;
2.549_{10} +6;	2.564_{10} +6;	2.567_{10} +6;	2.595_{10} +6;	2.599_{10} +6;
2.642_{10} +6;	2.619_{10} +6;	2.615_{10} +6;	2.612_{10} +6;	2.625_{10} +6;
2.644_{10} +6;	2.650_{10} +6;	2.661_{10} +6;	2.656_{10} +6;	

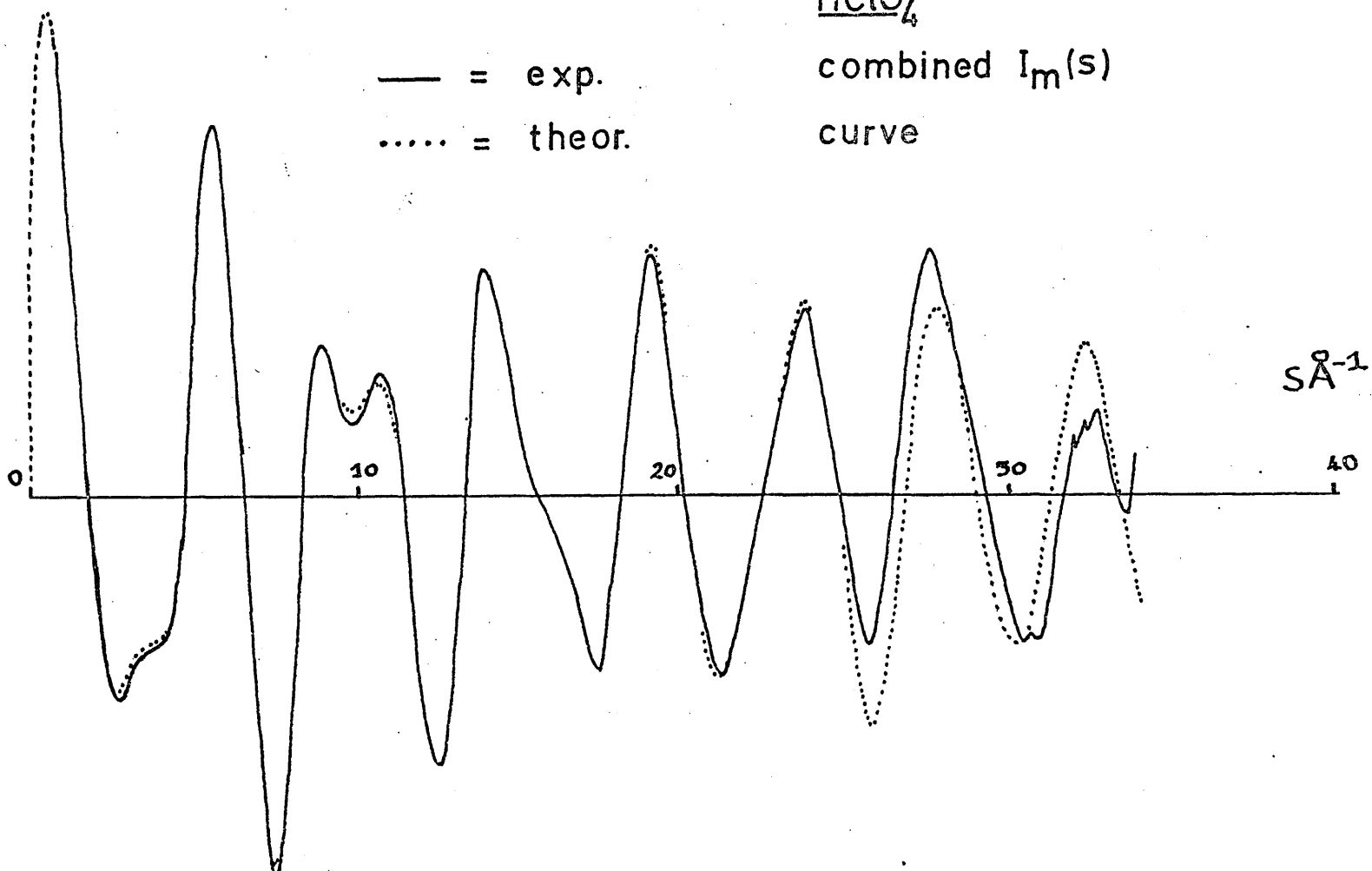

fig.10.1

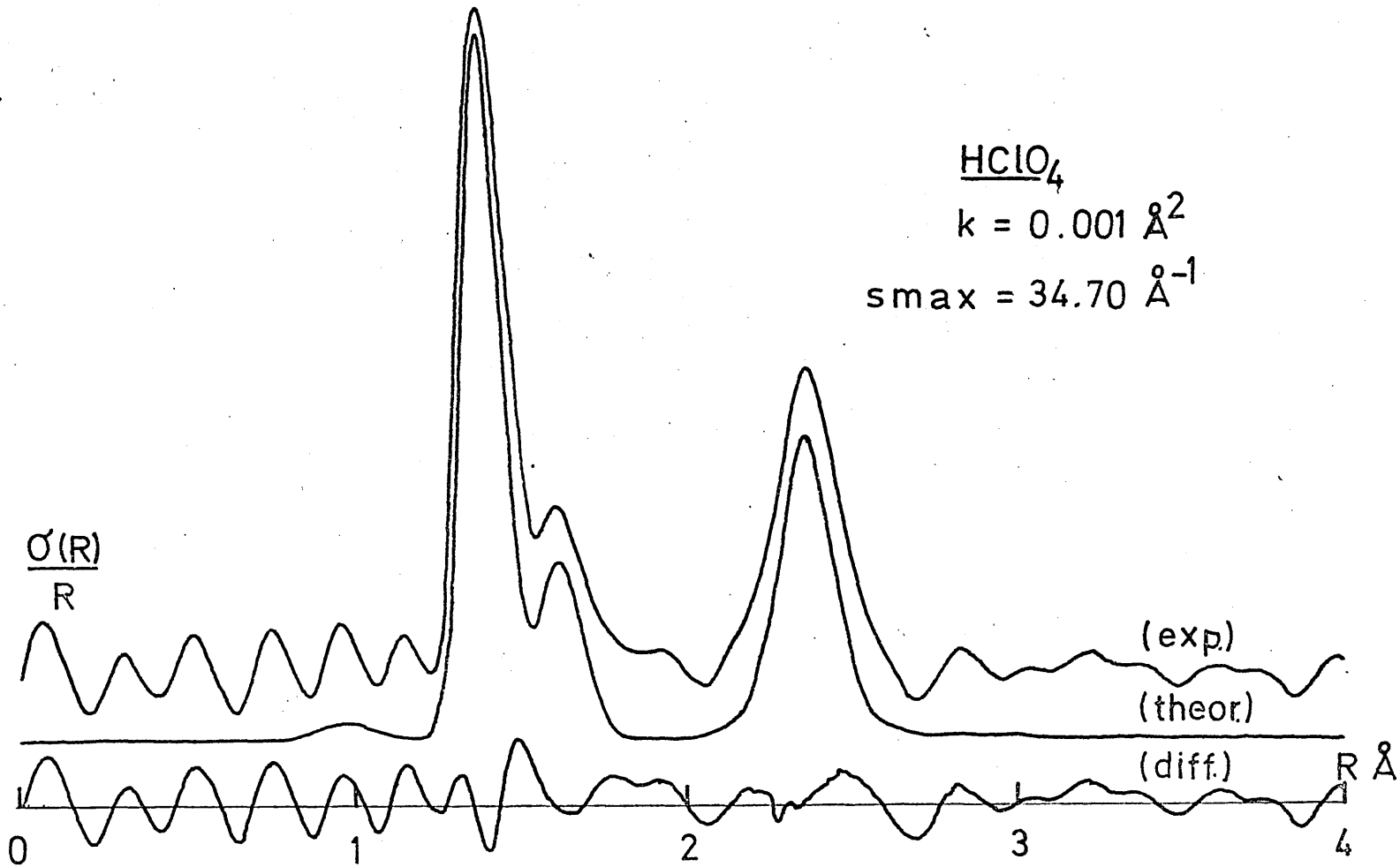

fig. 10.2

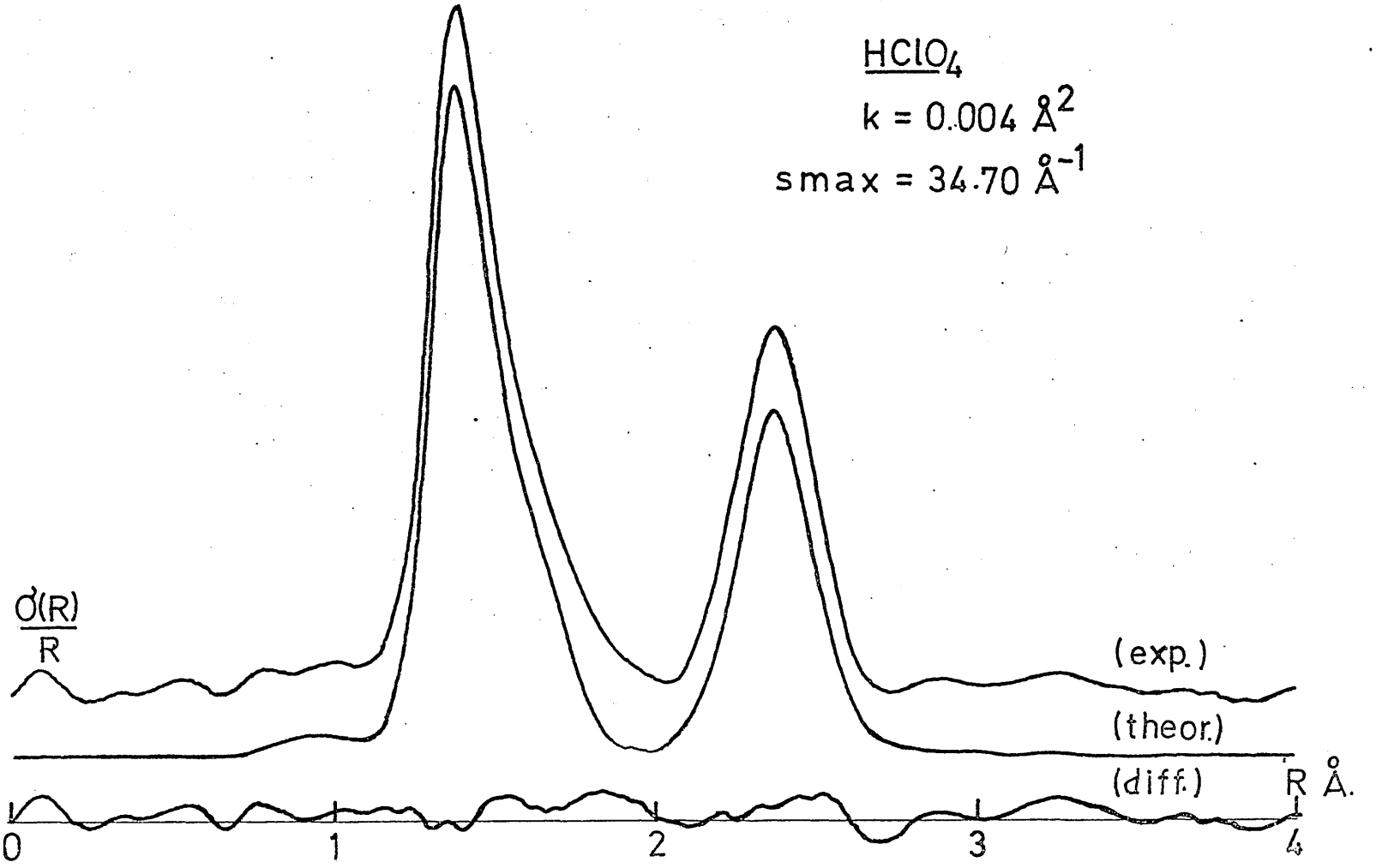

fig. 10.3

TABLE 10.3

Results of individual distance refinements

for $HClO_4$

jet to plate distance	100 cm	50 cm	25 cm
r_{Cl-Op} (Å)	1.4083	1.4083	1.4082
σ'	0.0013	0.0006	0.0013
r_{Cl-OH} (Å)	1.6398	1.6399	1.6289
σ'	0.0057	0.0021	0.0056
$r_{Op..Op}$ (Å)	2.3149	2.3689	2.3612
σ'	0.0045	0.0049	0.0099
R(%)	7.77	7.55	34.69
$\sum_w \Delta^2$	6.186×10^9	7.672×10^{10}	2.384×10^{13}

Notes: (1) In these refinements the u values were held constant at spectroscopic values, and r_{O-H} at 0.96 Å, and the angle ClOH at 113°.

(2) The σ' values are least squares e.s.d.'s.

(3) The r distances are the three independent parameters chosen to describe the ClO_4 tetrahedron, and the values quoted are $r_g(1)$ quantities.

TABLE 10.4

Results of ' all data combined ' refinements for $HClO_4$

parameter	combtwo	comb-scaled	combtwo	comb-scaled
r_{Cl-Op} (Å)	1.4074	1.4062	1.4071	1.4059
σ	0.0008	0.0006	0.0009	0.0007
r_{Cl-OH} (Å)	1.6293	1.6345	1.6387	1.6374
σ	0.0032	0.0025	0.0052	0.0036
$r_{Op..Op}$ (Å)	2.3497	2.3562	2.3638	2.3642
σ	0.0042	0.0039	0.0164	0.0110
u_{Cl-Op} (Å)	spect.	spect.	0.0444	0.0439
σ	-	-	0.0012	0.0010
u_{Cl-OH} (Å)	spect.	spect.	0.0700	0.0635
σ	-	-	0.0047	0.0036
$u_{Op..Op}$ (Å)	spect.	spect.	0.0781	0.0749
σ	-	-	0.0174	0.0140
$u_{Op..OH}$ (Å)	spect.	spect.	0.0677	0.0617
σ	-	-	0.0072	0.0071
R(%)	14.19	13.18	13.14	12.63
$\sum wΔ^2$	3.485×10^{10}	3.637×10^{10}	3.025×10^{10}	3.288×10^{10}

Note: The distances are $r_g(1)$ values and the H position was assumed as described in Table 10.3, note (1).

TABLE 10.5

The final structural parameters

for $HClO_4$

parameter	final result	reproducibility
r_{Cl-Op} (Å)	1.407	0.003
r_{Cl-OH} (Å)	1.635	0.011
$r_{Op..Op}$ (Å)	2.359	0.027
$r_{Op..OH}$ (Å)	2.410	0.048
$\widehat{OpClOp}$ (°)	113.9	2.1
$\widehat{OpClOH}$ (°)	104.5	2.8
u_{Cl-Op} (Å)	0.036	0.004
u_{Cl-OH} (Å)	0.062	0.013
$u_{Op..Op}$ (Å)	0.077	0.048
$u_{Op..OH}$ (Å)	0.065	0.022

Notes: (1) The amplitudes of vibration have been corrected for Born failure according to the methods of Chapter Eight.

(2) The above results were obtained by taking a straight average of the values given in the four columns of table 10.4, the O's being averaged, and reproducibilities calculated from them.

CHAPTER ELEVEN

AN ELECTRON DIFFRACTION INVESTIGATION OF GASEOUS PERCHLORYL FLUORIDE*

1. Introduction

In 1956, as a result of a gas phase infrared investigation, Lide and Mann[69] proposed a C_{3v} tetrahedral model (see fig. 6.1) for the molecule of perchloryl fluoride ($FClO_3$). In 1965 Lide confirmed this symmetry by microwave spectroscopy[70] and determined the distance of the centre of mass of the system from the Cl^{35} atom.

The present electron diffraction investigation of the compound was undertaken to obtain accurate structural parameters and root mean square amplitudes of vibration for the $FClO_3$ molecule, it being intended to compare the amplitudes determined with corresponding spectroscopic results calculated from the infrared data of ref. 69.

2. Experimental

The sample of perchloryl fluoride used in experiments was donated by the Pennsalt Chemical Corporation of Pennsylvania U.S.A. No difficulty was experienced in recording diffraction patterns at all four jet-to-plate distances, and a summary of the experimental conditions adopted is given in table 11.1.

* A preliminary account of this work has been given in ref. 98.

Four uphill curves are listed in table 11.2, and the final experimental combined $I_m(s)$ function is presented graphically in figure 11.1. Two radial distribution curves calculated from this function using damping constants of 0.001 and 0.004 A^{o2}, are shown in figures 11.2 and 11.3 respectively, and of these, the first achieves a resolution of the two types of bonded internuclear distance present in the molecule. The C_{3v} structure proposed in references 69 and 70 is evidently confirmed.

3. Results

The $FClO_3$ tetrahedron was defined by the three internuclear distances R_{Cl-Op}, R_{Cl-F}, and $R_{Op..Op}$. In least squares refinements these parameters were varied independently, and the amplitudes of vibration u_{Cl-Op}, u_{Cl-F}, $u_{Op..Op}$ and $u_{Op..F}$ were also refinable. The dependent distance $R_{Op..F}$ was calculated after each least squares cycle by means of the perchloric acid subroutine discussed in Appendix Five, and to avoid the necessity of modifying this computer procedure, an imaginary atom of zero scattering factor was assumed.

Results of four single distance refinements are presented in table 11.3. The hundred centimetre parameters quoted in the first column of this table are

distinctly high when compared with those of the other three columns, but since no unusually high values were obtained on carrying out all-data-combined refinements (see table 11.4) it may be concluded that these values correspond to a least squares false minimum, and do not indicate experimental error. Table 11.4 also shows that , unlike the case of perchloric acid (see Chapter Ten) the Op..Op distance in $FClO_3$ is well determined, whether root mean square amplitudes of vibration are refined simultaneously or not. This fact probably indicates that the tetrahedron edges of the perchloryl fluoride molecule differ more in size than do the corresponding distances in $HClO_4$. Final structural parameters for perchloryl fluoride, obtained by averaging the columns of table 11.4, are listed in table 11.5.

4. Discussion

It is clear from table 11.5 that in $FClO_3$ and Cl_2O_7 the ClO3 groups present are basically similar, the relevant heptoxide parameters having been determined by Beagley[81] as $R_{Cl-Op} = 1.405$ Å and $OpClOp = 115.2^{o}$. The perchloryl fluoride R_{Cl-Op} bond length of 1.403 Å appears, however, to be significantly shorter than the corresponding distance in perchloric acid (1.407 Å)

whilst its valence angle OpClOp of 116.2° is considerably larger than the corresponding $HClO_4$ value of 113.9°. This latter result is subject, however, to a large uncertainty (2.1°) and hence this difference may not be as significant as it appears. It is of interest that the ClF bond length of 1.617 Å obtained by the present work is somewhat shorter than the r_e value determined for chlorine monofluoride by microwave spectroscopy[71], and shorter still than the Cl-F single bond length of 1.66 Å consistent with Beagley's tetrahedral covalent radii[99] for oxygen and fluorine and a single bond value of 1.700 Å for the Cl-O distance.

From the structural results listed in table 11.5, a value of 0.171 Å was calculated for the distance of the centre of mass of the Cl^{35} species of $FClO_3$ from the chlorine atom (this point lies between Cl and F) and a value of 5276 Mc/sec was obtained for the rotational constant B of this same isotopic species. These quantities, which are subject to errors of 0.013 Å and 40 Mc/sec respectively, may be compared with the corresponding results of 0.154 Å and 5258.7 Mc/sec determined by Lide[70]. Such a comparison indicates that if the bond lengths given in table 11.5 are accepted as correct, then an OpClOp valence angle of 115.2° would be more consistent with the microwave position

for the centre of mass, and hence it is probable that a compromise value of 115.7° is the best estimate which can be given at present for the OpClOp angle in $FClO_3$.

Both the Cl-Op and Cl-F distances in $FClO_3$ are shorter than single bond values, and it is clear from the Cl-Op shortening of ~ 0.3 Å, that this bond has a large amount of double bond character, larger probably than that appropriate to the corresponding internuclear distances in Cl_2O_7 and $HClO_4$. On the other hand, the shortening of ~ 0.04 Å observed for the Cl-F bond is surprisingly small, when it is considered that in $FClO_3$ the central chlorine atom must be depleted of electrons to a large extent by the sigma bonds which it forms, and that the fluorine atom has two lone pairs of electrons apparently available for π bonding. Unlike the peripheral oxygen atoms, however, which evidently donate electrons into the d_{z^2} and $d_{x^2-y^2}$ orbitals on chlorine[95], the fluorine atom appears to retain its p electrons. Indeed, it seems possible that some of the Cl-F shortening observed merely results from a hybridisation change from sp^3 to sp, and if this is so it must be inferred that the amount of π character in the Cl-F bond of perchloryl fluoride is less even than that of the Cl-OH bond in $HClO_4$. The slight shortening of the Cl-Op distance in $FClO_3$ relative to

that of $HClO_4$, is presumably attributable to the electron-withdrawing properties of the fluorine atom which should cause an increased positive charge on chlorine, and so enhance the amount of $d\pi$-$p\pi$ bonding present in the peripheral Cl-O bonds.

Finally, it is of interest that the amplitudes of vibration obtained by the present study, and listed in table 11.5, are in good agreement with those calculated from spectroscopic data in Chapter Six.

TABLE 11.1

A summary of experimental details

for the perchloryl fluoride investigation

jet to plate distance	100 cm	50 cm	25 cm	11 cm
wavelength (A)	0.051205	0.051205	0.051205	0.051205
e.s.d.	0.000020	0.000020	0.000020	0.000020
sample temperature (^{o}K)	193	193	193	193
nozzle temperature (^{o}K)	293	293	293	293
gas temperature assumed (^{o}K)	243	243	243	243
number of plates used	4	4	6	4
quality	rather dark	good	good	good to light
number of traces measured (AMDM)	4	4	6	8

TABLE 11.2

$FClO_3$ intensity data as combined uphill curves

range (1): s = 0.86 by 0.02 to 9.02 Å^{-1}

8.121_{10} +2;	8.604_{10} +2;	9.143_{10} +2;	9.694_{10} +2;	1.023_{10} +3;
1.073_{10} +3;	1.124_{10} +3;	1.174_{10} +3;	1.226_{10} +3;	1.285_{10} +3;
1.352_{10} +3;	1.427_{10} +3;	1.507_{10} +3;	1.593_{10} +3;	1.682_{10} +3;
1.772_{10} +3;	1.861_{10} +3;	1.948_{10} +3;	2.032_{10} +3;	2.113_{10} +3;
2.191_{10} +3;	2.266_{10} +3;	2.338_{10} +3;	2.408_{10} +3;	2.475_{10} +3;
2.541_{10} +3;	2.608_{10} +3;	2.676_{10} +3;	2.746_{10} +3;	2.818_{10} +3;
2.888_{10} +3;	2.956_{10} +3;	3.021_{10} +3;	3.083_{10} +3;	3.141_{10} +3;
3.195_{10} +3;	3.246_{10} +3;	3.294_{10} +3;	3.340_{10} +3;	3.386_{10} +3;
3.429_{10} +3;	3.474_{10} +3;	3.521_{10} +3;	3.568_{10} +3;	3.616_{10} +3;
3.664_{10} +3;	3.709_{10} +3;	3.754_{10} +3;	3.796_{10} +3;	3.839_{10} +3;
3.880_{10} +3;	3.921_{10} +3;	3.962_{10} +3;	4.004_{10} +3;	4.045_{10} +3;
4.084_{10} +3;	4.123_{10} +3;	4.160_{10} +3;	4.196_{10} +3;	4.234_{10} +3;
4.273_{10} +3;	4.313_{10} +3;	4.354_{10} +3;	4.395_{10} +3;	4.435_{10} +3;
4.474_{10} +3;	4.513_{10} +3;	4.553_{10} +3;	4.596_{10} +3;	4.639_{10} +3;
4.685_{10} +3;	4.732_{10} +3;	4.783_{10} +3;	4.837_{10} +3;	4.892_{10} +3;
4.952_{10} +3;	5.015_{10} +3;	5.083_{10} +3;	5.155_{10} +3;	5.228_{10} +3;
5.303_{10} +3;	5.379_{10} +3;	5.456_{10} +3;	5.535_{10} +3;	5.619_{10} +3;
5.708_{10} +3;	5.801_{10} +3;	5.896_{10} +3;	5.993_{10} +3;	6.092_{10} +3;
6.194_{10} +3;	6.299_{10} +3;	6.408_{10} +3;	6.520_{10} +3;	6.635_{10} +3;
6.753_{10} +3;	6.873_{10} +3;	6.996_{10} +3;	7.119_{10} +3;	7.246_{10} +3;
7.376_{10} +3;	7.512_{10} +3;	7.651_{10} +3;	7.794_{10} +3;	7.939_{10} +3;
8.085_{10} +3;	8.229_{10} +3;	8.377_{10} +3;	8.527_{10} +3;	8.681_{10} +3;
8.841_{10} +3;	9.004_{10} +3;	9.167_{10} +3;	9.328_{10} +3;	9.494_{10} +3;
9.659_{10} +3;	9.824_{10} +3;	9.995_{10} +3;	1.017_{10} +4;	1.034_{10} +4;
1.050_{10} +4;	1.067_{10} +4;	1.082_{10} +4;	1.097_{10} +4;	1.113_{10} +4;
1.128_{10} +4;	1.144_{10} +4;	1.160_{10} +4;	1.176_{10} +4;	1.192_{10} +4;
1.207_{10} +4;	1.222_{10} +4;	1.238_{10} +4;	1.253_{10} +4;	1.268_{10} +4;
1.282_{10} +4;	1.297_{10} +4;	1.312_{10} +4;	1.327_{10} +4;	1.343_{10} +4;
1.358_{10} +4;	1.374_{10} +4;	1.389_{10} +4;	1.404_{10} +4;	1.419_{10} +4;
1.433_{10} +4;	1.447_{10} +4;	1.462_{10} +4;	1.478_{10} +4;	1.493_{10} +4;
1.509_{10} +4;	1.525_{10} +4;	1.542_{10} +4;	1.559_{10} +4;	1.575_{10} +4;
1.591_{10} +4;	1.606_{10} +4;	1.621_{10} +4;	1.636_{10} +4;	1.652_{10} +4;
1.670_{10} +4;	1.688_{10} +4;	1.706_{10} +4;	1.722_{10} +4;	1.738_{10} +4;
1.754_{10} +4;	1.771_{10} +4;	1.788_{10} +4;	1.807_{10} +4;	1.827_{10} +4;
1.845_{10} +4;	1.864_{10} +4;	1.882_{10} +4;	1.901_{10} +4;	1.920_{10} +4;
1.940_{10} +4;	1.961_{10} +4;	1.983_{10} +4;	2.007_{10} +4;	2.032_{10} +4;
2.057_{10} +4;	2.082_{10} +4;	2.107_{10} +4;	2.132_{10} +4;	2.159_{10} +4;
2.188_{10} +4;	2.217_{10} +4;	2.245_{10} +4;	2.273_{10} +4;	2.302_{10} +4;
2.330_{10} +4;	2.359_{10} +4;	2.390_{10} +4;	2.422_{10} +4;	2.454_{10} +4;
2.486_{10} +4;	2.517_{10} +4;	2.549_{10} +4;	2.583_{10} +4;	2.617_{10} +4;

TABLE 11.2 (cont'd)

2.652_{10} +4;	2.687_{10} +4;	2.722_{10} +4;	2.757_{10} +4;	2.793_{10} +4;
2.830_{10} +4;	2.866_{10} +4;	2.902_{10} +4;	2.939_{10} +4;	2.975_{10} +4;
3.010_{10} +4;	3.045_{10} +4;	3.080_{10} +4;	3.116_{10} +4;	3.151_{10} +4;
3.186_{10} +4;	3.222_{10} +4;	3.258_{10} +4;	3.295_{10} +4;	3.331_{10} +4;
3.367_{10} +4;	3.403_{10} +4;	3.437_{10} +4;	3.470_{10} +4;	3.503_{10} +4;
3.534_{10} +4;	3.567_{10} +4;	3.598_{10} +4;	3.629_{10} +4;	3.658_{10} +4;
3.686_{10} +4;	3.713_{10} +4;	3.739_{10} +4;	3.765_{10} +4;	3.789_{10} +4;
3.813_{10} +4;	3.836_{10} +4;	3.859_{10} +4;	3.883_{10} +4;	3.906_{10} +4;
3.927_{10} +4;	3.946_{10} +4;	3.963_{10} +4;	3.977_{10} +4;	3.990_{10} +4;
4.002_{10} +4;	4.014_{10} +4;	4.025_{10} +4;	4.037_{10} +4;	4.049_{10} +4;
4.059_{10} +4;	4.066_{10} +4;	4.071_{10} +4;	4.073_{10} +4;	4.072_{10} +4;
4.072_{10} +4;	4.071_{10} +4;	4.070_{10} +4;	4.073_{10} +4;	4.070_{10} +4;
4.063_{10} +4;	4.050_{10} +4;	4.033_{10} +4;	4.017_{10} +4;	4.007_{10} +4;
3.999_{10} +4;	3.996_{10} +4;	3.996_{10} +4;	3.992_{10} +4;	3.981_{10} +4;
3.967_{10} +4;	3.949_{10} +4;	3.934_{10} +4;	3.916_{10} +4;	3.900_{10} +4;
3.882_{10} +4;	3.863_{10} +4;	3.842_{10} +4;	3.822_{10} +4;	3.800_{10} +4;
3.778_{10} +4;	3.756_{10} +4;	3.734_{10} +4;	3.711_{10} +4;	3.688_{10} +4;
3.665_{10} +4;	3.642_{10} +4;	3.619_{10} +4;	3.598_{10} +4;	3.575_{10} +4;
3.553_{10} +4;	3.532_{10} +4;	3.510_{10} +4;	3.488_{10} +4;	3.467_{10} +4;
3.447_{10} +4;	3.428_{10} +4;	3.410_{10} +4;	3.392_{10} +4;	3.374_{10} +4;
3.356_{10} +4;	3.340_{10} +4;	3.324_{10} +4;	3.309_{10} +4;	3.294_{10} +4;
3.280_{10} +4;	3.264_{10} +4;	3.249_{10} +4;	3.236_{10} +4;	3.225_{10} +4;
3.216_{10} +4;	3.209_{10} +4;	3.204_{10} +4;	3.198_{10} +4;	3.192_{10} +4;
3.186_{10} +4;	3.181_{10} +4;	3.177_{10} +4;	3.175_{10} +4;	3.171_{10} +4;
3.168_{10} +4;	3.166_{10} +4;	3.167_{10} +4;	3.169_{10} +4;	3.174_{10} +4;
3.182_{10} +4;	3.191_{10} +4;	3.200_{10} +4;	3.210_{10} +4;	3.217_{10} +4;
3.226_{10} +4;	3.231_{10} +4;	3.232_{10} +4;	3.236_{10} +4;	3.251_{10} +4;
3.268_{10} +4;	3.292_{10} +4;	3.322_{10} +4;	3.350_{10} +4;	3.372_{10} +4;
3.394_{10} +4;	3.411_{10} +4;	3.431_{10} +4;	3.455_{10} +4;	3.479_{10} +4;
3.504_{10} +4;	3.529_{10} +4;	3.555_{10} +4;	3.582_{10} +4;	3.609_{10} +4;
3.639_{10} +4;	3.668_{10} +4;	3.698_{10} +4;	3.729_{10} +4;	3.760_{10} +4;
3.791_{10} +4;	3.825_{10} +4;	3.859_{10} +4;	3.892_{10} +4;	3.923_{10} +4;
3.956_{10} +4;	3.988_{10} +4;	4.021_{10} +4;	4.056_{10} +4;	4.090_{10} +4;
4.124_{10} +4;	4.159_{10} +4;	4.194_{10} +4;	4.231_{10} +4;	4.269_{10} +4;
4.308_{10} +4;	4.344_{10} +4;	4.381_{10} +4;	4.415_{10} +4;	4.449_{10} +4;
4.483_{10} +4;	4.515_{10} +4;	4.547_{10} +4;	4.580_{10} +4;	4.614_{10} +4;
4.650_{10} +4;	4.688_{10} +4;	4.727_{10} +4;	4.761_{10} +4;	4.794_{10} +4;
4.823_{10} +4;	4.850_{10} +4;	4.877_{10} +4;	4.907_{10} +4;	4.937_{10} +4;
4.967_{10} +4;	4.998_{10} +4;	5.028_{10} +4;	5.056_{10} +4;	5.083_{10} +4;
5.109_{10} +4;	5.136_{10} +4;	5.163_{10} +4;	5.190_{10} +4;	5.213_{10} +4;
5.236_{10} +4;	5.254_{10} +4;	5.271_{10} +4;	5.287_{10} +4;	5.303_{10} +4;
5.319_{10} +4;	5.338_{10} +4;	5.358_{10} +4;	5.377_{10} +4;	

TABLE 11.2 (cont'd)

range (2): s = 2.40 by 0.05 to 17.90 $\mathring{A}^{-1}$

2.674_{10} +4;	2.774_{10} +4;	2.884_{10} +4;	3.000_{10} +4;	3.119_{10} +4;
3.241_{10} +4;	3.370_{10} +4;	3.510_{10} +4;	3.663_{10} +4;	3.831_{10} +4;
4.008_{10} +4;	4.196_{10} +4;	4.387_{10} +4;	4.574_{10} +4;	4.766_{10} +4;
4.966_{10} +4;	5.155_{10} +4;	5.331_{10} +4;	5.510_{10} +4;	5.703_{10} +4;
5.904_{10} +4;	6.109_{10} +4;	6.311_{10} +4;	6.506_{10} +4;	6.698_{10} +4;
6.890_{10} +4;	7.079_{10} +4;	7.270_{10} +4;	7.465_{10} +4;	7.657_{10} +4;
7.842_{10} +4;	8.031_{10} +4;	8.214_{10} +4;	8.397_{10} +4;	8.588_{10} +4;
8.801_{10} +4;	9.025_{10} +4;	9.261_{10} +4;	9.493_{10} +4;	9.732_{10} +4;
9.980_{10} +4;	1.024_{10} +5;	1.052_{10} +5;	1.082_{10} +5;	1.114_{10} +5;
1.148_{10} +5;	1.183_{10} +5;	1.219_{10} +5;	1.257_{10} +5;	1.295_{10} +5;
1.334_{10} +5;	1.375_{10} +5;	1.416_{10} +5;	1.458_{10} +5;	1.502_{10} +5;
1.545_{10} +5;	1.587_{10} +5;	1.625_{10} +5;	1.663_{10} +5;	1.698_{10} +5;
1.732_{10} +5;	1.763_{10} +5;	1.792_{10} +5;	1.819_{10} +5;	1.843_{10} +5;
1.864_{10} +5;	1.880_{10} +5;	1.893_{10} +5;	1.905_{10} +5;	1.912_{10} +5;
1.915_{10} +5;	1.915_{10} +5;	1.911_{10} +5;	1.902_{10} +5;	1.890_{10} +5;
1.876_{10} +5;	1.861_{10} +5;	1.845_{10} +5;	1.826_{10} +5;	1.801_{10} +5;
1.777_{10} +5;	1.754_{10} +5;	1.728_{10} +5;	1.701_{10} +5;	1.675_{10} +5;
1.650_{10} +5;	1.624_{10} +5;	1.596_{10} +5;	1.570_{10} +5;	1.547_{10} +5;
1.525_{10} +5;	1.506_{10} +5;	1.491_{10} +5;	1.477_{10} +5;	1.464_{10} +5;
1.454_{10} +5;	1.446_{10} +5;	1.441_{10} +5;	1.439_{10} +5;	1.441_{10} +5;
1.445_{10} +5;	1.451_{10} +5;	1.462_{10} +5;	1.476_{10} +5;	1.493_{10} +5;
1.513_{10} +5;	1.535_{10} +5;	1.557_{10} +5;	1.580_{10} +5;	1.608_{10} +5;
1.637_{10} +5;	1.664_{10} +5;	1.691_{10} +5;	1.721_{10} +5;	1.754_{10} +5;
1.784_{10} +5;	1.813_{10} +5;	1.843_{10} +5;	1.877_{10} +5;	1.909_{10} +5;
1.935_{10} +5;	1.958_{10} +5;	1.981_{10} +5;	2.006_{10} +5;	2.027_{10} +5;
2.046_{10} +5;	2.063_{10} +5;	2.077_{10} +5;	2.090_{10} +5;	2.101_{10} +5;
2.111_{10} +5;	2.120_{10} +5;	2.128_{10} +5;	2.131_{10} +5;	2.135_{10} +5;
2.141_{10} +5;	2.143_{10} +5;	2.142_{10} +5;	2.142_{10} +5;	2.144_{10} +5;
2.140_{10} +5;	2.133_{10} +5;	2.129_{10} +5;	2.129_{10} +5;	2.129_{10} +5;
2.126_{10} +5;	2.122_{10} +5;	2.119_{10} +5;	2.119_{10} +5;	2.122_{10} +5;
2.124_{10} +5;	2.125_{10} +5;	2.128_{10} +5;	2.135_{10} +5;	2.140_{10} +5;
2.145_{10} +5;	2.151_{10} +5;	2.158_{10} +5;	2.165_{10} +5;	2.172_{10} +5;
2.180_{10} +5;	2.191_{10} +5;	2.201_{10} +5;	2.210_{10} +5;	2.217_{10} +5;
2.226_{10} +5;	2.236_{10} +5;	2.246_{10} +5;	2.251_{10} +5;	2.255_{10} +5;
2.261_{10} +5;	2.267_{10} +5;	2.272_{10} +5;	2.275_{10} +5;	2.278_{10} +5;
2.283_{10} +5;	2.283_{10} +5;	2.278_{10} +5;	2.272_{10} +5;	2.272_{10} +5;
2.273_{10} +5;	2.268_{10} +5;	2.260_{10} +5;	2.252_{10} +5;	2.247_{10} +5;
2.244_{10} +5;	2.238_{10} +5;	2.231_{10} +5;	2.220_{10} +5;	2.208_{10} +5;
2.200_{10} +5;	2.197_{10} +5;	2.192_{10} +5;	2.184_{10} +5;	2.179_{10} +5;

2.177_{10} +5; 2.172_{10} +5; 2.169_{10} +5; 2.169_{10} +5; 2.170_{10} +5;
2.172_{10} +5; 2.173_{10} +5; 2.176_{10} +5; 2.186_{10} +5; 2.200_{10} +5;
2.210_{10} +5; 2.217_{10} +5; 2.227_{10} +5; 2.240_{10} +5; 2.256_{10} +5;
2.276_{10} +5; 2.295_{10} +5; 2.311_{10} +5; 2.322_{10} +5; 2.348_{10} +5;
2.379_{10} +5; 2.399_{10} +5; 2.408_{10} +5; 2.424_{10} +5; 2.452_{10} +5;
2.475_{10} +5; 2.495_{10} +5; 2.514_{10} +5; 2.533_{10} +5; 2.552_{10} +5;
2.570_{10} +5; 2.587_{10} +5; 2.599_{10} +5; 2.612_{10} +5; 2.625_{10} +5;
2.637_{10} +5; 2.647_{10} +5; 2.658_{10} +5; 2.666_{10} +5; 2.670_{10} +5;
2.674_{10} +5; 2.678_{10} +5; 2.679_{10} +5; 2.678_{10} +5; 2.677_{10} +5;
2.677_{10} +5; 2.677_{10} +5; 2.677_{10} +5; 2.677_{10} +5; 2.677_{10} +5;
2.678_{10} +5; 2.674_{10} +5; 2.665_{10} +5; 2.661_{10} +5; 2.664_{10} +5;
2.664_{10} +5; 2.663_{10} +5; 2.655_{10} +5; 2.639_{10} +5; 2.641_{10} +5;
2.660_{10} +5; 2.666_{10} +5; 2.655_{10} +5; 2.656_{10} +5; 2.661_{10} +5;
2.662_{10} +5; 2.660_{10} +5; 2.659_{10} +5; 2.663_{10} +5; 2.668_{10} +5;
2.674_{10} +5; 2.680_{10} +5; 2.686_{10} +5; 2.690_{10} +5; 2.696_{10} +5;
2.702_{10} +5; 2.713_{10} +5; 2.722_{10} +5; 2.729_{10} +5; 2.731_{10} +5;
2.736_{10} +5; 2.741_{10} +5; 2.747_{10} +5; 2.756_{10} +5; 2.766_{10} +5;
2.771_{10} +5; 2.777_{10} +5; 2.782_{10} +5; 2.784_{10} +5; 2.788_{10} +5;
2.797_{10} +5; 2.803_{10} +5; 2.803_{10} +5; 2.804_{10} +5; 2.810_{10} +5;
2.814_{10} +5; 2.814_{10} +5; 2.813_{10} +5; 2.817_{10} +5; 2.822_{10} +5;
2.826_{10} +5; 2.833_{10} +5; 2.841_{10} +5; 2.846_{10} +5; 2.847_{10} +5;
2.851_{10} +5; 2.856_{10} +5; 2.861_{10} +5; 2.869_{10} +5; 2.876_{10} +5;
2.886_{10} +5; 2.899_{10} +5; 2.906_{10} +5; 2.910_{10} +5; 2.918_{10} +5;
2.928_{10} +5;

range (3): s = 7.60 by 0.10 to 34.80 Å^{-1}

3.575_{10} +6; 3.691_{10} +6; 3.827_{10} +6; 3.974_{10} +6; 4.141_{10} +6;
4.300_{10} +6; 4.462_{10} +6; 4.623_{10} +6; 4.786_{10} +6; 4.934_{10} +6;
5.058_{10} +6; 5.151_{10} +6; 5.232_{10} +6; 5.276_{10} +6; 5.301_{10} +6;
5.308_{10} +6; 5.303_{10} +6; 5.278_{10} +6; 5.259_{10} +6; 5.251_{10} +6;
5.249_{10} +6; 5.232_{10} +6; 5.228_{10} +6; 5.235_{10} +6; 5.262_{10} +6;
5.295_{10} +6; 5.331_{10} +6; 5.387_{10} +6; 5.434_{10} +6; 5.488_{10} +6;
5.555_{10} +6; 5.597_{10} +6; 5.645_{10} +6; 5.675_{10} +6; 5.704_{10} +6;
5.696_{10} +6; 5.694_{10} +6; 5.683_{10} +6; 5.649_{10} +6; 5.592_{10} +6;

TABLE 11.2 (cont'd)

5.544_{10} +6;	5.501_{10} +6;	5.450_{10} +6;	5.407_{10} +6;	5.362_{10} +6;
5.320_{10} +6;	5.293_{10} +6;	5.287_{10} +6;	5.285_{10} +6;	5.304_{10} +6;
5.346_{10} +6;	5.394_{10} +6;	5.458_{10} +6;	5.535_{10} +6;	5.622_{10} +6;
5.714_{10} +6;	5.827_{10} +6;	5.931_{10} +6;	6.040_{10} +6;	6.151_{10} +6;
6.247_{10} +6;	6.336_{10} +6;	6.418_{10} +6;	6.471_{10} +6;	6.503_{10} +6;
6.531_{10} +6;	6.519_{10} +6;	6.517_{10} +6;	6.501_{10} +6;	6.476_{10} +6;
6.460_{10} +6;	6.430_{10} +6;	6.391_{10} +6;	6.377_{10} +6;	6.350_{10} +6;
6.342_{10} +6;	6.323_{10} +6;	6.313_{10} +6;	6.306_{10} +6;	6.308_{10} +6;
6.334_{10} +6;	6.363_{10} +6;	6.379_{10} +6;	6.425_{10} +6;	6.461_{10} +6;
6.480_{10} +6;	6.495_{10} +6;	6.522_{10} +6;	6.549_{10} +6;	6.577_{10} +6;
6.596_{10} +6;	6.601_{10} +6;	6.613_{10} +6;	6.603_{10} +6;	6.586_{10} +6;
6.559_{10} +6;	6.540_{10} +6;	6.517_{10} +6;	6.497_{10} +6;	6.502_{10} +6;
6.528_{10} +6;	6.538_{10} +6;	6.575_{10} +6;	6.616_{10} +6;	6.666_{10} +6;
6.719_{10} +6;	6.769_{10} +6;	6.827_{10} +6;	6.894_{10} +6;	6.965_{10} +6;
7.015_{10} +6;	7.068_{10} +6;	7.132_{10} +6;	7.182_{10} +6;	7.228_{10} +6;
7.252_{10} +6;	7.269_{10} +6;	7.285_{10} +6;	7.306_{10} +6;	7.292_{10} +6;
7.279_{10} +6;	7.244_{10} +6;	7.215_{10} +6;	7.178_{10} +6;	7.138_{10} +6;
7.111_{10} +6;	7.076_{10} +6;	7.044_{10} +6;	7.017_{10} +6;	7.003_{10} +6;
6.982_{10} +6;	6.973_{10} +6;	6.993_{10} +6;	6.998_{10} +6;	7.002_{10} +6;
7.027_{10} +6;	7.065_{10} +6;	7.074_{10} +6;	7.111_{10} +6;	7.134_{10} +6;
7.164_{10} +6;	7.204_{10} +6;	7.232_{10} +6;	7.257_{10} +6;	7.291_{10} +6;
7.335_{10} +6;	7.350_{10} +6;	7.376_{10} +6;	7.404_{10} +6;	7.427_{10} +6;
7.458_{10} +6;	7.485_{10} +6;	7.524_{10} +6;	7.570_{10} +6;	7.602_{10} +6;
7.645_{10} +6;	7.663_{10} +6;	7.696_{10} +6;	7.714_{10} +6;	7.757_{10} +6;
7.798_{10} +6;	7.823_{10} +6;	7.843_{10} +6;	7.853_{10} +6;	7.868_{10} +6;
7.869_{10} +6;	7.881_{10} +6;	7.886_{10} +6;	7.886_{10} +6;	7.867_{10} +6;
7.856_{10} +6;	7.847_{10} +6;	7.838_{10} +6;	7.811_{10} +6;	7.777_{10} +6;
7.767_{10} +6;	7.756_{10} +6;	7.755_{10} +6;	7.737_{10} +6;	7.720_{10} +6;
7.711_{10} +6;	7.722_{10} +6;	7.725_{10} +6;	7.743_{10} +6;	7.770_{10} +6;
7.782_{10} +6;	7.817_{10} +6;	7.840_{10} +6;	7.888_{10} +6;	7.948_{10} +6;
7.999_{10} +6;	8.027_{10} +6;	8.079_{10} +6;	8.117_{10} +6;	8.169_{10} +6;
8.211_{10} +6;	8.252_{10} +6;	8.284_{10} +6;	8.314_{10} +6;	8.354_{10} +6;
8.381_{10} +6;	8.378_{10} +6;	8.386_{10} +6;	8.415_{10} +6;	8.426_{10} +6;
8.423_{10} +6;	8.459_{10} +6;	8.527_{10} +6;	8.471_{10} +6;	8.436_{10} +6;
8.433_{10} +6;	8.442_{10} +6;	8.421_{10} +6;	8.411_{10} +6;	8.415_{10} +6;
8.405_{10} +6;	8.397_{10} +6;	8.412_{10} +6;	8.425_{10} +6;	8.437_{10} +6;
8.434_{10} +6;	8.431_{10} +6;	8.438_{10} +6;	8.439_{10} +6;	8.441_{10} +6;
8.458_{10} +6;	8.479_{10} +6;	8.495_{10} +6;	8.514_{10} +6;	8.527_{10} +6;
8.543_{10} +6;	8.575_{10} +6;	8.610_{10} +6;	8.658_{10} +6;	8.693_{10} +6;
8.762_{10} +6;	8.824_{10} +6;	8.902_{10} +6;	8.919_{10} +6;	8.921_{10} +6;
8.919_{10} +6;	8.970_{10} +6;	9.005_{10} +6;	9.031_{10} +6;	9.087_{10} +6;
9.152_{10} +6;	9.162_{10} +6;	9.198_{10} +6;	9.232_{10} +6;	9.254_{10} +6;
9.261_{10} +6;	9.290_{10} +6;	9.319_{10} +6;	9.303_{10} +6;	9.332_{10} +6;
9.336_{10} +6;	9.346_{10} +6;	9.350_{10} +6;	9.353_{10} +6;	9.360_{10} +6;
9.347_{10} +6;	9.369_{10} +6;	9.397_{10} +6;	9.418_{10} +6;	9.439_{10} +6;
9.473_{10} +6;	9.488_{10} +6;	9.518_{10} +6;	9.557_{10} +6;	9.588_{10} +6;
9.607_{10} +6;	9.634_{10} +6;	9.663_{10} +6;		

TABLE 11.2 (concluded)

range (4): s = 26.84 by 0.22 to 42.42 $\mathring{A}^{-1}$

5.254_{10} +7;	5.312_{10} +7;	5.360_{10} +7;	5.388_{10} +7;	5.401_{10} +7;
5.420_{10} +7;	5.427_{10} +7;	5.424_{10} +7;	5.423_{10} +7;	5.425_{10} +7;
5.439_{10} +7;	5.462_{10} +7;	5.458_{10} +7;	5.471_{10} +7;	5.481_{10} +7;
5.485_{10} +7;	5.493_{10} +7;	5.527_{10} +7;	5.563_{10} +7;	5.625_{10} +7;
5.675_{10} +7;	5.733_{10} +7;	5.812_{10} +7;	5.946_{10} +7;	5.945_{10} +7;
5.911_{10} +7;	5.937_{10} +7;	5.944_{10} +7;	5.958_{10} +7;	5.971_{10} +7;
5.972_{10} +7;	6.014_{10} +7;	5.995_{10} +7;	5.974_{10} +7;	6.019_{10} +7;
6.055_{10} +7;	6.062_{10} +7;	6.108_{10} +7;	6.146_{10} +7;	6.172_{10} +7;
6.224_{10} +7;	6.274_{10} +7;	6.290_{10} +7;	6.317_{10} +7;	6.379_{10} +7;
6.439_{10} +7;	6.453_{10} +7;	6.474_{10} +7;	6.497_{10} +7;	6.553_{10} +7;
6.585_{10} +7;	6.590_{10} +7;	6.607_{10} +7;	6.641_{10} +7;	6.657_{10} +7;
6.681_{10} +7;	6.711_{10} +7;	6.740_{10} +7;	6.786_{10} +7;	6.844_{10} +7;
6.875_{10} +7;	6.929_{10} +7;	6.964_{10} +7;	7.040_{10} +7;	7.058_{10} +7;
7.104_{10} +7;	7.179_{10} +7;	7.140_{10} +7;	7.180_{10} +7;	7.213_{10} +7;
7.253_{10} +7;	7.289_{10} +7;	7.323_{10} +7;	7.364_{10} +7;	7.399_{10} +7;
7.448_{10} +7;	7.518_{10} +7;	7.558_{10} +7;	7.606_{10} +7;	7.623_{10} +7;
7.671_{10} +7;	7.728_{10} +7;	7.780_{10} +7;	7.824_{10} +7;	7.860_{10} +7;
7.915_{10} +7;	7.989_{10} +7;	8.033_{10} +7;	8.071_{10} +7;	8.133_{10} +7;

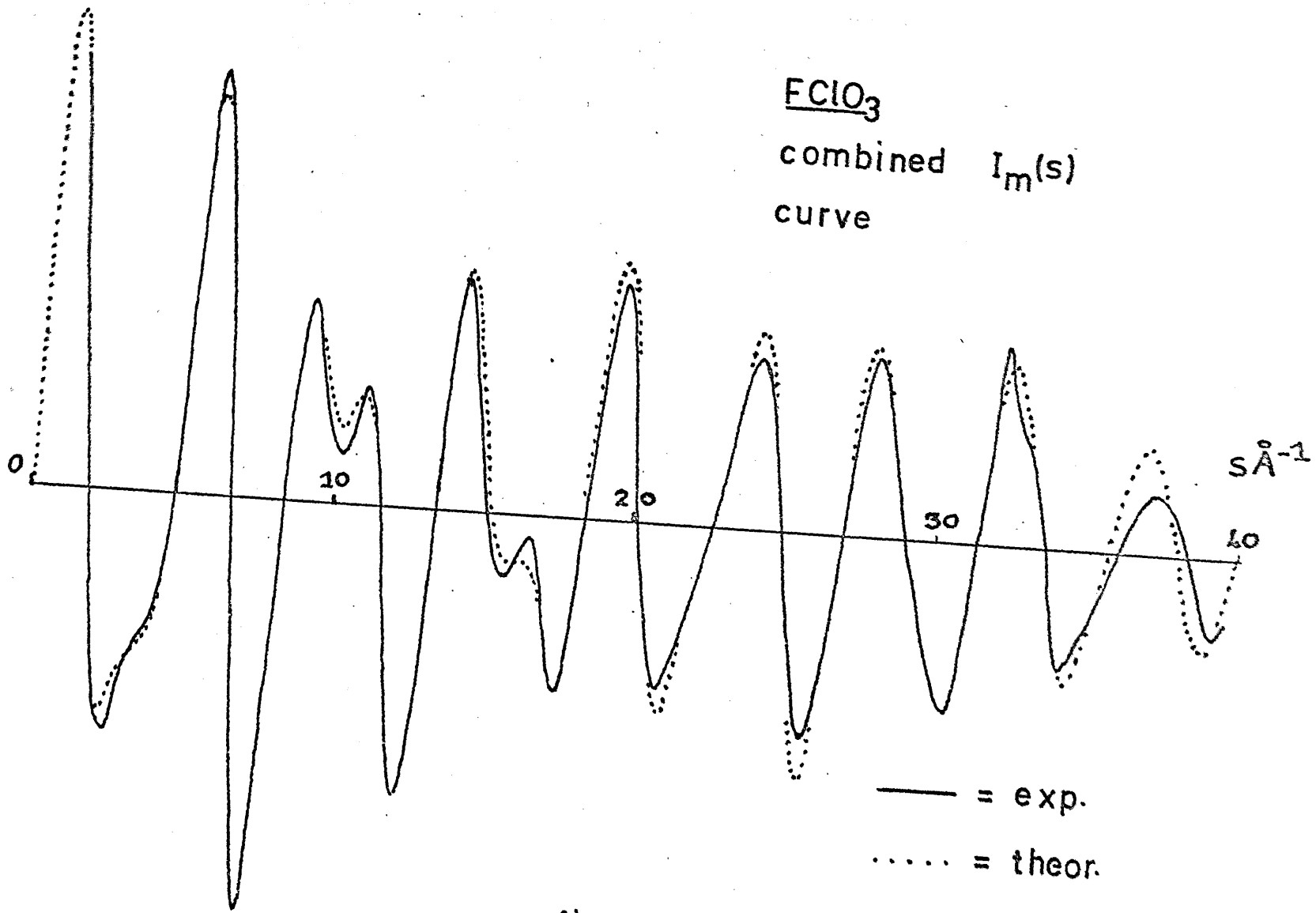

fig. 11.1

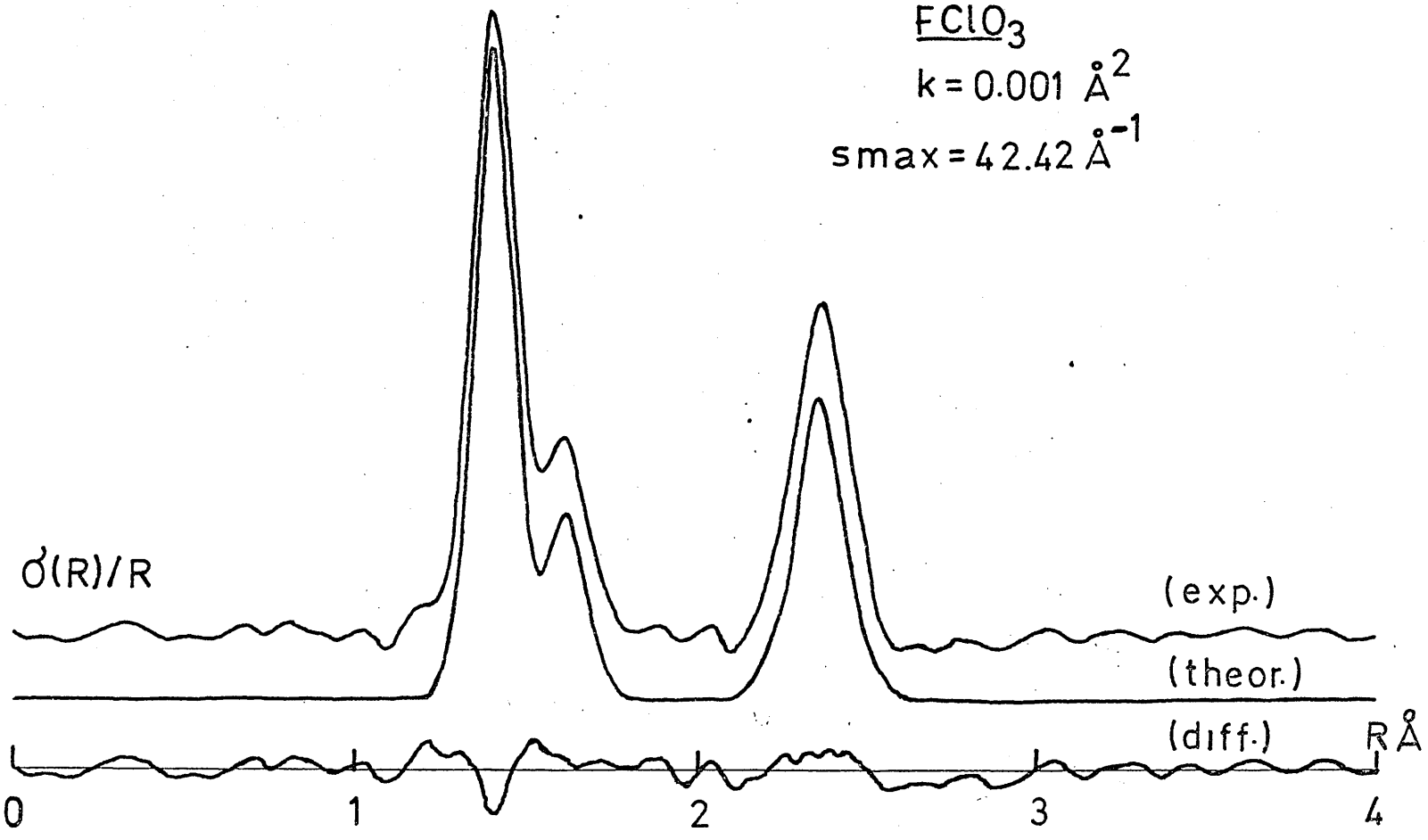

fig. 11.2

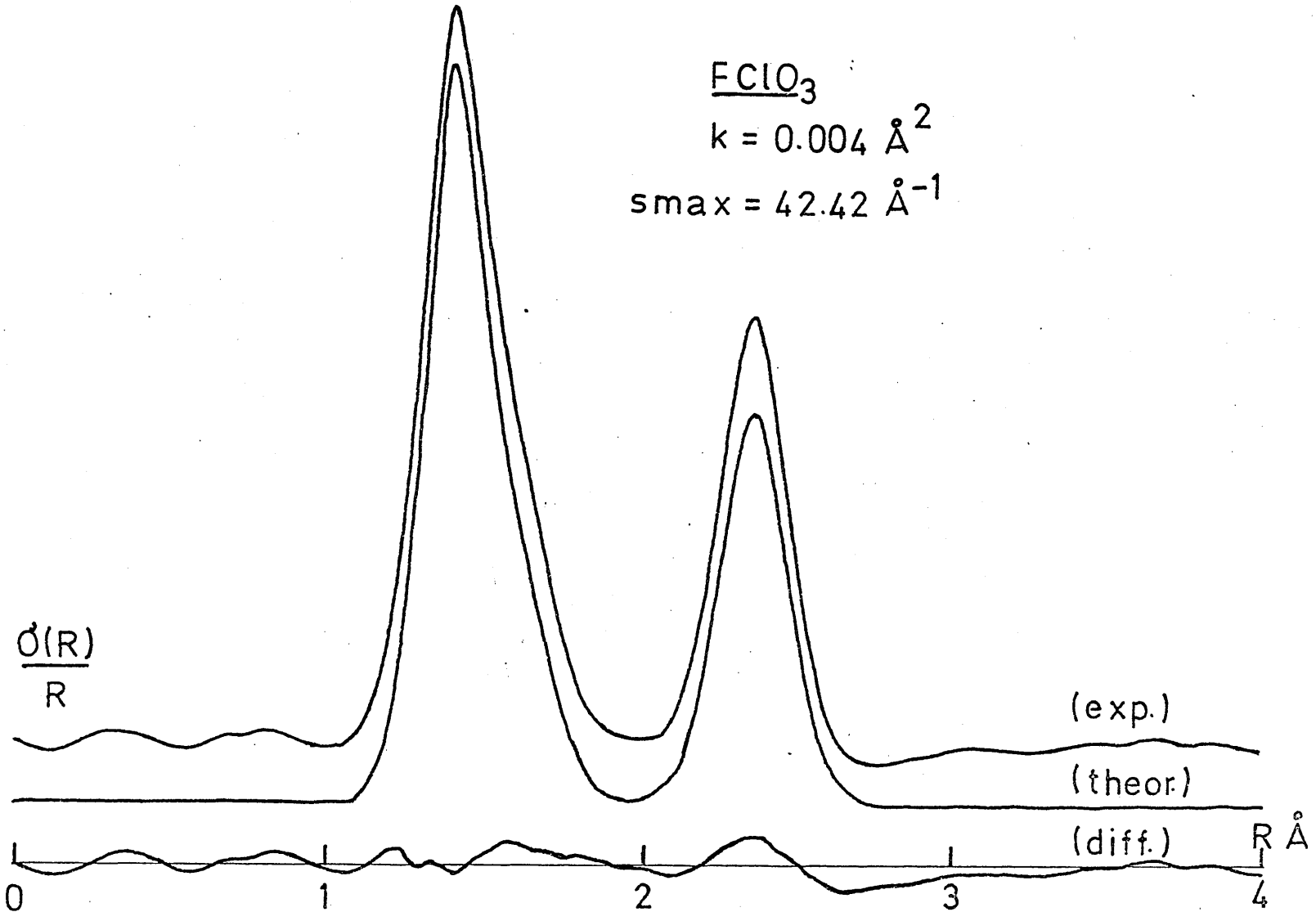

fig. 11.3

TABLE 11.3

Results of individual distance refinements

for $FClO_3$

jet to plate distance	100 cm	50 cm	25 cm	11 cm
r_{Cl-Op} (Å)	1.4073	1.4020	1.4034	1.4034
σ'	0.0004	0.0004	0.0006	0.0016
r_{Cl-F} (Å)	1.6811	1.6181	1.6106	1.6329
σ'	0.0023	0.0014	0.0021	0.0085
$r_{Op..Op}$ (Å)	2.4285	2.3805	2.3731	2.3405
σ'	0.0010	0.0024	0.0080	0.0318
R(%)	3.12	5.69	16.59	62.02
$\sum w\Delta^2$	3.305×10^9	6.803×10^{10}	1.419×10^{14}	8.097×10^{15}

Notes: (1) In these refinements the u values were held constant at spectroscopic values.

(2) The r distances are the three independent parameters chosen to describe the $FClO_3$ tetrahedron. The values quoted are $r_g^3(1)$ quantities.

(3) The σ' values are least squares e.s.d.'s.

(4) The results of the hundred centimetre refinement may correspond to a false minimum of the $\Sigma w\Delta^2$ function, as they are distinctly different from those of the remaining three columns.

TABLE 11.4

Results of ' all data combined ' refinements for $FClO_3$

parameter	combtwo	comb-scaled	combtwo	comb-scaled
r_{Cl-Op} (Å)	1.4033	1.4030	1.4035	1.4032
σ'	0.0004	0.0003	0.0004	0.0004
r_{Cl-F} (Å)	1.6122	1.6158	1.6183	1.6208
σ'	0.0015	0.0012	0.0015	0.0014
$r_{Op..Op}$(Å)	2.3753	2.3786	2.3863	2.3868
σ'	0.0033	0.0022	0.0026	0.0023
u_{Cl-Op} (Å)	spect.	spect.	0.0436	0.0427
σ'	-	-	0.0005	0.0005
u_{Cl-F} (Å)	spect.	spect.	0.0464	0.0485
σ'	-	-	0.0014	0.0014
$u_{Op..Op}$(Å)	spect.	spect.	0.0501	0.0509
σ'	-	-	0.0026	0.0023
$u_{Op..F}$ (Å)	spect.	spect.	0.0648	0.0671
σ'	-	-	0.0026	0.0024
R(%)	11.55	11.36	10.06	10.02
$\sum w\Delta^2$	5.581×10^{10}	5.469×10^{10}	4.213×10^{10}	5.939×10^{10}

TABLE 11.5

The final structural parameters

for $FClO_3$

parameter	final result	reproducibility
r_{Cl-Op} (Å)	1.403	0.002
r_{Cl-F} (Å)	1.617	0.005
$r_{Op..Op}$ (Å)	2.382	0.008
$r_{Op..F}$ (Å)	2.341	0.020
$\widehat{OpClOp}$ (°)	116.2	0.7
$\widehat{OpClF}$ (°)	101.4	1.1
u_{Cl-Op} (Å)	0.035	0.002
u_{Cl-F} (Å)	0.042	0.005
$u_{Op..Op}$ (Å)	0.051	0.008
$u_{Op..F}$ (Å)	0.066	0.008

Notes: (1) The amplitudes of vibration have been corrected for Born failure according to the methods of Chapter Eight.

(2) The above results were obtained by taking a straight average of the values given in the four columns of table 11.4, the O's being averaged, and reproducibilities calculated from them.

CHAPTER TWELVE

AN ELECTRON DIFFRACTION INVESTIGATION OF GASEOUS CHLORINE DIOXIDE

1. Introduction

Chlorine dioxide (ClO_2) has been extensively studied by a number of physical methods. The most recent electron diffraction investigation[92] of the compound, by Dunitz and Hedberg in 1950, determined structural parameters for the molecule with moderate accuracy, but did not obtain values for root mean square amplitudes of vibration.

An infrared study of gaseous chlorine dioxide, by Nielsen and Woltz[86] in 1952, established the harmonic frequencies of vibration of the normal isotopic species, and resolved rotational fine structure, but a lack of similar information about the O^{18} species prevented a determination of the four force constants necessary to define the molecule's harmonic force field.

In 1954 Ward[100] used the results of Nielsen and Woltz, together with ultraviolet spectroscopic data obtained by Coon[101], to calculate accurate structural parameters for ClO_2, and his results have subsequently been confirmed by a microwave study[102] published by Curl et al.[83] in 1961. In 1962, microwave spectroscopy

was also used to produce reliable values for the four force constants of the harmonic potential function.

The present electron diffraction work was undertaken to confirm the structural results of references 100 and 102, and also to obtain values for the root mean square amplitudes of vibration of the internuclear distances present in ClO_2. It was intended to compare these amplitudes with spectroscopic results calculated from the force constant data of reference 83.

2. Experimental

Chlorine dioxide was prepared by the action of sulphuric acid on potassium chlorate as described in reference 103 (second method given). A summary of the experimental conditions adopted during the electron diffraction study is given in table 12.1. Eleven centimetre jet-to-plate distance data were not included in this investigation on account of the small part such data had previously been found to play in determining structural parameters.

The uphill curves obtained are listed in table 12.2, and the final experimental combined $I_m(s)$ curve is presented graphically in figure 12.1. A Fourier transform of this function is shown in figure 12.2, and the excessively large ' noise ripple ' visible

in this radial distribution curve between R = 0 and R = 1 Å, may presumably be ascribed to the deviation between the experimental and theoretical $I_m(s)$ functions at $s \sim 18$ Å^{-1}. Figure 12.2 immediately confirms the angular symmetric nature of the chlorine dioxide molecule, and the rather short Cl-O bonds present.

3. Results

In least squares refinements the molecule was defined by the internuclear distances R_{Cl-O} and $R_{O..O}$, and these were refined independently together with their corresponding root mean square amplitudes of vibration. Results of single distance refinements are listed in table 12.3 and show a reasonable consistency from one jet-to-plate distance to another. Results of combtwo and combscaled all-data-combined refinements are listed in table 12.4, and a final set of structural parameters, obtained by averaging the columns of this table, are listed in table 12.5.

4. Discussion

The results obtained by the present work are compared with those of Curl[102] and Ward[100] in table 12.6. The agreement achieved is good, but since the microwave result is uncertain, at least by normal

microwave standards, and is not in any case an r_s or r_e value, no definite conclusion can be reached about the real accuracy achieved by the present study. Clearly any error involved in the Cl-O $r_g(1)$ distance, cannot be in excess of few thousandths of an Angstrom unit, but more than this cannot be said. The valence angle of the molecule is naturally rather poorly determined on account of the low A factor of the O..O internuclear distance.

The amplitudes of vibration obtained by the present work are in fairly good agreement with those calculated spectroscopically, and listed in tables 8.5 and 12.6. The difference of 0.004 Å between the two u_{Cl-O} results which is larger than would be expected from the well determined nature of R_{Cl-O}, is presumably a consequence of the poor twentyfive centimetre R factor of table 12.3.

The 0.23 Å shortening of the Cl-O bond length in ClO_2 relative to the Cl-O single bond value (1.70 Å) implies a considerable amount of double bond character, and it is evident from the nature of the molecule, that any π bonding present will be complicated by the fact that both p and d orbitals on chlorine may be involved. Molecular orbital calculations by Wagner[104], have confirmed these ideas, and have predicted that the bonds in ClO_2 possess considerable π bond orders, fifty percent of this bonding being of d character.

TABLE 12.1

A summary of experimental details

for the chlorine dioxide investigation

jet to plate distance	100 cm	50 cm	25 cm	-
wavelength (A)	0.051172	0.051172	0.051172	
e.s.d.	0.000020	0.000020	0.000020	
sample temperature (^{o}K)	233	233	233	
nozzle temperature (^{o}K)	333	333	333	
gas temperature assumed (^{o}K)	283	283	283	
number of plates used	6	6	2	
quality	good	good	good to light	
number of traces measured (AMDM)	6	6	10	

TABLE 12.2

ClO_2 intensity data as combined uphill curves

range (1): s = 0.86 by 0.020 to 9.00 $Å^{-1}$

6.507_{10}	+2;	6.907_{10}	+2;	7.340_{10}	+2;	7.752_{10}	+2;	8.190_{10}	+2;
8.599_{10}	+2;	8.989_{10}	+2;	9.388_{10}	+2;	9.825_{10}	+2;	1.033_{10}	+3;
1.090_{10}	+3;	1.155_{10}	+3;	1.227_{10}	+3;	1.304_{10}	+3;	1.380_{10}	+3;
1.461_{10}	+3;	1.542_{10}	+3;	1.621_{10}	+3;	1.699_{10}	+3;	1.777_{10}	+3;
1.854_{10}	+3;	1.929_{10}	+3;	2.001_{10}	+3;	2.070_{10}	+3;	2.137_{10}	+3;
2.207_{10}	+3;	2.275_{10}	+3;	2.348_{10}	+3;	2.426_{10}	+3;	2.507_{10}	+3;
2.586_{10}	+3;	2.667_{10}	+3;	2.745_{10}	+3;	2.821_{10}	+3;	2.894_{10}	+3;
2.966_{10}	+3;	3.038_{10}	+3;	3.107_{10}	+3;	3.174_{10}	+3;	3.240_{10}	+3;
3.304_{10}	+3;	3.371_{10}	+3;	3.438_{10}	+3;	3.508_{10}	+3;	3.584_{10}	+3;
3.662_{10}	+3;	3.739_{10}	+3;	3.817_{10}	+3;	3.893_{10}	+3;	3.966_{10}	+3;
4.038_{10}	+3;	4.108_{10}	+3;	4.179_{10}	+3;	4.249_{10}	+3;	4.319_{10}	+3;
4.387_{10}	+3;	4.455_{10}	+3;	4.523_{10}	+3;	4.591_{10}	+3;	4.659_{10}	+3;
4.728_{10}	+3;	4.795_{10}	+3;	4.858_{10}	+3;	4.921_{10}	+3;	4.980_{10}	+3;
5.037_{10}	+3;	5.095_{10}	+3;	5.155_{10}	+3;	5.216_{10}	+3;	5.279_{10}	+3;
5.341_{10}	+3;	5.401_{10}	+3;	5.463_{10}	+3;	5.526_{10}	+3;	5.589_{10}	+3;
5.655_{10}	+3;	5.722_{10}	+3;	5.788_{10}	+3;	5.851_{10}	+3;	5.914_{10}	+3;
5.974_{10}	+3;	6.035_{10}	+3;	6.102_{10}	+3;	6.174_{10}	+3;	6.247_{10}	+3;
6.325_{10}	+3;	6.402_{10}	+3;	6.477_{10}	+3;	6.550_{10}	+3;	6.623_{10}	+3;
6.697_{10}	+3;	6.770_{10}	+3;	6.842_{10}	+3;	6.915_{10}	+3;	6.990_{10}	+3;
7.069_{10}	+3;	7.150_{10}	+3;	7.233_{10}	+3;	7.320_{10}	+3;	7.408_{10}	+3;
7.493_{10}	+3;	7.578_{10}	+3;	7.660_{10}	+3;	7.744_{10}	+3;	7.832_{10}	+3;
7.924_{10}	+3;	8.021_{10}	+3;	8.123_{10}	+3;	8.232_{10}	+3;	8.342_{10}	+3;
8.455_{10}	+3;	8.567_{10}	+3;	8.683_{10}	+3;	8.799_{10}	+3;	8.908_{10}	+3;
9.012_{10}	+3;	9.116_{10}	+3;	9.227_{10}	+3;	9.339_{10}	+3;	9.458_{10}	+3;
9.580_{10}	+3;	9.704_{10}	+3;	9.826_{10}	+3;	9.945_{10}	+3;	1.006_{10}	+4;
1.018_{10}	+4;	1.032_{10}	+4;	1.045_{10}	+4;	1.060_{10}	+4;	1.074_{10}	+4;
1.089_{10}	+4;	1.103_{10}	+4;	1.118_{10}	+4;	1.132_{10}	+4;	1.147_{10}	+4;
1.162_{10}	+4;	1.177_{10}	+4;	1.193_{10}	+4;	1.209_{10}	+4;	1.227_{10}	+4;
1.245_{10}	+4;	1.262_{10}	+4;	1.279_{10}	+4;	1.296_{10}	+4;	1.313_{10}	+4;
1.330_{10}	+4;	1.348_{10}	+4;	1.369_{10}	+4;	1.390_{10}	+4;	1.410_{10}	+4;
1.430_{10}	+4;	1.449_{10}	+4;	1.468_{10}	+4;	1.487_{10}	+4;	1.507_{10}	+4;
1.527_{10}	+4;	1.548_{10}	+4;	1.571_{10}	+4;	1.595_{10}	+4;	1.620_{10}	+4;
1.644_{10}	+4;	1.668_{10}	+4;	1.691_{10}	+4;	1.714_{10}	+4;	1.738_{10}	+4;
1.762_{10}	+4;	1.785_{10}	+4;	1.809_{10}	+4;	1.833_{10}	+4;	1.858_{10}	+4;
1.884_{10}	+4;	1.910_{10}	+4;	1.937_{10}	+4;	1.964_{10}	+4;	1.989_{10}	+4;
2.015_{10}	+4;	2.041_{10}	+4;	2.067_{10}	+4;	2.092_{10}	+4;	2.118_{10}	+4;
2.143_{10}	+4;	2.169_{10}	+4;	2.195_{10}	+4;	2.221_{10}	+4;	2.248_{10}	+4;
2.273_{10}	+4;	2.299_{10}	+4;	2.326_{10}	+4;	2.353_{10}	+4;	2.381_{10}	+4;
2.409_{10}	+4;	2.435_{10}	+4;	2.461_{10}	+4;	2.485_{10}	+4;	2.509_{10}	+4;

TABLE 12.2 (cont'd)

2.533_{10} +4;	2.558_{10} +4;	2.584_{10} +4;	2.608_{10} +4;	2.632_{10} +4;
2.653_{10} +4;	2.674_{10} +4;	2.696_{10} +4;	2.719_{10} +4;	2.745_{10} +4;
2.771_{10} +4;	2.797_{10} +4;	2.822_{10} +4;	2.845_{10} +4;	2.867_{10} +4;
2.887_{10} +4;	2.905_{10} +4;	2.924_{10} +4;	2.941_{10} +4;	2.959_{10} +4;
2.977_{10} +4;	2.994_{10} +4;	3.011_{10} +4;	3.027_{10} +4;	3.042_{10} +4;
3.057_{10} +4;	3.070_{10} +4;	3.085_{10} +4;	3.100_{10} +4;	3.115_{10} +4;
3.128_{10} +4;	3.140_{10} +4;	3.152_{10} +4;	3.163_{10} +4;	3.174_{10} +4;
3.184_{10} +4;	3.194_{10} +4;	3.204_{10} +4;	3.211_{10} +4;	3.215_{10} +4;
3.217_{10} +4;	3.220_{10} +4;	3.221_{10} +4;	3.223_{10} +4;	3.226_{10} +4;
3.230_{10} +4;	3.233_{10} +4;	3.236_{10} +4;	3.238_{10} +4;	3.239_{10} +4;
3.238_{10} +4;	3.237_{10} +4;	3.236_{10} +4;	3.233_{10} +4;	3.231_{10} +4;
3.228_{10} +4;	3.225_{10} +4;	3.220_{10} +4;	3.214_{10} +4;	3.206_{10} +4;
3.199_{10} +4;	3.192_{10} +4;	3.187_{10} +4;	3.180_{10} +4;	3.174_{10} +4;
3.166_{10} +4;	3.157_{10} +4;	3.147_{10} +4;	3.138_{10} +4;	3.129_{10} +4;
3.122_{10} +4;	3.114_{10} +4;	3.103_{10} +4;	3.091_{10} +4;	3.079_{10} +4;
3.066_{10} +4;	3.054_{10} +4;	3.044_{10} +4;	3.034_{10} +4;	3.024_{10} +4;
3.014_{10} +4;	3.003_{10} +4;	2.992_{10} +4;	2.982_{10} +4;	2.973_{10} +4;
2.964_{10} +4;	2.956_{10} +4;	2.948_{10} +4;	2.942_{10} +4;	2.934_{10} +4;
2.925_{10} +4;	2.916_{10} +4;	2.907_{10} +4;	2.900_{10} +4;	2.894_{10} +4;
2.887_{10} +4;	2.881_{10} +4;	2.874_{10} +4;	2.867_{10} +4;	2.862_{10} +4;
2.858_{10} +4;	2.853_{10} +4;	2.850_{10} +4;	2.847_{10} +4;	2.843_{10} +4;
2.840_{10} +4;	2.836_{10} +4;	2.833_{10} +4;	2.830_{10} +4;	2.827_{10} +4;
2.824_{10} +4;	2.824_{10} +4;	2.824_{10} +4;	2.826_{10} +4;	2.827_{10} +4;
2.829_{10} +4;	2.830_{10} +4;	2.833_{10} +4;	2.836_{10} +4;	2.841_{10} +4;
2.846_{10} +4;	2.852_{10} +4;	2.857_{10} +4;	2.861_{10} +4;	2.865_{10} +4;
2.870_{10} +4;	2.874_{10} +4;	2.879_{10} +4;	2.886_{10} +4;	2.893_{10} +4;
2.903_{10} +4;	2.913_{10} +4;	2.923_{10} +4;	2.933_{10} +4;	2.943_{10} +4;
2.954_{10} +4;	2.965_{10} +4;	2.975_{10} +4;	2.987_{10} +4;	2.998_{10} +4;
3.009_{10} +4;	3.020_{10} +4;	3.031_{10} +4;	3.043_{10} +4;	3.056_{10} +4;
3.070_{10} +4;	3.085_{10} +4;	3.101_{10} +4;	3.116_{10} +4;	3.130_{10} +4;
3.145_{10} +4;	3.160_{10} +4;	3.177_{10} +4;	3.195_{10} +4;	3.214_{10} +4;
3.231_{10} +4;	3.247_{10} +4;	3.262_{10} +4;	3.276_{10} +4;	3.291_{10} +4;
3.307_{10} +4;	3.322_{10} +4;	3.337_{10} +4;	3.349_{10} +4;	3.361_{10} +4;
3.376_{10} +4;	3.392_{10} +4;	3.411_{10} +4;	3.433_{10} +4;	3.456_{10} +4;
3.481_{10} +4;	3.504_{10} +4;	3.525_{10} +4;	3.545_{10} +4;	3.564_{10} +4;
3.582_{10} +4;	3.598_{10} +4;	3.614_{10} +4;	3.632_{10} +4;	3.651_{10} +4;
3.669_{10} +4;	3.688_{10} +4;	3.709_{10} +4;	3.730_{10} +4;	3.753_{10} +4;
3.774_{10} +4;	3.795_{10} +4;	3.817_{10} +4;	3.839_{10} +4;	3.861_{10} +4;
3.884_{10} +4;	3.906_{10} +4;	3.928_{10} +4;	3.948_{10} +4;	3.969_{10} +4;
3.989_{10} +4;	4.011_{10} +4;	4.036_{10} +4;	4.063_{10} +4;	4.088_{10} +4;
4.111_{10} +4;	4.131_{10} +4;	4.150_{10} +4;	4.167_{10} +4;	4.185_{10} +4;
4.205_{10} +4;	4.227_{10} +4;	4.250_{10} +4;	4.272_{10} +4;	4.293_{10} +4;
4.314_{10} +4;	4.336_{10} +4;	4.359_{10} +4;		

TABLE 12.2 (cont'd)

range (2): s = 2.40 by 0.05 to 17.95 $\mathring{A}^{-1}$

1.682_{10} +4;	1.738_{10} +4;	1.794_{10} +4;	1.848_{10} +4;	1.901_{10} +4;
1.951_{10} +4;	1.998_{10} +4;	2.047_{10} +4;	2.102_{10} +4;	2.166_{10} +4;
2.233_{10} +4;	2.302_{10} +4;	2.368_{10} +4;	2.432_{10} +4;	2.501_{10} +4;
2.577_{10} +4;	2.654_{10} +4;	2.728_{10} +4;	2.805_{10} +4;	2.885_{10} +4;
2.972_{10} +4;	3.066_{10} +4;	3.167_{10} +4;	3.277_{10} +4;	3.396_{10} +4;
3.515_{10} +4;	3.623_{10} +4;	3.732_{10} +4;	3.850_{10} +4;	3.975_{10} +4;
4.111_{10} +4;	4.252_{10} +4;	4.393_{10} +4;	4.531_{10} +4;	4.673_{10} +4;
4.833_{10} +4;	4.989_{10} +4;	5.144_{10} +4;	5.306_{10} +4;	5.474_{10} +4;
5.623_{10} +4;	5.764_{10} +4;	5.926_{10} +4;	6.098_{10} +4;	6.265_{10} +4;
6.416_{10} +4;	6.559_{10} +4;	6.711_{10} +4;	6.869_{10} +4;	7.024_{10} +4;
7.175_{10} +4;	7.315_{10} +4;	7.449_{10} +4;	7.577_{10} +4;	7.700_{10} +4;
7.816_{10} +4;	7.916_{10} +4;	7.993_{10} +4;	8.043_{10} +4;	8.093_{10} +4;
8.159_{10} +4;	8.211_{10} +4;	8.238_{10} +4;	8.253_{10} +4;	8.277_{10} +4;
8.290_{10} +4;	8.261_{10} +4;	8.210_{10} +4;	8.174_{10} +4;	8.138_{10} +4;
8.078_{10} +4;	8.009_{10} +4;	7.943_{10} +4;	7.868_{10} +4;	7.784_{10} +4;
7.697_{10} +4;	7.612_{10} +4;	7.526_{10} +4;	7.442_{10} +4;	7.354_{10} +4;
7.268_{10} +4;	7.183_{10} +4;	7.093_{10} +4;	6.979_{10} +4;	6.867_{10} +4;
6.775_{10} +4;	6.708_{10} +4;	6.643_{10} +4;	6.594_{10} +4;	6.551_{10} +4;
6.506_{10} +4;	6.453_{10} +4;	6.407_{10} +4;	6.369_{10} +4;	6.333_{10} +4;
6.310_{10} +4;	6.309_{10} +4;	6.318_{10} +4;	6.341_{10} +4;	6.365_{10} +4;
6.401_{10} +4;	6.451_{10} +4;	6.496_{10} +4;	6.532_{10} +4;	6.573_{10} +4;
6.628_{10} +4;	6.681_{10} +4;	6.752_{10} +4;	6.827_{10} +4;	6.906_{10} +4;
6.981_{10} +4;	7.042_{10} +4;	7.095_{10} +4;	7.165_{10} +4;	7.267_{10} +4;
7.357_{10} +4;	7.445_{10} +4;	7.531_{10} +4;	7.625_{10} +4;	7.711_{10} +4;
7.802_{10} +4;	7.872_{10} +4;	7.922_{10} +4;	7.947_{10} +4;	7.993_{10} +4;
8.051_{10} +4;	8.107_{10} +4;	8.145_{10} +4;	8.198_{10} +4;	8.255_{10} +4;
8.309_{10} +4;	8.352_{10} +4;	8.412_{10} +4;	8.479_{10} +4;	8.525_{10} +4;
8.560_{10} +4;	8.607_{10} +4;	8.645_{10} +4;	8.671_{10} +4;	8.705_{10} +4;
8.759_{10} +4;	8.809_{10} +4;	8.847_{10} +4;	8.879_{10} +4;	8.881_{10} +4;
8.863_{10} +4;	8.849_{10} +4;	8.870_{10} +4;	8.888_{10} +4;	8.867_{10} +4;
8.843_{10} +4;	8.843_{10} +4;	8.868_{10} +4;	8.870_{10} +4;	8.830_{10} +4;
8.783_{10} +4;	8.770_{10} +4;	8.765_{10} +4;	8.730_{10} +4;	8.689_{10} +4;
8.643_{10} +4;	8.572_{10} +4;	8.475_{10} +4;	8.417_{10} +4;	8.368_{10} +4;
8.322_{10} +4;	8.257_{10} +4;	8.186_{10} +4;	8.090_{10} +4;	8.029_{10} +4;
7.988_{10} +4;	7.953_{10} +4;	7.876_{10} +4;	7.780_{10} +4;	7.703_{10} +4;
7.670_{10} +4;	7.643_{10} +4;	7.616_{10} +4;	7.601_{10} +4;	7.587_{10} +4;
7.560_{10} +4;	7.544_{10} +4;	7.527_{10} +4;	7.497_{10} +4;	7.485_{10} +4;
7.516_{10} +4;	7.537_{10} +4;	7.532_{10} +4;	7.530_{10} +4;	7.586_{10} +4;
7.693_{10} +4;	7.767_{10} +4;	7.783_{10} +4;	7.780_{10} +4;	7.849_{10} +4;

TABLE 12.2 (cont'd)

7.967$_{10}$ +4; 8.042$_{10}$ +4; 8.063$_{10}$ +4; 8.062$_{10}$ +4; 8.131$_{10}$ +4;
8.232$_{10}$ +4; 8.309$_{10}$ +4; 8.369$_{10}$ +4; 8.490$_{10}$ +4; 8.608$_{10}$ +4;
8.669$_{10}$ +4; 8.722$_{10}$ +4; 8.801$_{10}$ +4; 8.855$_{10}$ +4; 8.894$_{10}$ +4;
8.973$_{10}$ +4; 9.092$_{10}$ +4; 9.159$_{10}$ +4; 9.175$_{10}$ +4; 9.221$_{10}$ +4;
9.305$_{10}$ +4; 9.380$_{10}$ +4; 9.437$_{10}$ +4; 9.485$_{10}$ +4; 9.527$_{10}$ +4;
9.568$_{10}$ +4; 9.615$_{10}$ +4; 9.681$_{10}$ +4; 9.741$_{10}$ +4; 9.789$_{10}$ +4;
9.799$_{10}$ +4; 9.796$_{10}$ +4; 9.795$_{10}$ +4; 9.807$_{10}$ +4; 9.826$_{10}$ +4;
9.836$_{10}$ +4; 9.846$_{10}$ +4; 9.851$_{10}$ +4; 9.830$_{10}$ +4; 9.798$_{10}$ +4;
9.785$_{10}$ +4; 9.793$_{10}$ +4; 9.785$_{10}$ +4; 9.755$_{10}$ +4; 9.701$_{10}$ +4;
9.666$_{10}$ +4; 9.649$_{10}$ +4; 9.644$_{10}$ +4; 9.651$_{10}$ +4; 9.661$_{10}$ +4;
9.646$_{10}$ +4; 9.619$_{10}$ +4; 9.591$_{10}$ +4; 9.589$_{10}$ +4; 9.590$_{10}$ +4;
9.601$_{10}$ +4; 9.597$_{10}$ +4; 9.554$_{10}$ +4; 9.491$_{10}$ +4; 9.451$_{10}$ +4;
9.428$_{10}$ +4; 9.387$_{10}$ +4; 9.349$_{10}$ +4; 9.374$_{10}$ +4; 9.420$_{10}$ +4;
9.406$_{10}$ +4; 9.349$_{10}$ +4; 9.319$_{10}$ +4; 9.325$_{10}$ +4; 9.329$_{10}$ +4;
9.329$_{10}$ +4; 9.350$_{10}$ +4; 9.371$_{10}$ +4; 9.378$_{10}$ +4; 9.383$_{10}$ +4;
9.369$_{10}$ +4; 9.355$_{10}$ +4; 9.364$_{10}$ +4; 9.382$_{10}$ +4; 9.440$_{10}$ +4;
9.496$_{10}$ +4; 9.547$_{10}$ +4; 9.565$_{10}$ +4; 9.599$_{10}$ +4; 9.609$_{10}$ +4;
9.651$_{10}$ +4; 9.720$_{10}$ +4; 9.799$_{10}$ +4; 9.855$_{10}$ +4; 9.916$_{10}$ +4;
9.964$_{10}$ +4; 1.001$_{10}$ +5; 1.007$_{10}$ +5; 1.016$_{10}$ +5; 1.025$_{10}$ +5;
1.034$_{10}$ +5; 1.043$_{10}$ +5; 1.051$_{10}$ +5; 1.062$_{10}$ +5; 1.078$_{10}$ +5;
1.091$_{10}$ +5; 1.099$_{10}$ +5; 1.109$_{10}$ +5; 1.123$_{10}$ +5; 1.138$_{10}$ +5;
1.151$_{10}$ +5; 1.162$_{10}$ +5; 1.174$_{10}$ +5; 1.185$_{10}$ +5; 1.193$_{10}$ +5;
1.199$_{10}$ +5; 1.205$_{10}$ +5; 1.216$_{10}$ +5; 1.227$_{10}$ +5; 1.239$_{10}$ +5;
1.249$_{10}$ +5; 1.259$_{10}$ +5;

range (3): s = 7.60 by 0.10 to 35.00 $\mathring{A}^{-1}$

4.739$_{10}$ +5; 4.886$_{10}$ +5; 4.992$_{10}$ +5; 5.141$_{10}$ +5; 5.310$_{10}$ +5;
5.435$_{10}$ +5; 5.552$_{10}$ +5; 5.732$_{10}$ +5; 5.859$_{10}$ +5; 6.005$_{10}$ +5;
6.127$_{10}$ +5; 6.301$_{10}$ +5; 6.361$_{10}$ +5; 6.412$_{10}$ +5; 6.495$_{10}$ +5;
6.537$_{10}$ +5; 6.593$_{10}$ +5; 6.627$_{10}$ +5; 6.649$_{10}$ +5; 6.688$_{10}$ +5;
6.750$_{10}$ +5; 6.806$_{10}$ +5; 6.847$_{10}$ +5; 6.780$_{10}$ +5; 6.765$_{10}$ +5;
6.722$_{10}$ +5; 6.715$_{10}$ +5; 6.693$_{10}$ +5; 6.677$_{10}$ +5; 6.655$_{10}$ +5;
6.866$_{10}$ +5; 6.810$_{10}$ +5; 6.429$_{10}$ +5; 6.395$_{10}$ +5; 6.348$_{10}$ +5;
6.263$_{10}$ +5; 6.203$_{10}$ +5; 6.098$_{10}$ +5; 6.024$_{10}$ +5; 5.993$_{10}$ +5;
5.949$_{10}$ +5; 5.953$_{10}$ +5; 5.958$_{10}$ +5; 6.014$_{10}$ +5; 6.081$_{10}$ +5;
6.131$_{10}$ +5; 6.282$_{10}$ +5; 6.391$_{10}$ +5; 6.389$_{10}$ +5; 6.646$_{10}$ +5;
6.792$_{10}$ +5; 6.823$_{10}$ +5; 7.004$_{10}$ +5; 7.191$_{10}$ +5; 7.363$_{10}$ +5;
7.444$_{10}$ +5; 7.586$_{10}$ +5; 7.757$_{10}$ +5; 7.857$_{10}$ +5; 7.877$_{10}$ +5;

TABLE 12.2 (concluded)

7.985_{10} +5;	8.089_{10} +5;	8.090_{10} +5;	8.118_{10} +5;	8.146_{10} +5;
8.155_{10} +5;	8.176_{10} +5;	8.134_{10} +5;	8.142_{10} +5;	8.084_{10} +5;
8.089_{10} +5;	8.069_{10} +5;	8.003_{10} +5;	8.000_{10} +5;	7.923_{10} +5;
7.906_{10} +5;	7.905_{10} +5;	7.904_{10} +5;	7.850_{10} +5;	7.828_{10} +5;
7.791_{10} +5;	7.853_{10} +5;	7.851_{10} +5;	7.856_{10} +5;	7.974_{10} +5;
7.888_{10} +5;	7.907_{10} +5;	7.956_{10} +5;	8.008_{10} +5;	8.097_{10} +5;
8.264_{10} +5;	8.374_{10} +5;	8.406_{10} +5;	8.502_{10} +5;	8.635_{10} +5;
8.918_{10} +5;	8.878_{10} +5;	8.885_{10} +5;	9.005_{10} +5;	9.136_{10} +5;
9.221_{10} +5;	9.275_{10} +5;	9.428_{10} +5;	9.954_{10} +5;	9.482_{10} +5;
9.555_{10} +5;	9.534_{10} +5;	9.472_{10} +5;	9.552_{10} +5;	9.586_{10} +5;
9.507_{10} +5;	9.464_{10} +5;	9.402_{10} +5;	9.338_{10} +5;	9.328_{10} +5;
9.354_{10} +5;	9.325_{10} +5;	9.242_{10} +5;	9.232_{10} +5;	9.262_{10} +5;
9.240_{10} +5;	9.213_{10} +5;	9.268_{10} +5;	9.258_{10} +5;	9.238_{10} +5;
9.236_{10} +5;	9.243_{10} +5;	9.274_{10} +5;	9.372_{10} +5;	9.369_{10} +5;
9.441_{10} +5;	9.471_{10} +5;	9.548_{10} +5;	9.634_{10} +5;	9.752_{10} +5;
9.670_{10} +5;	9.828_{10} +5;	9.902_{10} +5;	1.004_{10} +6;	1.009_{10} +6;
1.011_{10} +6;	1.013_{10} +6;	1.024_{10} +6;	1.030_{10} +6;	1.041_{10} +6;
1.045_{10} +6;	1.048_{10} +6;	1.055_{10} +6;	1.064_{10} +6;	1.072_{10} +6;
1.063_{10} +6;	1.075_{10} +6;	1.082_{10} +6;	1.071_{10} +6;	1.069_{10} +6;
1.067_{10} +6;	1.070_{10} +6;	1.072_{10} +6;	1.073_{10} +6;	1.068_{10} +6;
1.070_{10} +6;	1.069_{10} +6;	1.066_{10} +6;	1.068_{10} +6;	1.068_{10} +6;
1.072_{10} +6;	1.070_{10} +6;	1.074_{10} +6;	1.078_{10} +6;	1.080_{10} +6;
1.085_{10} +6;	1.097_{10} +6;	1.110_{10} +6;	1.127_{10} +6;	1.126_{10} +6;
1.123_{10} +6;	1.128_{10} +6;	1.170_{10} +6;	1.139_{10} +6;	1.150_{10} +6;
1.160_{10} +6;	1.168_{10} +6;	1.179_{10} +6;	1.187_{10} +6;	1.193_{10} +6;
1.209_{10} +6;	1.208_{10} +6;	1.208_{10} +6;	1.208_{10} +6;	1.205_{10} +6;
1.216_{10} +6;	1.224_{10} +6;	1.233_{10} +6;	1.238_{10} +6;	1.232_{10} +6;
1.232_{10} +6;	1.234_{10} +6;	1.225_{10} +6;	1.228_{10} +6;	1.236_{10} +6;
1.236_{10} +6;	1.241_{10} +6;	1.239_{10} +6;	1.236_{10} +6;	1.238_{10} +6;
1.236_{10} +6;	1.239_{10} +6;	1.248_{10} +6;	1.254_{10} +6;	1.252_{10} +6;
1.266_{10} +6;	1.266_{10} +6;	1.268_{10} +6;	1.266_{10} +6;	1.266_{10} +6;
1.280_{10} +6;	1.286_{10} +6;	1.288_{10} +6;	1.287_{10} +6;	1.298_{10} +6;
1.313_{10} +6;	1.325_{10} +6;	1.333_{10} +6;	1.332_{10} +6;	1.337_{10} +6;
1.347_{10} +6;	1.357_{10} +6;	1.370_{10} +6;	1.378_{10} +6;	1.386_{10} +6;
1.386_{10} +6;	1.397_{10} +6;	1.410_{10} +6;	1.428_{10} +6;	1.417_{10} +6;
1.415_{10} +6;	1.433_{10} +6;	1.440_{10} +6;	1.450_{10} +6;	1.451_{10} +6;
1.463_{10} +6;	1.475_{10} +6;	1.482_{10} +6;	1.480_{10} +6;	1.477_{10} +6;
1.480_{10} +6;	1.487_{10} +6;	1.503_{10} +6;	1.498_{10} +6;	1.510_{10} +6;
1.521_{10} +6;	1.521_{10} +6;	1.521_{10} +6;	1.525_{10} +6;	1.535_{10} +6;
1.553_{10} +6;	1.571_{10} +6;	1.588_{10} +6;	1.590_{10} +6;	1.598_{10} +6;
1.609_{10} +6;	1.623_{10} +6;	1.632_{10} +6;	1.638_{10} +6;	1.650_{10} +6;
1.666_{10} +6;	1.689_{10} +6;	1.690_{10} +6;	1.698_{10} +6;	1.701_{10} +6;
1.729_{10} +6;	1.727_{10} +6;	1.737_{10} +6;	1.751_{10} +6;	1.764_{10} +6;

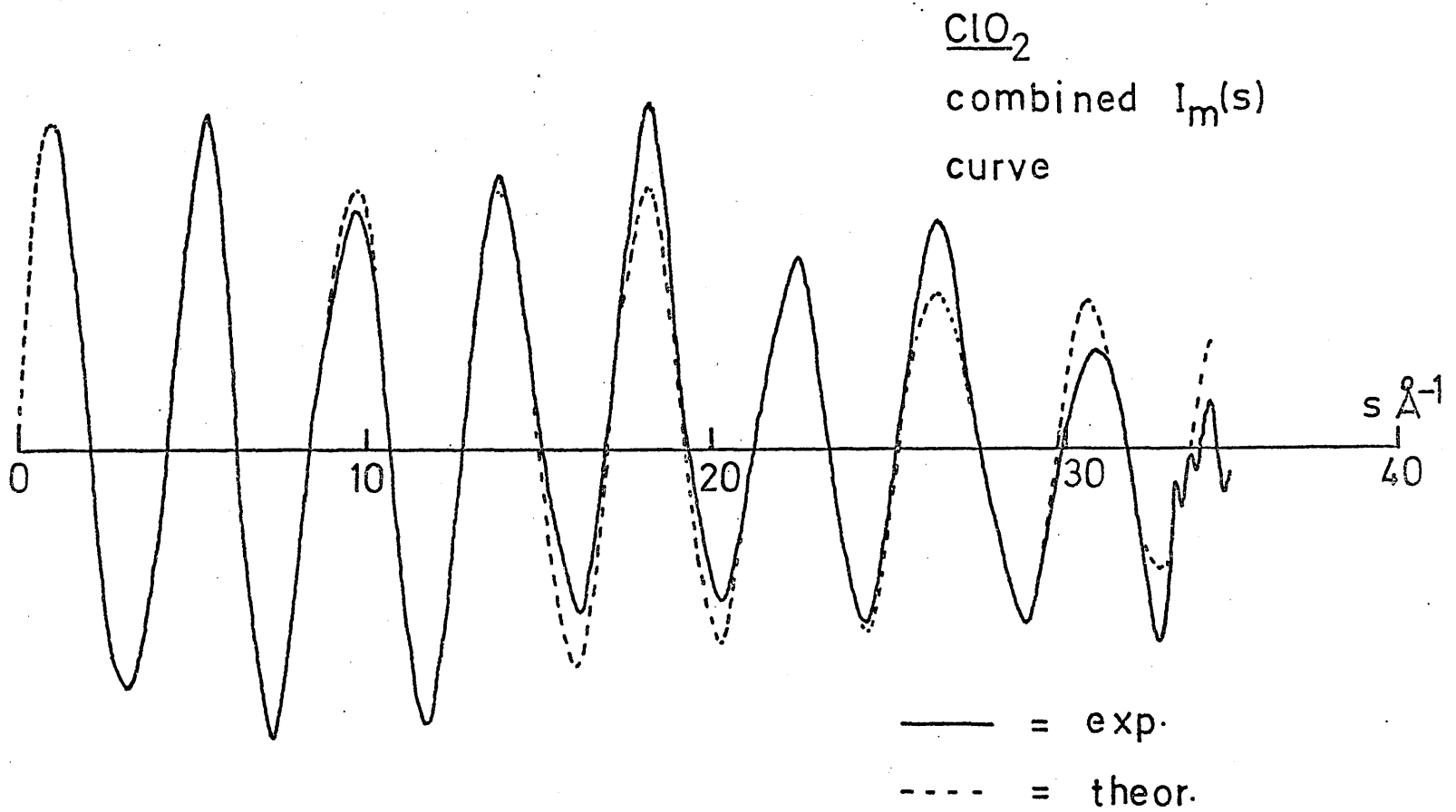

fig.12.1

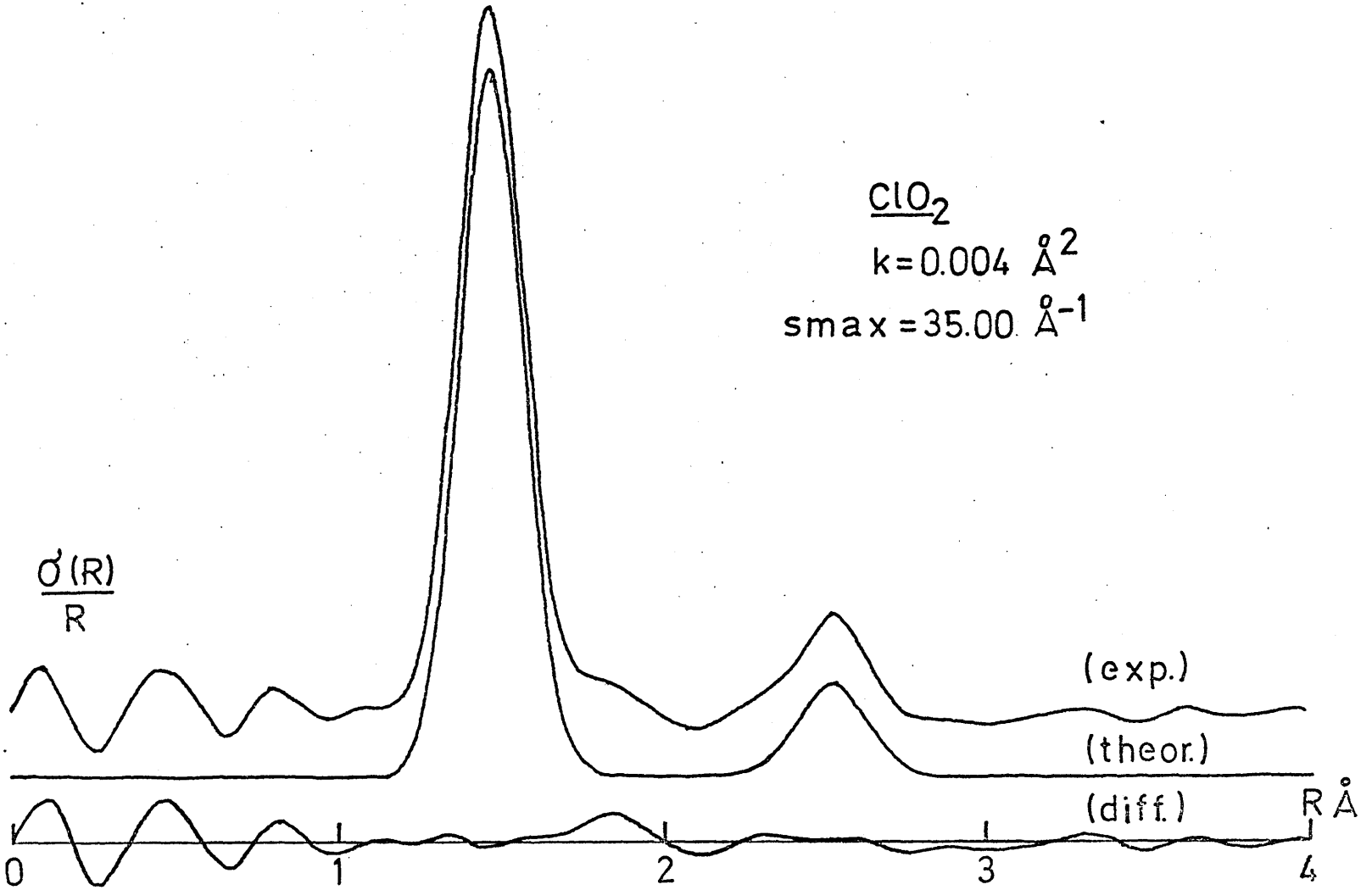

fig.12.2

TABLE 12.3

Results of individual distance refinements for ClO_2

jet to plate distance	100 cm	50 cm	25 cm
r_{Cl-O} (Å)	1.4773	1.4759	1.4731
σ'	0.0004	0.0006	0.0014
$r_{O..O}$ (Å)	2.5255	2.5365	2.5061
σ'	0.0027	0.0042	0.0134
R(%)	4.44	8.63	37.58
$\sum w\Delta^2$	2.994×10^9	5.135×10^{10}	2.194×10^{13}

Notes: (1) u values were held constant at spectroscopic values.

(2) σ''s are least squares e.s.d.'s.

(3) r values are $r_g(1)$ distances.

TABLE 12.4

Results of ' all data combined ' refinements

for ClO_2

parameter	combtwo	comb-scaled
r_{Cl-O} (Å)	1.4750	1.4743
σ'	0.0008	0.0006
$r_{O..O}$ (Å)	2.5251	2.5210
σ'	0.0070	0.0051
u_{Cl-O} (Å)	0.0429	0.0426
σ'	0.0010	0.0009
$u_{O..O}$ (Å)	0.0629	0.0595
σ'	0.0077	0.0060
R(%)	14.70	13.29
$\sum w\Delta^2$	1.055×10^{11}	1.100×10^{11}

Notes: (1) The distances are $r_g(1)$ values.

(2) The σ' s are least squares e.s.d.'s.

(3) The amplitudes have not been corrected for failure of the Born approximation.

TABLE 12.5

The final structural parameters

for ClO_2

parameter	final result	reproducibility
r_{Cl-O} (Å)		
$r_g(1)$	1.475	0.003
$r_g(0)$	1.476	0.003
r_e	1.471	0.003
$r_{O..O}$ (Å)		
$r_g(1)$	2.523	0.019
$r_g(0)$	2.525	0.019
$\angle OClO$ (°)	117.6($r_g(1)$)	1.3
u_{Cl-O} (Å)	0.035	0.003
$u_{O..O}$ (Å)	0.061	0.021

Notes: (1) These results were obtained by taking a straight average of the results presented in the two columns of the previous table. The O's were averaged and reproducibilities calculated from them according to the methods of Chapter Four.

(2) The u_{Cl-O} value has been corrected for failure of the Born approximation.

TABLE 12.6

A comparison of

the structural parameters obtained for ClO_2

with values derived by other methods

parameter	present study $r_g(1)$ values	microwave study ref.102	UV + IR studies ref.100	microwave force field* ref.83
r_{Cl-O} (Å)	1.475	1.473	1.472	-
estimated error	0.003	0.01	0.005	-
$\widehat{OClO}$ (°)	117.6	117.6	117.4	-
estimated error	1.3	1.0	0.2	-
u_{Cl-O} (Å)	0.035	-	-	0.039
estimated error	0.003	-	-	0.001
$u_{O..O}$ (Å)	0.061	-	-	0.063
estimated error	0.021	-	-	0.003

* The amplitudes were calculated by the author from the force constants published in this reference. These results are also included in table 8.5. The errors quoted are essentially subjective and are not based on exact calculation.

CHAPTER THIRTEEN

AN ELECTRON DIFFRACTION INVESTIGATION OF GASEOUS SULPHUR DIOXIDE

1. Introduction

In 1940, an electron diffraction study of gaseous sulphur dioxide by Schomaker and Stephenson[105], established the dimensions of the SO_2 molecule with moderate precision, but did not determine values for root mean square amplitudes of vibration. Subsequently, several microwave investigations of the compound have been carried out, and among these may be mentioned the studies of Dailey et al.,[106] Crable and Smith,[107] Sirvetz,[108] Kivelson[109] and the most recent investigation by Morino et al.[110] In most of these publications accurate molecular dimensions are stated, and in Morino's treatment the equilibrium molecular structure is very accurately determined.

The infrared investigation of gaseous SO_2 by Shelton, Nielsen and Fletcher in 1953,[87] established the harmonic frequencies of vibration of the normal isotopic species, but it remained for Polo and Wilson[84] to study the O^{18} substituted compound by the same technique and so determine the force constants of the harmonic potential function. Their results are in

excellent agreement with corresponding values determined by Kivelson[109] by microwave spectroscopy.

Recently, while the present work was in progress, Haase and Winnewisser published a high accuracy electron diffraction investigation of SO_2[111], and obtained an equlibrium S-O bond length in excellent agreement with Morino's result.

The present investigation was originally undertaken to obtain accurate electron diffraction structural parameters and amplitudes of vibration for the molecule, it being intended to compare the amplitudes determined with corresponding results calculated from the force constant data of Polo and Wilson.

2. Experimental

A commercial sample of sulphur dioxide was used to obtain diffraction patterns, and a summary of the experimental conditions employed is given in table 13.1. Owing to a technical fault, the electron beam showed a slight tremor, and for this reason data were not collected at the hundred centimetre jet-to-plate distance. For the same reason solid sample patterns were recorded at the fifty centimetre distance.

Uphill curves are listed in table 13.2, and the experimental combined $I_m(s)$ function is shown in figure

13.1. A corresponding Fourier transform is presented in figure 13.2, and indicates the angular symmetric nature of the molecule and the rather short S-O bonds present. The ' noise ripple ' prominent in this $\sigma(R)/R$ curve at $R \sim 0.5$ Å is presumably a consequence of the deviation between the theoretical and experimental $I_m(s)$ functions which occurs near $s = 10$ Å^{-1}.

3. Results

For the purposes of least squares refinement the molecule was defined by the internuclear distances R_{S-O} and $R_{O..O}$, and these were varied independently together with their corresponding root mean square amplitudes of vibration. Results of single distance refinements are presented in table 13.3, whilst those obtained by combtwo and combscaled all-data-combined refinements are listed in table 13.4. The final parameters for the SO_2 system, obtained by averaging the columns of table 13.4, are presented in table 13.5.

4. Discussion

If all relevant error limits are taken into account, the molecular dimensions obtained by the present work are in satisfactory agreement with corresponding results produced by the electron diffraction study of reference

105, as well as the results of the early microwave investigations.[106-108] In view, however, of the considerable accuracy of the most recent published electron diffraction work by Haase and Winnewisser[111], and of the microwave study by Morino et al.,[110] it is of interest to compare the results of these authors ($r_g(1)$ from ref. 111 and r_e from ref. 110) with the $r_g(1)$ and r_e S-O bond lengths determined by the present work. Such a comparison is made in table 13.6, and the following remarks may be made on the agreements evident in this table.

The SO_2 valence angle obtained by the present study is, within its rather large but understandable error limit of 1.2^o, in agreement with the corresponding values given by Morino and Haase and Winnewisser, but in view of the error limit mentioned, this comparison is not a particularly critical one. It is of much greater significance to consider the S-O bond lengths listed in table 13.6. The r_e distances obtained for the S-O bonds by the electron diffraction study of reference 111 and the microwave work of Morino are in very good agreement with eachother, but are both about 0.004 $\mathring{A}$ greater than the corresponding value determined by the present investigation. Of this difference, only about 0.003 $\mathring{A}$ can be justified if the random and

systematic errors normally assumed (which in this case amount to 0.002 Å) have added to them an extra 0.001 Å, to take into account the omission of hundred centimetre data, and the error of about twentyfive percent which the 'a' factor of the Morse potential is subject to. The fact that a difference of as much as 0.004 Å is observed seems to suggest that the systematic error of the diffraction experiment is greater than originally anticipated. It is significant that both single distance refinements produce an $r_g(1)$ S-O bond length which is lower than Haase and Winnewisser's $r_g(1)$ result (see table 13.6) and therefore it seems likely that the beam wavelength has been subject to a greater error than the one part in two thousand normally ascribed to it. It is also possible, however, that the beam tremor mentioned previously gave rise to systematic error in the microdensitometer traces measured.

The amplitudes of vibration obtained are in very good agreement with the spectroscopic values listed in tables 8.5 and 13.6. Haase and Winnewisser's amplitude results are not in quite such good agreement even after Born correction has been applied.

As for ClO_2, the considerable bond shortening of 0.26 Å of the S-O bond relative to a single bond estimate of 1.69 Å [95], indicates considerable double bond character. This conclusion has been confirmed

by Moffitt [111A], who has carried out molecular orbital calculations on SO_2 and has proposed a high π bond order, both d and p orbitals on sulphur being involved in this bonding.

TABLE 13.1

A summary of experimental details

for the sulphur dioxide investigation

jet to plate distance	-	50 cm	25 cm	-
wavelength (A)		0.051183	0.051183	
e.s.d.		0.000015	0.000015	
sample temperature (^{o}K)		213	213	
nozzle temperature (^{o}K)		293	293	
gas temperature assumed (^{o}K)		253	253	
number of plates used		4	5	
quality		good	rather light	
number of traces measured (AMDM)		8	10	

TABLE 13.2

SO_2 intensity data as combined uphill curves

range (1): s = 2.40 by 0.05 to 17.85 Å^{-1}

2.604$_{10}$ +4;	2.694$_{10}$ +4;	2.785$_{10}$ +4;	2.872$_{10}$ +4;	2.952$_{10}$ +4;
3.028$_{10}$ +4;	3.105$_{10}$ +4;	3.187$_{10}$ +4;	3.277$_{10}$ +4;	3.371$_{10}$ +4;
3.466$_{10}$ +4;	3.567$_{10}$ +4;	3.673$_{10}$ +4;	3.777$_{10}$ +4;	3.879$_{10}$ +4;
3.987$_{10}$ +4;	4.098$_{10}$ +4;	4.199$_{10}$ +4;	4.302$_{10}$ +4;	4.416$_{10}$ +4;
4.540$_{10}$ +4;	4.669$_{10}$ +4;	4.815$_{10}$ +4;	4.968$_{10}$ +4;	5.118$_{10}$ +4;
5.269$_{10}$ +4;	5.425$_{10}$ +4;	5.592$_{10}$ +4;	5.766$_{10}$ +4;	5.945$_{10}$ +4;
6.132$_{10}$ +4;	6.322$_{10}$ +4;	6.514$_{10}$ +4;	6.715$_{10}$ +4;	6.928$_{10}$ +4;
7.138$_{10}$ +4;	7.349$_{10}$ +4;	7.567$_{10}$ +4;	7.790$_{10}$ +4;	8.025$_{10}$ +4;
8.262$_{10}$ +4;	8.495$_{10}$ +4;	8.721$_{10}$ +4;	8.954$_{10}$ +4;	9.196$_{10}$ +4;
9.448$_{10}$ +4;	9.694$_{10}$ +4;	9.929$_{10}$ +4;	1.016$_{10}$ +5;	1.040$_{10}$ +5;
1.063$_{10}$ +5;	1.086$_{10}$ +5;	1.108$_{10}$ +5;	1.130$_{10}$ +5;	1.152$_{10}$ +5;
1.173$_{10}$ +5;	1.192$_{10}$ +5;	1.209$_{10}$ +5;	1.225$_{10}$ +5;	1.239$_{10}$ +5;
1.252$_{10}$ +5;	1.264$_{10}$ +5;	1.275$_{10}$ +5;	1.286$_{10}$ +5;	1.294$_{10}$ +5;
1.300$_{10}$ +5;	1.306$_{10}$ +5;	1.312$_{10}$ +5;	1.314$_{10}$ +5;	1.313$_{10}$ +5;
1.312$_{10}$ +5;	1.311$_{10}$ +5;	1.310$_{10}$ +5;	1.307$_{10}$ +5;	1.301$_{10}$ +5;
1.295$_{10}$ +5;	1.288$_{10}$ +5;	1.280$_{10}$ +5;	1.272$_{10}$ +5;	1.264$_{10}$ +5;
1.255$_{10}$ +5;	1.245$_{10}$ +5;	1.235$_{10}$ +5;	1.224$_{10}$ +5;	1.214$_{10}$ +5;
1.206$_{10}$ +5;	1.198$_{10}$ +5;	1.189$_{10}$ +5;	1.180$_{10}$ +5;	1.174$_{10}$ +5;
1.168$_{10}$ +5;	1.164$_{10}$ +5;	1.160$_{10}$ +5;	1.157$_{10}$ +5;	1.156$_{10}$ +5;
1.154$_{10}$ +5;	1.153$_{10}$ +5;	1.153$_{10}$ +5;	1.154$_{10}$ +5;	1.157$_{10}$ +5;
1.161$_{10}$ +5;	1.166$_{10}$ +5;	1.171$_{10}$ +5;	1.178$_{10}$ +5;	1.187$_{10}$ +5;
1.194$_{10}$ +5;	1.203$_{10}$ +5;	1.213$_{10}$ +5;	1.224$_{10}$ +5;	1.234$_{10}$ +5;
1.245$_{10}$ +5;	1.257$_{10}$ +5;	1.269$_{10}$ +5;	1.281$_{10}$ +5;	1.293$_{10}$ +5;
1.305$_{10}$ +5;	1.318$_{10}$ +5;	1.332$_{10}$ +5;	1.347$_{10}$ +5;	1.360$_{10}$ +5;
1.372$_{10}$ +5;	1.383$_{10}$ +5;	1.395$_{10}$ +5;	1.410$_{10}$ +5;	1.424$_{10}$ +5;
1.436$_{10}$ +5;	1.447$_{10}$ +5;	1.461$_{10}$ +5;	1.473$_{10}$ +5;	1.485$_{10}$ +5;
1.497$_{10}$ +5;	1.509$_{10}$ +5;	1.522$_{10}$ +5;	1.534$_{10}$ +5;	1.544$_{10}$ +5;
1.552$_{10}$ +5;	1.562$_{10}$ +5;	1.572$_{10}$ +5;	1.583$_{10}$ +5;	1.593$_{10}$ +5;
1.603$_{10}$ +5;	1.613$_{10}$ +5;	1.624$_{10}$ +5;	1.633$_{10}$ +5;	1.640$_{10}$ +5;
1.646$_{10}$ +5;	1.654$_{10}$ +5;	1.664$_{10}$ +5;	1.673$_{10}$ +5;	1.679$_{10}$ +5;
1.684$_{10}$ +5;	1.689$_{10}$ +5;	1.698$_{10}$ +5;	1.707$_{10}$ +5;	1.713$_{10}$ +5;
1.715$_{10}$ +5;	1.715$_{10}$ +5;	1.728$_{10}$ +5;	1.748$_{10}$ +5;	1.754$_{10}$ +5;
1.742$_{10}$ +5;	1.733$_{10}$ +5;	1.740$_{10}$ +5;	1.738$_{10}$ +5;	1.729$_{10}$ +5;
1.720$_{10}$ +5;	1.715$_{10}$ +5;	1.712$_{10}$ +5;	1.710$_{10}$ +5;	1.708$_{10}$ +5;
1.704$_{10}$ +5;	1.699$_{10}$ +5;	1.693$_{10}$ +5;	1.687$_{10}$ +5;	1.683$_{10}$ +5;
1.679$_{10}$ +5;	1.674$_{10}$ +5;	1.669$_{10}$ +5;	1.663$_{10}$ +5;	1.658$_{10}$ +5;
1.655$_{10}$ +5;	1.653$_{10}$ +5;	1.654$_{10}$ +5;	1.652$_{10}$ +5;	1.648$_{10}$ +5;
1.645$_{10}$ +5;	1.645$_{10}$ +5;	1.644$_{10}$ +5;	1.645$_{10}$ +5;	1.653$_{10}$ +5;
1.657$_{10}$ +5;	1.656$_{10}$ +5;	1.655$_{10}$ +5;	1.660$_{10}$ +5;	1.667$_{10}$ +5;
1.675$_{10}$ +5;	1.683$_{10}$ +5;	1.691$_{10}$ +5;	1.701$_{10}$ +5;	1.709$_{10}$ +5;

1.717_{10} +5; 1.728_{10} +5; 1.744_{10} +5; 1.757_{10} +5; 1.766_{10} +5;
1.776_{10} +5; 1.790_{10} +5; 1.803_{10} +5; 1.816_{10} +5; 1.832_{10} +5;
1.847_{10} +5; 1.860_{10} +5; 1.874_{10} +5; 1.890_{10} +5; 1.905_{10} +5;
1.916_{10} +5; 1.928_{10} +5; 1.943_{10} +5; 1.959_{10} +5; 1.971_{10} +5;
1.983_{10} +5; 1.995_{10} +5; 2.003_{10} +5; 2.012_{10} +5; 2.023_{10} +5;
2.032_{10} +5; 2.038_{10} +5; 2.046_{10} +5; 2.053_{10} +5; 2.060_{10} +5;
2.068_{10} +5; 2.076_{10} +5; 2.082_{10} +5; 2.084_{10} +5; 2.088_{10} +5;
2.091_{10} +5; 2.094_{10} +5; 2.100_{10} +5; 2.105_{10} +5; 2.105_{10} +5;
2.101_{10} +5; 2.102_{10} +5; 2.106_{10} +5; 2.108_{10} +5; 2.106_{10} +5;
2.105_{10} +5; 2.103_{10} +5; 2.101_{10} +5; 2.100_{10} +5; 2.099_{10} +5;
2.097_{10} +5; 2.096_{10} +5; 2.095_{10} +5; 2.092_{10} +5; 2.091_{10} +5;
2.089_{10} +5; 2.086_{10} +5; 2.082_{10} +5; 2.078_{10} +5; 2.074_{10} +5;
2.072_{10} +5; 2.072_{10} +5; 2.071_{10} +5; 2.071_{10} +5; 2.070_{10} +5;
2.066_{10} +5; 2.064_{10} +5; 2.063_{10} +5; 2.061_{10} +5; 2.058_{10} +5;
2.057_{10} +5; 2.056_{10} +5; 2.058_{10} +5; 2.058_{10} +5; 2.056_{10} +5;
2.053_{10} +5; 2.052_{10} +5; 2.055_{10} +5; 2.059_{10} +5; 2.061_{10} +5;
2.064_{10} +5; 2.069_{10} +5; 2.074_{10} +5; 2.078_{10} +5; 2.082_{10} +5;
2.089_{10} +5; 2.097_{10} +5; 2.102_{10} +5; 2.108_{10} +5; 2.115_{10} +5;
2.123_{10} +5; 2.132_{10} +5; 2.143_{10} +5; 2.153_{10} +5; 2.163_{10} +5;
2.173_{10} +5; 2.183_{10} +5; 2.194_{10} +5; 2.211_{10} +5; 2.231_{10} +5;
2.246_{10} +5; 2.255_{10} +5; 2.262_{10} +5; 2.269_{10} +5; 2.279_{10} +5;
2.293_{10} +5; 2.306_{10} +5; 2.319_{10} +5; 2.330_{10} +5; 2.344_{10} +5;

range (2): s = 7.60 by 0.10 to 34.70 Å^{-1}

1.108_{10} +6; 1.128_{10} +6; 1.151_{10} +6; 1.173_{10} +6; 1.200_{10} +6;
1.224_{10} +6; 1.247_{10} +6; 1.272_{10} +6; 1.304_{10} +6; 1.329_{10} +6;
1.354_{10} +6; 1.382_{10} +6; 1.406_{10} +6; 1.425_{10} +6; 1.446_{10} +6;
1.466_{10} +6; 1.479_{10} +6; 1.496_{10} +6; 1.511_{10} +6; 1.530_{10} +6;
1.541_{10} +6; 1.559_{10} +6; 1.575_{10} +6; 1.582_{10} +6; 1.588_{10} +6;
1.603_{10} +6; 1.610_{10} +6; 1.612_{10} +6; 1.618_{10} +6; 1.624_{10} +6;
1.634_{10} +6; 1.635_{10} +6; 1.625_{10} +6; 1.611_{10} +6; 1.602_{10} +6;
1.592_{10} +6; 1.583_{10} +6; 1.569_{10} +6; 1.559_{10} +6; 1.549_{10} +6;
1.548_{10} +6; 1.535_{10} +6; 1.529_{10} +6; 1.534_{10} +6; 1.534_{10} +6;
1.544_{10} +6; 1.547_{10} +6; 1.557_{10} +6; 1.577_{10} +6; 1.594_{10} +6;
1.614_{10} +6; 1.631_{10} +6; 1.656_{10} +6; 1.680_{10} +6; 1.707_{10} +6;
1.736_{10} +6; 1.759_{10} +6; 1.783_{10} +6; 1.805_{10} +6; 1.826_{10} +6;

TABLE 13.2 (concluded)

1.844_{m} +6;	1.861_{m} +6;	1.880_{m} +6;	1.891_{m} +6;	1.904_{m} +6;
1.917_{m} +6;	1.916_{m} +6;	1.916_{m} +6;	1.924_{m} +6;	1.916_{m} +6;
1.916_{m} +6;	1.916_{m} +6;	1.911_{m} +6;	1.908_{m} +6;	1.907_{m} +6;
1.906_{m} +6;	1.900_{m} +6;	1.902_{m} +6;	1.897_{m} +6;	1.894_{m} +6;
1.895_{m} +6;	1.887_{m} +6;	1.886_{m} +6;	1.887_{m} +6;	1.882_{m} +6;
1.881_{m} +6;	1.880_{m} +6;	1.890_{m} +6;	1.891_{m} +6;	1.908_{m} +6;
1.899_{m} +6;	1.906_{m} +6;	1.919_{m} +6;	1.930_{m} +6;	1.943_{m} +6;
1.963_{m} +6;	1.978_{m} +6;	1.999_{m} +6;	2.014_{m} +6;	2.036_{m} +6;
2.052_{m} +6;	2.068_{m} +6;	2.089_{m} +6;	2.110_{m} +6;	2.122_{m} +6;
2.148_{m} +6;	2.152_{m} +6;	2.165_{m} +6;	2.173_{m} +6;	2.180_{m} +6;
2.182_{m} +6;	2.190_{m} +6;	2.196_{m} +6;	2.191_{m} +6;	2.200_{m} +6;
2.191_{m} +6;	2.182_{m} +6;	2.184_{m} +6;	2.178_{m} +6;	2.174_{m} +6;
2.171_{m} +6;	2.170_{m} +6;	2.165_{m} +6;	2.157_{m} +6;	2.153_{m} +6;
2.158_{m} +6;	2.154_{m} +6;	2.149_{m} +6;	2.153_{m} +6;	2.153_{m} +6;
2.159_{m} +6;	2.161_{m} +6;	2.172_{m} +6;	2.177_{m} +6;	2.185_{m} +6;
2.200_{m} +6;	2.214_{m} +6;	2.232_{m} +6;	2.251_{m} +6;	2.262_{m} +6;
2.268_{m} +6;	2.274_{m} +6;	2.286_{m} +6;	2.291_{m} +6;	2.308_{m} +6;
2.332_{m} +6;	2.337_{m} +6;	2.354_{m} +6;	2.364_{m} +6;	2.376_{m} +6;
2.389_{m} +6;	2.392_{m} +6;	2.403_{m} +6;	2.420_{m} +6;	2.425_{m} +6;
2.429_{m} +6;	2.440_{m} +6;	2.444_{m} +6;	2.445_{m} +6;	2.445_{m} +6;
2.446_{m} +6;	2.450_{m} +6;	2.441_{m} +6;	2.448_{m} +6;	2.444_{m} +6;
2.437_{m} +6;	2.441_{m} +6;	2.436_{m} +6;	2.433_{m} +6;	2.433_{m} +6;
2.437_{m} +6;	2.438_{m} +6;	2.441_{m} +6;	2.443_{m} +6;	2.446_{m} +6;
2.450_{m} +6;	2.454_{m} +6;	2.464_{m} +6;	2.481_{m} +6;	2.489_{m} +6;
2.500_{m} +6;	2.511_{m} +6;	2.519_{m} +6;	2.539_{m} +6;	2.552_{m} +6;
2.558_{m} +6;	2.574_{m} +6;	2.588_{m} +6;	2.590_{m} +6;	2.610_{m} +6;
2.621_{m} +6;	2.643_{m} +6;	2.660_{m} +6;	2.653_{m} +6;	2.660_{m} +6;
2.672_{m} +6;	2.679_{m} +6;	2.689_{m} +6;	2.700_{m} +6;	2.710_{m} +6;
2.712_{m} +6;	2.719_{m} +6;	2.720_{m} +6;	2.720_{m} +6;	2.726_{m} +6;
2.723_{m} +6;	2.730_{m} +6;	2.732_{m} +6;	2.738_{m} +6;	2.738_{m} +6;
2.747_{m} +6;	2.755_{m} +6;	2.750_{m} +6;	2.746_{m} +6;	2.742_{m} +6;
2.743_{m} +6;	2.742_{m} +6;	2.749_{m} +6;	2.753_{m} +6;	2.752_{m} +6;
2.762_{m} +6;	2.766_{m} +6;	2.771_{m} +6;	2.782_{m} +6;	2.787_{m} +6;
2.795_{m} +6;	2.805_{m} +6;	2.819_{m} +6;	2.827_{m} +6;	2.839_{m} +6;
2.852_{m} +6;	2.858_{m} +6;	2.875_{m} +6;	2.886_{m} +6;	2.892_{m} +6;
2.899_{m} +6;	2.914_{m} +6;	2.923_{m} +6;	2.933_{m} +6;	2.947_{m} +6;
2.948_{m} +6;	2.967_{m} +6;	2.973_{m} +6;	2.971_{m} +6;	2.978_{m} +6;
2.980_{m} +6;	2.985_{m} +6;	3.001_{m} +6;	3.012_{m} +6;	3.013_{m} +6;
3.014_{m} +6;	3.022_{m} +6;	3.038_{m} +6;	3.052_{m} +6;	3.048_{m} +6;
3.062_{m} +6;	3.061_{m} +6;	3.068_{m} +6;	3.075_{m} +6;	3.075_{m} +6;
3.081_{m} +6;	3.088_{m} +6;	3.102_{m} +6;	3.139_{m} +6;	3.127_{m} +6;
3.120_{m} +6;	3.129_{m} +6;	3.143_{m} +6;	3.140_{m} +6;	3.150_{m} +6;
3.143_{m} +6;	3.155_{m} +6;			

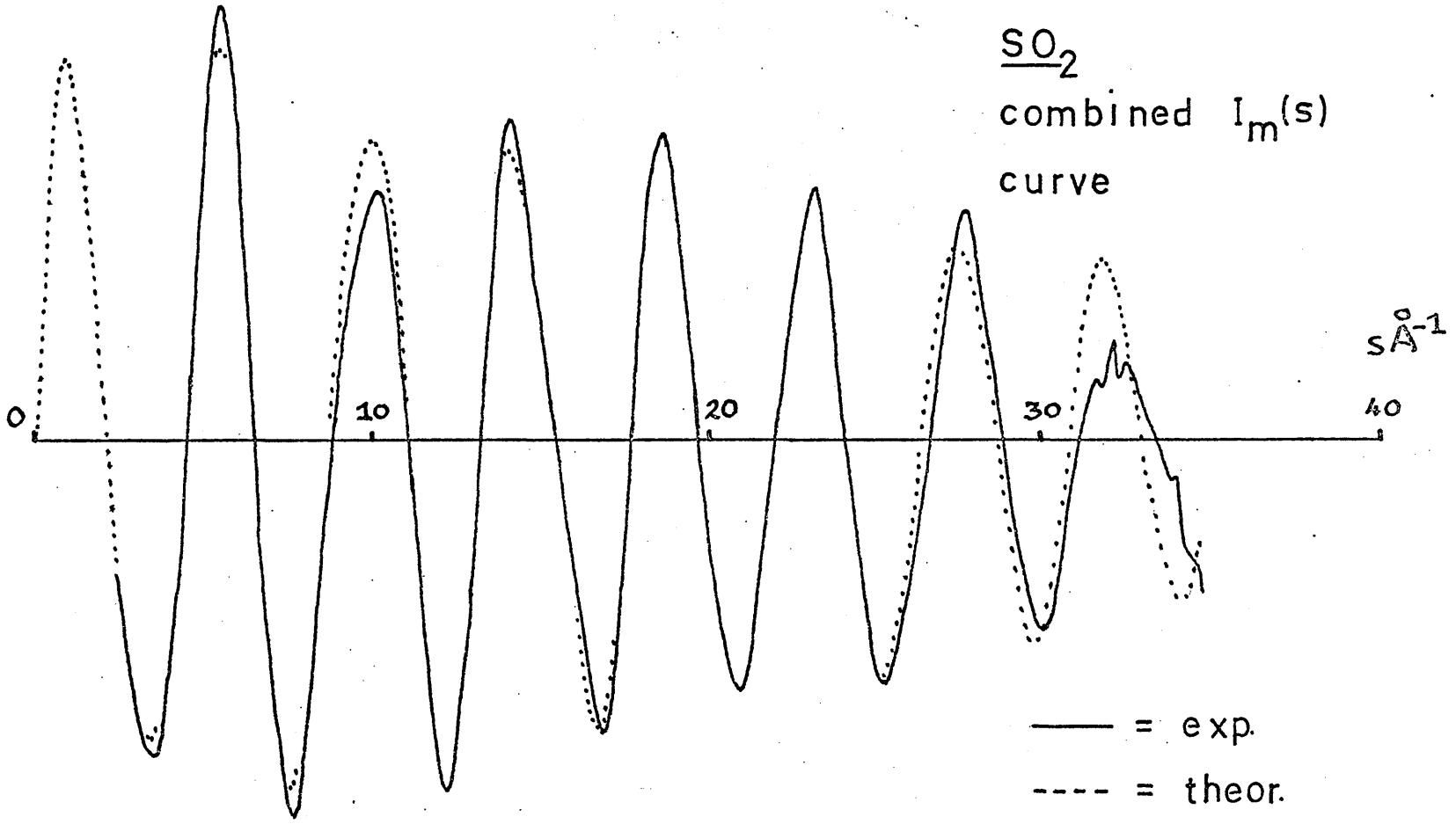

fig. 13.1

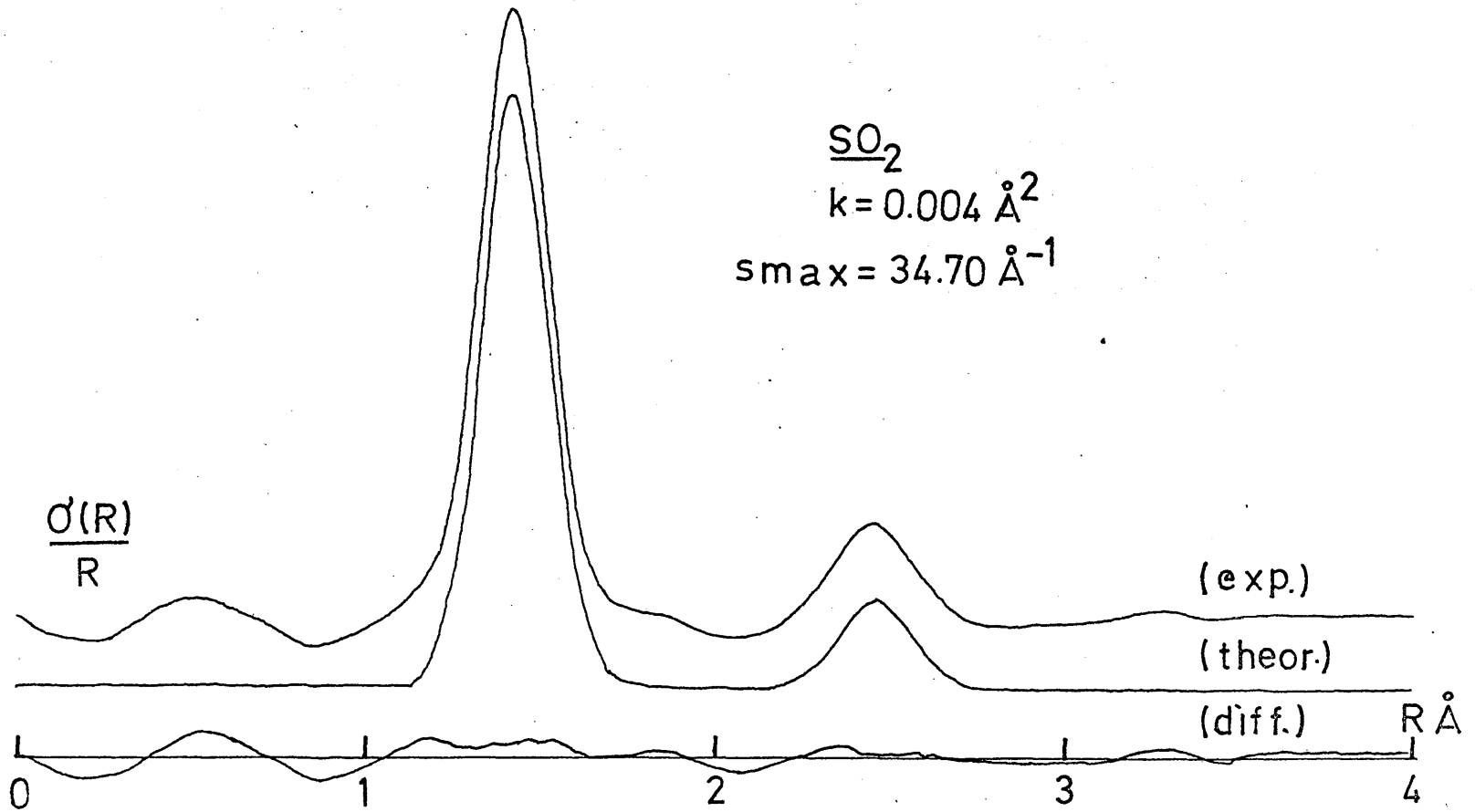

fig.13.2

TABLE 13.3

Results of individual distance refinements for SO_2

jet to plate distance	50 cm	25 cm
r_{S-O} (Å)	1.4331	1.4307
σ'	0.0007	0.0006
$r_{O..O}$ (Å)	2.4712	2.4520
σ'	0.0056	0.0063
R(%)	12.63	19.37
$\sum w\Delta^2$	1.898×10^{11}	1.322×10^{13}

Notes: (1) u values were held constant at spectroscopic values.

(2) σ''s are least squares e.s.d.'s.

(3) r values are $r_g(1)$ distances.

TABLE 13.4

Results of ' all data combined ' refinements for SO_2

parameter	combtwo	comb-scaled
r_{S-O} (Å)	1.4310	1.4309
σ'	0.0005	0.0005
$r_{O..O}$ (Å)	2.4647	2.4661
σ'	0.0040	0.0038
u_{S-O} (Å)	0.0423	0.0413
σ'	0.0008	0.0009
$u_{O..O}$ (Å)	0.0481	0.0459
σ'	0.0043	0.0045
R(%)	12.57	15.08
$\sum w\Delta^2$	3.181 x 10^{11}	4.784 x 10^{11}

Notes: (1) The distances are $r_g(1)$ values.

(2) The σ''s are least squares e.s.d.'s.

(3) The amplitudes have not been corrected for failure of the Born approximation.

TABLE 13.5

The final structural parameters

for SO_2

parameter	final result	reproducibility
r_{S-O} (Å)		
$r_g(1)$	1.431	0.002
$r_g(0)$	1.432	0.002
r_e	1.427	0.002
$r_{O..O}$ (Å)		
$r_g(1)$	2.465	0.013
$r_g(0)$	2.466	0.013
$\widehat{OSO}$ (°)	118.9($r_g(1)$)	1.2
u_{S-O} (Å)	0.035	0.003
$u_{O..O}$ (Å)	0.047	0.012

Notes: (1) These results were obtained by taking a straight average of the results presented in the two columns of the previous table. The O's were averaged and reproducibilities calculated from them according to the methods of Chapter 4.

(2) The u_{S-O} value has been corrected for failure of the Born approximation.

TABLE 13.6

A comparison of

the structural parameters obtained for SO_2

with values derived by other methods

parameter	present study	microwave study ref. 110	recent e.d. study ref. 111	IR force field* ref. 84
r_{S-O} (Å)				
$r_g(1)$	1.431		1.4361	
error	0.002		0.001	
r_e	1.427	1.4308	1.4309	
error	0.002	0.0002	0.001	
$\widehat{OSO}$ (°)	118.9 ($r_g(1)$)	119.32 (r_e)	118.98 ($r_g(1)$)	
error	1.2	0.03	0.5	
u_{S-O} (Å)	0.035		0.044**	0.035
error	0.003		0.002	0.001
$u_{O..O}$ (Å)	0.047		0.072	0.055
error	0.012		0.002	0.003

* The amplitudes were calculated by the author from the force constants published in this reference. The errors quoted are essentially subjective.

**This amplitude has not been corrected but is the published value.

CHAPTER FOURTEEN

AN ELECTRON DIFFRACTION INVESTIGATION OF SULPHUR TRIOXIDE VAPOUR

1. Introduction

In 1938 Palmer published a low accuracy electron diffraction study[112] of sulphur trioxide vapour, and showed, that within the error limits of his experiment, the molecule is planar with a threefold axis of symmetry. In this investigation values were not obtained for the root mean square amplitudes of vibration.

A recent infrared study[85] of the vapour, carried out by Krakow and Lord, has determined the force constants necessary to define the molecule's harmonic potential function, and these results have been slightly modified by Stølevik et al.[88], and used to calculate root mean square amplitudes of vibration, and the expected shrinkage effect.

The present electron diffraction investigation was undertaken to obtain a more accurate S-O bond length than was determined by Palmer, and also root mean square amplitudes of vibration for comparison with the results of reference 88.

2. Experimental

A commercial sample of sulphur trioxide was used to obtain diffraction patterns, and a summary of the experimental conditions adopted is given in table 14.1. Owing to a slight tremor in the electron beam, data were not collected at the hundred centimetre jet-to-plate distance, and the wavelength was determined from powder patterns recorded at fifty centimetres. The sample showed a marked tendency to condense out on the nozzle tip, despite the high nozzle temperature adopted, and the sample temperature had to be carefully regulated to prevent this occurring. Accordingly, long exposure times were impossible, and the twentyfive centimetre plates obtained were underexposed and somewhat unsatisfactory.

Uphill curves are listed in table 14.2, and the experimental combined $I_m(s)$ function is shown graphically in figure 14.1. Its Fourier transform is presented in figure 14.2, and indicates the planar, symmetrical nature of the molecule.

3. Results

In least squares refinements SO_3 was treated as an XY_3 system with a threefold axis of symmetry, but was not assumed planar. The two internuclear distances

S-O and O..O were refined as independent parameters, together with their corresponding root mean square amplitudes of vibration.

Results for the single distance refinements carried out are listed in table 14.3, and show good consistency, whilst results obtained by combtwo and combscaled refinements of the all-distances-combined intensity data, are given in table 14.4. The residuals quoted in this latter table are unusually low, and this is a consequence of the fact that poor quality data beyond the $s = 25$ A^{o-1} limit were omitted. Final structural parameters for the molecule are presented in table 14.5.

4. Discussion

The planar nature of the sulphur trioxide molecule is confirmed within the experimental error limits involved. No shrinkage effect is observed, but the uncertainty in $R_{O..O}$ is a good deal larger than the anticipated 0.002 A calculated for this effect in reference 88.

The S-O bond length agrees with the corresponding result obtained by Palmer of 1.43 A^{o}, if his error limit of 0.02 A^{o} is taken into account, and is evidently about 0.015 A^{o} shorter than the S-O distance in SO_2. Such a result is consistent with the force constant of

10.6 md/Å calculated for the S-O bond in SO_3 by Krakow and Lord, when this latter result is compared with the value of 10.02 md/Å obtained for SO_2 by Polo and Wilson.[84] The difference between these two force constants is just what would be expected for the bond shortening of 0.015 Å observed.

The amplitudes of vibration determined by the present work are in extremely poor agreement with the spectroscopic results (0.035 and 0.054 Å) of reference 88, and also with the results obtained for SO_2 in the previous chapter. Such differences are too large to be explained in terms of the poor quality of the twentyfive centimetre data, and it seems likely that traces of some impurity, such as sulphur dioxide, must have been present in the vapour studied.

It is evident from the shortness of the S-O distance obtained for SO_3 (single bond value 1.69 Å[95]) that this bond involves a considerable amount of double bond character. This has been confirmed by molecular orbital calculations carried out in 1950 by Moffitt[111A], who concluded that the sulphur d orbitals are involved to a considerable extent in π bonding to oxygen. Moffitt predicted that the bond order of the S-O bond in SO_3 should be greater than that of the corresponding bond in SO_2, a conclusion which is confirmed by the present work.

TABLE 14.1

A summary of experimental details

for the sulphur trioxide investigation

jet to plate distance	-	50 cm	25 cm	-
wavelength (A)		0.051183	0.051183	
e.s.d.		0.000015	0.000015	
sample temperature (^{o}K)		268	268	
nozzle temperature (^{o}K)		353	353	
gas temperature assumed (^{o}K)		310	310	
number of plates used		4	5	
quality		good	very light	
number of traces measured (AMDM)		8	10	

TABLE 14.2

SO_3 intensity data as combined uphill curves

range (1): s = 2.40 by 0.05 to 17.85 $Å^{-1}$

1.613$_{10}$ +4;	1.668$_{10}$ +4;	1.722$_{10}$ +4;	1.772$_{10}$ +4;	1.819$_{10}$ +4;
1.864$_{10}$ +4;	1.911$_{10}$ +4;	1.965$_{10}$ +4;	2.023$_{10}$ +4;	2.084$_{10}$ +4;
2.147$_{10}$ +4;	2.215$_{10}$ +4;	2.286$_{10}$ +4;	2.353$_{10}$ +4;	2.418$_{10}$ +4;
2.489$_{10}$ +4;	2.555$_{10}$ +4;	2.606$_{10}$ +4;	2.653$_{10}$ +4;	2.717$_{10}$ +4;
2.790$_{10}$ +4;	2.862$_{10}$ +4;	2.936$_{10}$ +4;	3.014$_{10}$ +4;	3.093$_{10}$ +4;
3.173$_{10}$ +4;	3.255$_{10}$ +4;	3.340$_{10}$ +4;	3.425$_{10}$ +4;	3.515$_{10}$ +4;
3.612$_{10}$ +4;	3.713$_{10}$ +4;	3.820$_{10}$ +4;	3.934$_{10}$ +4;	4.057$_{10}$ +4;
4.185$_{10}$ +4;	4.319$_{10}$ +4;	4.456$_{10}$ +4;	4.595$_{10}$ +4;	4.739$_{10}$ +4;
4.900$_{10}$ +4;	5.071$_{10}$ +4;	5.243$_{10}$ +4;	5.412$_{10}$ +4;	5.586$_{10}$ +4;
5.770$_{10}$ +4;	5.974$_{10}$ +4;	6.186$_{10}$ +4;	6.389$_{10}$ +4;	6.589$_{10}$ +4;
6.795$_{10}$ +4;	7.003$_{10}$ +4;	7.210$_{10}$ +4;	7.406$_{10}$ +4;	7.587$_{10}$ +4;
7.757$_{10}$ +4;	7.926$_{10}$ +4;	8.083$_{10}$ +4;	8.234$_{10}$ +4;	8.365$_{10}$ +4;
8.471$_{10}$ +4;	8.560$_{10}$ +4;	8.647$_{10}$ +4;	8.728$_{10}$ +4;	8.786$_{10}$ +4;
8.824$_{10}$ +4;	8.843$_{10}$ +4;	8.853$_{10}$ +4;	8.854$_{10}$ +4;	8.837$_{10}$ +4;
8.791$_{10}$ +4;	8.724$_{10}$ +4;	8.658$_{10}$ +4;	8.587$_{10}$ +4;	8.503$_{10}$ +4;
8.403$_{10}$ +4;	8.297$_{10}$ +4;	8.191$_{10}$ +4;	8.077$_{10}$ +4;	7.955$_{10}$ +4;
7.825$_{10}$ +4;	7.690$_{10}$ +4;	7.557$_{10}$ +4;	7.425$_{10}$ +4;	7.294$_{10}$ +4;
7.157$_{10}$ +4;	7.028$_{10}$ +4;	6.925$_{10}$ +4;	6.832$_{10}$ +4;	6.740$_{10}$ +4;
6.654$_{10}$ +4;	6.589$_{10}$ +4;	6.530$_{10}$ +4;	6.460$_{10}$ +4;	6.397$_{10}$ +4;
6.356$_{10}$ +4;	6.341$_{10}$ +4;	6.335$_{10}$ +4;	6.336$_{10}$ +4;	6.352$_{10}$ +4;
6.366$_{10}$ +4;	6.393$_{10}$ +4;	6.435$_{10}$ +4;	6.495$_{10}$ +4;	6.557$_{10}$ +4;
6.616$_{10}$ +4;	6.686$_{10}$ +4;	6.757$_{10}$ +4;	6.832$_{10}$ +4;	6.906$_{10}$ +4;
6.984$_{10}$ +4;	7.071$_{10}$ +4;	7.164$_{10}$ +4;	7.248$_{10}$ +4;	7.319$_{10}$ +4;
7.403$_{10}$ +4;	7.501$_{10}$ +4;	7.597$_{10}$ +4;	7.673$_{10}$ +4;	7.740$_{10}$ +4;
7.810$_{10}$ +4;	7.896$_{10}$ +4;	7.981$_{10}$ +4;	8.055$_{10}$ +4;	8.116$_{10}$ +4;
8.170$_{10}$ +4;	8.205$_{10}$ +4;	8.262$_{10}$ +4;	8.333$_{10}$ +4;	8.398$_{10}$ +4;
8.465$_{10}$ +4;	8.527$_{10}$ +4;	8.566$_{10}$ +4;	8.602$_{10}$ +4;	8.654$_{10}$ +4;
8.717$_{10}$ +4;	8.760$_{10}$ +4;	8.825$_{10}$ +4;	8.901$_{10}$ +4;	8.960$_{10}$ +4;
9.007$_{10}$ +4;	9.050$_{10}$ +4;	9.091$_{10}$ +4;	9.136$_{10}$ +4;	9.201$_{10}$ +4;
9.273$_{10}$ +4;	9.322$_{10}$ +4;	9.375$_{10}$ +4;	9.452$_{10}$ +4;	9.510$_{10}$ +4;
9.555$_{10}$ +4;	9.614$_{10}$ +4;	9.686$_{10}$ +4;	9.730$_{10}$ +4;	9.750$_{10}$ +4;
9.790$_{10}$ +4;	9.853$_{10}$ +4;	9.910$_{10}$ +4;	9.922$_{10}$ +4;	9.922$_{10}$ +4;
9.930$_{10}$ +4;	9.967$_{10}$ +4;	9.999$_{10}$ +4;	9.992$_{10}$ +4;	9.975$_{10}$ +4;
9.958$_{10}$ +4;	9.945$_{10}$ +4;	9.910$_{10}$ +4;	9.862$_{10}$ +4;	9.815$_{10}$ +4;
9.783$_{10}$ +4;	9.741$_{10}$ +4;	9.669$_{10}$ +4;	9.598$_{10}$ +4;	9.540$_{10}$ +4;
9.488$_{10}$ +4;	9.435$_{10}$ +4;	9.362$_{10}$ +4;	9.288$_{10}$ +4;	9.212$_{10}$ +4;
9.138$_{10}$ +4;	9.079$_{10}$ +4;	9.040$_{10}$ +4;	8.992$_{10}$ +4;	8.930$_{10}$ +4;
8.874$_{10}$ +4;	8.838$_{10}$ +4;	8.799$_{10}$ +4;	8.764$_{10}$ +4;	8.744$_{10}$ +4;

TABLE 14.2 (cont'd)

8.744_{10} +4;	8.777_{10} +4;	8.870_{10} +4;	8.906_{10} +4;	8.851_{10} +4;
8.792_{10} +4;	8.819_{10} +4;	8.895_{10} +4;	8.964_{10} +4;	9.039_{10} +4;
9.092_{10} +4;	9.140_{10} +4;	9.185_{10} +4;	9.265_{10} +4;	9.372_{10} +4;
9.487_{10} +4;	9.580_{10} +4;	9.670_{10} +4;	9.784_{10} +4;	9.917_{10} +4;
1.004_{10} +5;	1.012_{10} +5;	1.022_{10} +5;	1.033_{10} +5;	1.046_{10} +5;
1.058_{10} +5;	1.069_{10} +5;	1.078_{10} +5;	1.086_{10} +5;	1.094_{10} +5;
1.106_{10} +5;	1.115_{10} +5;	1.122_{10} +5;	1.128_{10} +5;	1.137_{10} +5;
1.146_{10} +5;	1.151_{10} +5;	1.155_{10} +5;	1.162_{10} +5;	1.169_{10} +5;
1.174_{10} +5;	1.177_{10} +5;	1.180_{10} +5;	1.184_{10} +5;	1.191_{10} +5;
1.194_{10} +5;	1.193_{10} +5;	1.193_{10} +5;	1.199_{10} +5;	1.206_{10} +5;
1.208_{10} +5;	1.205_{10} +5;	1.202_{10} +5;	1.203_{10} +5;	1.204_{10} +5;
1.206_{10} +5;	1.208_{10} +5;	1.210_{10} +5;	1.210_{10} +5;	1.213_{10} +5;
1.215_{10} +5;	1.215_{10} +5;	1.215_{10} +5;	1.220_{10} +5;	1.224_{10} +5;
1.222_{10} +5;	1.217_{10} +5;	1.220_{10} +5;	1.224_{10} +5;	1.226_{10} +5;
1.225_{10} +5;	1.226_{10} +5;	1.225_{10} +5;	1.226_{10} +5;	1.227_{10} +5;
1.228_{10} +5;	1.232_{10} +5;	1.239_{10} +5;	1.241_{10} +5;	1.235_{10} +5;
1.229_{10} +5;	1.229_{10} +5;	1.228_{10} +5;	1.228_{10} +5;	1.230_{10} +5;
1.232_{10} +5;	1.232_{10} +5;	1.228_{10} +5;	1.228_{10} +5;	1.226_{10} +5;
1.225_{10} +5;	1.225_{10} +5;	1.228_{10} +5;	1.227_{10} +5;	1.230_{10} +5;
1.238_{10} +5;	1.244_{10} +5;	1.242_{10} +5;	1.240_{10} +5;	1.244_{10} +5;
1.247_{10} +5;	1.252_{10} +5;	1.258_{10} +5;	1.265_{10} +5;	1.271_{10} +5;
1.277_{10} +5;	1.282_{10} +5;	1.291_{10} +5;	1.299_{10} +5;	1.303_{10} +5;
1.312_{10} +5;	1.325_{10} +5;	1.332_{10} +5;	1.336_{10} +5;	1.345_{10} +5;
1.360_{10} +5;	1.370_{10} +5;	1.378_{10} +5;	1.384_{10} +5;	1.387_{10} +5;

range (2): s = 7.60 by 0.10 to 34.7 Å^{-1}

5.046_{10} +5;	5.185_{10} +5;	5.350_{10} +5;	5.490_{10} +5;	5.674_{10} +5;
5.860_{10} +5;	5.996_{10} +5;	6.151_{10} +5;	6.309_{10} +5;	6.425_{10} +5;
6.554_{10} +5;	6.683_{10} +5;	6.750_{10} +5;	6.835_{10} +5;	6.952_{10} +5;
6.987_{10} +5;	7.056_{10} +5;	7.103_{10} +5;	7.199_{10} +5;	7.245_{10} +5;
7.331_{10} +5;	7.471_{10} +5;	7.583_{10} +5;	7.638_{10} +5;	7.791_{10} +5;
7.880_{10} +5;	7.887_{10} +5;	7.944_{10} +5;	7.996_{10} +5;	8.068_{10} +5;
8.085_{10} +5;	8.013_{10} +5;	8.020_{10} +5;	7.943_{10} +5;	7.849_{10} +5;
7.767_{10} +5;	7.572_{10} +5;	7.484_{10} +5;	7.512_{10} +5;	7.127_{10} +5;
7.060_{10} +5;	6.934_{10} +5;	6.795_{10} +5;	6.735_{10} +5;	6.695_{10} +5;
6.717_{10} +5;	6.737_{10} +5;	6.779_{10} +5;	6.902_{10} +5;	7.013_{10} +5;
7.114_{10} +5;	7.264_{10} +5;	7.461_{10} +5;	7.691_{10} +5;	7.883_{10} +5;
8.012_{10} +5;	8.232_{10} +5;	8.432_{10} +5;	8.588_{10} +5;	8.689_{10} +5;
8.813_{10} +5;	8.917_{10} +5;	9.094_{10} +5;	9.199_{10} +5;	9.244_{10} +5;
9.280_{10} +5;	9.216_{10} +5;	9.233_{10} +5;	9.275_{10} +5;	9.302_{10} +5;
9.304_{10} +5;	9.338_{10} +5;	9.276_{10} +5;	9.283_{10} +5;	9.306_{10} +5;

TABLE 14.2 (concluded)

9.325_{10} +5;	9.223_{10} +5;	9.162_{10} +5;	9.242_{10} +5;	9.447_{10} +5;
9.417_{10} +5;	9.164_{10} +5;	9.153_{10} +5;	9.078_{10} +5;	9.056_{10} +5;
9.064_{10} +5;	9.104_{10} +5;	9.077_{10} +5;	9.000_{10} +5;	9.061_{10} +5;
9.151_{10} +5;	9.175_{10} +5;	9.244_{10} +5;	9.275_{10} +5;	9.301_{10} +5;
9.414_{10} +5;	9.545_{10} +5;	9.617_{10} +5;	9.741_{10} +5;	9.882_{10} +5;
1.011_{10} +6;	1.026_{10} +6;	1.046_{10} +6;	1.059_{10} +6;	1.073_{10} +6;
1.094_{10} +6;	1.116_{10} +6;	1.125_{10} +6;	1.132_{10} +6;	1.138_{10} +6;
1.147_{10} +6;	1.150_{10} +6;	1.161_{10} +6;	1.167_{10} +6;	1.163_{10} +6;
1.169_{10} +6;	1.179_{10} +6;	1.192_{10} +6;	1.175_{10} +6;	1.183_{10} +6;
1.178_{10} +6;	1.175_{10} +6;	1.180_{10} +6;	1.181_{10} +6;	1.183_{10} +6;
1.189_{10} +6;	1.185_{10} +6;	1.183_{10} +6;	1.180_{10} +6;	1.185_{10} +6;
1.197_{10} +6;	1.198_{10} +6;	1.210_{10} +6;	1.215_{10} +6;	1.226_{10} +6;
1.249_{10} +6;	1.258_{10} +6;	1.265_{10} +6;	1.276_{10} +6;	1.284_{10} +6;
1.284_{10} +6;	1.303_{10} +6;	1.316_{10} +6;	1.343_{10} +6;	1.351_{10} +6;
1.347_{10} +6;	1.365_{10} +6;	1.375_{10} +6;	1.389_{10} +6;	1.404_{10} +6;
1.417_{10} +6;	1.432_{10} +6;	1.449_{10} +6;	1.471_{10} +6;	1.476_{10} +6;
1.490_{10} +6;	1.514_{10} +6;	1.524_{10} +6;	1.521_{10} +6;	1.531_{10} +6;
1.544_{10} +6;	1.549_{10} +6;	1.553_{10} +6;	1.559_{10} +6;	1.559_{10} +6;
1.562_{10} +6;	1.586_{10} +6;	1.573_{10} +6;	1.585_{10} +6;	1.588_{10} +6;
1.584_{10} +6;	1.591_{10} +6;	1.596_{10} +6;	1.610_{10} +6;	1.609_{10} +6;
1.618_{10} +6;	1.635_{10} +6;	1.650_{10} +6;	1.664_{10} +6;	1.667_{10} +6;
1.679_{10} +6;	1.700_{10} +6;	1.724_{10} +6;	1.726_{10} +6;	1.735_{10} +6;
1.750_{10} +6;	1.772_{10} +6;	1.784_{10} +6;	1.794_{10} +6;	1.809_{10} +6;
1.825_{10} +6;	1.847_{10} +6;	1.860_{10} +6;	1.877_{10} +6;	1.895_{10} +6;
1.896_{10} +6;	1.906_{10} +6;	1.919_{10} +6;	1.929_{10} +6;	1.946_{10} +6;
1.944_{10} +6;	1.949_{10} +6;	1.959_{10} +6;	1.972_{10} +6;	1.981_{10} +6;
1.993_{10} +6;	2.002_{10} +6;	2.013_{10} +6;	2.016_{10} +6;	2.029_{10} +6;
2.034_{10} +6;	2.040_{10} +6;	2.051_{10} +6;	2.057_{10} +6;	2.058_{10} +6;
2.064_{10} +6;	2.059_{10} +6;	2.067_{10} +6;	2.082_{10} +6;	2.094_{10} +6;
2.086_{10} +6;	2.090_{10} +6;	2.104_{10} +6;	2.106_{10} +6;	2.112_{10} +6;
2.109_{10} +6;	2.122_{10} +6;	2.146_{10} +6;	2.170_{10} +6;	2.171_{10} +6;
2.203_{10} +6;	2.184_{10} +6;	2.205_{10} +6;	2.210_{10} +6;	2.218_{10} +6;
2.231_{10} +6;	2.256_{10} +6;	2.253_{10} +6;	2.265_{10} +6;	2.280_{10} +6;
2.305_{10} +6;	2.307_{10} +6;	2.327_{10} +6;	2.341_{10} +6;	2.355_{10} +6;
2.371_{10} +6;	2.373_{10} +6;	2.403_{10} +6;	2.416_{10} +6;	2.420_{10} +6;
2.444_{10} +6;	2.445_{10} +6;	2.462_{10} +6;	2.476_{10} +6;	2.495_{10} +6;
2.515_{10} +6;	2.522_{10} +6;	2.532_{10} +6;	2.536_{10} +6;	2.563_{10} +6;
2.595_{10} +6;	2.606_{10} +6;	2.611_{10} +6;	2.630_{10} +6;	2.646_{10} +6;
2.650_{10} +6;	2.664_{10} +6;	2.682_{10} +6;	2.701_{10} +6;	2.721_{10} +6;
2.725_{10} +6;	2.739_{10} +6;			

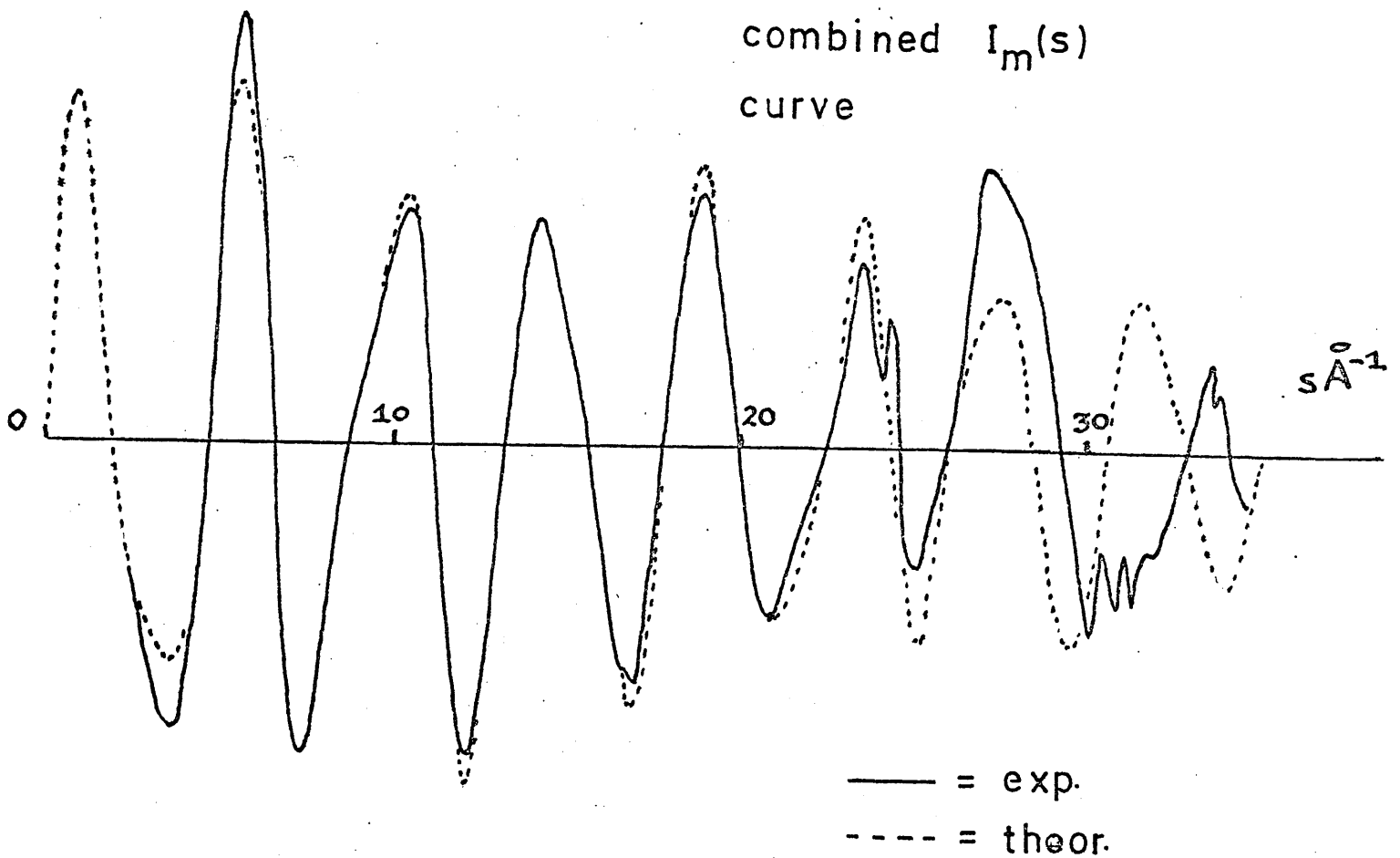

fig. 14.1

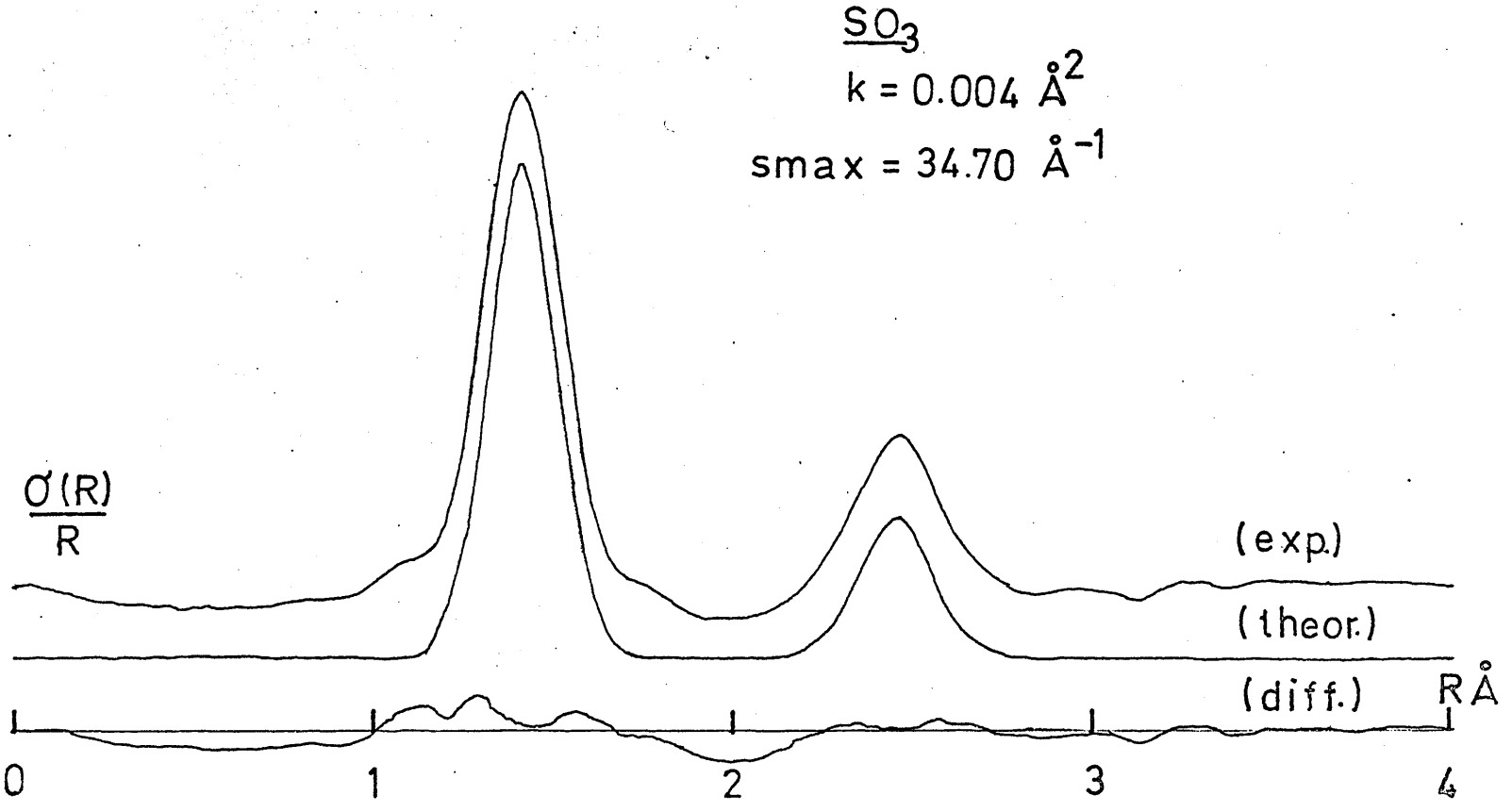

fig. 14.2

TABLE 14.3

Results of individual distance refinements for SO_3

jet to plate distance	50 cm	25 cm
r_{S-O} (Å)	1.4158	1.4153
σ'	0.0008	0.0017
$r_{O..O}$ (Å)	2.4589	2.4478
σ'	0.0028	0.0081
R(%)	11.86	45.37
$\sum w\Delta^2$	1.233×10^{11}	4.976×10^{13}

Notes: (1) u values were held constant at spectroscopic values.

(2) σ''s are least squares e.s.d.'s.

(3) r values are $r_g(1)$ distances.

TABLE 14.4

Results of ' all data combined ' refinements

for SO_3

(data limited to smax = 25 A^{o-1})

parameter	combtwo	comb-scaled
r_{S-O} (Å)	1.4170	1.4160
σ'	0.0005	0.0005
$r_{O..O}$ (Å)	2.4564	2.4551
σ'	0.0021	0.0021
u_{S-O} (Å)	0.0536	0.0516
σ'	0.0009	0.0010
$u_{O..O}$ (Å)	0.0712	0.0636
σ'	0.0023	0.0023
R(%)	9.97	10.19
$\sum w\Delta^2$	9.054×10^{10}	1.598×10^{11}

Notes: (1) The distances are $r_g(1)$ values.

(2) The σ''s are least squares e.s.d.'s.

(3) The amplitudes have not been corrected for failure of the Born approximation.

(4) The intensity data beyond s = 25 A^{o-1} was omitted in these refinements because of its extremely poor quality, and hence the R factors are lower than normal.

TABLE 14.5

The final structural parameters

for SO_3

parameter	final result	reproducibility
r_{S-O} (Å)		
$r_g(1)$	1.417	0.002
$r_g(0)$	1.418	0.002
r_e	1.413	0.002
$r_{O..O}$ (Å)		
$r_g(1)$	2.456	0.007
$r_g(0)$	2.457	0.007
$\widehat{OSO}$ (°)	120.1 * ($r_g(0)$)	0.6
u_{S-O} (Å)	0.048	0.003
$u_{O..O}$ (Å)	0.067	0.007

Notes: (1) These results were obtained by taking a straight average of the results presented in the two columns of the previous table. The O's were averaged and reproducibilities calculated from them according to the methods of Chapter Four.

(2) The u_{S-O} value has been corrected for failure of the Born approximation.

* This angle cannot in actual fact have a value $> 120^\circ$ for an XY_3 model.

CHAPTER FIFTEEN

SOME GENERAL CONCLUSIONS BASED ON THE RESULTS OF CHAPTERS NINE TO FOURTEEN

1. Introduction

In this chapter a discussion is given of the principal sources of error likely to have affected the accuracy of the results presented in Chapters Nine to Fourteen, and this discussion is followed by an attempt to make an empirical estimate of the overall magnitudes of these errors, by comparing certain of the R_{ij}, and all of the u_{ij} values obtained, with corresponding results determined by other physical methods. Finally, several modifications to the experimental and computational procedures of Chapters Three and Four are suggested, these being intended to reduce both the systematic and the random errors involved.

2. Systematic error sources

A single jet-to-plate distance $L_m(s)$ curve consists of two matching series of s-scale and intensity results, and if it is assumed that the methods of Chapter Three and of Chapter Four have been employed to determine this

function, then each of the two sets of numbers will be subject to both random and systematic errors. Of these two classes of error, only the random uncertainties can be reduced by the averaging procedures of Chapter Four, such as processing a large number of microdensitometer traces, and recording these latter from several photographic plates.

In the present work, the $I_m(s)$ intensities obtained were subject to errors of the first type as a result of random uncertainties in the microdensitometer readings, and randomly distributed irregularities on the photographic plates scanned. They were also liable to errors of the second type from correlation of microdensitometer measurements, and from possible systematic errors in the background, sector correction, and blackness correction functions assumed.

Similarly, the s-scale values obtained were subject to errors of the first type from random uncertainties in the microdensitometer scan motion, from random errors in the centres calculated for the microdensitometer traces, and from random errors involved in centering the diffraction pattern relative to the light beam of the microdensitometer each time a trace was recorded. The s-scale results were also subject to uncertainties of the second type from

systematic error in the microdensitometer scan interval, error in the assumed beam wavelength, and error in the assumed jet-to-plate distance.

In addition to uncertainty from the above sources, the R_{ij} and u_{ij} parameters obtained by fitting a single distance $I_m(s)$ curve by equation 2.46, were subject to systematic errors from the approximate nature of this theoretical intensity function, as it neglects (a) the $\cos \Delta\eta_{ij}$ factor, (b) sample size and beam width effects, and (c) the effects of anharmonicity of vibration, i.e. neglect of the $-x_{ij}s^2$ term of equation 2.42.

The above sources of systematic error will now be considered in turn.

(1) Errors arising from microdensitometer measurement

It may be assumed that intensities measured by means of the automatic instrument were subject to a minimum amount of correlation error, and also, since the scan interval of this instrument was checked and found to be free from systematic error, it may be assumed that the microdensitometer contribution to s-scale systematic uncertainty was negligible.

This did not seem to be also true of the manual microdensitometer measuring procedure. The results presented in Chapter Nine show, that in the case of the Cl_2O investigation, the manual instrument, and

the tracing and reading-off procedures associated with it, seemed to introduce fairly large systematic uncertainties into the $I_m(s)$ functions determined.

(2) Background errors

Since the backgrounds adopted in the investigations of Chapters Nine to Fourteen were all rigorously hand-smoothed, it is likely that the corresponding $I_m(s)$ curves obtained were subject to systematic errors, and indeed deviations between experimental and theoretical $I_m(s)$ functions are visible in several of the figures presented in Chapters Nine to Fourteen, and these may in most cases be ascribed to incorrectly drawn background curves. It may be assumed, however, that although the amplitudes of vibration were almost certainly affected by these errors, the R_{ij} distances were unlikely to have been subject to any real error from this source.

(3) Errors in the sector correction function

As for the background error, the amplitudes of vibration were probably the only parameters affected by systematic errors in this function.

(4) Errors in the blackness correction function

Again it may be assumed that only the amplitudes of vibration were affected.

(5) The wavelength error

The wavelength was probably subject to a random error of about one part in two thousand, and it may be assumed that any additional systematic error in this quantity was a good deal smaller. The wavelength error is particularly serious as its relative uncertainty is transmitted directly into the R_{ij} parameters measured.

(6) The jet-to-plate distance error

The jet-to-plate distance was subject to a random relative error which naturally increased as the camera distance decreased. Even for twentyfive centimetre data, this error may be considered to have been considerably less than one part in a thousand. The jet-to-plate error is particularly serious too, for like the wavelength it affects the R_{ij} distances fairly directly. Unlike the wavelength error, however, this source of uncertainty is averaged out somewhat by refining data collected at more than one camera distance. Systematic error arising from expansion or contraction of the measuring rods was assumed negligible.

(7) Failure of the first Born approximation

It was realised that for the compounds studied, the Cl-O, Cl-F and S-O amplitudes of vibration obtained by least squares refinement, were subject to systematic errors of between ten and twenty percent

(see ref. 14 for discussion) and after refinement this error was eliminated as described in Chapter Eight. The R_{ij} parameters corresponding to these amplitudes were not subject to error from this source.

(8) Sample size and beam width effects

In the absence of experimental information about the densities of the intersecting molecular and electron beams, no reliable estimate of these effects can be made. It is probable, however, that only the amplitudes of vibration were significantly affected.

(9) Neglect of the $-x_{ij}s^2$ term

As a result of this neglect, each $r_g(1)$ distance obtained, should, if x_{ij} is positive, be a little short, but calculation showed, that for most of the bonded distances present in the molecules studied in Chapters Nine to Fourteen, the error introduced in this way ought to have been a good deal smaller than one part in a thousand, particularly for the shortest Cl-O and S-O bond lengths measured.

The following general remarks may be added to the above comments:

(a) the R_{ij} results obtained in previous chapters were most likely to have been affected by error sources (5) and (6) above, and the amplitudes of vibration by sources (2), (3), (4) and (8), that is if systematic

errors are alone considered, and (b) in view of the facts (i) that data collected at several jet-to-plate distances were used in the final least squares refinements, and (ii) that many of the systematic errors discussed above must to some extent cancel out, it may be concluded that the parameters obtained by all-data-combined refinements will be subject to smaller systematic uncertainties than would be expected by simply adding all of the single jet-to-plate distance systematic errors together. It should be added, however, that any scale factor errors made when combining the single distance data sets, will affect the amplitudes of vibration.

It was decided at the outset of the work described in this thesis to assign a random error of three least squares refinement standard deviations to each of the R_{ij} parameters obtained, and to combine this with a total systematic error of one part in two thousand presumed to arise mainly from sources (5) and (6). In view of the considerable difficulty in assessing the systematic error appropriate to the amplitudes of vibration it was decided to quote a three standard deviations error alone.

In the above discussion a number of assumptions have been made about error sizes, and in the section

which follows, an attempt is made to justify or to contradict these assumptions, by the empirical approach of comparing certain of the R_{ij} and u_{ij} parameters listed in Chapters Nine to Fourteen with corresponding results obtained by other physical methods such as microwave spectroscopy and vibrational calculations.

3. The success of the procedures followed in Chapters Nine to Fourteen

If the success of the averaging processes described in Chapter Four is judged in terms of the R factors (residuals) attained in carrying out single distance least squares refinements, then the summary of such refinements, given in table 15.1, enables the following general remarks to be made.

(1) It becomes increasingly difficult to average out random errors as the jet-to-plate distance decreases, particularly when the automatic microdensitometer is used (Note: all of the results of table 15.1 were obtained from automatically collected data.).

(2) Underexposed photographic plates lead, as might be expected, to high residuals, and should be omitted from studies wherever possible.

(3) The success of using as many plates as possible for any one jet-to-plate distance is indicated.

(4) It is clearly more important to average several

traces recorded from several plates than to average a similar number of traces recorded from a single plate.

It should, however, be commented that the very high Cl_2O twentyfive centimetre residual is not entirely consistent with the above conclusions, as four traces were averaged from four good quality plates, and a somewhat lower R factor should have been achieved. It seems likely that the small number of traces taken, together with a poor choice of optical wedge were the causes of this bad result, and if this explanation is correct, an additional conclusion may be written as, (5) Care should be observed when choosing an optical wedge before trace recording.

Turning now to wavelength errors, table 15.2 collects together a series of wavelength measurements made for the purposes of the six investigations described in this thesis. As these investigations occupied about one year, it is evident from this table, that the wavelength drift is small, and occurs fairly slowly. It seems likely from the figures quoted, that the random error attributable to any one measurement is in the order of one part in two thousand, and although systematic error in this quantity, arising from an incorrect TlCl lattice parameter cannot be completely excluded, published results for this compound [58] seem

to suggest that its lattice spacing is very accurately determined.

The general consistency of the results listed in the columns of the single distance refinement tables of Chapters Nine to Fourteen, suggests that random errors in the jet-to-plate distances were satisfactorily small.

When attempting to assess the relative errors appropriate to the best determined bond lengths of Chapters Nine to Fourteen, it is unfortunate that only in the case of the SO_2 investigation is it possible to compare an electron diffraction bond length (the r_e S-O distance: see Chapter Thirteen) with an accurate, and exactly equivalent microwave result. Similar comparisons made in other chapters (for Cl_2O and ClO_2) are limited in significance on account of the non-equivalence of the distances involved, e.g. an $r_g(1)$ parameter has been compared with an r_o result etc., and in view of the uncertainty involved, the only meaningful general conclusion which can be reached from the previous six chapters is that the error appropriate to a well determined bond length measured by the technique of Chapters Three and Four, does not seem to be greater than one part in four thousand. In the case where a definite comparison is possible (i.e. for SO_2) the

difference between the r_e S-O distances measured by the present work and by microwave spectroscopy, is in fact about three parts in a thousand, and since the expected error for this bond length must be about two parts in a thousand (see Chapter Thirteen) the larger difference actually found could perhaps be taken as an indication that the systematic error estimate of the previous section is a good deal too small. It is impossible, however, to be sure of this in the absence of other similar tests, particularly in view of the special circumstances of the SO_2 investigation discussed in Chapter Thirteen.

If the SO_3 results are ignored (see Chapter Fourteen) then the agreement between the electron diffraction and spectroscopic amplitudes of vibration shown in table 15.3 (composed of data taken from Chapters Six to Fourteen) is very good by normal electron diffraction standards. It appears, however, that even a well-determined amplitude is subject to an error of at least three percent, and such accuracy is not really good enough to enable molecular force fields to be accurately determined. The results obtained do, however, confirm earlier assumptions that the background, sector correction, blackness correction and sample size errors are not unusually large.

4. Suggestions for further improvement

As a result of the previous discussions, the following suggestions may be put forward for reducing the random and systematic errors likely to affect parameters determined by the methods of Chapters Three and Four.

(1) Measurement of the wavelength by means of at least two different solid sample substances in order to investigate and reduce systematic error in λ.

(2) Collection of twentyfive and eleven centimetre plates in batches of two, each batch being obtained by a separate experiment involving a separate calibration of the jet-to-plate distance.

(3) Adoption of a more stringent averaging procedure for twentyfive and eleven centimetre data, in which at least two traces are taken from each of a minimum of six plates.

(4) Improvement of equation 2.46 by including the Born failure cosine term, and the anharmonicity constant x_{ij}.

(5) In cases where extreme accuracy is required, an investigation could be carried out in duplicate after photographic plates were obtained. Thus two separate uphill and background curves would be obtained for each camera distance, and final all-data-combined least squares results could be averaged.

(6) Regular checking of the sector and blackness correction functions is obviously desirable.

TABLE 15.1

	Cl_2O	$HClO_4$	$FClO_3$	ClO_2	SO_2	SO_3
distance cm	100	100	100	100	-	-
number of plates	4	4	4	6	-	-
quality	good	good	good to dark	good	-	-
number of traces	4	4	4	6	-	-
R(%)	4.63	7.77	3.12	4.44	-	-
distance cm	50	50	50	50	50	50
number of plates	4	4	4	6	4	4
quality	good	good	good	good	good	good
number of traces	4	4	4	6	8	8
R(%)	12.91	7.55	5.69	8.63	12.63	11.86

continued on next page.

TABLE 15.1

(continued)

	Cl_2O	$HClO_4$	$FClO_3$	ClO_2	SO_2	SO_3
distance cm	25	25	25	25	25	25
number of plates	4	1	6	2	5	5
quality	good	very light	good	good to light	light	very light
number of traces	4	8	6	10	10	10
R(%)	41.72	34.7	16.59	37.58	19.37	45.37

TABLE 15.2

investigation	wavelength	e.s.d.
Cl_2O	0.051162 Å	0.000015
$HClO_4$	0.051190 Å	0.000022
$FClO_3$	0.051205 Å	0.000020
ClO_2	0.051172 Å	0.000020
SO_2, SO_3	0.051183 Å	0.000015

TABLE 15.3

molecule and distance	e.d. u value (Å)	error limit	spec. u value (Å)	error limit
Cl_2O				
Cl-O	0.052	0.004	0.051	0.001
Cl..Cl	0.063	0.006	0.068	0.002
$HClO_4$				
Cl-OH	0.062	0.013	0.046	0.004
Cl-Op	0.036	0.004	0.036	0.002
Op..Op	0.077	0.048	0.054	0.003
Op..OH	0.065	0.022	0.064	0.004
$FClO_3$				
Cl-F	0.042	0.005	0.043	0.003
Cl-Op	0.035	0.002	0.036	0.002
Op..Op	0.051	0.008	0.053	0.003
Op..F	0.066	0.008	0.061	0.004
ClO_2				
Cl-O	0.035	0.003	0.039	0.001
O..O	0.061	0.021	0.063	0.002
SO_2				
S-O	0.035	0.003	0.035	0.001
O..O	0.047	0.012	0.055	0.002
SO_3				
S-O	0.048	0.003	0.035	0.001
O..O	0.067	0.007	0.054	0.002

CHAPTER SIXTEEN

FORCE CONSTANT - BOND LENGTH AND FORCE CONSTANT - BOND ORDER RELATIONSHIPS FOR THE CHLORINE - OXYGEN BOND

1. Introduction

In this chapter a revision is made of certain force constant - bond length, force constant - bond order and bond length - bond order relationships originally stated for the Cl-O bonded distance by Robinson[75] in 1963. Such a revision seems worthwhile not only in view of the results presented in previous chapters of this thesis, but also in the light of certain recently published papers on Cl-O containing compounds, particularly reference 82 on the infrared spectrum of dichlorine monoxide.

2. The force constant - bond length relation

The problem of relating force constant to bond length is a fairly old one. In 1934 Badger[113] proposed the relationship $k = A/(R_e-B)^3$ for diatomic molecules, where k is the stretching force constant, and R_e is the equilibrium internuclear distance. In the same year Clark[114] suggested an alternative relation for diatomics this being $k = C/R_e^6$. In these two expressions A, B

and C are constants which depend on the nature of the atom pair forming the molecule. Clark's equation has in fact been applied with some success to linkages occurring in polyatomic molecules as well, and in connection with this latter application Linnett has proposed[115] the modified version of this function, $k = C/R_e^n$ where n is a constant which also depends on the nature of the atom pair forming the bond concerned.

In the present work, an attempt was made to apply the last of the above equations to the case of the Cl-O bonded distance, by plotting $\log_{10}k_{Cl-O}$ against $\log_{10}R_{Cl-O}$ for four key molecules. Clearly, if Linnett's function is applicable, a straight line graph should be obtained, of gradient (-n) and intercept $\log_{10}C$. Considerable care was taken in deciding which molecules to select for the purposes of making this plot, but the final choice was based on the following requirements, (a) the molecules considered were required to have Cl-O bond lengths accurate to at least 0.01 Å, and corresponding stretching force constants accurate to better than ten percent, and (b) the Cl-O bond lengths selected were required to be distributed at approximately equal intervals across the distance range of 1.4 to 1.7 Å considered. In view of condition (a) it is hardly surprising that only small molecules were included in

the final set of four chosen. This key set of Cl-O containing systems is listed in table 16.1, together with corresponding assumed bond lengths and force constants.

For $FClO_3$, the Cl-Op bond length is an $r_g(1)$ value selected from the results presented in Chapter Eleven, and the force constant assigned to it was taken from Chapter Six. The bond length assumed for ClO_2 is the r_e result given in Chapter Twelve, and the Cl-O stretching force constant adopted was taken from reference 83. In the case of the ClO radical the internuclear distance quoted is an r_o value obtained from an electron spin resonance study by Carrington et al.,[123] and differs considerably from the earlier, and apparently erroneous result of 1.546 Å given by Durie and Ramsay[117], as a result of an ultraviolet study. The ClO stretching force constant assumed in table 16.1 was calculated from a measurement of the fundamental frequency of vibration of the radical published by Porter.[116] For dichlorine monoxide, the bond length adopted was calculated by averaging the r_e result obtained in Chapter Nine with the microwave r_s value of reference 93. The Cl-O stretching force constant was taken from reference 82. It should be noted that all of the error limits quoted in table 16.1 were assigned

by the present writer, and some of them are subjective, not being based on systematic calculation.

A plot of k_{Cl-O} against R_{Cl-O} is shown in figure 16.1, and in this diagram the four points obtained lie close to a smooth curve. A corresponding graph of $\log_{10}k_{Cl-O}$ against $\log_{10}R_{Cl-O}$ is presented in figure 16.2, and the points indicated in this figure conform reasonably well to the straight line relationship predicted by Clark and Linnett. The amount of linearity achieved is in fact surprisingly good when it is recalled that for polyatomic molecules stretching force constants have to take into account the force required to alter non-bonded distances, as well as to stretch the valence bonds principally concerned. The success attained in figure 16.2 probably indicates that the contributions from non-bonded interactions are small, for the molecules considered in the present work.

A straight line was fitted to the four points plotted in figure 16.2, by means of the least squares approach, and the equation obtained was,

$$\log_{10}k_{Cl-O} = (-6.23)\log_{10}R_{Cl-O} + 1.89 \quad .. \quad 16.1.$$

The corresponding linear function given by Robinson[75] is also presented graphically in figure 16.2 (broken line, and may be seen to deviate considerably from equation 16.1 above.

Equation 16.1 was used to calculate bond lengths for the ions ClO^-, ClO_2^-, ClO_3^- and ClO_4^- using force constants calculated by averaging each of the sets of force constant results collected for these species by Robinson,[75] and set out in Table 1 of his paper. No observed internuclear distance seems to be available for the ClO^- ion, but the bond lengths calculated for the other systems (see table 16.2) are in good agreement with observed results taken from reference 95. A bond length calculated for HOCl using an average force constant estimated from results presented in references 80 and 81A, is also given in table 16.2, but does not agree at all well with an observed value obtained by Ashby,[124] as a result of a high resolution infrared study of the absorption band corresponding to the O-H stretching frequency. This lack of agreement strongly suggests that the Cl-O stretching force constant obtained by Hedberg and Badger[80], and also by Schwager and Arkell[81A], of very nearly 3.9 md/Å, is too high, and is presumably based on a wrongly assigned Cl-O stretching frequency. The value of approximately 720 wave numbers measured by both sets of authors can be shown to be too high for a bond length of 1.689 Å, as this distance should presumably have a force constant of around 2.9 md/Å, and a stretching frequency

of about 650 wave numbers.

The rather long Cl-O distances evidently appropriate to ClO^- and to HOCl are definitely to be expected in view of the lone pairs of electrons on chlorine which, as is stated in reference 95, should have the effect of inhibiting $d\pi$-$p\pi$ bonding between this atom and oxygen. The fact that the bond length of ClO^- is shorter than the Cl-O distance found in HOCl or for that matter in methyl hypochlorite (CH_3OCl)* may be rationalised in terms of a change in hybridisation of the oxygen atom in going from an sp^3 state in HOCl to an sp state in ClO^-, and in terms of the increased availability of p electrons on the O atom of the ion, for back-bonding to chlorine.

In the above calculations, the errors quoted for the force constants of the species HOCl, ClO^-, ClO_2^-, ClO_3^- and ClO_4^- were estimated from the spread of data (see table 1 of ref. 75) used to make the averages mentioned above.

If a force constant of 3.9 md/Å is accepted for the O_3Cl-OH bond in perchloric acid (see Chapter Seven) then a bond length of 1.62 Å is predicted for this molecule by equation 16.1. This result is in reasonable agreement with the observed value of

* See ref. 120 for $R_{Cl-O} = 1.67(0.02)$ Å.

1.635(0.011) Å obtained in Chapter Ten, if the error of 0.5 md/Å appropriate to this force constant is considered.

3. The force constant - bond order relation

As is well known, C-C bonds in a large number of compounds (e.g. benzene, naphthalene etc.) may be assigned non-integer bond orders larger than one, the bonding involved in such cases being interpreted in a wave mechanical sense in terms of a sigma and π component. Of these two , the π bonding is normally described in terms of sideways overlap of p atomic orbitals on adjacent carbon atoms. In a similar way generalised bond orders can be assigned to Cl-O bonds, but owing to the fact that the d orbitals on chlorine can in certain cases become involved in forming the π component of any particular bond, as well as p orbitals, the π bonding in Cl-O containing molecules tends to be fairly complex. Thus for ClO_4^-, Cruickshank has assigned[95] a π bond order of 0.5 to each of the Cl-O bonds present in this ion, and has interpreted the bonding involved in terms of overlap of two p orbitals on each digonally hybridised oxygen atom, with the d_{z^2} and $d_{x^2-y^2}$ orbitals on chlorine. In ClO_2, however,

Wagner has concluded that both the d and p orbitals on chlorine are involved in π bonding.

In the present work a force constant - bond order relationship was set up by making four assumptions. The first of these was that the relationship between force constant and bond order is linear, an assumption which has been discussed, and to some extent justified in reference 118, whilst the remaining three were the assumptions of bond orders of 1.67 and 1 for the Cl-Op and Cl-OCl bonds in Cl_2O_7 (see ref. 81) and 1.5 for the Cl-O distance in ClO_4^-. The force constants assigned to these bonds in setting up the linear relationship between ' n ' the bond order and k the Cl-O stretching force constant, are shown in table 16.3, and those quoted for Cl_2O_7 were obtained by carrying out a simplified normal coordinate analysis on an approximate C_{2v} model of the heptoxide based on the structural results of reference 81. The spectroscopic information assumed was obtained from reference 119. A plot of n, the bond order against k is given in figure 16.3, and the three points obtained conform well to a straight line, though when errors in k are considered, this agreement is seen to be possibly fortuitous. The equation obtained is,

$$n = (0.11)k + 0.69 \quad \text{.....16.2,}$$

and by eliminating k between equations 16.1 and 16.2 above, the relationship

$$n = (8.54)R_{Cl-O}^{-6.23} + 0.69 \quad \ldots\ldots 16.3,$$

a graphic representation of which is shown in figure 16.4, can be derived.

Equation 16.2 can be used to calculate bond orders from force constant data pertaining to Cl-O containing compounds, and some results of this kind are listed in table 16.4. The trend of increasing bond order evident in this table for the ions ClO^-, ClO_2^- and ClO_3^-, is that predicted by Wagner,[104] as a result of molecular orbital calculations. Wagner concluded in fact that the Cl-O bonds in the above species involve $d\pi$-$p\pi$ multiple bonding only, and indeed such bonding would be expected to increase as the central chlorine atom becomes more and more positively charged by the addition of oxygen atoms to it. It should be commented, however, that Wagner's bond orders differ numerically from those of table 16.4, which are essentially valence bond results (see reference 95).

It is also of interest that for ClO and ClO_2, the n values determined by the present work, fit into the general scheme of table 16.4, in a manner entirely consistent with Wagner's set of calculated results, and that for $HClO_4$ and $FClO_3$, the bond orders listed in

table 16.4 are consistent with the arguements of Chapters Ten and Eleven. For the Cl-O bond in HOCl, however, it is quite clear that the bond order given in table 16.4 is higher than would be expected for a Cl-O distance of 1.689 Å, but this ' anomaly ' can be explained in terms of an erroneous stretching force constant as has already been proposed in the previous section. Some calculated bond orders are plotted against observed bond length in figure 16.4, and all lie close to the theoretical function, equation 16.3.

4. Conclusion

Linear $\log_{10}k_{Cl-O}$ versus $\log_{10}R_{Cl-O}$, and 'n' versus k_{Cl-O} relationships have been established for Cl-O bonds in general, and can be used to predict Cl-O distances and bond orders from force constant data. Thus Arkell and Schwager[121] have suggested a force constant of 1.29 md/Å for the Cl-O bond in Cl-O-O and relations 16.1 and 16.2 above predict a bond length of 1.93 Å, and a bond order of 0.83 for this species. A similar treatment of such molecules as CH_3OClO_3 and $FOClO_3$ would be interesting from the point of view of the $d\pi$-$p\pi$ bonding theory, but unfortunately no detailed spectroscopic data seem to be available for these systems at present.

TABLE 16.1

Key data used to construct

figs. 16.1 and 16.2

molecule	k_{Cl-O} md/A	estimated error	bond length (Å)	error with respect to r_e
$FClO_3$	9.3	0.5	1.403	0.005
ClO_2	7.0	0.3	1.471	0.003
ClO	4.9	0.2	1.571	0.008
Cl_2O	2.8	0.1	1.694	0.005

For the origins of the data presented in this table, see text.

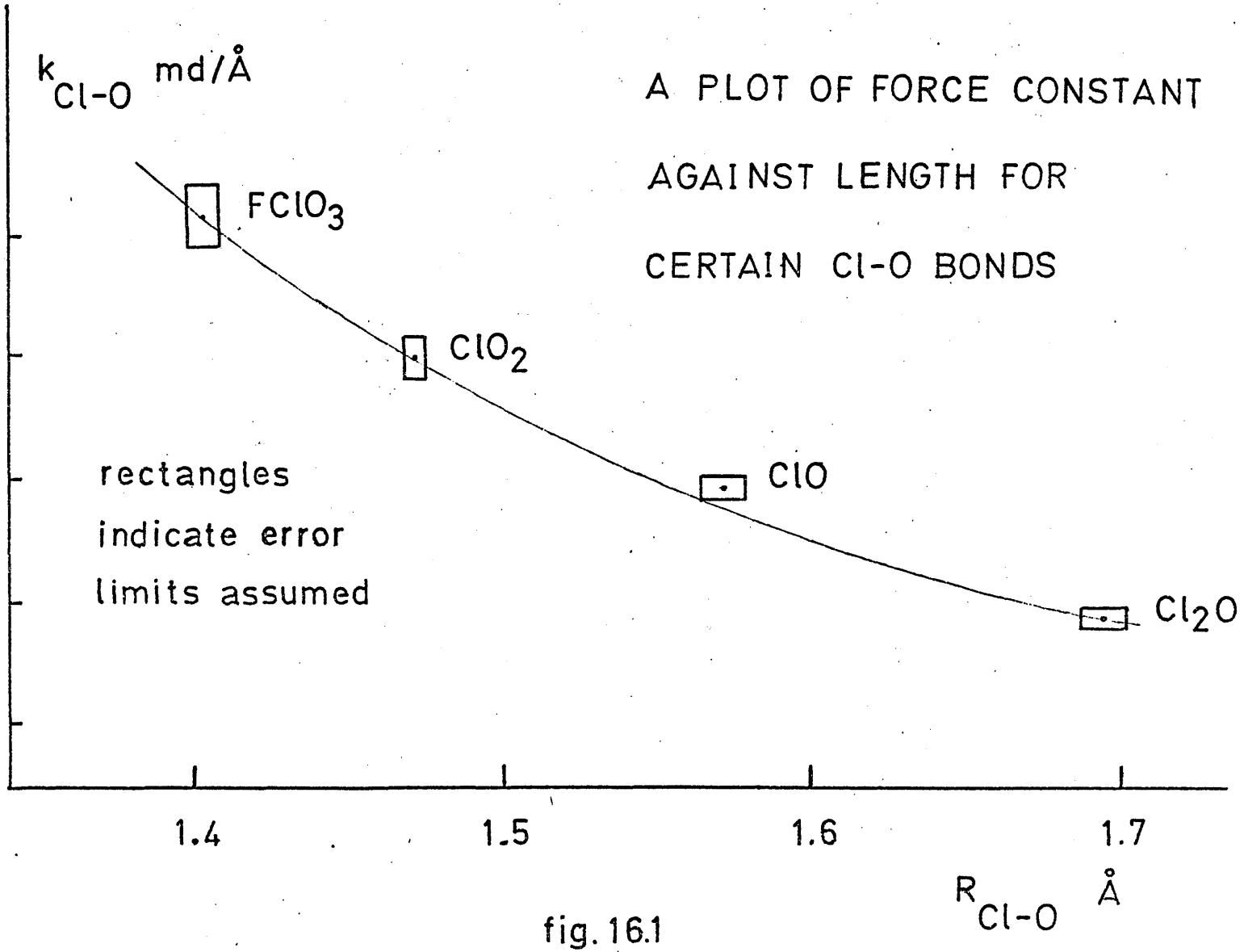
k_{Cl-O} md/Å
A PLOT OF FORCE CONSTANT AGAINST LENGTH FOR CERTAIN Cl-O BONDS
$FClO_3$
ClO_2
ClO
Cl_2O
rectangles indicate error limits assumed
9
7
5
3
1
1.4
1.5
1.6
1.7
R_{Cl-O} Å

fig. 16.1

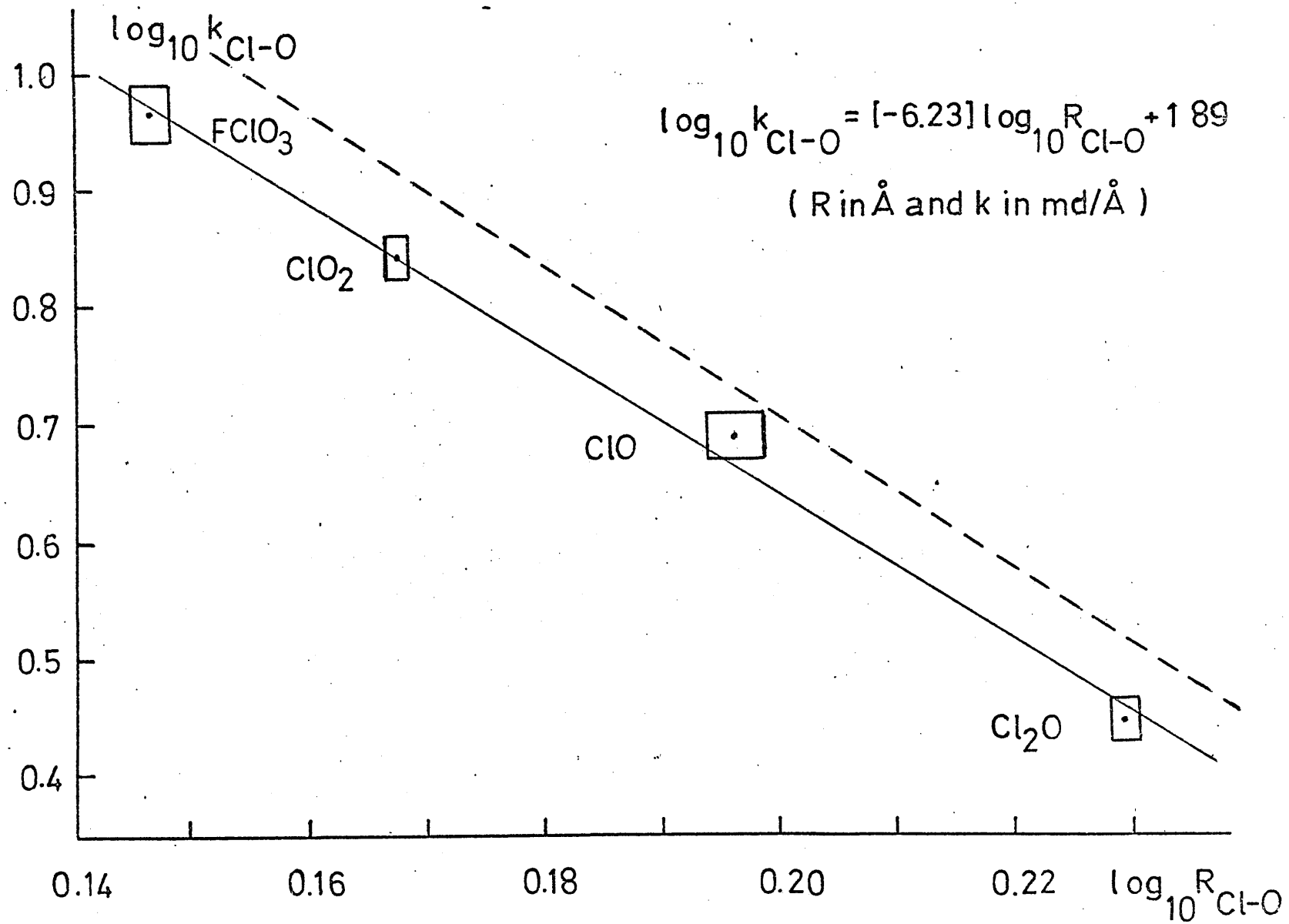
log10 kCl-O
1.0
0.9
0.8
0.7
0.6
0.5
0.4
FClO3
ClO2
ClO
Cl2O
log10 kCl-O = [-6.23] log10 RCl-O + 1 89
(R in Å and k in md/Å)
0.14
0.16
0.18
0.20
0.22
log10 RCl-O

fig. 16.2

TABLE 16.2

Some Cl-O bond lengths

calculated using

the empirical force constant - bond length

relationship

molecule or ion	ClO^-	HOCl	ClO_2^-	ClO_3^-	ClO_4^-
k_{Cl-O} assumed md/Å	3.3	3.9	4.6	6.8	7.4
estimated error in k	0.1	0.2	0.6	0.2	0.8
calculated Cl-O bond length	1.66	1.62	1.57	1.48	1.46
calculated error in R_{Cl-O}	0.01	0.02	0.03	0.01	0.03
observed value for R_{Cl-O}	-	1.689	1.57	1.46	1.46
error in observed R_{Cl-O}	-	0.006	0.03*	0.01*	0.01*

For the origins of the data presented in this table, see text.

* These are X-ray e.s.d.'s.

TABLE 16.3

Key data used to construct

fig. 16.3

molecule or ion	k_{Cl-O} assumed (md/Å)	estimated error	assumed bond order 'n'
Cl_2O_7			
Cl-Op	8.8	0.5	1.67
Cl-OCl	2.7	0.2	1.0
ClO_4^-	7.4	0.8	1.5

For the origins of the data presented in this table, see text.

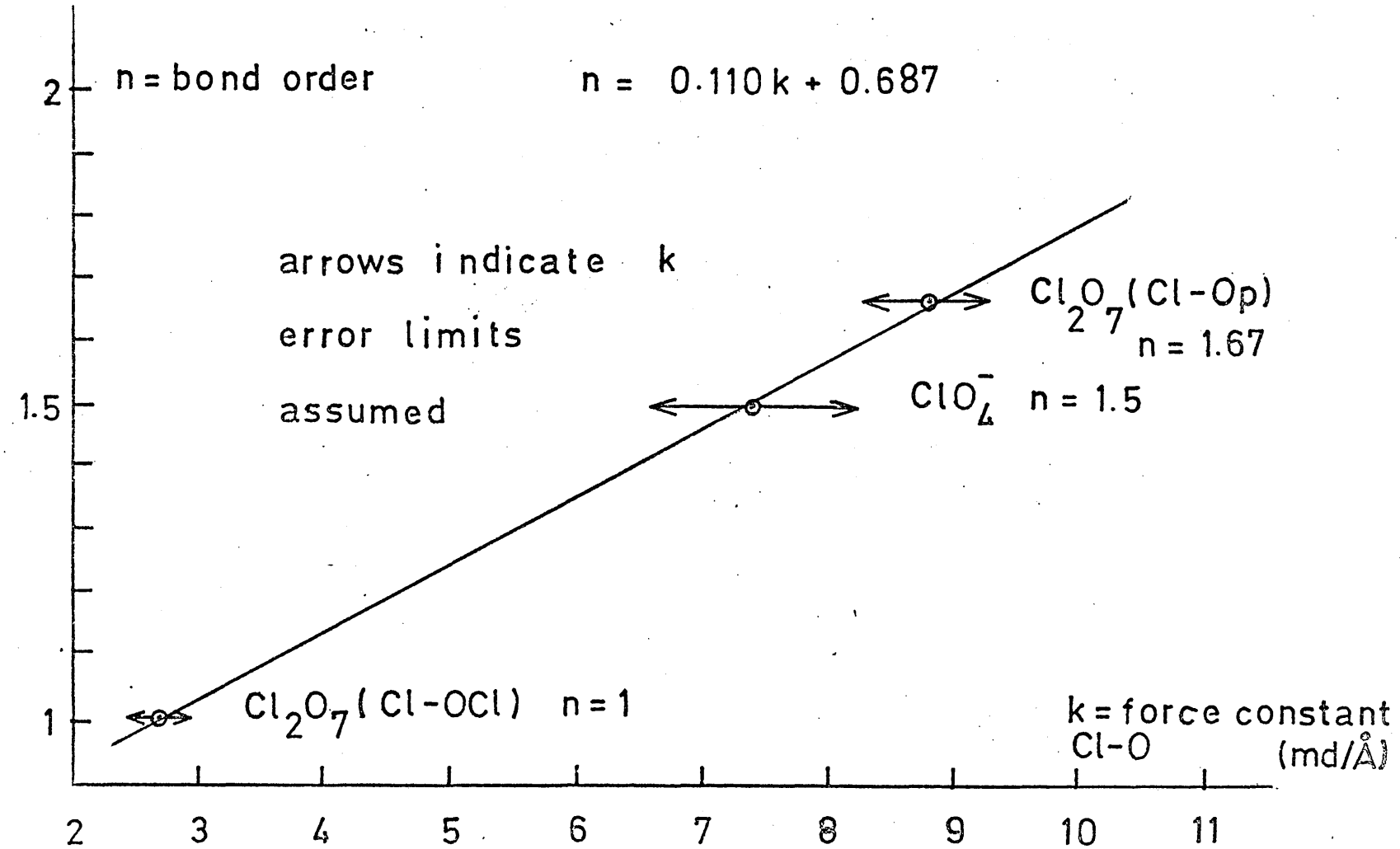
n = bond order
n = 0.110 k + 0.687
arrows indicate k
error limits
assumed
Cl_2O_7 (Cl-Op)
n = 1.67
ClO_4^- n = 1.5
Cl_2O_7 (Cl-OCl) n = 1
k = force constant
Cl-O
(md/Å)
2
1.5
1
2
3
4
5
6
7
8
9
10
11

fig 16.3

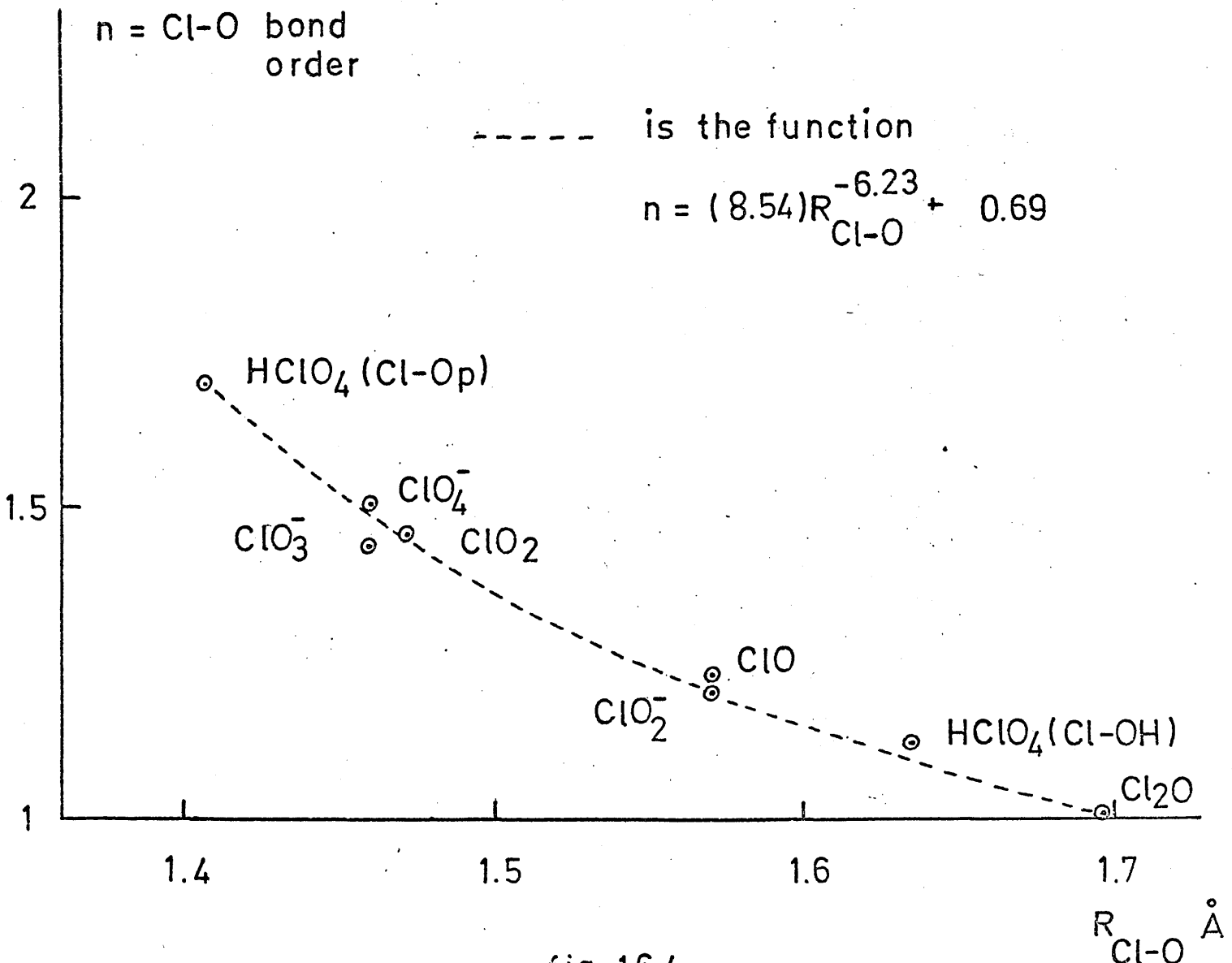
n = Cl-O bond order
is the function
$n = (8.54)R_{Cl-O}^{-6.23} + 0.69$
2
1.5
1
$HClO_4$ (Cl-Op)
ClO_4^-
ClO_3^-
ClO_2
ClO
ClO_2^-
$HClO_4$ (Cl-OH)
Cl_2O
1.4
1.5
1.6
1.7
R_{Cl-O} Å

fig 16.4

TABLE 16.4

Some Cl-O bond orders

calculated using

the force constant - bond order

relationship

molecule	k_{Cl-O} assumed (md/Å)	calculated bond order (n)	observed bond length (Å)
$HClO_4$			
Cl-OH	3.9(0.5)	1.12(0.06)	1.635(0.011)
Cl-Op	9.2(0.5)	1.70(0.06)	1.407(0.005)
$FClO_3$	9.3(0.5)	1.71(0.06)	1.403(0.005)
ClO_2	7.0(0.3)	1.46(0.02)	1.471(0.003)
ClO_3^-	6.8(0.2)	1.44(0.03)	1.46 (0.01)
ClO	4.9(0.2)	1.23(0.02)	1.571(0.008)
ClO_2^-	4.6(0.6)	1.20(0.07)	1.57 (0.03)
HOCl	3.9(0.2)	1.12(0.02)	1.689(0.006)
ClO^-	3.3(0.1)	1.05(0.01)	-

For origins of the data presented in this table, see text.

Error limits are written in parenthesis.

APPENDIX ONE

THE g MATRIX COMPUTER PROGRAMME

1. Introduction

If the vibrational motion of a molecular system is treated classically, in the manner outlined in Chapter Five, and if the coordinates used to describe this motion, are a set of internal displacement values s_i, then the molecular kinetic energy of vibration T, is given by $2T = \dot{\underline{s}}'(\underline{g}^{-1})\dot{\underline{s}}$, and the secular determinant which emerges on application of Lagrange's equations, is $|\underline{gf} - \underline{E}\lambda| = 0$. These results have already been quoted in Chapter Five, and it is the purpose of this appendix to discuss a method of computing the inverse kinetic energy matrix g from details of the molecular geometry and the atomic masses.

2. Theory

The origin of the matrix $\underline{g}^{-1}$ and hence of g, has been discussed in the fourth chapter of reference (62), where g^{-1} is obtained by considering a linear transformation from Cartesian displacement coordinates, to a set of s_i values. For the purposes of the present appendix, it will suffice to say that the elements $g_{tt'}$ of g are given by,

$$g_{tt'} = \sum_{\alpha} \left(\frac{1}{m_\alpha}\right)^{**} \underline{s}_{t\alpha} \cdot \underline{s}_{t'\alpha} \quad \text{..... A1.1,}$$

where the summation extends over all atoms in the molecule, and the vectors $\underline{s}_{t\alpha}$ and $\underline{s}_{t'\alpha}$ depend on which atom α is concerned, and on the nature of the internal coordinates s_t and $s_{t'}$ to which the element $g_{tt'}$ corresponds. These vectors are discussed and formulated for certain types of internal displacement coordinate, in a paper [122] by Decius, in which they are written in terms of unit vectors directed along interatomic distances, the scalar coefficients being functions of bond lengths and valence angles.

The formulae given in this paper are restricted to three coordinate types, these being respectively, a change in a bonded distance, r_{ij}, a change in a valence angle, a_{ijk}, and a change in a torsional angle, t_{ijkl}. For a description of these, and of the internal coordinates, R_{ij}, A_{ijk}, and T_{ijkl} which correspond to them, reference should be made to Chapter Four of textbook (62). The subscript coding system used is self-evident, as the integer numbers i,j etc., simply refer to the atoms, in terms of which the coordinates are defined. Sometimes, if there is no ambiguity produced, an abbreviated form a_{ik} is used for a_{ijk},

** m_α = mass of atom α.

and similarly t_{il} for t_{ijkl}. Examples of this alternative symbolism are given in Table 6.3, and in several other tables of Chapters Six and Seven. The internal coordinates R_{ij}, $A_{i(j)k}$, and $T_{i(jk)l}$ which are the actual equilibrium distances and angles themselves, should be distinguished from the changes r_{ij} etc., which correspond to them. The special sign convention applicable to the T_{ijkl}'s which is defined in Chapter Four of reference (62), on page 60, should also be carefully noted.

The computer programme described below calculates each $g_{tt'}$ element according to equation A1.1 above, and as a good many of the $\underline{s}_{t\alpha}$ vectors are always zero, it is only necessary to sum scalar products over those atoms common to both coordinates s_t and $s_{t'}$. Thus, if s_t and $s_{t'}$ are the coordinates r_{ij} and a_{ijk}, summation over atoms i and j is all that is required.

The standard formulae for the $\underline{s}_{t\alpha}$ vectors, adopted as part of the present computer programme, were taken from paper (122), and not from Chapter Four of reference (62), as one of the torsional formulae given there is in error.

The g matrix programme not only computes the $g_{tt'}$ elements, but transforms this array to the block-diagonal form $\underline{G}$, using the matrix $\underline{U}'$ appearing in the

transformation to symmetry coordinates, $\underline{S} = \underline{U}'\underline{s}$. The transformation to $\underline{G}$ is stated mathematically in equation 5.9 of Chapter Five.

3. The g matrix computer programme

The text of the g matrix programme follows at the end of this section. The programme is written in Algol, for use on an English Electric K.D.F.9 computer, and in the present work, was compiled by a Whetstone compiler.

Calculations for Cl_2O_7, involving twentyone internal displacement coordinates including two torsional ones, required about twelve minutes for completion. The nature of the data input to the programme for use in these calculations, is best described by taking perchloryl fluoride (see Chapter Six) as an example.

The atomic numbering system chosen for this molecule is shown in figure 6.1, and the choice of internal, and internal displacement, coordinates in Table 6.3. The data input sequence based on these coordinates, must take the following form (see programme text for the symbolism used).

; Title = The g and G matrices for perchloryl fluoride ;
n = the number of atoms in the molecule = 5 ;

m = the number of internal coordinates = 10 ;

$\underline{C}$(nx3) = the matrix of Cartesian coordinates for the atoms 1-5 of perchloryl fluoride, the molecule being referred to some suitable choice of axes, this choice being arbitrary = x1;y1;z1; x2;y2;z2; x3;y3;z3; x4;y4;z4; x5;y5;z5;

$\underline{M}$(nx1) = the matrix of atomic masses = 35;19;16;16;16;

$\underline{I}$(mx4) = the code description matrix, a code being necessary to define the ten internal displacement coordinates. Each row of the matrix corresponds to one of the coordinates, and four integer numbers are required. Thus, for an r_{ij} type, the row reads i;j;0;0; for an a_{ijk} type i;j;k;0; and for a t_{ijkl} type i;j;k;l; For perchloryl fluoride, and the set of s_i values, s_{12}, r_{13} etc., the matrix is:
1;2;0;0; 1;3;0;0; 1;4;0;0; 1;5;0;0; 3;1;4;0; 3;1;5;0; 4;1;5;0; 2;1;3;0; 2;1;4;0; 2;1;5;0; where each set of four numbers is a row of $\underline{I}$, and the order of rows is that of the coordinates.

The next step is to feed in values for the internal coordinates S_{12}, R_{13} etc., and hence the data input sequence continues,

p = a return to label, or continue, directive (equal to zero for return, and 1 for continue) = 0 ;

i;j; the indices which label the first coordinate S_{12},

hence i = 1; and j = 2; (Note: if angles a_{ijk} and t_{ijkl} are involved, the corresponding pairs of indices required are ik and il, as two numbers are required to define the elements of the matrices PR(nxn),PA(nxn) and PT(nxn) which store the distance and angle parameters, and which are now in process of being filled.)

PR(1,2) = magnitude of S_{12} in $\overset{o}{A}$ = 1.61 ;

Now, as p is zero the computer returns to L1 and continues reading in distances,

p = 0; i = 1; j = 3; PR(1,3) = 1.402;

p = 0; i = 1; j = 4; PR(1,4) = 1.402;

p = 1; i = 1; j = 5; PR(1,5) = 1.402;

Now, since p = 1, the computer moves to L2 and reads in angle parameters,

p = 0; i = 3; j = 4; PA(3,4) = 115.1;

p = 0; i = 3; j = 5; PA(3,5) = 115.1;

p = 0; i = 4; j = 5; PA(4,5) = 115.1;

p = 0; i = 2; j = 3; PA(2,3) = 103.0;

p = 0; i = 2; j = 4; PA(2,4) = 103.0;

p = 1; i = 2; j = 5; PA(2,5) = 103.0;

Since p = 1, the computer moves to L3, and reads in torsion parameters. There are none for $FClO_3$, but at least one dummy parameter must be included before passing on to the next item of input. This parameter

could be written,

p = 1; i = 1; j = 4; PT(1,4) = -100.0; This set of values (with the exception of p) is quite arbitrary.

In order to factor the g matrix, the elements of the U' transformation matrix are required, and these are indicated in Table 6.5 of Chapter Six. Since most of these are zero, the computer first zeros all the U'(1,s) quantities, and then reads in the non-zero elements according to the scheme,

k = return or continue directive (compare with p) = 0; 1;s; the indices of the first element. Hence l = 1; and s = 1;

U'(1,1) = the first element = 1.0; The input continues,

o; 2; 2; 0.5773;

.; .; .; .....;

1; 10; 10; 0.7070; →

The final value of k indicates that the process of reading in U' matrix elements has been completed, and the arrow indicates that the data input has also come to an end.

The computing procedure which follows, may be summarised:

(a) the $g_{tt'}$ elements are considered in turn, and for

each pair of internal displacement coordinates s_t and $s_{t'}$, the integer labels of the common atoms are determined from the rows of the I matrix.

(b) the $\underline{s}_{t\alpha}$ vectors for s_t are then computed for each of these common atoms, by resolving the literature vector formulae into components along the directions of the axes used to define the atomic coordinates. Parameters stored in the matrices PR and PA are required for this calculation. The same procedure is then carried out for the $\underline{s}_{t'\alpha}$ vectors.

(c) the sum of scalar products $1/m_\alpha(\underline{s}_{t\alpha}.\underline{s}_{t'\alpha})$ is carried out over all of the common atoms, and this sum is the required element $g_{tt'}$.

(d) the g matrix is output in rows, the order of the elements corresponding to that of the input s_t elements.

(e) the g matrix is transformed by the matrices U' and U, to the block-diagonal matrix G, and this is also output in rows, the order of the S_t being that implied by the form of U'.

The g matrix computer programme was tested by calculating the g and G matrices for Cl_2O_7 (a C_{2v} model was used as described in Chapter Sixteen) for which the elements $g_{tt'}$ and $G_{tt'}$ had previously been calculated by hand. Similar tests were made for $HClO_4$ and several other molecules. All tests were found to be satisfactory.

```
begin  comment  This program finds the g matrix for
                any molecule.  A set of internal
                displacement coordinates is used.
                These coordinates can be of three
                kinds.  A change in an interatomic
                distance,  a change in a valence
                angle,  a change in dihedral angle.
                The g matrix is then transformed
                into the G matrix by the matrix U
                which is formed by considering the
                symmetry properties of the molecule;

       real     SX1,SY1,SZ1,SX2,SY2,SZ2,C1,C2,EX,EY,
                EZ,ex,ey,ez,VX,VY,VZ,VTX,VTY,VTZ;

       integer  m,n,a,b,c,d,i,j,k,l,p,q,r,s,int,x;

       open(20);  open(10);  open(30);
       copy text(20,30,[;;]);
       n:=read(20);  m:= read(20);

       begin  real  array   C[1:n,1:3],M[1:n],
                            PR[1:n,1:n],
                            PA[1:n,1:n],PT[1:n,1:n],
                            g,U,V,Ug,G[1:m,1:m],
                            SCALAR[1:4];
              integer  array   I[1:m,1:4],N[1:4];

              real  procedure  COT(aa);
                    value  aa;
                    real   aa;
                    begin    COT:= cos(aa)/sin(aa);
                    end procedure;

              real  procedure  COSEC(bb);
                    value  bb;
                    real   bb;
                    begin    COSEC:=1.0/sin(bb);
                    end procedure;

              procedure  UNITVEC(cax,cay,caz,cbx,cby,
                                 cbz,eabx,eaby,eabz,
                                 aaa,bbb);
              value  cax,cay,caz,cbx,cby,cbz,aaa,bbb;
              real   cax,cay,caz,cbx,cby,cbz,eabx,eaby,
                     eabz;
              integer  aaa,bbb;
```

```
begin  eabx:=(cbx-cax)×PR[aaa,bbb];
       eaby:=(cby-cay)×PR[aaa,bbb];
       eabz:=(cbz-caz)×PR[aaa,bbb];
end  procedure;
procedure  VP(ax,ay,az,bx,by,bz,vpx,
                vpy,vpz);
value  ax,ay,az,bx,by,bz;
real   ax,ay,az,bx,by,bz,vpx,vpy,vpz;
begin  vpx:=(ay×bz)-(az×by);
       vpy:=(az×bx)-(ax×bz);
       vpz:=(ax×by)-(ay×bx);
end  procedure;
procedure  VTP(ax,ay,az,bx,by,bz,cx,
                 cy,cz,vtpx,vtpy,vtpz);
value  ax,ay,az,bx,by,bz,cx,cy,cz;
real  ax,ay,az,bx,by,bz,cx,cy,cz,vtpx,
      vtpy,vtpz;
begin  vtpx:=(ay×bx×cy)-(ay×by×cx)-
             (az×bz×cx)+(az×bx×cz);
       vtpy:=(az×by×cz)-(az×bz×cy)-
             (ax×bx×cy)+(ax×by×cx);
       vtpz:=(ax×bz×cx)-(ax×bx×cz)-
             (ay×by×cz)+(ay×bz×cy);
end  procedure;
procedure MMULT(A,B,C,y);
value A,B,y;
integer y;
real array A,B,C;
begin integer u,v,w;
for u:=1 step 1 until y do
for v:=1 step 1 until y do
begin
C[u,v]:=0.0;
for w:=1 step 1 until y do
C[u,v]:=C[u,v]+A[u,w]×B[w,v]
end;
end procedure;
procedure TRANS(A,B,y);
value A,y;
integer y;
real array A,B;
begin integer u,v;
for u:=1 step 1 until y do
for v:=1 step 1 until y do
B[u,v]:=A[v,u]
end procedure;
```

```
        for i:=1 step 1 until n do
        for j:=1 step 1 until 3 do
        C[i,j]:=read(20);

        for i:=1 step 1 until n do
        M[i]:=read(20);

        for i:=1 step 1 until m do
        for j:=1 step 1 until 4 do
        I[i,j]:=read(20);


L1:   p:=read(20);  i:=read(20);  j:=read(20);
      PR[i,j]:=read(20); PR[i,j]:=1.0/PR[i,j];
      PR[j,i]:=PR[i,j];
      if p=0 then goto L1;
L2:   p:=read(20);  i:=read(20);  j:=read(20);
      PA[i,j]:=read(20);  PA[i,j]:=PA[i,j]/57.2957795;
      PA[j,i]:=PA[i,j];
      if p=0 then goto L2;
L3:   p:=read(20);  i:=read(20);  j:=read(20);
      PT[i,j]:=read(20);  PT[i,j]:=PT[i,j]/57.2957795;
      PT[j,i]:=PT[i,j];
      if p=0 then goto L3;


      for i:=1  step 1 until m  do
      for j:=i  step 1 until m  do
      begin
      for p:=1 step 1 until 4 do
          begin  N[p]:=0;
          if I[i,p]=I[j,1]then N[p]:=I[i,p];
          if I[i,p]=I[j,2]then N[p]:=I[i,p];
          if I[i,p]=I[j,3]then N[p]:=I[i,p];
          if I[i,p]=I[j,4]then N[p]:=I[i,p];
          end;
      for p:=1 step 1 until 4 do
      if N[p]≠0 then
          begin  r:=0;  for q:=1 step 1 until 4 do
                        begin  if I[i,q]≠0 then
                               r:=r+1;
                        end;
          int:=2;  a:=I[i,1];  b:=I[i,2];  c:=I[i,3];
          d:=I[i,4];
```

```
            if r=2 then goto R;
            if r=3 then goto A;
            if r=4 then goto T;

R:          if N[p]=a then goto RA;
            if N[p]=b then goto RB;

RA:         UNITVEC(C[b,1],C[b,2],C[b,3],C[a,1],C[a,2],
                    C[a,3],EX,EY,EZ,b,a);
            SX2:=EX;  SY2:=EY;  SZ2:=EZ;
            goto FIN;
RB:         x:=a;  a:=b;  b:=x;
            goto RA;

A:          if N[p]=a then goto AA;
            if N[p]=b then goto AB;
            if N[p]=c then goto AC;

AA:         UNITVEC(C[a,1],C[a,2],C[a,3],C[b,1],C[b,2],
                    C[b,3],EX,EY,EZ,a,b);
            UNITVEC(C[b,1],C[b,2],C[b,3],C[c,1],C[c,2],
                    C[c,3],ex,ey,ez,b,c);
            VTP(EX,EY,EZ,EX,EY,EZ,ex,ey,ez,VTX,VTY,VTZ);
            C1:=PR[b,a]×COSEC(PA[a,c]);
            SX2:=C1×VTX;  SY2:=C1×VTY;  SZ2:=C1×VTZ;
            goto FIN;
AC:         x:=a;  a:=c;  c:=x;  goto AA;
AB:         UNITVEC(C[a,1],C[a,2],C[a,3],C[b,1],C[b,2],
                    C[b,3],EX,EY,EZ,a,b);
            UNITVEC (C[b,1],C[b,2],C[b,3],C[c,1],C[c,2],
                     C[c,3],ex,ey,ez,b,c);
            VTP(EX,EY,EZ,EX,EY,EZ,ex,ey,ez,VTX,VTY,VTZ);
            C1:=PR[b,a]×COSEC(PA[a,c]);
            SX2:=-C1×VTX;  SY2:=-C1×VTY;  SZ2:=-C1×VTZ;
            UNITVEC(C[c,1],C[c,2],C[c,3],C[b,1],C[b,2],
                    C[b,3],EX,EY,EZ,c,b);
            UNITVEC(C[b,1],C[b,2],C[b,3],C[a,1],C[a,2],
                    C[a,3],ex,ey,ez,b,a);
            VTP(EX,EY,EZ,EX,EY,EZ,ex,ey,ez,VTX,VTY,VTZ);
            C1:=PR[b,c]×COSEC(PA[a,c]);
            SX2:=SX2-C1×VTX;  SY2:=SY2-C1×VTY;
            SZ2:=SZ2-C1×VTZ;
            goto FIN;
```

```
T:      if N[p]= a  then goto TA;
        if N[p]= b  then goto TB;
        if N[p]= c  then goto TC;
        if N[p]= d  then goto TD;

TA:     UNITVEC(C[a,1],C[a,2],C[a,3],C[b,1],C[b,2],
                C[b,3],EX,EY,EZ,a,b);
        UNITVEC(C[b,1],C[b,2],C[b,3],C[c,1],C[c,2],
                C[c,3],ex,ey,ez,b,c);
        VP(EX,EY,EZ,ex,ey,ez,VX,VY,VZ);
        C1:=-PR[a,b]×COSEC(PA[a,c])↑2.0;
        SX2:=C1×VX;  SY2:=C1×VY;  SZ2:=C1×VZ;
        goto FIN;
TB:     UNITVEC(C[a,1],C[a,2],C[a,3],C[b,1],C[b,2],
                C[b,3],EX,EY,EZ,a,b);
        UNITVEC(C[b,1],C[b,2],C[b,3],C[c,1],C[c,2],
                C[c,3],ex,ey,ez,b,c);
        VP(EX,EY,EZ,ex,ey,ez,VX,VY,VZ);
        VTP(ex,ey,ez,EX,EY,EZ,ex,ey,ez,VTX,VTY,VTZ);
        C1:=(PR[a,b]×COSEC(PA[a,c])-PR[b,c]×
             cos(PT[a,d])×COT(PA[b,d])-PR[b,c]×
             COT(PA[a,c]))×COSEC(PA[a,c]);

        C2:=-PR[b,c]×COT(PA[b,d])×sin(PT[a,d])×
             COSEC(PA[a,c]);
        SX2:=C1×VX+C2×VTX;  SY2:=C1×VY+C2×VTY;
        SZ2:=C1×VZ+C2×VTZ;
        goto FIN;
TC:     x:=a;  a:=d;  d:=x;  x:=b;  b:=c;  c:=x;
        goto TB;
TD:     x:=a;  a:=d;  d:=x;  x:=b;  b:=c;  c:=x;
        goto TA;


FIN:    int:=int-1;   if int≠0 then
                      begin  SX1:=SX2;
                      SY1:=SY2;  SZ1:=SZ2;
                      r:=0;
                      for q:=1 step 1 until
                      4 do
                      begin
                      if I[j,q]≠0
                      then r:=r+1;
                      end;
                      a:=I[j,1]; b:=I[j,2];
                      c:=I[j,3]; d:=I[j,4];
```

```
                                        if r=2 then goto R;
                                        if r=3 then goto A;
                                        if r=4 then goto T;
                                        end;


            SCALAR[p] :=SX1xSX2+SY1xSY2+SZ1xSZ2;
            SCALAR[p] := SCALAR[p]/M[N[p]];

            end
            else      SCALAR[p]:=0.0;

      g[i,j]:=SCALAR[1]+SCALAR[2]+SCALAR[3]+
                  SCALAR[4];
        end;

for i:=1 step 1 until m do
for j:=i step 1 until m do
g[j,i]:=g[i,j];

gap(10,300);
write text(30,[[cc]UNFACTORED**G**MATRIX[cc]]);
for i:=1 step 1 until m do
begin for j:=1 step 1 until m do
      begin
      write(30,format([-nd.ddddddddd;ss]),g[i,j]);
      write(10,format([-nd.ddddddddd;ss]),g[i,j]);
      if j=10 then
              begin
              write text(30,[[c]]);
              write text(10,[[c]]);
              end;
      if j=20 then
              begin
              write text(30,[[c]]);
              write text(10,[[c]]);
              end;
      end;
write text(30,[[cccc]]);
write text(10,[[cccc]]);
end;

for i:=1 step 1 until m do
for j:=1 step 1 until m do
U[i,j]:=0.0;
```

```
L4:     k:=read(20);  l:=read(20);  s:=read(20);
        U[l,s]:=read(20);  if k=0 then goto L4;
        TRANS(U,V,m);  MMULT(U,g,Ug,m);
        MMULT(Ug,V,G,m);

        gap(10,300);
        write text(30,[[cc]FACTORED**G**MATRIX[cc]]);
        for i:=1 step 1 until m do
        begin
        for jj:=1 step 1 until m do
            begin
            write(30,format([-nd.ddddddddd;ss]),G[i,j]);
            write(10,format([-nd.ddddddddd;ss]),G[i,j]);
            if j=10 then
                    begin
                    write text (30,[[c]]);
                    write text(10,[[c]]);
                    end;
            if j=20 then
                    begin
                    write text (30 ,[[c]]);
                    write text(10,[[c]]);
                    end;
            end;
        write text(30,[[cccc]]);
        write text(10,[[cccc]]);
        end;


end;

close(20);   close(30);   close(10);

end→
```

APPENDIX TWO

THE EIGENVALUES PROGRAMME

1. Introduction

In Chapter Five it was stated that the basic equation of the classical approach to molecular vibration, involves finding the eigenvalues of an unsymmetrical matrix $\underline{gf}$ (or $\underline{GF}$), and the present appendix describes a computer programme written to carry out this calculation for matrices of low order.

2. Theory

The method of solution adopted is that known as the trace method, and it is described in reference (62), on page 216. This method involves finding the coefficients of the polynomial in λ , obtained by expanding the determinantal equation $|\underline{GF} - \underline{E}\lambda| = 0$, and this is done by evaluating the traces of successive powers of the matrix $\underline{GF}$. The programme then finds the required zeros of the polynomial by Newton's iterative method[67]. The lowest root is found first, and then divided out to produce a new polynomial in λ , whose order is one less than that of the original one. The new polynomial is treated in the same way. The lowest zero is found, divided out, and a polynomial of

order two less than the original, is produced. This procedure is repeated until all the eigenvalues of the GF matrix have been isolated.

A number of disadvantages of the above procedure should be mentioned. Firstly, it is rather time-consuming, and the time required for complete solution increases dramatically with increasing order of the matrix to be solved. Secondly, the method is subject to error from a number of sources, these errors being also accentuated as the order increases. Thus the coefficients of the original polynomial equation, must be subject to numerical round-off errors, as they are calculated by carrying out a large number of matrix multiplications. In addition, the method of dividing out each root as it is isolated, cannot be regarded as completely satisfactory, for any error in the first root leads to errors in the coefficients of the polynomial obtained on division, and this error is transmitted to the second root. In this way errors must accumulate as successive roots are calculated.

In order to investigate the seriousness of the error sources discussed, various matrices of order less than eight, whose eigenvalues were accurately known, were used to test the programme, and even for a matrix of order seven, all eigenvalues were obtained

accurate to at least the fifth place of decimals. In the iterative process the accuracy to which each root was calculated was kept constant at 10^{-7}. It is not of course possible to make this quantity indefinitely small, as sources of numerical error in the iterative process cause the latter to diverge, if the accuracy required is set at too high a value. As a result of the tests it was assumed that the method was adequate for the purposes of the calculations described in Chapters Six and Seven.

2. The data input requirements

The text of the eigenvalues programme follows at the end of this section. The programme is written in Algol for use on an English Electric K.D.F.9 computer. In the present work it was compiled by a Whetstone compiler, and took only a few seconds to solve a matrix of order four, but around twelve minutes for one of order seven. The sequence of data necessary for the calculation, is as follows,

DV = output device number = 10 or 30;

y = the number of GF matrices to be solved;

tol = the error permitted in each root extracted by Newton's method. This was held at 10^{-7};

*n = the order of the matrices G,F, and GF.

trial = a value lower than the lowest root expected. This might, for example, be set at -0.5 for the vibrational problem;

$\underline{G}$ (nxn) = the elements of the $\underline{G}$ matrix in rows;

$\underline{F}$ (nxn) = the elements of the $\underline{F}$ matrix in rows;

For more sets of data return to *.

The eigenvalues are output in order of increasing magnitude, and each is converted to a wavenumber value using the relation $w = 1302.9\lambda^{\frac{1}{2}}$, which is given in reference (62) on page 266. These wavenumbers were output for comparison with observed spectral values.

The above programme does not of course calculate the eigenvectors necessary for obtaining the transformation to normal coordinates. In simple cases, these were found by hand, whilst for matrices of order greater than four, they were found using a standard linear equations computer programme.

If for any reason the iterative process diverges a failure message ROOTS COMPLEX is output, and the calculation is terminated.

```
begin comment  This program reads in two matrices G and
               F and forms from them the product matrix
               A equal to GF.  It then finds the
               eigenvalues of A by the trace method and
               converts these into wavenumber values;

      real     r,s,func,diff,tol,trial,correct,waves;

      integer  y,n,a,b,c,i,j,DV;


      open(20);  DV:= read(20);  open(DV);
      y:=read(20);  tol:= read(20);
REPEAT:
      n:= read(20);  trial:= read(20);

      begin real array A,B,E,G,F[1:n,1:n],CI,C,D[0:n],
                       T[1:n];

      procedure MMULT(X,Y,Z,x);
        value X,Y,x;
        integer x;
        real array X,Y,Z;
        begin integer u,v,w;
        for u:=1 step 1 until x do
        for v:=1 step 1 until x do
        begin  Z[u,v]:=0.0;
        for w:=1 step 1 until x do
        Z[u,v]:=Z[u,v]+X[u,w]xY[w,v]
        end;
        end procedure ;

      procedure  TRACE(X,x,p);
        value X,x;
        integer x;
        real  p;
        real array X;
        begin integer u;   p:=0.0;
        for u:=1 step 1 untilx do
        p:=p+X[u,u];
        end procedure;


      procedure FUNCTION(P,t,p,x);
        value P,t,p;
        integer p;
        real t,x;
        real array P;
```

```
    begin integer u;  x:=0.0;
    for u:=0 step 1 until p do
    x:=x+P[u]×t↑u;
    end procedure;

  procedure DIFFERENTIATE(P,Q,p);
    valueP,p;
    integer p;
    real array P,Q;
    begin integer u;
    for u:=0 step 1 until p do
    Q[u]:=P[u+1]×(u+1);
    Q[p+1]:=0.0;
    end procedure ;

  procedure DIVIDE(P,t,p);
    value t,p;
    integer p;
   real t;
    real array P;
    begin integer u,v;
    for u:=0 step 1 until p do
    begin
    P[u]:=0.0;
    for v:=u+1 step 1 until p+1 do
    P[u]:=P[u]+P[v]×t↑(v-u-1);
    end;
    P[p+1]:=0.0;
    end procedure;



for i:=1 step 1 until n do
forj:= 1 step 1 until n do
G[i,j] :=read(20);
for i:=1 step 1 until n do
for j:=1 step 1 until n do
F[i,j]:=read(20);

MMULT(G,F,A,n);

TRACE(A,n,T[1]);  MMULT(A,A,B,n);

TRACE(B,n,T[2]);
a:=2;
```

```
L1:   a:=a+1;   MMULT(A,B,E,n);   TRACE(E,n,T[a]);
      if a<n then goto L2 else gotoL3;
L2:   a:=a+1;   MMULT(A,E,B,n);   TRACE(B,n,T[a]);
      if a<n then goto L1 else goto L3;
L3:   CI[0]:=1.0;
      for i:=1 step 1 until n do
      begin  CI[i]:=0.0;
      for j:=0 step 1 until i-1 do
      CI[i] := CI[i] + T[i-j ]×CI[j];
      CI[i]:=-CI[i]/i;
      end;
      for i:=0 step 1 until n do
      C[i]:=CI[n-i];

      b:=n;  c:=n-1;
L4:   DIFFERENTIATE (C,D,c);
      correct:= +100.0;
L5:   FUNCTION(C,trial,b,func);
      FUNCTION(D,trial,c,diff);
      r:=-func/diff;   s:=correct-r;
      if s<0 then goto FAIL;
      correct:=r;
      trial:=trial+correct;
      if abs(correct)<tol then goto L6 else goto L5;
L6:   write text (DV,[[c]EIGENVALUE**IS**EQUAL**TO****]);
      write(DV,format([-nd.ddddd;]),trial);
      write text (DV,[***OR***]);
      waves:=sqrt(trial)×1302.9;
      write(DV,format([-nddd.dd;]),waves);
      write text (DV,[****WAVE**NUMBERS**]);
      b:=b-1;  c:=c-1;
      if b=0 then goto L8 else gotoL7;
L7:   DIVIDE(C,trial,b);
      goto L4;
L8:   end;

      y:=y-1;   if y≠0 then goto REPEAT;
      goto L9;
FAIL: write text(DV,[[c]ROOTS*COMPLEX]);

L9:   close(20);  close(DV);


end→
```

APPENDIX THREE

THE FORCE CONSTANT VARIATION PROCEDURE

Before a vibrational secular equation can be set up, the matrix $\underline{f}$ must be known, and unlike the $\underline{g}$ matrix, this cannot be calculated for a molecule from a knowledge of its structure. Indeed, the whole object of normal coordinate calculations is to find $\underline{f}$, using the observed vibrational frequencies as data.

Since the number of observed frequencies is usually smaller than the number of $\underline{f}$ matrix elements to be determined, even when data for several isotopic species are available, it is necessary to make the approximation of valence forces (see Chapter Five), and to limit the number of non-zero $\underline{f}$ matrix elements to that of the observed frequencies. All other force constants are then assumed zero.

Even when this approximation is made, it is not usually possible to write down equations for the non-zero constants in terms of the observed frequencies, and hence to calculate them directly. Instead, rather indirect methods must be adopted to determine these constants, and the present appendix describes one of these, an iterative procedure, which was used in the calculations of Chapters Six and Seven.

In this procedure, a trial matrix $\underline{f}$ is set up, containing guessed values for the diagonal elements, and those cross-terms which have been assumed non-zero. The values chosen for these elements are then fed into the force constant variation programme, together with the elements of each block of the $\underline{G}$ matrix, and wavenumber values for the observed spectral frequencies. These latter are grouped according to their symmetry species, each group corresponding to a particular block. The input $\underline{f}$ elements are then used by the programme to construct the blocks of $\underline{F}$, and the secular equations defined by the products of each $\underline{G}$ block, with its corresponding $\underline{F}$ block, are solved using the methods described in Appendix Two. In fact the eigenvalues programme of Appendix Two is included in the variation programme as a special subroutine.

The calculated frequencies are compared with the observed values, and the quantity,

$$\sum_i (W_{obs} - W_{calc})_i^2 \qquad \ldots \text{A3.1,}$$

calculated by summing over all frequencies. A small change* is then made to one of the non-zero $\underline{f}$ elements, the others being held constant at their trial values. The secular equations are reconstructed and solved again to enable the sum A3.1 to be re-evaluated. If

* In the present work this had the value 0.05.

this sum is found to be less than its previous value, a second small change of equal magnitude and sign is made to the $\underline{f}$ matrix element previously varied. If, on the other hand, it is increased, the change is still made, but its sign is reversed. When a point is reached at which it is impossible to reduce the sum A3.1 by making a change in either direction, then the $\underline{f}$ matrix element varied is allowed to remain constant at its new optimum value, and the procedure repeated for a second force constant, and so on, for all of the non-zero $\underline{f}$ matrix elements. This process is then repeated by returning to the first force constant varied and working through all of the constants again. Thus, by a cyclic process, the function A3.1 is minimised a final set of optimum values being obtained for the non-zero force constants. At this stage the final values obtained for these constants, and the corresponding calculated frequencies, are output by the programme.

The programme text is not included in this appendix, as it is rather long, and constitutes a straightforward application of the principles outlined above. For $FClO_3$ and $HClO_4$ a six constant force field was used and convergence achieved after four full cycles of variation. The cross-terms were initially set equal to zero.

APPENDIX FOUR

A COMPUTER PROGRAMME FOR THE XOX ANGULAR SYMMETRIC SYSTEM

In this appendix the text is given of a computer programme used to calculate frequency and root mean square amplitude values for various XOX angular symmetric molecules (see Chapter Eight). The programme is written in Algol for use on the K.D.F.9 computer, and in the present work was compiled by a Whetstone compiler. Calculations required only a few seconds for completion and the programme was tested using results published for NO_2 by Cyvin[27].

The programme assumes as internal displacement coordinates, changes in the two bonded distances, and a change in the valence angle. It follows the theory outlined in Chapter Five and in reference (27), and calculates the elements of the g matrix from input structural data. It also inputs the four constants required to define the f matrix, and by transforming to symmetry coordinates constructs the G and F matrices, and finds the eigenvalues of the two blocks appearing in the GF matrix. The three vibrational frequencies which result are output in wavenumber values. The transformation relating the symmetry coordinates to

the normal coordinates, is next calculated from a set of eigenvectors, and this is used to determine the transformation of the internal displacement coordinates to the normal coordinates. Following this the two changes in interatomic distance for an XOX molecule, that is the change in OX which is already a chosen internal coordinate, and the change in the X..X non-bonded distance, are related linearly to the normal coordinates, and the amplitude values u_{OX} and $u_{X..X}$ calculated, and output in Angstrom units.

The data sequence required is,

DV = output device number = 10 or 30;

Title; p = the number of separate calculations to be completed; MX = the mass of X in a.m.u.'s;

MO = the mass of O in a.m.u.'s; A = the valence angle in degrees; R = the OX bond length in Å;

T = the absolute temperature;

* f1 = force constant f_r ;

f2 = force constant f_{rr};

f3 = force constant $f_{r\theta}$;

f4 = force constant f_θ ; Note: for the meaning and units of these latter four quantities, see Chapter Eight.

Return to * for more sets of data.

```
begin comment  This program finds the fundamental
               frequencies and mean amplitudes of
               vibration  for a symmetrical,angular,
               XOX molecule at temperature T degrees
               Kelvin.   It uses a variable force
               field f and a fixed molecular geometry.
               It outputs principally the fundamental
               frequencies in cm-1 , and the mean
               amplitudes of vibration, UOX and UX..X
               in Angstrom units;

      real     MX,MO,A,R,T,g1,g2,g3,g4,G11,G12,G22,
               G33,f1,f2,f3,f4,F11,F12,F22,F33,GF11,
               GF12,GF21,GF22,GF33,D,E,X,Y,Z,L11,L12,
               L21,L22,L33,N1,N2,N3,N11,N12,N21,N22,
               N33,WN1,WN2,WN3,K11,K12,K13,K31,K32,
               beta,C1,C2,C3,UOX,UXX;

      integer  DV,p,g,G,N,K,eigs,fr1,fr2,fr3;


      real procedure   sinh(a);   value a;   real a;
           begin real  S,term;    integer n;
                       n:=0;  term:=a;   S:=a;   a:=a↑2;
                  for  n:=n+2 while abs(term)>10-6 do
                  begin term:=termxa/n/(n+1); S:=S+term;
                  end;
                  sinh:=S;
           end;


      real procedure  cosh(b);   value b;   real b;
           begin real C,TERM;    integer m;
                      m:=2;   TERM:=b↑2/2.0;
                      C:=1.0+TERM;
                      b:=b↑2;
                  for  m:=m+2 while abs(TERM)>10-6 do
                  begin TERM := TERMxb/m/(m-1);
                        C:=C+TERM;
                  end;
                  cosh:=C;
           end;


     open(20);   DV:= read(20);   open(DV);
     copy text   (20,DV,[;;1);
```

```
        p:= read(20);  MX:= read(20);  MO:= read(20);
        A:= read(20);  R:= read(20);  T:= read(20);
        A:=A/57.30;
        g1:= 1.0/MX + 1.0/MO;
        g2:= cos(A)/MO;
        g3:= -sin(A)/(RxMO);
        g4:= 2.0/(MXxRT2)+2.0x(1-cos(A))/(RT2xMO);

        G11:= g1+g2;
        G12:= sqrt(2.0)xg3;
        G22:= g4;
        G33:= g1-g2;

RETURN: g:= read(20);  G:=read(20);  N:=read(20);
        K:=read(20);  eigs:=read(20);
        f1:=read(20); f2:=read(20); f3:=read(20);
        f4:=read(20);
        F11:= f1+f2;
        F12:= sqrt(2.0)xf3;
        F22:= f4;
        F33:= f1-f2;
        GF11:=G11xF11+G12xF12;
        GF12:=G11xF12+G12xF22;
        GF21:=G12xF11+G22xF12;
        GF22:=G12xF12+G22xF22;
        GF33:=G33xF33;
        D:=GF11+GF22;
        E:=(GF11xGF22)-(GF12xGF21);
        X:=(D+sqrt(DT2-4.0xE))/2;
        Y:=(D-sqrt(DT2-4.0xE))/2;
        Z:=GF33;
        L11:=1;
        L12:=1;
        L21:=(X-GF11)/GF12;
        L22:=(Y-GF11)/GF12;
        L33:=1;
        N1:=sqrt(X/(F11+2.0xF12xL21+F22xL21T2));
        N2:=sqrt(Y/(F11+2.0xF12xL22+F22xL22T2));
        N3:=sqrt(Z/F33);
        N11:=N1;
        N12:=N2;
        N21:=N1xL21;
        N22:=N2xL22;
        N33:=N3;

        WN1 :=sqrt(X)x1302.9;
        WN2 :=sqrt(Y)x1302.9;
        WN3 :=sqrt(Z)x1302.9;
```

```
K11:=N11/sqrt(2.0);
K12:=N12/sqrt(2.0);
K13:=N33/sqrt(2.0);
K31:=(sqrt(2.0)xsin(A/2)xN11)+(RxcosA/2)xN21);
K32:=(sqrt(2.0)xsin(A/2)xN12)+(RxcosA/2)xN22);
beta:= (2.998x6.6252)/(20x1.3805xT);

C1  := cosh(betaxWN1)/sinh(betaxWN1);
C2  := cosh(betaxWN2)/sinh(betaxWN2);
C3  := cosh(betaxWN3)/sinh(betaxWN3);

UOX := sqrt((K11↑2x16.866xC1)/WN1 +
            (K12↑2x16.866xC2)/WN2+
            (K13↑2x16.866xC3)/WN3);

UXX := sqrt((K31↑2x16.866xC1)/WN1 +
            (K32↑2x16.866xC2)/WN2);

write text (DV,[[c]RESULTS*FOR*RUN****]);
write (DV,format([ddd;c]),p);
write text (DV,[[c]FORCE*FIELD*USED***
            f1,f2,f3,f4;*[c]]);

fr1:=format([-nd.dd;c]);
write(DV,fr1,f1);
write(DV,fr1,f2);
write(DV,fr1,f3);
write(DV,fr1,f4);
write text(DV,[[c]FUNDAMENTAL*FREQUENCIES*W1,W2,W3,
            *IN*WAVE*NUMBERS;[c]]);
fr2:=format([-nddd.d;c]);
write(DV,fr2,WN1);
write(DV,fr2,WN2);
write(DV,fr2,WN3);
write text(DV,[[c]THE*MEAN*AMPLITUDES*OF*VIBRATION*
            UOX*and*UXX;[c]]);
fr3:=format([-nd.dddddd;c]);
write(DV,fr3,UOX);
write(DV,fr3,UXX);
p:=p-1;     if  p≠0 then goto RETURN;
close(20);   close(DV);

end→
```

APPENDIX FIVE

PROCEDURE DEPENDENTS FOR PERCHLORIC ACID

This appendix contains the text of a subroutine which formed part of the least squares refinement programme used to obtain R_{ij} and u_{ij} parameters for $HClO_4$. The purpose of the routine is to calculate certain dependent internuclear distances from a set of five independent values, namely those refined by the least squares procedure. A set of partial derivatives, necessary for the correct functioning of the least squares method, are also calculated.

The numbering system chosen for the C_s model of perchloric acid is shown in figure 7.1. This model contains fifteen interatomic distances and these may be classified as follows into eight non-equivalent types,

S = magnitude of S_{12}.

U = magnitude of U_{16}.

D = magnitude of D_{26}.

R = magnitude of R_{13}, R_{14}, and R_{15}.

P = magnitude of P_{34}, P_{35}, and P_{45}.

X = magnitude of X_{23}, X_{24}, and X_{25}.

Y = magnitude of Y_{64}, and Y_{65}.

Z = magnitude of Z_{63}.

Only the first five of the eight quantities S,U,D,R,P,X,Y,and Z are independent of oneanother, and the three remaining values X,Y, and Z may be written as functions of the general sort,

$X = f_1(S,U,D,R,P)$; $Y = f_2(S,U,D,R,P)$: $Z = f_3(S,U,D,R,P)$;

The procedure whose text is given below uses input values for S,U,D,R and P to calculate X,Y and Z, formulae derived from geometrical considerations being applied. In addition the cosines of the three valence angles possible for this model are also calculated and output. Finally the series of partial derivatives,

$$\frac{\partial X}{\partial S}, \quad \frac{\partial X}{\partial U}, \quad \ldots\ldots \quad \frac{\partial Z}{\partial R}, \quad \frac{\partial Z}{\partial P},$$

are calculated from analytical formulae obtained by differentiating the functions f_1, f_2, and f_3 above. These terms are stored as the elements of a matrix C.

```
procedure DEPENDENTS;
begin comment This procedure calculates the dependent
              distances for the five plus three model
              of perchloric acid as well as the
              partial derivative matrix C;
      real    S,U,D,RR,P,X,Y,Z,
              a,b,m,n,q,e,f,g,h,i,
              as,au,ad,bs,bu,bd,
              ms,mu,md,ns,nu,nd,qr,qp,
              cosA,cosB,cosG;
      integer k,l,f1,f2;

      f1:=format([-nd.ddddc]);  f2:=format([-nd.dddds]);
      S:=R[1];  U:=R[2];  D:=R[3];  RR:=R[4];  P:=R[5];
      comment Calculation of the dependent distances;
      i:=S×D;
      a:=2×S↑2×D↑2+2×U↑2×S↑2+2×U↑2×D↑2-S↑4-D↑4-U↑4;
      b:=S↑2+D↑2-U↑2;  m:=sqrt(a)/(2×i);
      n:=b/(2×i);  q:=sqrt(RR↑2-P↑2/3);  e:=S+q;
      f:=S-D×n+q;
      g:=D×m+P/sqrt(3);  h:=D×m-P/(sqrt(3)×2);
      X:=sqrt(P↑2/3+e↑2);
      Y:=sqrt(g↑2+f↑2);
      Z:=sqrt(P↑2/4+h↑2+f↑2);
      if r[6]=1 then R[6]:=X;
      if r[7]=1 then R[7]:=Y;
      if r[8]=1 then R[8]:=Z;
      comment Calculation of three angles as cosines;
      cosA:=(2×RR↑2-P↑2)/(2×RR↑2);
      cosB:=(RR↑2+S↑2-X↑2)/(2×RR×S);
      cosG:=(S↑2+D↑2-U↑2)/(2×S×D);
      write text(30,[[ccc]PERCHLORIC*ACID*MODEL*A[ccc]]);
      write text(30,[ANGLE*COSINES[c]]);
      write text(30,[COS*OPCLOP*EQUALS*****]);
      write(30,f1,cosA);
      write text(30,[COS*OPCLOB*EQUALS*****]);
      write(30,f1,cosB);
      write text(30,[COS*CLOBH**EQUALS*****]);
      write(30,f1,cosG);
      writetext(30,[[ccc]]);
      comment  Calculation of the C matrix;
      as:=4×S×(D↑2+U↑2-S↑2);
      au:=4×U×(S↑2+D↑2-U↑2);
      ad:=4×D×(S↑2+U↑2-D↑2);
      bs:=2×S;  bu:=-2×U;  bd:=2×D;
```

```
        ms:=(as×0.25)/(sqrt(a)×S×D)-(0.5×sqrt(a))/(S↑2×D);
        mu:=(au×0.25)/(sqrt(a)×S×D);
        md:=(ad×0.25)/(sqrt(a)×S×D)-(0.5×sqrt(a))/(D↑2×S);
        ns:=(bs×0.5)/i-(b×0.5)/(D×S↑2);
        nu:=(bu×0.5)/i;
        nd:=(bd×0.5)/i-(b×0.5)/(D↑2×S);
        qr:=RR/q;  qp:=-P/(3×q);
        for k:=1 step 1 until 8 do
        for l:=1 step 1 until 5 do
        if k≠l then C[k,l]:=0 else C[k,l]:=1.0;
        C[6,1]:=e/X;  C[6,2]:=0;  C[6,3]:=0;
        C[6,4]:=(e×qr)/X;  C[6,5]:=(P/3+e×qp)/X;
        C[7,1]:=(g×D×ms+f×(1-D×ns))/Y;
        C[7,2]:=(g×D×mu-f×D×nu)/Y;
        C[7,3]:=(g×(D×md+m)-f×(nd×D+n))/Y;
        C[7,4]:=(f×qr)/Y;
        C[7,5]:=(g/sqrt(3)+f×qp)/Y;
        C[8,1]:=(h×D×ms+f×(1-D×ns))/Z;
        C[8,2]:=(h×D×mu-f×D×nu)/Z;
        C[8,3]:=(h×(D×md+m)-f×(D×nd+n))/Z;
        C[8,4]:=(f×qr)/Z;
        C[8,5]:=(P/4-h/(2×sqrt(3))+(f×qp))/Z;
end DEPENDENTS;
```

LIST OF REFERENCES

1. R. Wierl, Ann. Physik, 8, 521 (1931).
2. P. Debye, Phys. Zeitshr., 40, 66, 404 (1939).
3. C. Finbak, Avhandl. Norske Vid. Acad. Oslo, Mat.-Naturv. Kl., 13 (1937).
4. P. Debye, J. Chem. Phys., 9, 55 (1941).
5. J. Karle, J. Chem. Phys., 13, 155 (1945).
6. J. Karle, J. Chem. Phys., 15, 202 (1947).
7. I. Karle and J. Karle, J. Chem. Phys., 17, 1052 (1949).
8. J. Karle and H. Hauptman, J. Chem. Phys., 18, 875 (1950).
9. J. Karle and I. Karle, J. Chem. Phys., 18, 957 (1950).
10. I. Karle and J. Karle, J. Chem. Phys., 18, 963 (1950).
11. V. Schomaker and R. Glauber, Nature, 170, 290 (1952).
12. J. A. Ibers and J. A. Hoerni, Acta Cryst., 7, 405 (1954).
13. L. S. Bartell and L. O. Brockway, Nature, 171, 978 (1953).
14. R. A. Bonham and T. Ukaji, J. Chem. Phys., 36, 72 (1962).
15. J. Karle and R. A. Bonham, J. Chem. Phys., 40, 1396 (1964).
16. H. M. Seip, Selected Topics in Structure Chemistry, Universitetsforlaget, Oslo (1967).
17. J. Karle, J. Chem. Phys., 35, 963 (1961).
18. T. Iijima and R. A. Bonham, Acta Cryst., 16, 1061 (1963).
19. R. A. Bonham and T. Iijima, J. Phys. Chem., 67, 2266 (1963).
20. T. Iijima and R. A. Bonham, J. Phys. Chem., 67, 2769 (1963).
21. L. S. Bartell, J. Chem. Phys., 23, 1219 (1955).
22. K. Kuchitsu and L. S. Bartell, J. Chem. Phys., 35, 1945 (1961).

23. L. S. Bartell, K. Kuchitsu and R. J. de Neui, J. Chem. Phys., 35, 1211 (1961).

24. K. Kuchitsu and L. S. Bartell, J. Chem. Phys., 36, 2470 (1962).

25. Y. Morino, J. Chem. Phys., 36, 1108 (1962).

26. A. Reitan, Acta Chem. Scand., 12, 131, 785 (1958).

27. S. J. Cyvin, Acta Polytech. Scand., Physics Series No. 6 (1960).

28. A. Almenningen, O. Basiansen and J. Munthe-Kaas, Acta Chem. Scand., 10, 261 (1956).

29. Y. Morino, Acta Cryst., 13, 1107 (1960).

30. S. Cyvin and E. Meisingseth, Acta Chem. Scand., 15, 1289 (1961).

31. O. Bastiansen, L. Hedberg and K. Hedberg, J. Chem. Phys., 27, 1311 (1957).

32. L. S. Bartell, D. A. Kohl, B. L. Carroll and R. M. Gavin Jr., J. Chem. Phys., 42, 3079 (1965).

33. Y. Morino, K. Kuchitsu and Y. Murata, Acta Cryst., 16, A129 (1963).

34. K. Hedberg and M. Iwasaki, Acta Cryst., 17, 529 (1964).

35. A. Almenningen, O. Bastiansen, R. Seip and H. M. Seip, Acta Chem. Scand., 18, 2115 (1964).

36. L. S. Bartell, L. O. Brockway and R. H. Schwendeman, J. Chem. Phys., 23, 1854 (1955).

37. R. A. Bonham and L. S. Bartell, J. Chem. Phys., 31, 702 (1959).

38. O. Bastiansen, O. Hassel and F. Risberg, Acta Chem. Scand., 9, 232 (1955).

39. O. Bastiansen and P. N. Skancke, Adv. Chem. Physics, Vol. Three, 323 (1960).

40. A. Almenningen, O. Bastiansen, A. Haaland and H. M. Seip, Angew. Chem. (Internat. Edit.) 4, 819 (1965).

41. N. F. Mott and H. S. W. Massey, The Theory of Atomic Collisions, Third Ed., Oxford University Press (1965).

42. L. S. Rodberg and R. H. Thaler, Introduction to the Quantum Theory of Scattering, Academic Press (1967).

43. E. Merzbacher, Quantum Mechanics, John Wiley and Sons (1961).

44. L. I. Shiff, Quantum Mechanics, Second Ed., McGraw-Hill, New York (1955).

45. P. A. M. Dirac, The Principles of Quantum Mechanics, Fourth Ed., Oxford University Press (1958).

46. N. F. Mott and I. N. Sneddon, Wave Mechanics and its Applications, Oxford University Press (1948).

47. V. P. Spiridonov, N. G. Rambidi and N. V. Alekseev, J. Struct. Chem., 4, 717 (1963).

48. N. G. Rambidi, V. P. Spiridonov and N. V. Alekseev, J. Struct. Chem., 3, 331 (1962).

49. H. Faxen and J. Holtsmark, Zeits. f. Physik., 45, 307 (1927).

50. M. Born, Zeits. f. Physik, 37, 863 (1926).

51. M. Born, Zeits. f. Physik, 38, 803 (1926).

52. L. O. Brockway, Usp. Fiz. Nauk., 17, 175, 280 (1937).

53. L. Pauling and L. O. Brockway, J. Am. Chem. Soc., 57, 2684 (1935).

54. S. H. Bauer, J. Chem. Phys., 18, 27 (1950).

55. K. Kuchitsu, Bull. Chem. Soc. Japan, 32, 748 (1959).

56. J. Rundgren, Arkiv f. Fysik, 35, 31 (1967).

57. L. Wegmann, J. Haase and W. Zeil, Proceedings of the Sixth International Congress for Electron Microscopy, 259 (1966).

58. P. G. Hambling, Acta Cryst., 6, 98 (1953).

59. B. Beagley, D. W. J. Cruickshank, T. G. Hewitt and A. Haaland, Trans. Farad. Soc., 63, 836 (1967).

60. H. P. Hanson, F. Herman, J. D. Lea and S. Skillman, HFS Atomic Structure Factors, R. A. Welch Foundation of Texas.

61. H. Margenau and G. M. Murphy, The Mathematics of Physics and Chemistry, Vol. One, D. van Nostrand Comp. Inc., (1956).

62. E. B. Wilson Jr., J. C. Decius and P. C. Cross, Molecular Vibrations, McGraw-Hill, New York (1955).

63. Y. Morino, K. Kuchitsu and T. Shimanouchi, J. Chem. Phys., 20, 726 (1952).

64. Y. Morino, K. Kuchitsu, A. Takahashi and K. Maeda, J. Chem Phys., 21, 1927 (1953).

65. Y. Morino, E. Hirota, J. Chem. Phys., 23, 737 (1955).

66. E. T. Whittaker, Analytical Dynamics, Dover Press, New York (1944).

67. B. Noble, Numerical Methods: 1, Oliver and Boyd Ltd. (1964).

68. B. Crawford and J. Overend, J. Mol. Spec., 12, 307 (1964).

69. D. R. Lide Jr. and D. E. Mann, J, Chem. Phys., 25, 1128 (1956).

70. D. R. Lide Jr., J. Chem. Phys., 43, 3767 (1965).

71. D. A. Gilbert, A. Roberts and P. A. Griswold, Phys. Rev., 76, 1723L (1949).

72. E. A. Jones, T. F. Parkinson and T. G. Burke, J. Chem. Phys., 18, 235 (1950).

73. D. F. Smith, J. Chem Phys., 21, 609 (1953).

74. D. A. Long and D. T. L. Jones, Trans. Farad. Soc., 59, 273 (1963).

75. E. A. Robinson, Can. J. Chem., 41, 3021 (1963).

76. H. Siebert, Z. Anorg. Allgem. Chem., 275, 225 (1954).

77. P. A. Akishin, L. V. Vilkov and V. Rosolovskii, Kristallografiya, 4, 353 (1959).

78. A. Simon and M. Weist, Z. Anorg. Allgem. Chem., 268, 301 (1952).

79. P. A. Giguere and R. Savoie, Can. J. Chem., 40, 495 (1962).

80. K. Hedberg and R. M. Badger, J. Chem. Phys., 19, 508 (1951).

81. B. Beagley, Trans. Farad. Soc., 61, 1821 (1965).

81 A. I. Schwager and A. Arkell, J. Am. Chem. Soc., 89, 6006 (1967).

82. M. M. Rochkind and G. C. Pimentel, J. Chem. Phys., 42, 1361 (1965).

83. M. G. K. Pillai and R. F. Curl, Spectrochim. Acta, 18, 1382 (1962).

84. S. R. Polo and M. K. Wilson, J. Chem Phys., 22, 900 (1954).

85. B. Krakow and R. L. Lord, J. Chem. Phys., 44, 3640 (1966).

86. A. H. Nielsen and P. J. H. Woltz, J. Chem. Phys., 20, 1878 (1952).

87. R. D. Shelton, A. H. Nielsen and W. H. Fletcher, J. Chem. Phys., 21, 2178 (1953).

88. R. Stolevik, B. Andersen, S. J. Cyvin and J. Brunvoll, Acta Chem. Scand., 21, 1581 (1967).

89. B. Beagley, A. H. Clark and D. W. J. Cruickshank, Chem. Comm., 458 (1966).

90. L. E. Sutton and L. O. Brockway, J. Am. Chem. Soc., 57, 473 (1935).

91. L. Pauling and L. O. Brockway, J. Am. Chem. Soc., 57, 2684 (1935).

92. J. D. Dunitz and K. Hedberg, J. Am. Chem. Soc., 72, 3108 (1950).

93. G. E. Herberich, P. H. Jackson and D. J. Millen, J. Chem. Soc (A), 336 (1966).

94. G. H. Cady, Inorg. Synth., 5, 156 (1957).

95. D. W. J. Cruickshank, J. Chem. Soc., 5486 (1961).

96. B. Beagley, A. H. Clark and T. G. Hewitt, J. Chem. Soc. (A), 658 (1968).

97. G. F. Smith, J. Am. Chem. Soc., 75, 184 (1953).

98. A. H. Clark, B. Beagley and D. W. J. Cruickshank, Chem. Comm., 14 (1968).

99. B. Beagley, Chem. Comm., 388 (1966).

100. J. K. Ward, Phys. Rev., 96, 845 (1954).

101. J. B. Coon, J. Chem. Phys., 14, 665 (1946).

102. R. F. Curl, J. L. Kinsey, J. G. Baker, D. H. Baird, G. R. Bird, R. F. Heidelberg, T. M. Sugden, D. R. Jenkins and C. N. Kenney, Phys. Rev., 121, 1119 (1961).

103. G. Brauer, Handbook of Preparative Inorganic Chemistry, Vol. One, Second Ed., Academic Press, 301 (1963).

104. E. L. Wagner, J. Chem. Phys., 37, 751 (1962).

105. V. Schomaker and D. P. Stevenson, J. Am. Chem. Soc., 62, 1270 (1940).

106. B. P. Dailey, S. Golden and E. B. Wilson Jr., Phys. Rev., 72, 872 (1947).

107. G. F. Crable and W. V. Smith, J. Chem. Phys., 19, 502 (1951).

108. M. H. Sirvetz, J. Chem. Phys., 19, 938 (1951).

109. D. Kivelson, J. Chem. Phys., 22, 904 (1954).

110. Y. Morino, Y. Kikuchi, S. Saito and E. Hirota, J. Mol. Spec., 13, 95 (1964).

111. J. Haase and M. Winnewisser, Zeit. Naturf., 61 (1968).

111A. W. Moffitt, Proc. Roy. Soc. (London) Ser. A, 200 409 (1950).

112. K. J. Palmer, J. Am. Chem. Soc., 60, 2360 (1938).

113. R. M. Badger, J. Chem. Phys., 2, 128 (1934).

114. C. H. D. Clark, Phil. Mag., 18, 459 (1934).

115. J. W. Linnett, Quart. Rev., 1, 73 (1947).

116. G. Porter, Discussions of Far. Soc., 960 (1950).

117. R. A. Durie and D. A. Ramsay, Can. J. Phys., 36, 35 (1958).

118. E. A. Robinson and M. W. Lister, Can. J. Chem., 41, 2988 (1963).

119. R. Savoie and P. A. Giguere, Can. J. Chem., 40, 991 (1962).

120. J. S. Rigden and S. S. Butcher, J. Chem. Phys., 40, 2109 (1964).

121. A. Arkell and I. Schwager, J. Am. Chem. Soc., 89, 5999 (1967).

122. J. C. Decius, J. Chem. Phys., 16, 1025 (1948).

123. A Carrington, P. N. Dyer and D. H. Levy, J. Chem. Phys., 47, 1756 (1967).

124. R. A. Ashby, J. Mol. Spec., 23, 439 (1967).